HEINRICH HEINE
UNIVERSITÄT DÜSSELDORF

Characterization of a lipoprotein CD1348 from *Clostridium difficile* and the viral infectivity factor of HIV-1

Inaugural-Dissertation

For the attainment of the title of doctor
in the Faculty of Mathematics and Natural Sciences
at the Heinrich Heine University Duesseldorf

Presented by

Rebecca Clemens

from Neuss

Duesseldorf, May 2018

From the Institute of Biochemistry
At the Heinrich Heine University Duesseldorf

Published by permission of the
Faculty of Mathematics and Natural Sciences
at Heinrich Heine University Duesseldorf

Supervisor: Prof. Dr. Lutz Schmitt
Co-supervisor: Prof. Dr. Holger Gohlke

Date of the oral examination: 02.07.2018

“Es scheint immer unmöglich, bis es vollbracht ist.”

(Nelson Mandela)

Abstract

Since the discovery of penicillin in 1928 by Alexander Flemming different types of antibiotics were discovered. One big group of antibiotics is targeting the cell wall synthesis of bacteria. ß-Lactams, like penicillin G, glycopeptides, like vancomycin and lipodepsipeptides like ramoplanin are the most prominent antibiotics targeting the cell wall. Some bacteria raise resistance against antibiotics via various resistance mechanisms. They are able to modify the target protein of the antibiotic or degrade the antibiotic. Because of the high number of antibiotic resistant strains a new treatment against bacteria has to be found. Promising candidates are the antimicrobial peptides especially the lantibiotics like nisin. Nisin is a post-translational modified peptide that is highly active against Gram-positive bacteria and is used in food industry as a preservative. Some human pathogens developed lantibiotic resistance systems. An operon encoding a three component ABC-transporter in *Clostridium difficile* (*C. difficile*) was discovered. This ABC-transporter, CprABC, was characterized and it is known that the system performs resistance against different lantibiotics, like subtilin, nisin and gallidermin. Also, a two-component system with a response regulator, CprR, and a histidine kinase, CprK, could be identified. With a closer look to this resistance system a lipoprotein encoded directly in front of the CprABC transporter could be identified. Comparing the operon with other resistance systems the lipoprotein CD1348, of *C. difficile* could be similar to NisI of *Lactococcus lactis* (*L. lactis*) an immunity protein or Nsr of *Streptococcus agalactiae* (*S. agalactiae*) a resistance protein. In this thesis, the CD1348 protein of *C. difficile* should be characterized and the function and the structure analysed. The purification could be established and with NMR and small-angle X-ray scattering (SAXS) measurements the calculated model of CD1348 could be proven. Also *in vivo* studies in *L. lactis* and *in vitro* interaction measurements with different lantibiotics were performed. No resistance in *L. lactis* cells expressing the CD1348 protein could be determined, till date.

Furthermore, an antibiotic and lantibiotic resistant strain was analysed via growth inhibition studies and lipid analysis. Via this study the lipid composition of the original *L. lactis* strain, which was not available till now, and the lipid composition of the resistant strain could be determined.

Additionally, a purification of secreted viral infectivity protein of HIV-1 expressed in *Escherichia coli* (*E. coli*) was tried to establish.

Zusammenfassung

Seit der Entdeckung von Penicillin durch Alexander Flemming 1928 wurden mehrere unterschiedliche Antibiotika entdeckt. Eine große Gruppe von Antibiotika hat als Angriffsziel die Zellwandsynthese von Bakterien. Die bekanntesten Antibiotika, welche die Zellwand angreifen, sind die ß-Lactame wie Penicillin G, die Glycopeptide wie Vancomycin und die Lipodepsipeptide wie Ramoplanin. Einige Bakterien sind in der Lage mit verschiedenen Mechanismen Resistenzen gegen Antibiotika zu entwickeln. Sie sind in der Lage die Angriffsziele der Antibiotika zu modifizieren oder auch durch Abbau die Antibiotika zu deaktivieren. Wegen der wachsenden Zahl an antibiotikaresistenten Bakterien müssen neue Behandlungsmöglichkeiten gefunden werden. Eine Alternative für Antibiotika sind die antimikrobiellen Peptide zu denen auch die Lantibiotika, wie Nisin, gehören. Nisin ist ein post-translational modifiziertes Peptid, welches sehr aktiv gegen Gram-positive Bakterien ist und schon seit langem in der Lebensmittelindustrie als Konservierungsmittel eingesetzt wird. Einige Human Pathogene haben auch gegen Lantibiotika Resistenzmechanismen entwickelt. Ein Operon mit einem drei Komponenten ABC-Transporter wurde auch in *Clostridium difficile* (*C. difficile*) gefunden. Dieser ABC-transporter, CprABC, ist charakterisiert und es wurde herausgefunden, dass er Resistenz gegenüber mehreren Lantibiotika, wie Subtilin, Nisin und Gallidermin vermittelt. Auch ein zwei-komponenten System mit einem Responseregulator, CprR, und einer Histidinkinase, CprK konnte in *C. difficile* identifiziert werden. Bei näherer Betrachtung dieses Resistenzsystems wurde ein Lipoprotein entdeckt, welches direkt vor dem CprABC Transporter kodiert ist. Ein Vergleich dieses Operons mit anderen bekannten Resistenzsystemen zeigte, dass das Lipoprotein CD1348 ähnlich zu dem Immunitätsprotein NisI aus *Lactococcus lactis* (*L. lactis*) und dem Resistenzprotein Nsr aus *Streptococcus agalactiae* (*S. agalactiae*) sein könnte.

In dieser Arbeit wurde das CD1348 Protein aus *C. difficile* charakterisiert, es sollte die Funktion und die Struktur gelöst werden. Mit der in dieser Arbeit etablierten Reinigung des Proteins konnten NMR und SAXS Messungen zur Ermittlung der Richtigkeit des errechneten Modells durchgeführt werden. Mit *in vivo* Studien in *L. lactis* und *in vitro* Interaktionsstudien mit unterschiedlichen Lantibiotika sollte die Funktion geklärt werden. Es konnte jedoch bisher keine Resistenzfunktion in *L. lactis* Zellen ermittelt werden.

Außerdem wurde in dieser Arbeit ein Antibiotika- und Lantibiotika-resistenter *L. lactis* Stamm mit Wachstumsinhibitionsstudien und einer Lipidanalyse näher charakterisiert.

Durch die Analyse der Lipide konnte nicht nur die Lipidzusammensetzung des resistenten Stamms, sondern auch die des originalen *L. lactis* Stamms ermittelt werden, welche bis heute nicht bekannt war.

Zusätzlich wurde eine Reinigung von sekretiertem viralen Infektionsfaktor Protein von HIV-1, welches in *Escherichia coli* (*E. coli*) exprimiert wurde, versucht zu etablieren.

Table of Contents

Abstract iv
Zusammenfassung v
Table of Contents vii
List of figures ix
List of tables x
Abbreviation xi
1. Introduction 1
1.1. Antibiotics 1
1.2. Cell wall synthesis as target of antibiotics 2
1.3. Antibiotic resistance 6
1.4. Antimicrobial peptides 7
1.5. Bacteriocins 8
1.6. Lantibiotics and their classification 9
1.7. Nisin 12
1.8. Lantibiotic resistance 13
1.8.1 Cell wall modification 14
1.8.2 Cell membrane modification 15
1.8.3 Lantibiotic Resistance Operons 16
1.9. ABC-transporter of lantibiotic resistance 17
1.10. Membrane associated proteins of lantibiotic resistance 19
1.11. Retroviruses 21
1.12. Human immunodeficiency virus (HIV) 22
1.13. Accessory proteins of HIV 22
1.14. Viral infectivity factor 24
2. Aims 26
3. Publications 27
3.1. Chapter I - Insight into Two ABC Transporter Families 28
3.2. Chapter II - Lantibiotic maturation complex 39
3.3. Chapter III - CD1348 lipoprotein from *Clostridium difficile* 66
3.4. Chapter IV - Lipid composition of *Lactococcus lactis* 102
3.5. Chapter V - Viral infectivity factor of HIV 142

4. General Discussion 167
4.1. Potential function of CD1348 167
4.2. Potential substrates of CD1348 174
4.3. Lipid composition of *L. lactis* 178
5. Literature 183
6. Curriculum vitae 198
7. List of Publications 200
8. Acknowledgment 201
9. Declaration 205

List of figures

Figure 1: Targets of different known antibiotic classes. 2
Figure 2: ß-Lactams. 3
Figure 3: Glycopeptides and Lipodepsiglycopeptides. 4
Figure 4: Structure of lipid II. 5
Figure 5: Structure of bacteriocins from Gram-negative and Gram-positive bacteria. 8
Figure 6: The four classes of lanthionine-generating enzymes. 10
Figure 7: Representative examples of lantibiotic classes. 11
Figure 8: Mode of action of nisin. 12
Figure 9: Mechanism of lantibiotic resistance. 14
Figure 10: Overview of the lantibiotic resistance operons belonging to the Lan- and Bce-type systems. 18
Figure 11: Cartoon representation of crystal structures of NisI and *Sa*Nsr and NMR structures of SpaI and MlbQ. 20
Figure 12: HIV-1 genome. 22
Figure 13: Complex formed by the Vif protein. 24
Figure 14: Functional domains of the Vif protein. 25
Figure 15: Amino acid NCBI blast of CD1348. 168
Figure 16: Cartoon representation of crystal structures of NisI and *Sa*Nsr and NMR structures of SpaI and model structure of CD1348. 169
Figure 17: Structures of CD1348 and two example structures from the structural blast... 171
Figure 18: Structure alignment of CD1348 and SMU.848. 173
Figure 19: Potential substrates of CD1348 compared to nisin. 176

List of tables

Table 1: Result of EBI structure blast of CD1348. 170
Table 2: Comparison of immunity protein NisI, resistance protein *Sa*Nsr and the potential resistance protein CD1348. 174
Table 3: Different bacteriocins produced by various *Clostridia* species. 175
Table 4: Phospholipid composition of three different used expression systems. 180

Abbreviation

ABC	ATP-binding cassette
ADP	adenosine-5-diposhpate
AMP	antimicrobial peptide
APOBEC3	apolipoprotein B mRNA editing enzyme catalytic polypeptide-like 3
ATP	adenosine-5-triphosphate
B. cereus	*Bacillus cereus*
B. subtilis	*Bacillus subtilis*
C. difficile	*Clostridium difficile*
CL	cardiolipin
Dha	dehydoalanine
Dhb	dehydroaminobutyric acid
DNA	deoxyribonucleic acid
HIV	human immunodeficiency virus
HK	histidine kinase
IMAC	immobilized metal ion affinity chromatography
K_D	dissociation constant
kDa	kilo Dalton
Lan	lanthionine
L. lactis	*Lactococcus lactis*
LTA	lipoteichoic acid
MALS	multi-angle light scattering
mM	milli molar
MRSA	methicillin-resistant *Staphylococcus aureus*
NBD	nucleotide binding domain
Ni	Nickel
nm	nano meter
nM	nano molar
NMR	nuclear magnetic resonance
NTA	nitrilotriacetic acid
PBP	penicillin-binding protein
PC	phosphatidylcholine
PE	phosphatidylethanolamine

PG	phosphatidylglycerol
PS	phosphatidylserine
µM	micro molar
RNA	ribonucleic acid
S. agalactiae	*Streptococcus agalactiae*
S. aureus	*Staphylococcus aureus*
SAXS	small-angle X-ray scattering
SEC	size exclusion chromatography
S. mutans	*Streptococcus mutans*
TCS	two-component signalling system
TLC	thin layer chromatography
TMD	transmembrane domain
Vif	viral infectivity factor
VRE	vancomycin-resistant *Enterococci*
VRSA	vancomycin-resistant *Staphylococcus aureus*
WTA	wall teichoic acid

Amino acid	**three letter code**	**one letter code**
Alanine	Ala	A
Arginine	Arg	R
Asparagine	Asn	N
Aspartic acid	Asp	D
Cysteine	Cys	C
Glutamic acid	Glu	E
Glutamine	Gln	Q
Glycine	Gly	G
Histidine	His	H
Isoleucine	Ile	I
Leucine	Leu	L
Lysine	Lys	K
Methionine	Met	M
Phenylalanine	Phe	F
Proline	Pro	P
Serine	Ser	S
Threonine	Thr	T
Tryptophan	Trp	W
Tyrosine	Tyr	Y
Valine	Val	V

1. Introduction

1.1. Antibiotics

In 1928 Alexander Flemming discovered penicillin and since then antibiotics became important for human health [1; 2]. Antibiotics are used for treatment of bacterial infections and resulted in an increased human life expectancy [2]. For example due to the usage of antibiotics the mortality rate by tuberculosis (50%) decreased [3]. Twenty antibiotic classes were discovered in between 1930 and 1962, for example in 1932 sulfonamides and in 1959 kanamycin [4; 5], since then only a few more classes were discovered. The antibiotics which reached the market meanwhile, are modifications of already known antibiotics like amoxicillin which is based on penicillin [3; 6]. Antibiotics are classified by their cellular component or target system. Beside this a separation in bactericidal and bacteriostatic drugs is possible. Bactericidal drugs induce cell death, whereas bacteriostatic drugs inhibit cell growth [7]. In general antibiotics can be distinguished due to their mode of action [5]. The four main targets of antibiotics are shown in Figure 1: nucleic acid synthesis (I), protein synthesis (II), metabolic pathway (III) and the cell wall synthesis (IV).

Nucleic acid synthesis (Figure 1) is one target of different antibiotics, for example quinolones, which are interacting with the nucleic acids synthesis machinery [8]. Quinolones bind to the DNA gyrase and topoisomerase IV, thereby inhibiting the bacterial DNA replication resulting in bacterial cell death [2; 9; 10; 11].

The protein synthesis (Figure 1) is also a target of antibiotic classes like chloramphenicol [2]. Chloramphenicol is highly specific in binding the peptidyl transferase of the 50S ribosomal subunit of the 70S ribosome (Figure 1) and by this inhibiting the peptide chain elongation. Chloramphenicol is active against Gram-positive as well as Gram-negative bacteria [12; 13; 14].

Sulfonamides are part of the antibiotics impacting the metabolic pathway as they inhibit the folate synthesis (Figure 1) [5]. The inhibition of folate synthesis results in a hindrance of replication of the bacterial cells as cells are no longer able to produce nucleotides [15].

The cell wall synthesis (Figure 1) of bacteria is a major target for antibiotics [16]. The first discovered antibiotic penicillin is part of the ß-lactam group which influence the cell wall synthesis of bacteria [17]. Glycopeptides, especially vancomycin and teicoplanin are used in clinical trials for their high potential against Gram-positive pathogens.

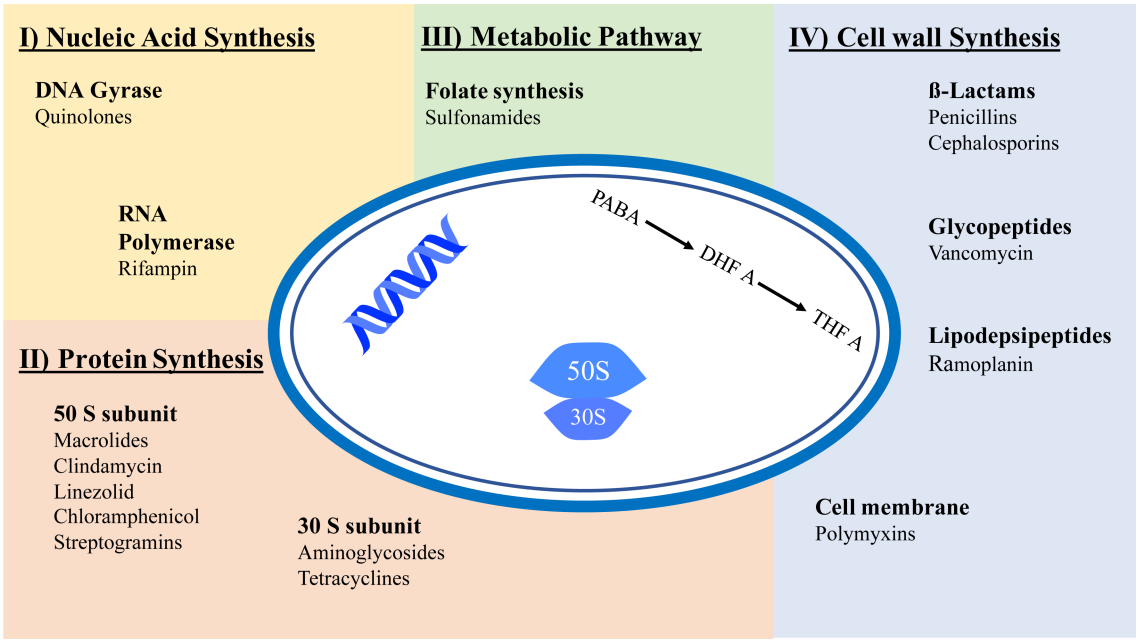

Figure 1: Targets of different known antibiotic classes.
A schematic bacterial cell is shown containing DNA, ribosome subunits, cell wall and the folate synthesis. There are antibiotics targeting the metabolic pathway like sulfonamides, some targeting the nucleic acid synthesis like quinolones, some are targeting protein synthesis like chloramphenicol and some are targeting the cell wall synthesis, like penicillin. Based on [5; 8].

Lipodepsiglycopeptides are a third group targeting the cell wall. Ramoplanin, a member of this group, is a good candidate for treatment against the human pathogen *Clostridium difficile* (*C. difficile*) [18; 19]. These antibiotics are highly specific targeting cell wall synthesis of bacteria [2; 16]. All in all, there are different antibiotics influencing the cell syntheses pathways. In the following chapter (1.2) antibiotics targeting the cell wall synthesis are described more in detail.

1.2. Cell wall synthesis as target of antibiotics

As mentioned in section 1.1 cell wall synthesis is an important target of different antibiotics. Three prominent antibiotic classes targeting cell wall synthesis are the ß-lactams, the glycopeptides and the lipodepsipeptides [2; 16]. ß-Lactams are one large group of antibiotics. They were the first discovered antibiotic group containing penicillin [1; 17; 20; 21]. All members of the ß-lactam family contain a ß-lactam ring within their molecular structure, like penicillin, cephalosporins and carbapenems [20; 21]. The difference between antibiotics of the ß-lactam group are the specific chemical structures. While penicillins contain a 6-aminopenicillanic acid, cephalosporins have a cephalosporin ring. There are varying penicillins known and synthetically developed, the only difference between these is

the chemical site group R (Figure 2) [3; 17; 21]. Cephalosporins and carbapenems are also members of the ß-lactam antibiotic family and can also have different site groups resulting in diverse antibiotic names [21].

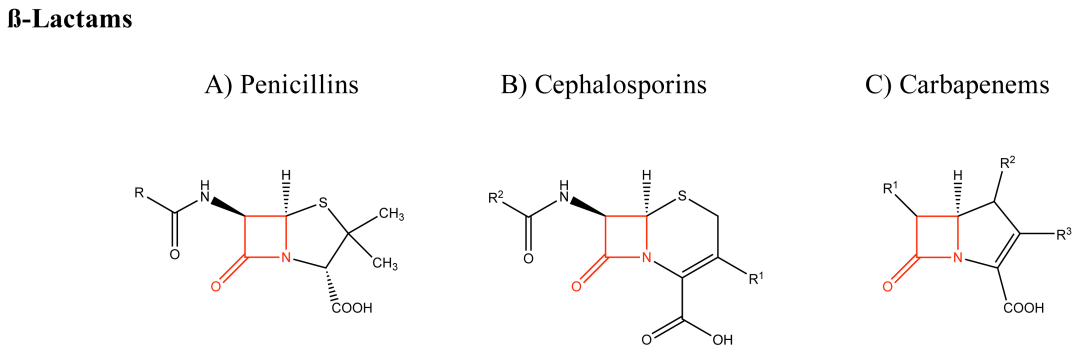

Figure 2: ß-Lactams.
Three different ß-lactam classes and their basic structure are shown. All classes penicillins, cephalosporins and carbapenems contain the ß-lactam ring depicted in red. Based on [21].

The mode of action of ß-lactam antibiotics is to inhibit the cell wall synthesis. ß-Lactams bind to the so-called penicillin-binding protein (PBP). Binding to the PBP results in inhibition of the crosslinking of peptidoglycans, and by this inhibiting transpeptidation in the bacterial cell wall. The inhibited transpeptidation causes a weakened cell wall and results in cell death due to the build-up osmotic pressure [20; 22; 23].

Glycopeptides are antibiotics produced by actinomycete, synthesized by non-ribosomal peptide synthase [16]. They contain unique tricyclic or tetracyclic heptapeptide cores [24]. Glycopeptides find clinical use in the treatment of bacterial infection caused by Gram-positive bacteria, *Staphylococci*, *Enterococci* and *Clostridia* [25]. The first discovered glycopeptide was vancomycin produced in the secondary metabolite by a soil bacteria *Streptomyces orientalis* discovered in 1950 [26; 27]. Vancomycin and teicoplanin, produced by *Actinoplanes teichomyceticus*, are the two glycopeptides used in clinical treatment (Figure 3) [2; 26].

Glycopeptides

Vancomycin

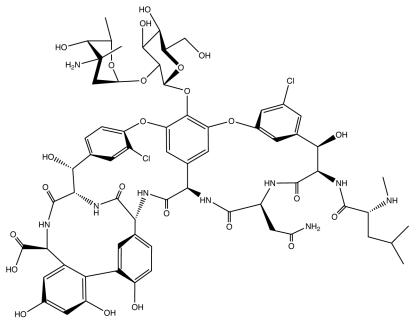

Teicoplanin

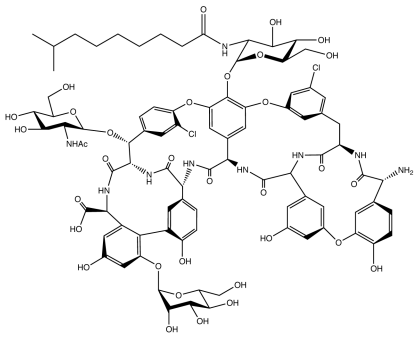

Lipodepsiglycopeptides

Ramoplanin

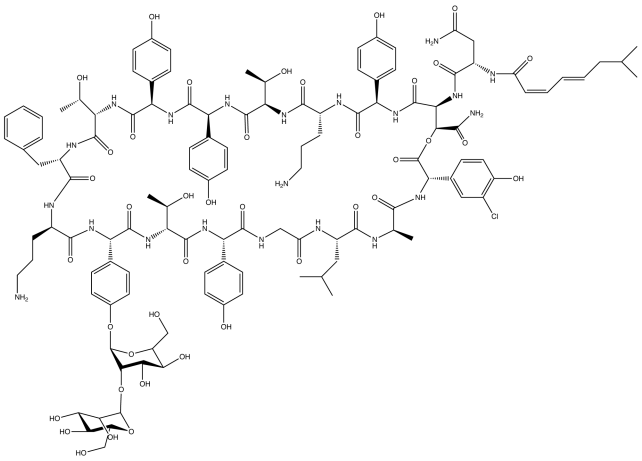

Figure 3: Glycopeptides and Lipodepsiglycopeptides.
Structure of the two main glycopeptides in clinical use vancomycin and teicoplanin. Beneath, the structure of one lipodepsiglycopeptide, ramoplanin A2, is shown. Based on [16].

Vancomycin was called “drug of last resort” for a long time, because of the use in treatment of the methicillin-resistant *Staphylococcus aureus* (MRSA) strain, one main reason for hospital-acquired infections [25]. The mode of action of glycopeptides is the inhibition of extracellular steps of peptidoglycan synthesis. They are interacting with the D-Ala-D-Ala terminus of the uncross-linked peptidoglycan pentapeptide. In detail, the glycopeptides interact with the D-Ala-D-Ala dipeptide via five hydrogen bonds. This eventuates in an inhibition of the transpeptidation and transglycosylation [27]. Due to steric hindrance, the formed complex is shielding the peptidoglycan from the penicillin-binding protein.

Lipodepsiglycopeptides are naturally derived and have antibacterial activity. They are short oligopeptides (up to 25 amino acids) with an N-terminal acylated fatty acid moiety (Figure 3) [16; 28]. One of the most prominent lipodepsipeptides is ramoplanin, isolated from *Actinoplanes sp.* ATCC 33076 as a mixture of three closely related compounds [16; 28; 29].

The fatty acid substituents, which are bound to the identical heptadecapeptide ring are the differing elements of the compounds [16; 30; 31].

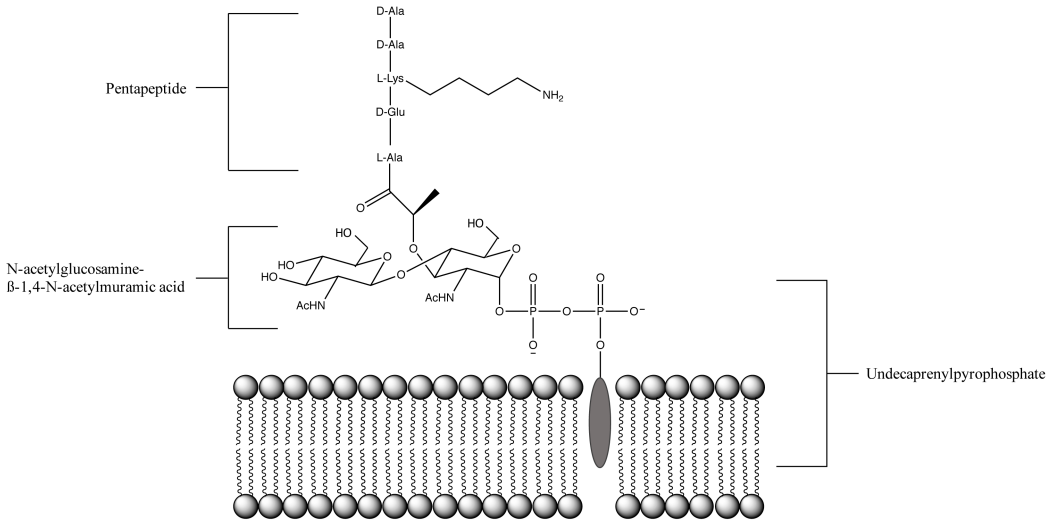

Figure 4: Structure of lipid II.
Lipid II is made up of an N-acetylglucosamine-ß-1,4-N-acetylmuramic acid disaccharide, connected to a undecaprenylpyrophosphate. The undecaprenyl membrane anchor is depicted as grey oval in the membrane. The muramic acid contains a pentapeptide with a lysine necessary for later cross-linking. Based on [32; 33].

Ramoplanin is combined of three different variants A1, A2 and A3. The most prominent variant is A2 which shows activity against a broad spectrum of Gram-positive pathogens (Figure 3). Ramoplanin is a promising candidate in treatment of the multi-resistant pathogen *C. difficile*, causing infections in the gastrointestinal tract resulting in a chronical disease and inflammation of the colon [19; 30]. It could be shown that ramoplanin binds to the cell wall precursor lipid II (Figure 4) and inhibits the peptidoglycan synthesis. Ramoplanin is binding to the pyrophosphate and the first sugar unit muramic acid (MurNAc) of lipid II, in a stoichiometric complex of 2:1 [31; 34; 35].

Although antibiotics are useful antagonists for bacterial infections, bacteria find adaptions resulting in resistance.

1.3. Antibiotic resistance

Since the first discovered antibiotic, antibiotic resistance has become a rising problem. Bacteria were able to develop varying mechanisms to bypass different antibiotics [2; 8; 16; 36]. Some developed resistance mechanisms are active efflux (I), inactivation via an enzyme (II) and modification of the drug target (III) [2; 36]. In general, the developed mechanisms are multifunctional and inhibit not only the activity of one antibiotic.

(I) The active removal of antibiotics is one resistance mechanism performed by different cells. One of the most important groups is the resistance-nodulation-cell division (RND) class [36; 37]. Well studied members are the AcrAB-TolC from *Escherichia coli* (*E. coli*) [38] and MexAB-OrpM from *Pseudomonas aeruginosa* [39].

(II) Antibiotic resistance performed by inactivation of antibiotics via enzymes are also described. The first described bacterial enzyme rising the penicillin resistance was the AmpC ß-lactamase [40]. ß-Lactamases are the most widespread resistance enzymes and have a high clinical importance [36]. ß-Lactamases are classified based on their amino acid sequences and functionality. ß-Lactamases can be divided in four classes (class A-D), which are based on the sequence similarity [41]. The classes A, C and D are so-called serine-ß-lactamases and group B are metallo-ß-lactamases [17; 42; 43]. Depending on whether they are serine- or metallo-ß-lactamase, they perform different chemical mechanisms to inactivate the ß-lactams. The serine-ß-lactamases need a catalytic serine, while the metallo-ß-lactamases need zinc ions for initiate the ß-lactam hydrolysis. Both mechanisms are targeting the ß-lactam centre and inactivate the ß-lactam through opening the ß-lactam ring [17; 36].

(III) Modification of the antibiotic target is another way to perform resistance in the bacterial cell. In fluoroquinolone resistant cells, resistance is created by a single mutation in the target genes *gyrA* or *gyrB* [36; 44; 45]. A short DNA sequence in these genes is known as quinolone resistance-determining region (QRDR). The mutation in this QRDR is resulting in an amino acid substitution and alters a structural change of the target protein of fluoroquinolone. As a consequence of this structural change the binding affinity of fluoroquinolone is decreased and results in a drug resistance [46]. Beside this mechanism, modifications in the 23S rRNA via the enzyme erythromycin ribosome methylation (Erm) are known to perform resistance against antibiotics like erythromycin [36; 47; 48]. The modification of the pentapeptide of the peptidoglycan is known to perform resistance against glycopeptides like vancomycin and teicoplanin. As vancomycin binds specific to the D-Ala-D-Ala pentapeptide and is highly active against Gram-positive bacteria, it was used for antibiotic resistant bacteria. Bacteria

come up with a change of the pentapeptide to a D-Ala-D-Lac or D-Ala-D-Ser. This change implies a 1000-fold lesser activity of vancomycin, as one single hydrogen bond is missing [16; 27; 49]. This modification in the peptidoglycan is a result of *van* operons. The proteins VanA, VanB and VanD are creating the D-Ala-D-Lac depsipeptide mutation, VanC, VanE and VanG proteins result in the D-Ala-D-Ser pentapeptide mutation [26; 49]. Resistance to the glycopeptides, vancomycin and teicoplanin are discovered in different Gram-positive bacteria: *Enterococcus, Erysipelothrix, Lactobacillus, Leuconostoc, Pediococcus* and *Staphylococcus*. The most prominent cells, having this resistance, are the vancomycin-resistant *Enterococcus* (VRE) and vancomycin-resistant *Staphylococcus aureus* (VRSA) [50; 51]. Also, a modification of the PBP can raise antibiotic resistance against ß-lactams. The ß-lactam is unable to bind to the altered PBP and consequently is less effective against the cell wall synthesis. The MRSA strain is the most prominent candidate creating this change. This strain generated a resistance against methicillin, a penicillin containing a big steric group at the penicillin backbone [20; 52]. Developing varying mechanisms against nearly all antibiotics rise the need for new antimicrobial agents against human pathogens.

1.4. Antimicrobial peptides

Since antibiotic resistance became a global health problem the need for new antimicrobial agents rises. Antimicrobial peptides (AMPs) are a promising group of new antimicrobial treatment [53; 54]. AMPs are a conserved component of the innate immune response in all organisms. All domains of life produce these kinds of peptides [55; 56; 57]. Alexander Flemming discovered the first AMP, lysozyme in 1922 [58]. Another early discovered AMP was nisin in 1928, which is produced by *Lactococcus lactis* (*L. lactis*) [59; 60]. Since then hundreds of AMPs have been discovered and it will become more in future. AMPs are defined as short (< 60 amino acids) overall positively charged (generally +2 to +9) amphipathic molecules. They have a broad antimicrobial spectrum and can have different mode of actions [61; 62; 63]. AMPs are active against nearly all organisms. They are antibacterial against Gram-positive and Gram-negative bacteria, antifungal against for example *Candida albicans* [64], antiparasitic against e.g. *Leishmania* [65] and also antiviral against for example human immunodeficiency virus (HIV-1) [62; 66]. Typically, AMPs mediated killing of microorganisms is performed via membrane permeation. The permeation can be catalysed by membrane-disruption or membrane-interaction resulting in pore formation [67]. Separated from this kind of membrane-disruptive peptides also non-

membrane disruptive peptides have been discovered. These peptides are able to interact with nucleic acids, protein synthesis and translation [68; 69]. There are numerous of classifications of the AMPs like biological source, functions and peptide properties [61; 70]. The most prominent classification is based on the three-dimensional structure. AMPs can be divided in four major classes: ß-sheet, α-helical, loop and extended peptides [55; 71; 72]. The first two mentioned classes are most common in nature.

1.5. Bacteriocins

AMPs produced by bacteria are called bacteriocins. Bacteriocins have a broad spectrum of activity, killing other related bacteria and also killing non-related ones [73]. Nisin is one of the best characterized bacteriocins and has been used in food industry the past 50 years [53]. Bacteriocins can be classified in Gram-positive produced bacteriocins and Gram-negative produced once [74]. In Gram-negative produced are colicins and microcins [74]. Colicins are antibacterial proteins, which can kill cells closely related to the producer strain. Colicins are organized in three domains, an N-terminal translocation domain, a central receptor-binding domain and a C-terminal cytoxic domain (Figure 5) [74; 75; 76]. Microcins are ribosomal synthesized hydrophobic antimicrobial peptides of low molecular weight (< 10 kDa). They are post-translational modified and produced as precursor peptides with an N-terminal leader peptide [74; 77; 78].
Bacteriocins of Gram-positive bacteria are classified in three classes, the lantibiotics, the non-lantibiotics and the bacteriolysins [53; 79].

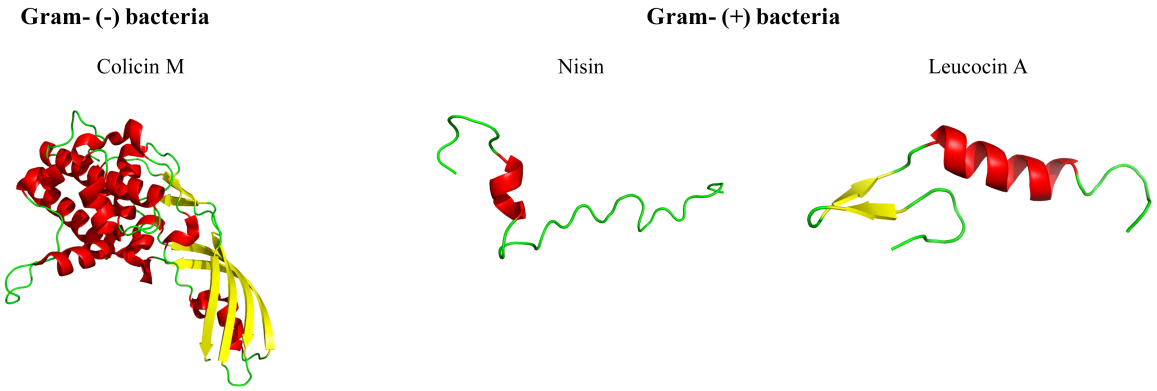

Figure 5: Structure of bacteriocins from Gram-negative and Gram-positive bacteria.
The crystallography structures of the bacteriocins colicin M (PDB code: 2XMX) from *E. coli*, NMR structure of nisin (PDB code: 1WCO) from *L. lactis* and the NMR structure of leucocin A (PDB code: 1CW6) from *Leuconostoc gelidum*.

Class I bacteriocins the lantibiotics are post-translational modified small membrane active peptides < 5 kDa big. They contain dehydrated amino acids and methyl- and lanthionine rings. Lantibiotics can be linear or globular peptides and are named based on the typical lanthionine rings, lanthionine containing antibiotics, lantibiotics. Nisin, subtilin and gallidermin are examples of this bacteriocin class. They are interacting with the membrane and can perform pore formation in a nanomolar range [80; 81; 82].
Class II bacteriocins are non-lanthionine unmodified peptides containing 30 - 60 (< 10 kDa) amino acids. Typical for the class II bacteriocins is the heat tolerance of these peptides. They are unmodified non-lanthionine containing peptides and positively charged. Class II bacteriocins are inducing the membrane permeabilization and they are also active in a nanomolar range [53; 74; 79]. Members of this bacteriocin class are leucocin A, lactacin F and reuterin 6 [79].
Class III bacteriocins are, in comparison to the other bacteriocins, large (> 30 kDa) heat labile antimicrobial proteins. They are subdivided in two groups. The group A, like enterolisin A which lysis the cell resulting in cell death. The group B like caseicin 80 belongs to the non-lytic proteins [53; 74; 79].

1.6. Lantibiotics and their classification

Lantibiotics are small ribosomal synthesized peptides. Lantibiotics are containing thioether cross links, which are installed with the help of the post-translational enzymes. The dehydration of serine or threonine forms the typical dehydrated amino acids like 2,3-didehydroalanine (Dha) and 2,3-didehydrobutyrine (Dhb). By a followed Michael-type addition of a neighboured cysteine thiol, resulting in the thioether bridges called methyl- and lanthionine rings [33; 83; 84]. These rings are related to the name of the lantibiotics, they are lanthionine containing antibiotics. Depending on the post-translational modification enzymes, four classes can be distinguished [32; 83; 84].

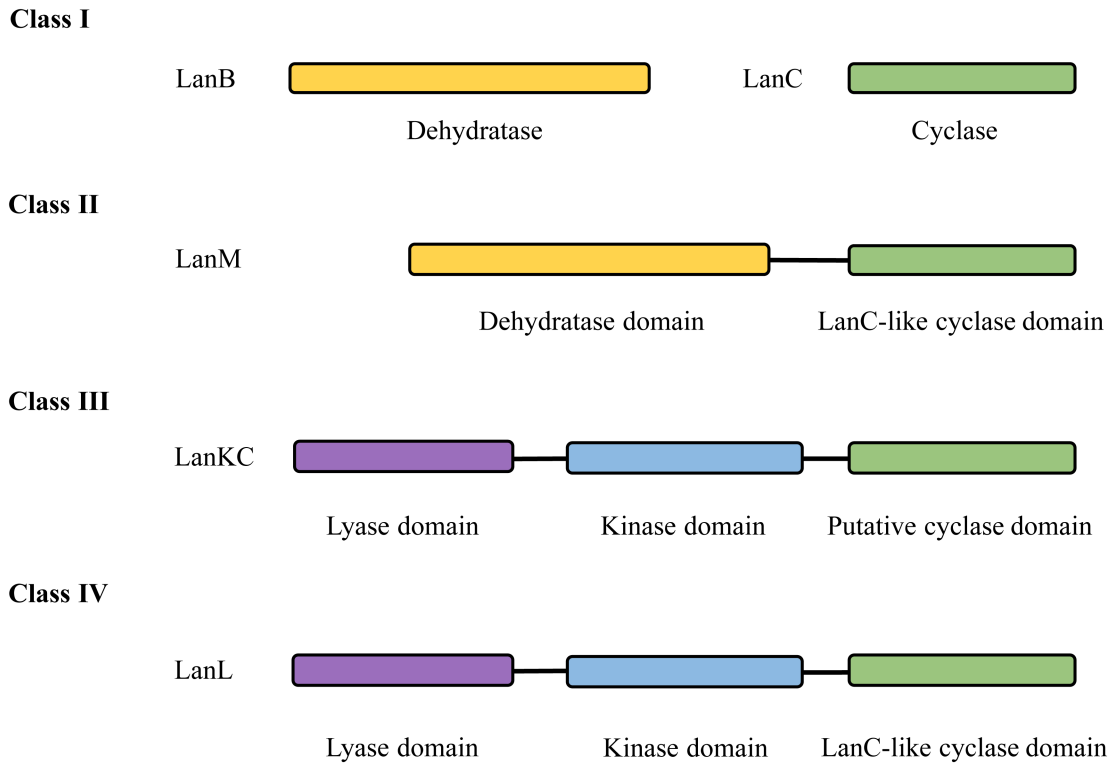

Figure 6: The four classes of lanthionine-generating enzymes.
Class I is characterized by two modification enzymes LanB and LanC. LanB is a dehydratase and LanC a cyclase. Class II contains one modification enzyme LanM, that includes a dehydratase and a LanC-like cyclase domain. Class III contains one modification enzyme with three distinct catalytic domains. A N-terminal lyase domain followed by a kinase domain and an C-terminal cyclase domain, lacking the LanC typical zinc binding motif. Class IV is mainly homolog to the class III enzyme. The difference is that the cyclase domain contains the zinc binding motif. Based on [83].

The operons of class I lantibiotics contain two modification enzyme families, the LanB and LanC (Figure 6) [32; 33; 85]. The LanB enzyme family (dehydratase) dehydrates serine and threonine and generates dehydrated amino acids, didehydroalanine (Dha) and didehydrobutyrine (Dhb) [86; 87]. The LanC enzyme family (cyclase) forms thioether bridges between the dehydrated amino acids and the thiol group of a neighbouring cysteine [88]. So lantibiotic characteristic (methyl-) lanthionine rings are formed [33; 84]. A zinc binding motif is characteristic for this enzyme family [88; 89]. Nisin, subtilin and gallidermin are members of class I lantibiotics (Figure 7) [32].

Class II lantibiotics contain a bifunctional synthetase LanM, which combines the dehydration and the cyclization reaction [32; 83]. LanM consists of an N-terminal dehydratase and a C-terminal cyclase domain. The dehydratase domain shows no homology to the LanB family while the C-terminal domain has 25% sequence similarity to LanC [83]. The cyclase domain also contains the zinc binding motif, like LanC. The most prominent members of this family are cinnamycin, lacticin 481 and mersacidin, which are showing antimicrobial activity against Gram-positive bacteria like all members of this class (Figure 7).

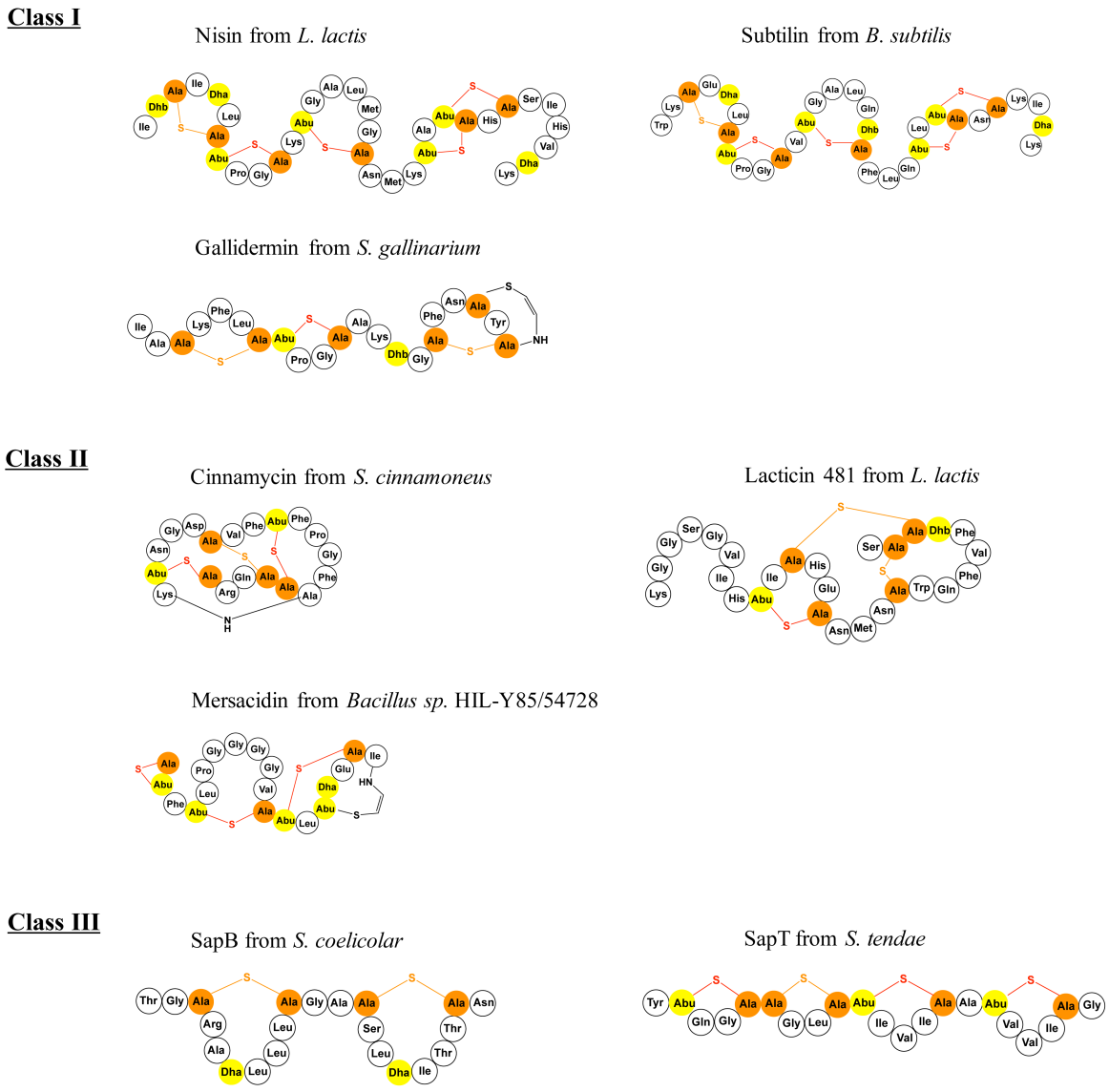

Figure 7: Representative examples of lantibiotic classes.
Class I structural examples of nisin, subtilin and gallidermin. Class II cinnamycin, lacticin 481 and mersacidin are chosen as examples of this class of lantibiotics. Class III the structure of SapB and SapT are shown. The dehydrated amino acids and the cysteines of the lantibiotics are highlighted in yellow and orange. The (methyl-) lanthionine rings are visualized in orange and red. Based on [32].

The first discovered class III lantibiotic was SapB containing two lanthionine rings and is produced by *Streptococcus coelicolar* [90]. These class III lantibiotics contain a LanKC modification enzyme. Distinct to the other classes enzyme LanKC contains three different domains, a lyase domain, a kinase and a cyclase domain (Figure 6). Interestingly the cyclase domain is lacking the zinc binding motif, which is unique for the lantibiotic modification enzymes [32]. SapB and SapT are the best-known members of this class (Figure 7). This kind of lantibiotics do not show an antimicrobial activity [83]. Since 2010 a fourth class of lantibiotics is known. The venezuelin was discovered in *Streptomyces venezuelae* [83; 91]. Like class III lantibiotics the modification enzyme is a tri-functional enzyme with a lyase, a

kinase and a cyclase domain. But different to the class III, the class IV cyclase domain contains the zinc binding motif (Figure 6) [83; 92].

1.7. Nisin

Nisin is one of the most studied and best characterized lantibiotics. It was discovered in 1928 and is produced by some *Lactococcus lactis* and *Streptococcus uberis* strains [59; 60; 93]. Nisin is an amphipathic molecule with a long hydrophobic N-terminal part and a short hydrophilic C-terminal part [94; 95]. It shows a broad antimicrobial activity and is active against several Gram-positive bacteria, like *Staphylococci*, *Streptococci*, *Bacilli* and *Enterococci*. The 3D solution structure of nisin was solved in 1991 via NMR [96]. Nisin can be divided in three regions, the N-terminal part containing the (methyl-) lanthionine rings A, B and C followed by the flexible hinge region and the C-terminal part containing the two intertwined rings D and E and the last six amino acids [97; 98]. Nisin has at least two main modes of action [99].

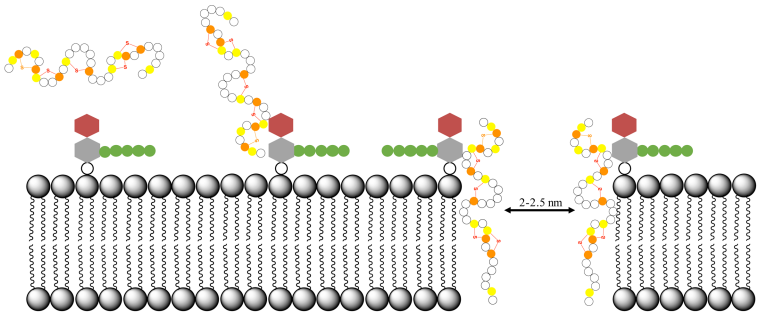

Figure 8: Mode of action of nisin.
First nisin binds with rings A and B to the diphosphate moiety of lipid II. By increased concentration of nisin a nisin-lipid II complex is formed and with the flexible hinge region nisin is able to insert the C-terminal part in the cytoplasmic membrane. Due to the nisin-lipid II complex containing eight nisin molecules and four lipid II molecules pores are formed. This build pore has a 2-2.5 nm diameter and leads to cell death. Based on [100].

First, it is able to bind to the peptidoglycan precursor molecule lipid II (Figure 8). Nisin binds via the first two (methyl-) lanthionine rings (A and B) to the diphosphate moiety of lipid II [101; 102]. The binding to the diphosphate moiety was determined via NMR in 2004 [101]. Because of this, the transglycosylation is blocked and the cell wall synthesis is inhibited [99]. Second, if the concentration of nisin increases to a certain threshold nisin forms a complex with lipid II [102]. Via the flexible hinge region and the two last rings nisin is able to flip into the membrane including pore formation (Figure 8) [99; 101; 103; 104]. This complex consists of eight nisin and four lipid II molecules with a diameter of 2 - 2.5 nm [102]. The pore results in the release of essential ions and small nutrients leading to cell death based on a collapse of the membrane potential [102]. Due to the pore formation nisin is highly active in nanomolar range [105].

1.8. Lantibiotic resistance

Lantibiotics are highly effective against several bacteria with the major targets cell wall and membrane. But like for antibiotics, bacteria are able to develop different resistance mechanisms against lantibiotics. Varying resistance mechanisms are known: Cell membrane and cell wall can be modified and also resistance operons containing a two-component system and an active transporter are known to perform resistance [67; 106; 107; 108; 109]. In the following parts the different resistance mechanisms are explained. In Figure 9 the resistance mechanisms are depicted. Some bacteria have a mixture of these resistance mechanisms.

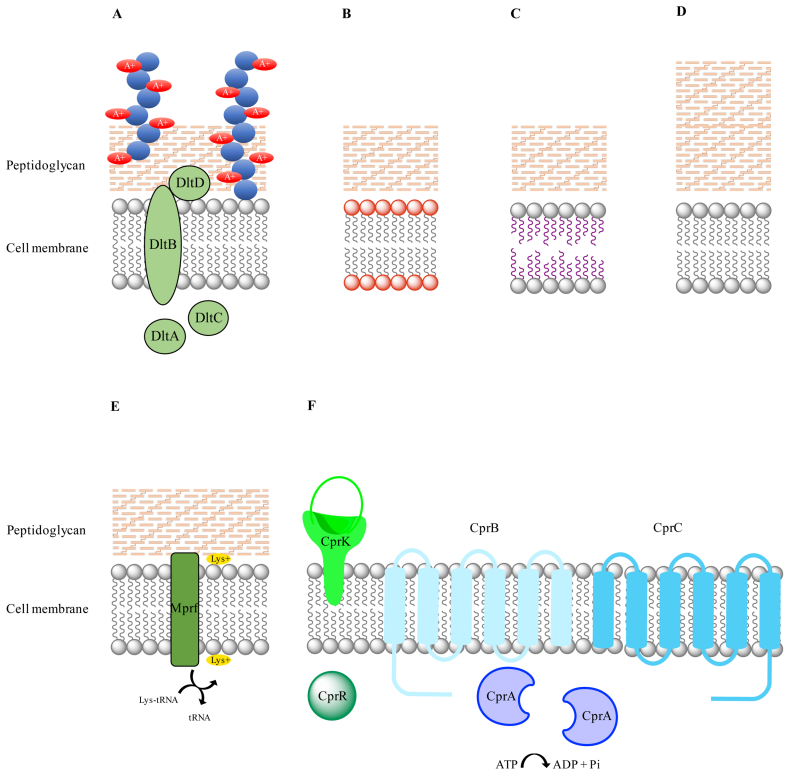

Figure 9: Mechanism of lantibiotic resistance.
A) D-alanylation of lipoteichoic acids (LTA) and wall teichoic acids (WTA) is performed via the *dltABCD* operon. Based on the change of the cell wall charge; the net charge is less negative and the lantibiotic cannot interact with the cell wall anymore. **B)** Phospholipid composition is changed and the interaction of lantibiotics is inhibited. **C)** Membrane fatty acids are changed and the membrane fluidity is reduced. **D)** A thicken cell wall can also result in lantibiotic resistance. **E)** Lysine esterification of phosphatidylglycerol (PG) by MprF, changes the negatively net charge. **F)** Resistance mechanism via a two-component system and an ABC-transporter. The two-component system is depicted in green, the histidine kinase (light green) and the response regulator (dark green) form the two-component system. The ABC-transporter is highlighted in blue. The nucleotide binding domain (dark blue) and the two transmembrane domains (light blue and cyan). As an example, the resistance system of *Clostridium difficile* is depicted. Based on [106].

1.8.1 Cell wall modification

The cell wall of Gram-positive bacteria in general contains a thick peptidoglycan structure. Additionally, teichoic acids are present polymers of phosphate and alditol. There are two different kinds of teichoic acids, the wall teichoic acids (WTAs) and the lipoteichoic acids (LTAs). The difference between these two groups is the binding position. While WTAs are binding to the muramic acids of peptidoglycan via phosphodiester, the LTAs are binding to the membrane glycolipid [110; 111]. A cell wall has a negative net charge generated by different phospholipids and the teichoic acids [112]. This negative net charge attracts the positive charged lantibiotics. Lantibiotics cannot interact with the cell wall if the net charge is changed. One known mechanism of bacteria to change the net charge of the cell wall is the *dlt* (D-alanyl-lipoteichoic acid) operon. This operon was characterized in many different species, e.g. *Staphylococcus, Streptococcus, Clostridium* and *Bacillus* and it contains four different genes *dltABCD* (Figure 9 A) [113; 114; 115; 116; 117; 118]. These genes are

responsible for the D-alanine esterification or D-anylation of the LTAs and the WTAs. The D-anylation reduces the negative charge by adding more positive charges to the teichoic acids cell wall and hinders the lantibiotic to interact [119].
Another reason for lantibiotic resistance can be the penicillin-binding protein (PBP). The PBP is also important for lantibiotic resistance instead of only antibiotic resistance [120]. Some strains which have an increased PBP expression show resistance against lantibiotics, like *Listeria monocytogenes* (*L. monocytogenes*) and *L. lactis* IL1403 [121; 122].

1.8.2 Cell membrane modification

Lantibiotic resistance can also be developed by changing the membrane composition which consists of different phospholipids. The composition is different between the different species, and can also vary under growth conditions and the growth phase. One of the most common phospholipid in bacteria is the phosphatidylglycerol (PG), which has a negatively charged head group [123]. In the different strains the percentage of PG can vary but most of the cells also contain cardiolipin (CL). It is known that nisin penetrates membranes containing a higher cardiolipin concentration more effective than membranes of PG, phosphatidylethanolamine (PE) or phosphatidylcholine (PC) [106]. The composition of the membrane has an important role for lantibiotic resistance. A resistant strain of *L. monocytogenes* Scott A is known which developed a membrane with more PG than CL against nisin (Figure 9 B) [67; 124]. A variation in the fatty acid composition is also able to provide resistance against lantibiotics beside these impacted by the head group of the phospholipids. An increase in saturated fatty acids within the membrane results in a more rigid membrane [67; 125]. Beside this, an increase in long chain fatty acids is known to perform resistance. All these changes result in reduced membrane fluidity and a more rigid membrane (Figure 9 C) [125; 126; 127].
It was discovered that some Gram-positive bacteria developed a way to change the negatively net charge of the membrane without a change of the main phospholipid [67; 128]. They use a lysine esterification of one of the hydroxyl groups of the PG and create a lysyl-phosphatidylglycerol (L-PG). The free amino groups give the PG a positively net charge. The protein which is responsible for this modification is the multiple peptide resistance factor (MprF). MprF is an integral lysyl-phosphatidylglycerol synthetase with two functional domains (Figure 9 E) [129; 130]. A hydrophilic cytoplasmic domain necessary for synthesize of the L-PG and a large hydrophobic domain responsible for the flipping of the

L-PG. Both domains are important for complete resistance as only if the L-PG is located in the outer layer of the membrane the resistance against lantibiotics can be performed [106; 129]. The MprF mediated resistance could be detected in different Gram-positive bacteria like *Staphylococcus aureus* (*S. aureus*) [128; 131], *Bacillus subtilis* (*B. subtilis*) [132], *Mycobacterius tuberculosis* (*M. tuberculosis*) [133].

An additional mechanism to perform resistance against lantibiotics in the membrane modification is the *fab* operon. A decreased expression of this operon results in lantibiotic resistance. Fab is involved in the saturation and elongation in the membrane synthesis. A decreased expression results in a reduced densely packed membrane which influences the ability of the lantibiotic interaction [121; 134].

1.8.3 Lantibiotic Resistance Operons

Expression of membrane or membrane associated proteins lead to a lantibiotic resistance. Lantibiotic resistance operons are containing a two-component system and an ATP binding cassette transporter (ABC-transporter). Based on the different components the two-component systems and the ABC-transporter can be divided in different groups. Various classes are described for the two-component systems (TCSs) while for the ABC-transporters two types are known. As the resistance machinery of Gram-positive bacteria against lantibiotics includes both components there are various options [67; 106; 135].

The two-component system consists mostly of two proteins, a histidine kinase and a response regulator [136]. The histidine kinase acts as sensor of the lantibiotic and is membrane bound. The response regulator mediates the cellular response [137]. A lot of two-component systems are identified in various Gram-positive bacteria. In general, they can be divided in two groups the BceRS like and the LiaRS like two-component systems. The BceRS system was first discovered in *B. subtilis* and is performing resistance against actagardine and mersacidin [138]. It was the first discovered two-component system of this type and is the name giving one. The kinase is missing the characteristic extracellular sensor domain and is called intramembrane sensing kinase [137; 139; 140]. This is a difference to kinases with this extracellular sensory domain, like EnvZ from *E. coli* a kinase of one of the best characterized two-component systems or SpaK from *B. subtilis*. Both are so called periplasmic sensing histidine kinases [135; 141]. The BceRS like kinases are functionally linked to homodimeric ABC-transporter [135; 137].

In contrast, the LiaRS like two-component system from *B. subtilis* is a special two-component system as it contains three proteins. The LiaRS like TCSs are containing the LiaR regulator, the LiaS kinase and the additional protein LiaF acting as a negative regulator of gene expression [142]. Some examples for this special type of two-component system are VraRS of *S. aureus*, LiaRS of *L. monocytogenes* and CeaRS of *L. lactis* [143; 144; 145; 146].

1.9. ABC-transporter of lantibiotic resistance

Some Gram-positive bacteria are able to perform an active resistance mechanism with an ATP binding cassette (ABC) transporter [135]. In general ABC-transporter transport or efflux the lantibiotics out of the cell. ABC-transporter use ATP to drive the transport of the substrate across the membrane. In general they consist of two different domains, the transmembrane domain (TMD), which is spanning through the membrane and the nucleotide binding domain (NBD), necessary for ATP binding and hydrolysis to generate the energy for the transport [147]. There are two different kinds of ABC-transporter known for lantibiotic resistance, the homodimeric ABC-transporter and the heterodimeric ABC-transporter [67; 135].

The homodimeric ABC-transporter involved in lantibiotic resistance were first discovered in *B. subtilis* and this kind of ABC-transporter are called BceAB (bacitracin efflux) type transporter [148]. The most BceAB type transporters have several substrates, even when they are structurally different to each other. There are several ABC-transporter of the BceAB type in different bacteria known. Examples are VraDE in *S. aureus* [149], PsdAB in *B. subtilis* [150], MbrAB in *Streptococcus mutans* (*S. mutans*) [151] and NsrFP in *Streptococcus agalactiae* (*S. agalactiae*) (Figure 10). These transporters are encoded next to a BceRS-like TCS. They contain one large TMD, containing ten transmembrane helices and one NBD, which is functional as a dimer. One of the most characteristic components of these transporter is the extracellular domain between helices VII and VIII [135]. The mechanism of the recognition of the different substrates has not been solved yet but it is suggested that the extracellular domain has an important role for the recognition [135].

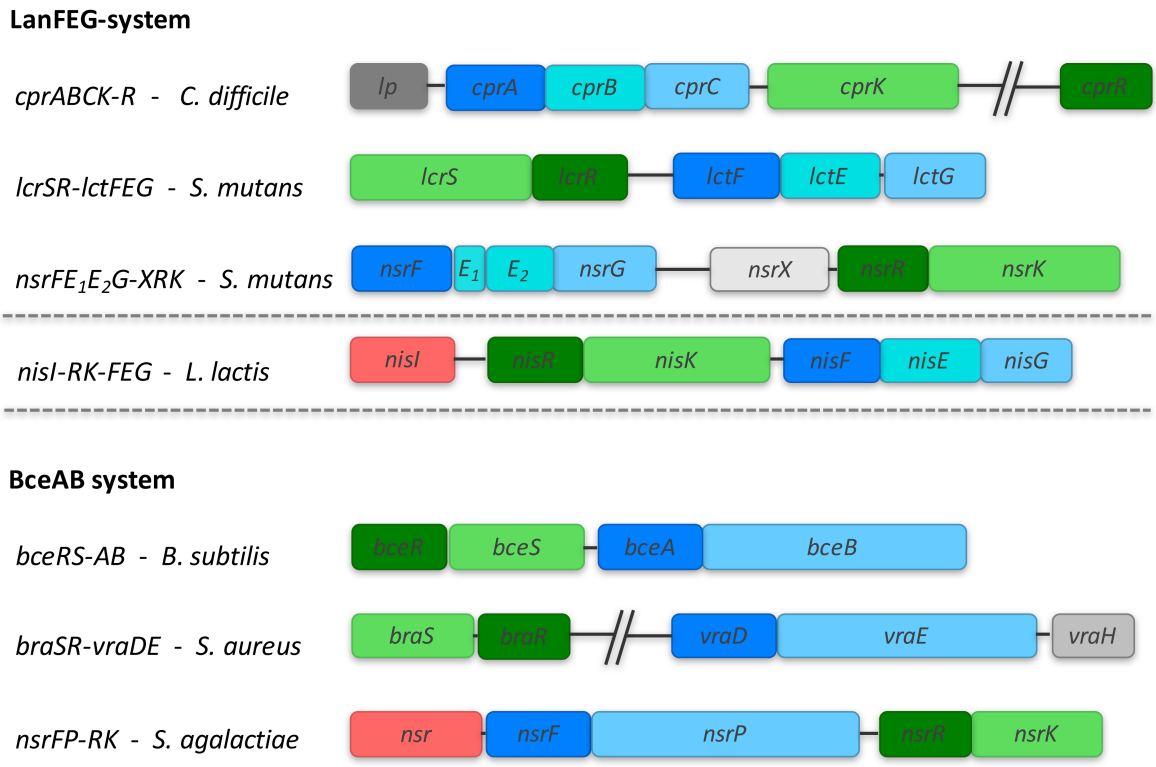

Figure 10: Overview of the lantibiotic resistance operons belonging to the Lan- and Bce-type systems.
Three operon structures, each are highlighted as representatives for the Lan and Bce group. For Lan-type these are *cprABCK-R* from *C. difficile*, *nsrFE₁E₂G-XRK* and *lcrSR-lctFEG* from *S. mutans*. Additionally, the *nisRK-FEG* system from *L. lactis* involved in nisin immunity is also highlighted. For Bce-type, the three representatives comprise of *bceRS-AB* from *B. subtilis*, *braSR-vraDE* from *S. aureus* and the *nsrFP-RK* system from *S. agalactiae*. The size of the genes corresponds directly with the gene length as deposited in the NCBI database. The TCSs with RR (dark green) and HK (light green); and the ABC transporters are shown in different shades of blue. In the BceAB system, the NBD is dark blue while the TMD is shown in light blue. The additional TMD present in the CprABC systems is shown in cyan. The proteins, which are part of the operon but the function has not been determined so far are shown in gray. In case of the *nis* and *nsr* operons, an additional membrane-associated protein is present which is colored in red. Taken from [152].

The heterodimeric ABC-transporter types are mainly recognized in lantibiotic producing bacteria, called LanFEG ABC-transporter, and normally have a narrow substrate range. In many cases the substrate is only the self-produced lantibiotic and highly identical variants. Examples are the EpiFEG which is able to transport gallidermin from *Staphylococcus gallinarium* (*S. gallinarium*) and epidermin from *Staphylococcus epidermidis* (*S. epidermidis*) but not nisin [135; 153]. They contain one NBD protein, working as dimer, and two TMD proteins. Two prominent members of these ABC-transporter types are the NisFEG and the SpaFEG [154; 155]. But NukFEG is also known [135; 156]. All of these are immunity transporters to protect the bacteria from the self-produced lantibiotic. There are only few resistance ABC-transporters of this type known. The CprABC (cationic antimicrobial peptide resistance) transporter from *C. difficile* is not associated with any lantibiotic biosynthesis genes and performs resistance, not immunity, separating it from the other members of the LanFEG family [106; 135]. Interestingly, this transporter has a broad spectrum of lantibiotics like the BceAB type transporter. It was shown that the CprABC

transporter is able to confer resistance against nisin, gallidermin and subtilin [157]. Suggestions are that the second ring motif, the proline and glycine, is important for the interaction and recognition of this ABC-transporter [157]. The CprABC transporter is expressed next to a histidine kinase, member of the periplasmic sensing histidine kinase. A response regulator was also found but is not located in the genome next to the other proteins [157; 158]. Also in *S. mutans* two transporters are known to perform resistance against lantibiotics, LctFEG and $NsrFE_1E_2G$ and these are members of this CprABC family (Figure 10) [143; 159]. The resistance operons are always the same, containing an ABC-transporter and a two-component system, no matter which family the transporter belongs to. These two components are responsible for the resistance against lantibiotics in different Gram-positive bacteria [135].

1.10. Membrane associated proteins of lantibiotic resistance

Additionally, to the ABC-transporter there are some strains expressing a resistance or immunity membrane associated protein. Nearly all self-producing strains contain an (auto)-immunity system containing a LanI protein and an ABC-transporter, independently of the produced class of lantibiotic [160]. The nisin system contains both a membrane associated LanI, NisI (Figure 11 B) and the ABC-transporter NisFEG mentioned above. This system is able to perform nearly a 100-fold higher nisin immunity in *L. lactis* compared to the immunity system lacking *L. lactis* strain [154; 161; 162; 163]. So, the bacteria carrying the immunity system are able to grow in presence of a high nisin concentration while bacteria lacking this system are dead. This seems to be a cooperatively mechanism as each protein alone induces 10-30% lesser immunity levels. Further examples of these immunity systems are also found in other lantibiotic producer strains. *B. subtilis* producing subtilin contains a SpaI (Figure 11 C) protein additionally to the SpaFEG transporter [164]. The epidermin and gallidermin producer strains *S. epidermidis* and *S. gallinarium* are also known to express immunity proteins EpiH and GdmH [153; 165; 166]. These immunity systems are highly active against the cell-produced lantibiotic but do not show a broad spectrum of immunity against different lantibiotics.

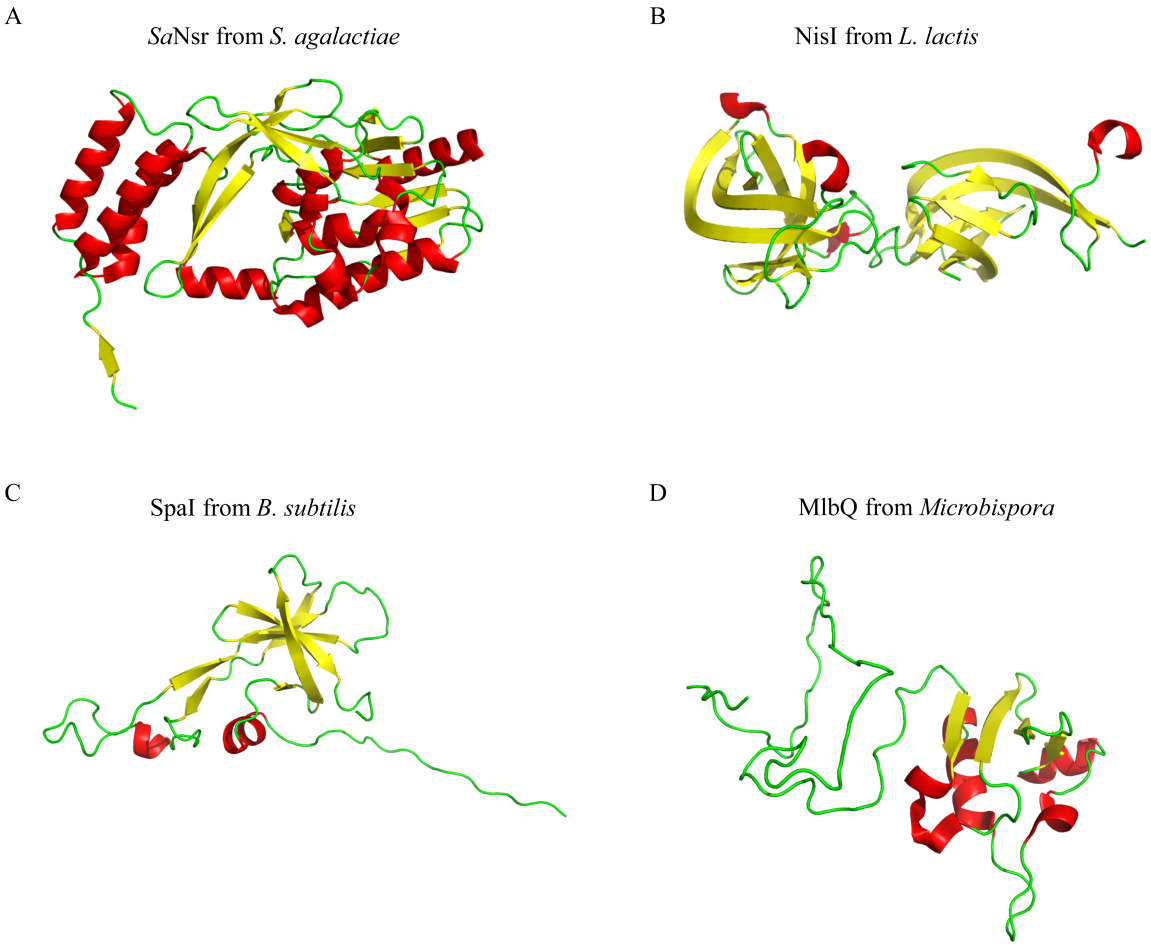

Figure 11: Cartoon representation of crystal structures of NisI and *Sa*Nsr and NMR structures of SpaI and MlbQ. A) The crystal structures of *Sa*Nsr from *S. agalactiae* (PDB code: 4Y68). B) The crystal structure of NisI from *L. lactis* (PDB code: 5XHB). C) NMR structure of SpaI from *B. subtilis* (PDB code: 2LVL). D) NMR structure of MlbQ from *Microbispora* ATCCPTA-5024 (PDB code: 2MVO). Depicted in red are the helices, in yellow the sheets and in green the loops.

NisI is an immunity protein of *L. lactis* and performs two different immunity mechanisms against nisin. The first characterized mechanism of NisI is the binding of nisin. Binding to nisin protects the bacteria against the mode of action of nisin [154; 161; 162; 167]. A second characterized mechanism is that the expressed NisI in presence of nisin is able to cluster the cells. This results in large cell chains up to 30 cells [162]. The clustering is able to impede nisin from binding to the lipid II and inhibit the pore formation [162]. Interestingly, this is a reversible mechanism and by removing nisin the cells are able to start growing normal again [162].

Some Gram-positive human pathogens produce one lantibiotic, but are highly resistant against another lantibiotic like *S. agalactiae,* which produces agalacticin but has a resistance system against nisin [168]. This system is highly resistant against nisin and contains a homodimeric ABC-transporter, NsrFP, mentioned above with a broad substrate spectrum of lantibiotics [169; 170]. Also, a membrane associated protein called *Sa*Nsr could be identified

and characterized (Figure 11 A). *Sa*Nsr is known to perform 20-fold of resistance to nisin in *L. lactis* strain compared to a sensitive strain [169; 171]. *Sa*Nsr is a serine protease and is active against nisin. It cleaves of the last six amino acids which results in a 100-fold less bactericidal activity of nisin [162; 172]. Another lipoprotein is MlbQ in *Microbispora* ATCC PTA-5024 from the NAI-107 biosynthetic gene cluster (Figure 11 D). This lipoprotein confers specific resistance to NAI-107-like lantibiotics [173; 174]. There are different mechanisms to prevent immunity or resistance with the help of membrane associated proteins. Comparing the gene cluster of different Gram-positive bacteria containing a resistance system a lipoprotein encoded in front of a three component ABC-transporter in *C. difficile* could be identified (Figure 10). The lipoprotein CD1348 is encoded directly in front of the CprABC transporter of *C. difficile*. This lipoprotein is uncharacterized but maybe it is able to perform resistance against some lantibiotics [157; 158]. This protein shows no homology to any known protein of these immunity and resistance systems but also NisI and Nsr are just showing 23% homology to each other and both are protecting the bacteria in total different mechanisms [175]. Also, no sequence homology to any other known protein could be determined. So, it could be interesting to characterize the CD1348 to solve a different way of resistance mechanism.

1.11. Retroviruses

Lantibiotics are not only active against bacteria but also DNA and RNA viruses, like retroviruses, are inhibited by some lantibiotics. One big group of RNA viruses are the retroviruses. A retrovirus is a single-stranded positive-sense RNA virus with a DNA intermediate. After the retrovirus entered the host cell the virus is able to produce DNA from its RNA genome with its own reverse transcriptase enzyme. An integrase enzyme incorporated the formed virus DNA in the host cell genome. At this point the host cell treats the virus DNA as part of own genome and translates and transcribes the viral genes in the same way like the own genes [176; 177; 178].

Retroviruses can be separated in in different sub groups. Here the α-retrovirus, β-retrovirus, γ-retrovirus, δ-retrovirus, ε-retrovirus and lentiviruses are known. One of the most prominent lentivirus is the human immunodeficiency virus (HIV) [178].

1.12. Human immunodeficiency virus (HIV)

HIV is a member of the lentivirus a subgroup of the retroviruses and can be divided in HIV-1 and HIV-2, while HIV-1 is the most common type occurring in patients [176; 179; 180]. HIV infections cause the acquired immunodeficiency syndrome (AIDS). Main characteristic is the reverse transcriptase enzyme using RNA as template for transcription into double stranded DNA. The HIV consists of three major genes the *env*, the *pol* and the *gag* gen (Figure 12) [181]. The *gag* encodes the virus matrix (MA), the capsid (CA), the nucleocapsid (NC) and the P6 precursor proteins (P6) [177; 182; 183]. The *pol* (polymerase) precursor protein encodes the protease (PR), the reverse transcriptase (RT) and the integrase (IN) [177; 181; 184]. The *env* gen encoded the monomeric envelope proteins containing two linked subunits, an outer subunit gp120 and the second subunit gp41 (Figure 12) [181; 184].

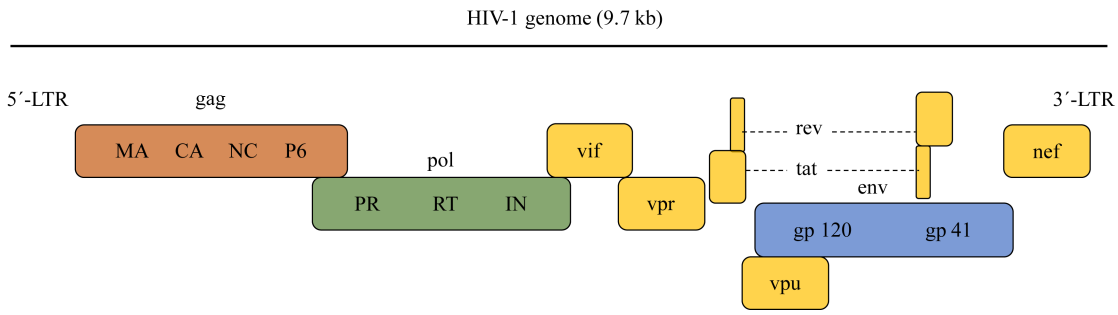

Figure 12: HIV-1 genome.
The operon contains the three structural genes *gag* (orange), *pol* (green) and *env* (blue). They are encoding the structure proteins of the HI-virus. *Gag* encodes the matrix (MA), the capsid (CA), the nucleocapsid (NC) and the P6 precursor protein (P6). The *pol* is encoding the proteasome (PR), the reverse transcriptase (RT) and the integrase (IN). The *env* gene encodes the outer subunit gp120 and the second subunit pg41.The genome also contains six accessory proteins depicted in yellow. Based on [184].

Additionally, to the three major genes there are encoded six so-called accessory proteins in the HIV genome.

1.13. Accessory proteins of HIV

Additional to the structural genes there are six accessory proteins known in the HIV genome, The Vpr, Nef, Tat, Rev, Vpu and Vif protein [185; 186; 187].

The Vpr (viral protein R) is a 96-amino acid 14 kDa small protein, encoded in central region of the HIV-1 genome. Vpr has two distinct functions, once the regulation of the nuclear translocation of the HIV-1 pre-integration complex (PIC) [188; 189]. The entry of the PIC is an essential step in the retroviral replication. Also, the induction of the cell cycle arrest in

infected proliferating cells is a function of Vpr. Additionally, some other activities could be observed [186; 188]. The stimulation of transcription of HIV-1 LTR and other promoters could be observed. Forming ion-selective channels and regulating the cell apoptosis are known activities of Vpr [190]. All these different functions are induced by interaction of Vpr with various different proteins of the host cell. The different functions are occurring at different times in the HIV replication cycle [189].

Tat (transactivator of transcription) and Rev (regulator of expression of virion) are two accessory proteins involved in the regulation of gene expression. Tat is one of the first proteins produced in the replication steps. Tat is 14 kDa big and is a potent transactivator required for the viral replication [191]. It is able to bind the transactivation-responsive region (TAR) a part of new transcribed RNA. This region mediates the phosphorylation of the polymerase II C-terminal domain [192]. The result of this interaction is the activation of the cellular transcription machinery to initiate transcription of the viral proteins [181; 193]. Rev is an 18 kDa big phosphoprotein which is involved in the nucleocytoplasmic transport of viral RNA. Rev is later expressed in the HIV replication cycles and forms multimers binding the Rev response element (RRE) [194]. After binding Rev exports unspliced viral mRNA, before they are processed by the human spliceosome. It could be shown that Rev can bind a number of cellular proteins which all contributes to the nuclear export of viral mRNA [181].

Nef (negative factor) is a 205 amino acid myristoylated phosphoprotein. Nef is dispensable for infection, its function is the down regulation of cell surface proteins [195]. The down regulated proteins are the cluster of differentiation (CD) 4 and the histocompatitibility complex I, resulting in the prevention of cell lysis of infected cell. Nef also down regulated the CTLA-4 to ensure T-cell activation [196]. Nef effects additional on the TCR signaling and combats the anti-viral SERINC proteins [197].

Vpu (viral protein U) is a 17 kDa viral protein. Vpu contains a hydrophobic membrane anchor and a phosphorylated cytoplasmic tail [198]. It is an integral membrane protein enhancing the budding of the viruses from the host cell. Vpu has two functions in the viral life cycle. Degradation of CD4 receptor preventing by this a formation of CD4 and HIV is one. Beside this Vpu can neutralize the cellular restriction factor tetherin [181].

Last of the six accessory proteins is the Vif (viral infectivity factor) protein a 23 kDa big protein targeting the cellular cytidine deaminases for ubiquitination and degradation. Vif is an interesting candidate for new drug development.

1.14. Viral infectivity factor

The viral infectivity factor protein is a 23 kDa big protein and is necessary for the HIV-1 replication in the human body. The Vif protein is one of the most interesting proteins in the HIV-1 drug development. It is forming a complex with 5 host cell proteins and degrades the human answer of the viral entry, the apolipoprotein B mRNA editing enzyme catalytic polypeptide-like 3 (APOBEC3) family.

There are proteins in the human body which have antiviral properties and negatively impact on the viral replication [199; 200; 201]. In humans are seven of the APOBEC3 proteins encoded the APOBEC3A, APOBEC3B, APOBEC3C, APOBEC3D, APOBEC3F, APOBEC3G and APOBEC3H [201; 202; 203]. The principal activity of APOBEC3 proteins is the cytidine deamination of single-stranded DNA, shown in biochemical and cell culture assays [204; 205]. Four of these proteins are able to reduce the HIV-1 replication. These proteins are A3D, A3F, A3H and A3G [206].

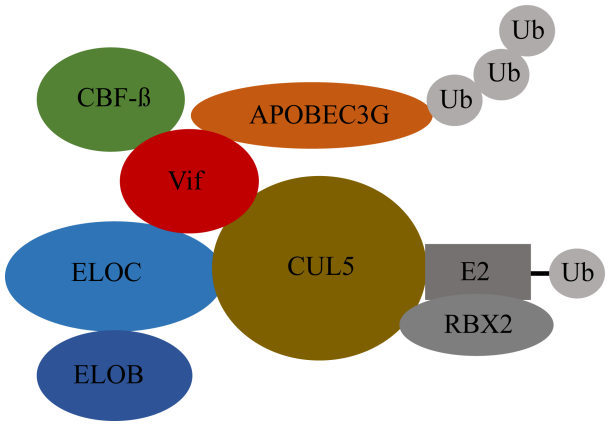

Figure 13: Complex formed by the Vif protein.
The complex is formed from the Vif protein to ubiquitinate and degrade the APOBEC3G protein. The Vif protein is recruiting the Cullin 5, CBF-ß and the adapter proteins Elongin C and B. This results in the degradation of the human immunity cytidine deaminase APOBEC3G. The corresponding binding domains are depicted in Figure 14. Based on [206].

Because of Vif this effect of reduced replication is not able to intervene in the HIV-1 replication in the host cell. The Vif protein uses the cellular Cullin-Ring ubiquitin ligase, leading to the ubiquitination and proteasomal degradation of the APOBEC3 protein and the virus can replicate itself without any hindrance [207; 208; 209].

This complex, which degrades the APOBEC3 proteins, is only able to be formed in presence of the Vif protein. Vif is a basic protein and it is well known characterized. The function and the corresponding binding sites are already known.

The formed complex, which is important for the degradation of the APOBEC3 is containing the Vif protein, the APOBEC3 protein, the transcription co-factor CBF-ß, the adapter proteins ELONGIN B and C, and the CULLIN-5 (Figure 13) [210].
The corresponding binding sites necessary for forming the complex are well characterized. The N-terminal part of the protein is not only necessary for RNA binding but also all-important APOBEC3 binding sites are located here as well [210]. The DRMR domain is known for binding the APOBEC3F while the YRHHY domain is necessary to bind the APOBEC3G [211; 212]. An additional APOBEC3F domain could be determined in the end of the N-terminal region of Vif which is the domain of the protein necessary for APOBEC3 binding (Figure 14) [213].

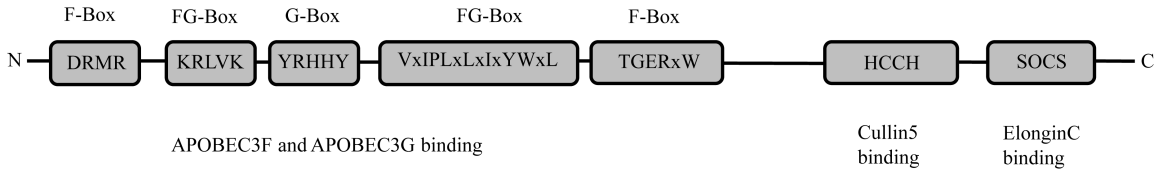

Figure 14: Functional domains of the Vif protein.
Shown are the known binding sites of the Vif protein. The N-terminus is known for binding RNA and more important binding the APOBEC3 proteins. Here are solved two FG-boxes where APOBEC3F and G can bind. Also, two F-boxes are known for APOBEC3F binding and one G-box is known to bind APOBEC3G. After the APOBEC3 binding domain the Cullin 5 binding site is located. The HCCH domain is also a zinc binding site which is important for Cullin 5 binding. The SOCS domain is for Elongin C binding responsible. Based on [179; 214].

Two FG-boxes, meaning APOBEC3F and APOBEC3G, are interacting with the Vif protein at the same domains could also be identified [213; 214]. The HCCH region is known for two different functions. Firstly, it is a zinc binding motif and secondly the interaction with the Cullin 5 is a function of this region [215; 216]. The so called SOCS box was identified as the Elongin C binding side [217].

2. Aims

Several membrane associated proteins in different Gram-positive bacteria performing immunity and resistance towards different lantibiotics are known. They usually belong to an operon cluster containing an ABC-transporter and a two-component system. Also in *Clostridium difficile* (*C. difficile*) such a system could be determined as well. This system performs resistance against different lantibiotics. In front of this system a lipoprotein CD1348 could be identified which is uncharacterized so far.
The first aim of this thesis was to establish the heterologous expression of the CD1348 protein of *C. difficile* in *Escherichia coli* and subsequently the purification of this protein. To determine if it is a resistance protein, different *in vivo* and *in vitro* studies were used. Further, a structural characterization with the help of crystallography, small-angle X-ray scattering (SAXS) and nuclear magnetic resonance (NMR) analysis of the lipoprotein CD1348 was performed.

Over the last years antibiotic resistance became a raising problem. There are different kinds of resistance mechanisms known for antibiotics and also lantibiotics. An antibiotic and lantibiotic resistant *Lactococcus lactis* (*L. lactis*) strain, which has a non-determined resistance mechanism, should be characterized. This strain was analysed with several lantibiotics and antibiotics to investigate against which types of antimicrobial agent it performs resistance. The second aim was to analyse this antibiotic and lantibiotic resistant *L. lactis* strain more in detail and to determine the resistance mechanism using different *in vivo* analyses for characterization.

The last aim of this thesis was to establish a high scale purification of pure viral infectivity factor (Vif) protein of human immunodeficiency virus (HIV-1) to perform interaction studies and structural analysis of the Vif protein with the APOBEC3 interaction protein.

3. Publications

Chapter I Insight into Two ABC Transporter Families

Insight into Two ABC Transporter Families Involved in Lantibiotic Resistance

Frontiers in Molecular Biosciences

Chapter II Lantibiotic maturation complex

Stoichiometry and structure of a lantibiotic maturation complex

Scientific reports

Chapter III CD1348 lipoprotein from *Clostridium difficile*

Characterization of CD1348 of the CprABC operon: Purification and interaction studies with different lantibiotics

In preparation

Chapter IV Lipid composition of *Lactococcus lactis*

Lantibiotic resistant *L. lactis* has an altered lipid composition

In preparation

Chapter V Viral infectivity factor of HIV

Purification and interaction studies of the viral infectivity factor of HIV

In preparation

3.1. Chapter I - Insight into Two ABC Transporter Families

Published in: Frontiers in Molecular Biosciences

Impact factor: 1.33
Own work: 45%
Writing the manuscript
Preparation of the figures

Insight into Two ABC Transporter Families Involved in Lantibiotic Resistance

Rebecca Clemens, Julia Zaschke-Kriesche, Sakshi Khosa and Sander H. J. Smits

frontiers in Molecular Biosciences

REVIEW
published: 22 January 2018
doi: 10.3389/fmolb.2017.00091

Insight into Two ABC Transporter Families Involved in Lantibiotic Resistance

*Rebecca Clemens, Julia Zaschke-Kriesche, Sakshi Khosa and Sander H. J. Smits**

Institute of Biochemistry, Heinrich-Heine-University Duesseldorf, Duesseldorf, Germany

Antimicrobial peptides, which contain (methyl)-lanthionine-rings are called lantibiotics. They are produced by several Gram-positive bacteria and are mainly active against these bacteria. Although these are highly potent antimicrobials, some human pathogenic bacteria express specific ABC transporters that confer resistance and counteract their antimicrobial activity. Two distinct ABC transporter families are known to be involved in this process. These are the Cpr- and Bce-type ABC transporter families, named after their involvement in cationic peptide resistance in *Clostridium difficile*, and bacitracin efflux in *Bacillus subtilis*, respectively. Both resistance systems differentiate to each other in terms of the proteins involved. Here, we summarize the current knowledge and describe the divergence as well as the common features present in both the systems to confer lantibiotic resistance.

Keywords: lanthionine ring, lantibiotic, nisin, resistance, antimicrobial peptide, *L. lactis*

OPEN ACCESS

Edited by:
Richard J. Bingham,
Department of Biological Sciences,
University of Huddersfield,
United Kingdom

Reviewed by:
Anastassios C. Papageorgiou,
University of Turku, Finland
Christopher Cooper,
University of Huddersfield,
United Kingdom

***Correspondence:**
Sander H. J. Smits
sander.smits@hhu.de

Specialty section:
This article was submitted to Structural Biology, a section of the journal Frontiers in Molecular Biosciences

Received: *28 August 2017*
Accepted: *08 December 2017*
Published: *22 January 2018*

Citation:
Clemens R, Zaschke-Kriesche J, Khosa S and Smits SHJ (2018) Insight into Two ABC Transporter Families Involved in Lantibiotic Resistance. Front. Mol. Biosci. 4:91. doi: 10.3389/fmolb.2017.00091

INTRODUCTION

The urging need for novel antibiotics has put small antimicrobial peptides (AMPs) into a particular focus. Especially, a large group of peptides called bacteriocins have been extensively studied for an application purpose as novel antibiotics. Bacteriocins are small, ribosomally-synthesized peptides of which some display a high potent antimicrobial activity (Tagg et al., 1976; Cotter et al., 2005b) and have been already used since decades as food preservatives or as antibiotic alternatives in biomedical applications (Cleveland et al., 2001; Cotter et al., 2012).

A large group within the bacteriocin family, are ***lan***thionine containing ***antibiotics*** termed lantibiotics. These lantibiotics are post-translationally modified peptides that contain dehydrated amino acids (Dehydrobutyrine and/or Dehydroalanine) and other unusual amino acid modifications (Jung, 1991; Willey and van der Donk, 2007; Bierbaum and Sahl, 2009; Alvarez-Sieiro et al., 2016). The Michael addition of a neighboring cysteine side chain residue to these dehydrated amino acids results in the formation of characteristic thioether bridges called lanthionine rings. These rings are primarily crucial for their high antimicrobial activity against mainly Gram-positive bacteria. The well-known lantibiotics nisin, gallidermin, and subtilin are highlighted in **Figure 1**. Lantibiotics are highly potent and nanomolar concentrations are already enough to fulfill their antimicrobial activity as observed for example for nisin produced by *Lactococcus lactis* species or subtilin produced by *Bacillus subtilis* (Delves-Broughton et al., 1996; Chatterjee et al., 2005).

In comparison to their high antimicrobial activity against Gram-positive bacteria, lantibiotics display a reduced effectiveness against Gram-negative bacteria. Many lantibiotics bind to lipid II or other peptidoglycan precursor inducing inhibition of cell wall synthesis. Some lantibiotics can subsequently form pores which lead to membrane leakage and rapid cell death (Héchard and Sahl, 2002; Bierbaum and Sahl, 2009). Due to their nanomolar activity, in combination with high stability

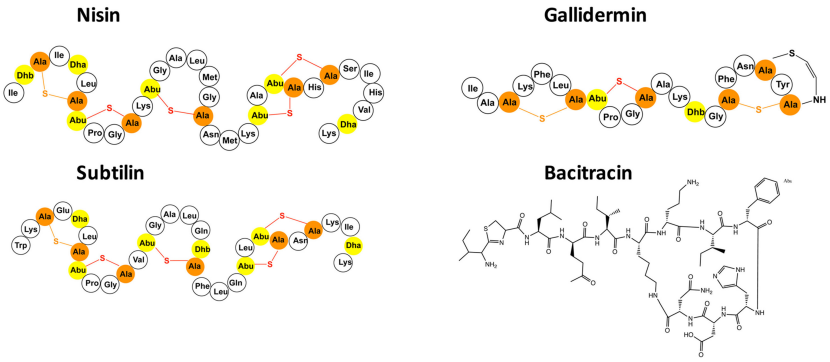

FIGURE 1 | Selected presentation of the lantibiotics nisin, gallidermin and subtilin as well as the bacteriocin bacitracin. The dehydrated amino acids and the cysteines of the lantibiotics are highlighted in yellow and orange. The (methyl-)lanthionine rings are visualized in orange and red.

against proteolytic digestion, lantibiotics are considered potential compounds for novel medical treatment.

A well-studied member of lantibiotics is nisin, which is produced by some *L. lactis* strains. It was shown that it is effective against the treatment of bacterial mastitis, methicillin-resistant *Staphylococcus aureus* (MRSA) and enterococcal infections (Brumfitt et al., 2002). Gallidermin and epidermin, produced by *Staphylococcus gallinarum* and *Staphylococcus epidermidis,* respectively, are some other examples of lantibiotics (Cotter et al., 2005a) and are associated with the treatment of acne, eczema, folliculitis, and impetigo.

The lantibiotic producer strains with a few exceptions, usually contain a single gene cluster, on which the structural genes for the lantibiotic itself, as well as for the modification and transport across the cellular membrane are located (Chatterjee et al., 2005; Willey and van der Donk, 2007; Alkhatib et al., 2012; Singh and Sareen, 2014). In many gene clusters, these genes are upregulated via a distinct two-component system (TCS) consisting of a histidine kinase (HK) and a response regulator (RR), which are located on the same gene cluster (Qiao et al., 1996). The upregulation is auto induced by its own lantibiotic (Kuipers et al., 1995).

Due to the high convergence of these gene clusters, it has been possible to detect potential lantibiotic gene clusters within newly sequenced genomes using *in silico* techniques (van Heel et al., 2013a). Such genome mining approaches have identified novel lantibiotic gene clusters in several species, such as the genes encoding for maddinglicin from *Clostridium maddingley*, agalacticin from *Streptococcus agalactiae*, bagelicin from *Streptococcus suis* and moraviensicin from *Enterococcus moraviensis* (van Heel et al., 2013b; Tracanna et al., 2017). These novel and mostly exotic lantibiotics can be expressed, modified and secreted by *L. lactis* using the well-characterized nisin biosynthetic machinery (van Heel et al., 2013b).

In order to prevent the activity of the secreted lantibiotic against their own membrane, the lantibiotic gene cluster contains additional genes (*lanI* and *lanFEG*), which form a lantibiotic (auto-)immunity system (Alkhatib et al., 2012). The *lanI* and *lanFEG* genes are conserved to a certain extent throughout the lantibiotic expressing bacteria (Alkhatib et al., 2012). Here LanI is a membrane-associated lipoprotein, which binds to the lantibiotic and thereby lowers the concentration of the lantibiotic reaching the membrane. Additionally, LanFEG forms an ABC transporter localized in the cellular membrane which effluxes the lantibiotic prior to pore formation (Stein et al., 2003, 2005; Draper et al., 2008, 2015).

Despite the odds, resistance against lantibiotics does exist and different resistance mechanisms have been unraveled so far. Resistance mechanisms comprise of modification in peptidoglycan or the cellular membrane (e.g., changes in phospholipid or fatty acid composition) as well as cell membrane modifications, such as lipopolysaccharides which are attached to the outer layer of the outer membrane of Gram-negative bacteria (Draper et al., 2015). Furthermore, some TCSs could be linked to lantibiotic resistance by upregulating the transcription of resistance-associated genes upon the presence of lantibiotic within the habitat of the bacteria. Other mechanisms resulting in resistance are the assembly of biofilms or the expression of resistance proteins such as the nisin resistance protein (NSR) found to be upregulated in nisin non-producing strains, inactivating nisin by specific proteolytic degradation (Sun et al., 2009). The lantibiotic resistance mechanisms have been nicely reviewed in detail in Draper et al. (2015).

Recently, several gene clusters were identified in various human pathogenic bacteria, which encode a lantibiotic resistance system based on the overexpression of membrane embedded proteins, that includes the presence of an ABC transporter (Khosa et al., 2013).

The expression of proteins within these gene clusters result in a detectable lantibiotic resistance. For example, resistance against nukacin ISK-I and lacticin 481 in *Streptococcus mutans* is mediated by the expression of *lcrSR-lctFEG* genes (Kawada-Matsuo et al., 2013a), while the expression of *cprABCK-R* operon in *Clostridium difficile* results in resistance against

different lantibiotics. Here, nisin, mutacin 1140, subtilin, and gallidermin were tested and resistance was observed (McBride and Sonenshein, 2011; Suárez et al., 2013). Furthermore, the proteins located on the *nsr* operon from *S. agalactiae* are together conferring resistance against nisin A, nisin H, and gallidermin (Khosa et al., 2016a,b; Reiners et al., 2017). All these resistance operons are characterized by the presence of a TCS consisting of a HK and a RR; as well as a membrane-embedded ATP-binding cassette (ABC) transporter (Gebhard, 2012; Khosa et al., 2013; Suárez et al., 2013). In some cases, an extra gene encoding a membrane-associated lipoprotein or a specific serine protease is present.

Upon examining these operons in detail, it was observed that the ABC transporters are responsible for lantibiotic resistance and can be divided into two groups: the CprABC-type and the BceAB-type ABC transporter family, both conferring resistance against lantibiotics and/or antimicrobial peptides in general.

Within this review, we will highlight these two lantibiotic resistance ABC transporter families and their corresponding gen clusters.

GENE CLUSTER ORGANIZATION OF ABC TRANSPORTERS INVOLVED IN LANTIBIOTIC RESISTANCE

The common feature of both operon types is the presence of a TCS, which upregulates the other genes by an external stimulus via binding of the lantibiotic. Furthermore, they both consist of an ABC transporter, which is thought to expel the lantibiotic once it has reached the bacterial membrane (**Figure 2**). In general, ABC transporter comprises of a transmembrane domain (TMD) and a nucleotide-binding domain (NBD). The NBD dimerizes upon binding of ATP, which is subsequently hydrolysed and the energy released is used to induce a conformational change within the TMD allowing substrate export or import. Furthermore, in some of these operons there is also the presence of either a lipoprotein or a membrane-associated specific protease.

CprABC-TYPE RESISTANCE OPERONS

Lantibiotic resistance operons belonging to the *Cpr* group contain three different genes encoding for an ABC transporter (one for the NBD and two different TMDs; highlighted in blue, **Figure 2**) and genes encoding a HK and RR, which build up the TCS. These transporters belong to the ABC-type 2 sub-family and on a genetic level closely resemble the immunity systems found in lantibiotic producing strains. This group is named after the most prominent member, the CprABC transporter from *C. difficile*, which confers resistance against nisin and gallidermin (McBride and Sonenshein, 2011; Suárez et al., 2013). Here, the NBD is encoded by *cprA* while *cprB* and *cprC* encode the two TMDs. CprB and CprC are of similar size and are predicted to contain six transmembrane helices each. Both CprB and CprC form a functional transporter together in the membrane as a heterodimer (**Figure 3**).

Other members of this group are *lcrSR-lctFEG* and *nsrFE$_1$E$_2$G-XRK*, both present in the genome of *S. mutans* (**Figure 2**). The encoded TMDs of this group contain six predicted transmembrane helices. They are upregulated via one promoter suggesting that they are expressed in equal stoichiometry. These ABC transporters, are closely related to the immunity ABC transporter LanFEG family, which consists of the NBD LanF and two TMDs LanE and LanG (as an example, the nisin immunity system called NisFEG is highlighted in **Figure 2**). These LanFEG ABC transporters are co-expressed in lantibiotic producer strains and have been shown to expel lantibiotics from the membrane preventing a suicidal effect (Stein et al., 2003, 2005; Alkhatib et al., 2012; AlKhatib et al., 2014b). The LanFEG genes are, in contrast to the Cpr group, encoded in a larger operon which also include genes for biosynthesis and transport machinery of the produced lantibiotic. Due to the operon similarity, one can assume that the *cpr* operons are evolutionary linked to the producing strains. Here however, only the genes for the resistance proteins are present and none of the biosynthetic machinery. Next to the ABC transporter genes, a TCS is present which consists of the HK and RR, which are distantly located on the chromosome (Suárez et al., 2013) (highlighted in green, **Figure 2**). These TCSs transfer the stimuli provided by the externally present lantibiotic into the cell and induce transcription of the genes.

BceAB RESISTANCE OPERON

Lantibiotic resistance operons belonging to the *Bce* group contain genes encoding for an ABC transporter, i.e., two different genes encoding one NBD and one large TMD (highlighted in blue, **Figure 2**). Additionally, a TCS is present consisting of a histidine kinase and response regulator. BceAB-type (ABC) transporters are putatively involved in antimicrobial peptide as well as lantibiotic removal from the lipid membrane (Gebhard and Mascher, 2011). They have been named after the transporter system from *B. subtilis*, which till date is the best characterized representative of *Bac*itracin *e*fflux (Bce) transporters, conferring resistance against the antimicrobial peptide bacitracin (Ohki et al., 2003; Rietkötter et al., 2008).

Based on the Transport Classification Database (TCDB), BceAB-type transporters belong to the peptide 7 exporter family (Saier et al., 2009). The BceAB-type transporters are composed of two components, a NBD (BceA) and a single TMD (BceB) (**Figure 2**). The TMD consists of ten predicted transmembrane helices (TMHs) and contain a large, extracellular domain (ECD$_L$ where L stands for lantibiotic) between transmembrane helices VII and VIII (**Figure 3**). This extracellular domain appears to be the hallmark of BceAB-type transporters and consists of ∼200–250 amino acids (Ohki et al., 2003; Rietkötter et al., 2008; Khosa et al., 2013; **Figure 3**).

Bioinformatically, ECD$_L$ are easy to detect and have been for example identified in the TMDs of the bacitracin resistance-associated ABC transporter BceAB in *Bacillus* species (Rietkötter et al., 2008), in the bacitracin and nisin resistance-associated ABC transporter VraDE in *S. aureus* (Hiron et al., 2011) and the nisin

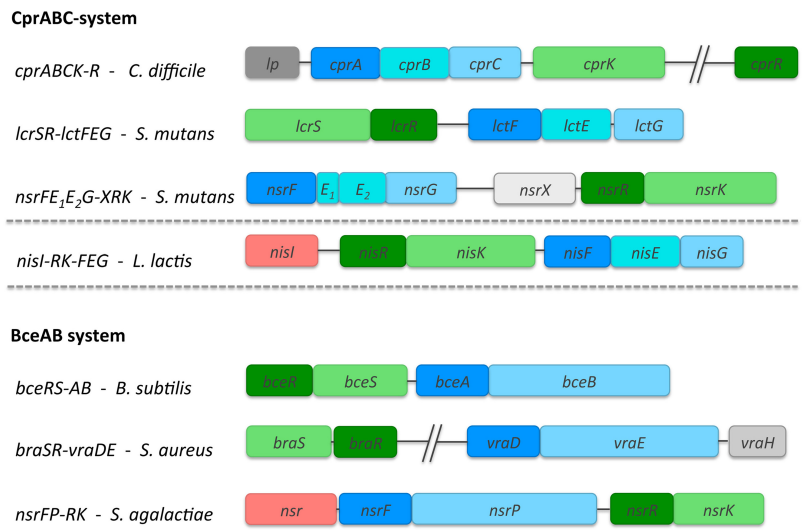

FIGURE 2 | Overview of the lantibiotic resistance operons belonging to the Cpr- and Bce- type systems. Three operon structures, each are highlighted as representatives for the Cpr and Bce group. For Cpr-type these are *cprABCK-R* from *C. difficile*, *nsrFE*$_1$*E*$_2$*G-XRK* and *lcrSR-lctFEG* from *S. mutans*. Additionally, the *nisRK-FEG* system from *L. lactis* involved in nisin immunity is also highlighted. For Bce-type, the three representatives comprise of *bceRS-AB* from *B. subtilis*, *braSR-vraDE* from *S. aureus* and the *nsrFP-RK* system from *S. agalactiae*. The size of the genes corresponds directly with the gene length as deposited in the NCBI database. The TCSs with RR (dark green) and HK (light green); and the ABC transporters are shown in different shades of blue. In the *bceAB* system, the NBD is dark blue while the TMD is shown in light blue. The additional TMD present in the *cprABC* systems is shown in cyan. The proteins, which are part of the operon but the function has not been determined so far are shown in gray. In case of the *nis* and *nsr* operons, an additional membrane-associated protein is present which is colored in red.

resistance-associated NsrFP in *S. agalactiae* (Khosa et al., 2013). These ECD$_L$ are found to be crucial for resistance determinants as they are supposed to recognize the lantibiotic extracellularly and subsequently induce the TCS-dependent signal transduction within the cell (Rietkötter et al., 2008; Hiron et al., 2011). Initial substrate binding usually occurs via these ECD$_L$, however, experimental evidence for this only has been indirectly proven via knockout studies (Falord et al., 2012).

In the Bce group, a BceRS-type TCS has co-evolved (Heijenoort, 1994; Dintner et al., 2011) composed of a response regulator (BceR) and a histidine kinase (BceS). The latter consists of two transmembrane helices with a short extracellular located loop of ∼25 amino acids. Such a small loop is unusual for HKs, which normally consists of roughly 115–125 amino acids. This suggested that the TCS lacks an extracellular domain normally present to detect an external stimulus and is therefore, categorized as a member of the intramembrane-sensing histidine kinase family (Mascher et al., 2003; Mascher, 2006). Members of this family have been shown to be responsible for the upregulation of the corresponding ABC-transporter in the presence of its specific lantibiotic (Staron et al., 2011).

In summary, three CprABC-type as well as BceAB-type ABC transporters are mentioned in detail, which are all well studied so far in order to highlight both their functional properties and the differences between these two groups. Within the CprABC group, we have included the NisFEG ABC transporter, which confers immunity against nisin in the producer strains. General characteristics including protein sequence, size, and function of these systems are listed in **Tables 1**, **2**.

CprABC RESISTANCE SYSTEMS

The CprABCK-R System from *C. difficile*

The operon of the *cpr* (*c*ationic antimicrobial *p*eptide *r*esistance) system from *C. difficile* consists of an ABC transporter and a TCS. The genetic organization of the Cpr system resembles the immunity system found in lantibiotic producing strains (see above).

The CprABC transporter from *C. difficile* is encoded by three different proteins: a nucleotide binding domain called CprA (26 kDa) and the two transmembrane domains called CprB and CprC (27 and 29 kDa, respectively; **Figure 3** and **Table 1**). Both of the TMDs have six predicted transmembrane helices and form a functional heterodimer (**Table 1**).

The TCS is composed of a RR *cprR* (CD3320) and a HK *cprK* (CD1352). The histidine kinase of the Cpr system contains an extracellular loop (113 aa) (**Table 1**), which has been proposed to be involved in sensing. Such a loop is a general feature of histidine kinases. The regulator does not directly belong to the *cpr* operon and is distantly located on the chromosome (McBride and Sonenshein, 2011; Suárez et al., 2013).

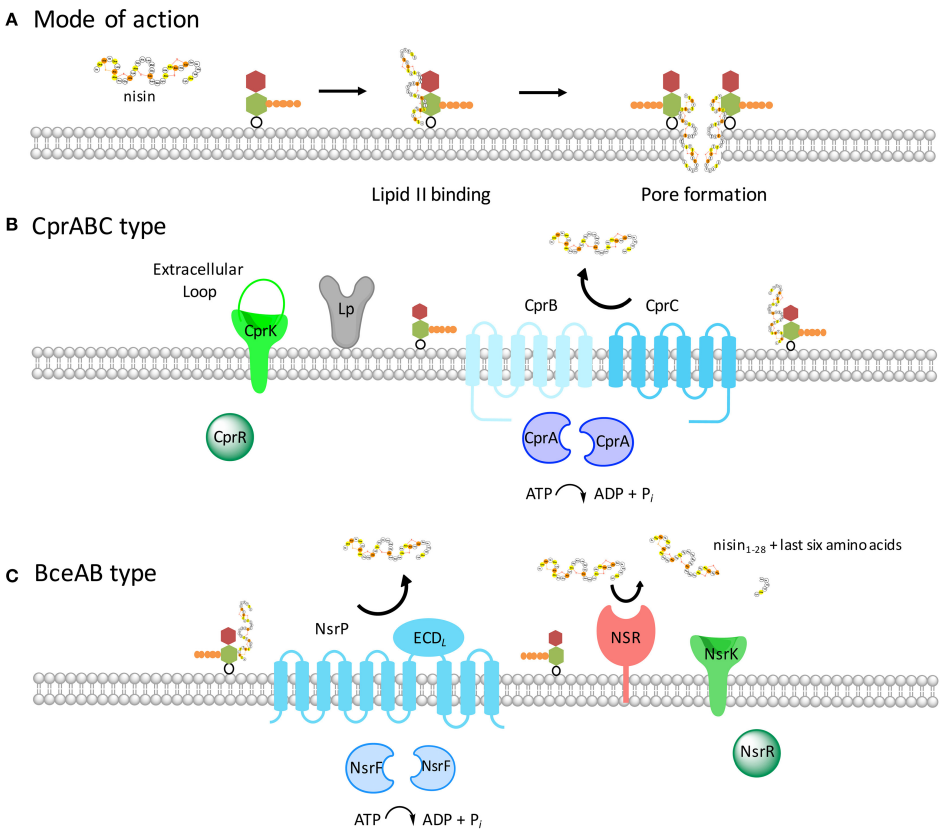

FIGURE 3 | Schematic representation of the two resistance systems of *C. difficile* and *S. agalactiae*. **(A)** The lantibiotic nisin A (see **Figure 1**) binds to the cell wall precursor lipid II, depicted with the N-acetyl glucosamine colored in red, the N-acetyl muramic acid shown in green and the pentapeptide presented in orange. The binding via the first two lanthionine rings of nisin to lipid II results growth inhibition and subsequently in pore formation. This results in rapid cell death already at nanomolar nisin concentrations. **(B)** The proteins encoded by the *cpr* operon are shown with the ABC transporter CprABC (depicted in blue) and the two-component system CprRK (depicted in green). The extracellular loop of the histidine kinase has also been shown. The lipoprotein adjacent to CprABC is depicted in gray. **(C)** The Nsr system of *S. agalactiae* is highlighted. The two-component system NsrRK and an efflux ABC transporter NsrFP are depicted in green and blue, respectively. The ECD_L present in the ABC transporter in between transmembrane helices seven and eight is indicated in cyan. Furthermore, an extra membrane-associated serine protease *Sa*NSR present in this system is shown in red. *Sa*NSR is a serine protease, which cleaves the last six amino acids of nisin off.

Within *C. difficile*, the *cpr* system has been shown to confer resistance against several lantibiotics such as nisin A, gallidermin, and subtilin. Although these lantibiotics are quite different in their amino acid composition, however the first two lanthionine rings are structurally conserved in their tertiary structure (Suárez et al., 2013), suggesting the importance of this region for the *cpr* genes to recognize lantibiotics. It was proposed that the lanthionine ring along with the proline and glycine residues form the sequence motif recognized by CprK resulting in signaling of the TCS CprK-CprR (Suárez et al., 2013).

The genes encoding the ABC transporter *cprABC* are regulated by *cprK-cprR* and are found adjacent to *cprK* in the genome. Insertional disruption of one of the transporter genes resulted in significant decrease in resistance against both nisin A and gallidermin. Hence, this TCS and ABC transporter pair contributes to the resistance of *C. difficile* toward many lantibiotics (Suárez et al., 2013). It has been shown that the addition of nisin induced the expression of CprABC, so it could be proven that the CprR is responsible for the upregulation (McBride and Sonenshein, 2011; Suárez et al., 2013).

Additionally, adjacent of the *cprABC* gene cluster, a lipoprotein is present (CD1348). Although, no involvement in lantibiotic resistance has been described so far, the genetic context resembles the BceAB system found in *S. agalactiae*, which contains the *Sa*NSR protein, a membrane associated resistance protein (see below). Interestingly, the lipoprotein is not upregulated by the presence of a lantibiotic or antimicrobial peptide and displays a basal expression level (Suárez et al., 2013).

TABLE 1 | Comparison of the different Cpr-type resistance systems with the TCS and the ABC transporter.

	CprABCK-R	*LcrSR-LctFEG*	*NsrFE$_1$E$_2$G-XRK*	*NisRK-FEG*
Organism	*C. difficile (Strain630)*	*S. mutans (UA159)*	*S. mutans (UA159)*	*L. lactis (NZ9700)*
Defense category	Resistance	Resistance	Resistance	Immunity
Resistance against	nisin A, subtilin, gallidermin, mutacin 1140, cinnamycin	lacticin 481, nukacin ISK-I	nisin A	nisin A
TMD [aa]	238 (B) 252 (C)	246 (E) 242 (G)	82 (E1) 171 (E2) 248 (G)	242 (E) 214 (G)
Oligomeric state	Dimer (B+C)	Dimer (E+G)	Trimer (G+E1+E2)	Dimer (E+G)
TMHs	6+6	6+6	6+2+4	6+6
NBD [aa]	235	255	234	225
Response regulator [aa]	219	229	219	229
Histidine kinase [aa]	462	437	460	447
Loop-cont. protein	Kinase	Kinase	Kinase	Kinase
Loop size [aa]	113	117	116	112

TABLE 2 | Comparison of the different Bce-type resistance machineries with the TCS and the ABC transporter.

	BceRS-AB	*BraSR-VraDE*	*NsrFP-RK*
Organism	*B. subtilis (Strain 168)*	*S. aureus (USA300)*	*S. agalactiae* (COH1)
Defense category	Resistance	Resistance	Resistance
Resistance against	bacitracin, actagardine, mersacidin	bacitracin, nisin A, daptomycin	nisin A, nisin H, gallidermin
TMD	646	626	651
Oligomeric state	Monomer	Monomer	Monomer
TMHs	10	10	10
NBD [aa]	253	252	250
Response regulator [aa]	231	221	222
Histidine kinase [aa]	334	295	262
ECD_L cont. protein	TMD	TMD	TMD
ECD_L size[aa]	216	195	220

The LcrSR-LctFEG and NsrFE$_1$E$_2$G-XRK Resistance Systems

S. mutans (UA159) has two resistance systems, namely, the LcrSR-LctFEG and NsrFE$_1$E$_2$G-XRK. Both consist of a TCS and an ABC transporter.

The LcrSR-LctFEG system confers resistance against lacticin 481 and nukacin ISK-I as determined with growth inhibition analyses (Kawada-Matsuo et al., 2013a,b).

Within this system, LcrR (26 kDa) is the RR and the LcrS (50 kDa) is the HK, which also contains an extracellular sensing loop (117aa) (**Table 1**). The ABC transporter consists of three different domains. The NBD LctF (29 kDa), which is important for the ATP binding and hydrolysis, and two transmembrane domains, LctE (28 kDa) and LctG (27 kDa), which each consist of six transmembrane helices each (Kawada-Matsuo et al., 2013b).

The NsrFE$_1$E$_2$G-XRK system contains a TCS NsrRK with the NsrR (25 kDa) as RR and the NsrK (53 kDa) as HK containing an extracellular loop of 116 amino acids. The ABC transporter system contains four proteins: the NBD NsrF (26 kDa) and the three TMDs NsrE$_1$E$_2$G. Here, the NsrG (28 kDa) has six transmembrane helices, the NsrE$_1$ (10 kDa) has two and NsrE$_2$ (20 kDa) has four transmembrane helices, so in total 12, which is similar to the other known ABC transporters. However, for NsrFE$_1$E$_2$G resistance against only nisin A was observed, which was examined using deletional mutants within the NsrRK system. For other tested lantibiotics like nukacin ISK-1, no resistance could be observed (Kawada-Matsuo et al., 2013b).

The NisFEG Immunity Transporter from *L. lactis*

In the self-immunity system of nisin producing strains, the cytoplasmic NisF (25 kDa) is composed of 225 amino (Siegers and Entian, 1995). Additionally, NisE (28 kDa) and NisG (24 kDa) are predominantly hydrophobic proteins, that form together an integral membrane part of the ABC transporter and are composed of six transmembrane helices each (Siegers and Entian, 1995). Using sequence similarity searches NisFEG likely exhibits a 2:1:1 stoichiometry to form a functional lantibiotic immunity LanFEG transporter (Siegers and Entian, 1995). Various gene knockout studies have shown that out of all the three genes of the ABC transporter, deletion of *nisE* gene has the most detrimental effect on immunity (Siegers and Entian, 1995).

The primarily function of NisFEG in providing immunity to the producer strain is the efflux of nisin molecules from the membrane before they can form pores (Stein et al., 2003; AlKhatib et al., 2014b). A similar function has been identified for the subtilin immunity ABC transporter SpaFEG, which is able to transport subtilin from the cytoplasmic membrane directly back into the exterior (Stein et al., 2005).

When expressed in the nisin sensitive *L. lactis* strain NZ9000, which does not carry the immunity genes *nisI* and *nisFEG* within its genome, NisFEG confers seven to eight fold of immunity when expressed alone (AlKhatib et al., 2014b).

The substrate specificity of NisFEG has been extensively studied. It has been shown that NisFEG recognizes the C-terminally located lanthionine ring and the last six amino acids of nisin as a reduction of 50% in the immunity provided by NisFEG was seen upon deletion of either of them (AlKhatib et al., 2014b).

THE Bce RESISTANCE SYSTEMS

BceRS-AB System from *B. subtilis*

The BceRS-AB system from *B. subtilis* consists of the ABC transporter, with NBD BceA (28 kDa) and TMD BceB (72 kDa), and the TCS with the response regulator BceR (27 kDa) and the histidine kinase BceS (39 kDa) (**Figure 3** and **Table 2**). Various

growth inhibition assays of strains expressing BceRS-AB and several deletion mutants have shown, that this system mediates resistance against actagardine, mersacidin, and bacitracin (Ohki et al., 2003; Staron et al., 2011).

For signal transduction purposes, both the BceAB ABC transporter as well as the TCS need to be present to confer a signal transduction inducing upregulation of the genes encoded on the operon. This is an unusual mode of signal transduction, as the HK cannot sense bacitracin alone, and needs the presence of the ABC transporter to sense the substrate in the surrounding. Furthermore, an ATP hydrolysis deficient transporter mutant highlighted that hydrolysis is required for this signaling process (Rietkötter et al., 2008). Based on random mutagenesis studies it was shown that the C-terminal part of the TMD BceB, specifically up to helix VIII is important for signaling and resistance of the BceAB-RS system in *B. subtilis* (Kallenberg et al., 2013).

The BceAB from *B. subtilis* has been to the best of our knowledge, the only system which has been purified and shown to form a multicomponent complex with its designated TCS BceRS upon binding of bacitracin (Dintner et al., 2014). These biochemical analyses of the BceAB and BceRS proteins showed that the TCS, more specifically the BceS module, and the transporter form a so-called sensory complex in the cytoplasmic membrane, where the kinase activity is relying on the BceAB transporter (Dintner et al., 2014). This further underlines the fact that the BceAB transporter from *B. subtilis* is directly involved in bacitracin sensing and consequently triggers the upregulation of its own gene by the TCS BceRS. This was further highlighted by mathematical modeling response dynamics of the Bce system, which suggested a direct correlation between the transport activity of BceAB, and the BceS kinase signaling activity (Fritz et al., 2015).

BceAB-like transporters are thought to recognize the target-peptide complex within the membrane and not the peptide as such (Bernard et al., 2007; Rietkötter et al., 2008). This idea is further strengthened by experiments suggesting that BceAB of *B. subtilis* does not export bacitracin, but instead acts as a flippase of the target molecule undecaprenyl pyrophosphate (UPP) to the cytoplasmic side of the membrane (Kingston et al., 2014), thereby removing the target of bacitracin. However, Surface Plasmon Resonance (SPR) spectroscopy studies of BceAB have shown that the TMD BceB binds bacitracin with a high affinity (K_D of 60 nM) in detergent solution and appears to be specific for the active bacitracin-Zn^{2+}-complexed form (Dintner et al., 2014). Although these results do not rule out that a bacitracin-UPP complex is recognized by BceAB, it suggests an effluxing mechanism for bacitracin. Random mutagenesis studies further highlighted, that the C-terminal part of the TMD BceB up to helix VIII is important for the signaling and the resistance of the BceRS-AB system in *B. subtilis* (Kallenberg et al., 2013).

The VraDE-BraRS from *S. aureus*

The VraDE-BraRS system of *S. aureus* is a system composed of the NBD VraD (28 kDa), the TMD VraE (70 kDa), the response regulator BraR (25 kDa), and the histidine kinase BraS (34 kDa). This system has been identified in *S. aureus* since only two of the 16 TCSs present have been linked to the Bce family. Here, the TCS GraRS (Meehl et al., 2007) and the VraDE-BraRS system, mediate cationic antimicrobial peptide resistance (Hiron et al., 2011).

The VraDE-BraRS system of *S. aureus* confers resistance against bacitracin, nisin A and daptomycin as determined via growth inhibition experiments of *S. aureus* (Hiron et al., 2011; Popella et al., 2016). Transcriptional fusions using the operon promoter revealed increased expression when induced with increasing sub-lethal bacitracin and nisin concentrations as previously observed for the BceRS/BceAB module of *B. subtilis* (Ohki et al., 2003; Hiron et al., 2011). The TCS BraRS activates transcription of the *BraDE* and *VraDE* operons, encoding two ABC transporters, which play distinct and original roles in bacitracin and nisin resistance. Here, VraDE is a specific detoxification system and is sufficient to confer resistance against bacitracin and nisin when expressed alone (Hiron et al., 2011) whereas BraDE and BraRS are involved in antibiotic sensing and signaling, respectively.

The ABC transporter VraDE is directly involved in bacitracin resistance. By using chimeric ABC transporter and domain-swapping variants, where the extracellular loop of VraD was exchanged by the one of VraE, it was observed that the extracellular domain of VraE is the determinant for bacitracin specificity (Hiron et al., 2011; Popella et al., 2016). Furthermore, it was shown that VraH, a small transmembrane protein, is further an essential component of the VraDE complex to form the functional VraDEH complex. VraH of *S. aureus* JE2 is a positively charged C-terminus containing a conserved YYKRREEKGK motif. The cytoplasmic VraD interacts with the transmembrane protein VraH. This complex however is formed only in the presence of VraE (Popella et al., 2016). Interestingly, VraH is only important for resistance against gallidermin. Nisin and bacitracin resistance appears to be independent of VraH. This is rather unexpected since gallidermin and nisin share the same structural and mechanistic features, whereas bacitracin is structurally unrelated. Additionally, gallidermin does not form pores in the membranes of most bacteria in contrast to nisin, indicating another mode of action (Popella et al., 2016).

The BraRS TCS has been shown to be specific for nisin and no upregulation occurred when using other antibiotics like vancomycin, fosfomycin, oxacillin, colistin, capreomycin, viomycin, or daptomycin (Hiron et al., 2011).

The NsrFP-RK System from *S. agalactiae*

The NsrFP-RK system from *S. agalactiae* is composed of the NBD NsrF (28 kDa), the TMD NsrP (74 kDa), the RR NsrR (25 kDa), and the HK NsrK (31 kDa) (characteristics of the proteins are listed in **Table 2**; Khosa et al., 2013). Further, the NsrFP-RK system includes an additional serine protease *Sa*NSR, which inactivates nisin by cleaving off the last six amino acids. *Sa*NSR is anchored in the membrane via a single transmembrane segment (Khosa et al., 2016a). This system confers resistance to multiple lantibiotics such as nisin A, nisin H, and gallidermin as determined with growth inhibition experiments in *L. lactis* (Khosa et al., 2013; Reiners et al., 2017). Furthermore, it was shown by SYTOX-green assay, that the resistance conferred

by the ABC transporter NsrFP is imparted by the inhibiting pore formation in the cell membrane and similar to the CprABC system (see above), it also recognizes specifically the N-terminal part of lantibiotics (Reiners et al., 2017), suggesting a common substrate specificity between these systems. For NsrFP, this was shown by a comprehensive mutational analysis of nisin and comparison of the fold of resistance (Reiners et al., 2017), thereby sensitively quantifying and comparing the growth inhibition studies between lantibiotics and their variants (AlKhatib et al., 2014a,b; Reiners et al., 2017). An advantage of the NsrFP system is their heterologous expression in *L. lactis*, which allows a mutational analysis, and holds true for the predominant substrate nisin A. Furthermore, the corresponding NsrR (RR) and NsrK (HK) are not present, which allowed the characterization of the NsrFP ABC transporter alone.

For NsrFP, an efflux transport activity has been reported (Reiners et al., 2017). Here, a peptide release assay revealed the transport direction of NsrFP. The efflux of nisin was shown by the amount of nisin present in the supernatant of the cell culture in comparison to a strain harboring an empty plasmid as well as a transport deficient mutant of NsrFP. Furthermore, NsrFP is the BceAB-type transporter that actually suggests an efflux transport direction using a peptide release assay. These results are similar to those previously obtained for the lantibiotic immunity transporters NisFEG and SpaFEG from *L. lactis* and *B. subtilis*, respectively, which have been shown to export their corresponding lantibiotics (Stein et al., 2003, 2005).

On the contrary, the TCS NsrRK of the Nsr system has been poorly described so far. Here, NsrR belongs to the large OmpR/PhoB subfamily of response regulators. The structure of the regulator NsrR has been solved by X-ray crystallography and a model in active dimeric DNA-bound state was postulated (Khosa et al., 2016b). This model revealed that the amino acids involved in phosphorylation, dimerization, as well as DNA-binding are conserved on sequence level throughout the family of regulators found in the BceAB resistance systems identified, so far. This suggests that other BceAB-type response regulators will probably have a similar tertiary structural arrangement.

An extra feature of the NsrFP-RK system is the presence of a membrane-associated serine protease in the operon called *Sa*NSR, which cleaves nisin at its C-terminus and the product $nisin_{1-28}$ has been shown to be 20–100 fold less effective against Gram-positive bacteria membranes (Sun et al., 2009; Khosa et al., 2016a).

The structure of *Sa*NSR was solved at 2.2 Å resolution and displays an N-terminal helical bundle, a protease cap and core domain. Within the latter, the highly conserved TASSAEM region is present. This region contains the active site and lies in a hydrophobic tunnel. Extensive computational modeling of the *Sa*NSR/nisin complex revealed that *Sa*NSR specifically recognizes the C-terminus of nisin, more specifically the last two lanthionine rings of nisin ensuring the exact coordination of the nisin cleavage site at the TASSAEM region (Khosa et al., 2016a). This clearly indicates that in contrast to the efflux mechanism of the ABC transporter NsrFP, *Sa*NSR is highly specific to confer resistance solely against nisin A.

FUTURE DIRECTIONS

Since (multi-) antibiotic resistant bacteria have rapidly evolved during the last decades, the urgent need for novel compounds is increasing. The secretion of antimicrobial peptides by microorganisms represent a giant pool of novel compounds, which can be used as initial lead structures to develop novel antibiotics.

Here, lantibiotics as small ribosomally-synthesized antimicrobial peptides became relevant and due to genome sequencing the number of identified lantibiotics is rapidly growing. Lantibiotics bind to the essential pyrophosphate-sugar moiety of the cell wall precursor lipid II. This is in contrast to well-known glycopeptide antibiotics vancomycin and teicoplanin, which bind to the D-Ala-D-alanyl group of lipid II (Draper et al., 2015). Due to this, it is believed that new resistance mechanisms against lantibiotics are hard to establish for bacteria.

However, inherent resistance against lantibiotics and antimicrobial peptides are already present and are mediated by ABC transporters, Cpr- and Bce-type transporter, which are present in most human pathogenic bacterial strains. This hampers a wide usage of lantibiotics against severe bacterial infections.

The Cpr ABC transporters resembles the known LanFEG transporter found in lantibiotic producer strains, involved in (auto-)immunity suggesting an evolutionary link. In contrast, the Bce-type ABC transporters appear to be a novel and unique transporter family, interacting directly with the TCS in the presence of the lantibiotic (Khosa et al., 2013; Dintner et al., 2014). Mechanistically, both families are not very well-understood. For the Cpr systems, it has been observed that they are able to expel the lantibiotic from the membrane back into the extracellular media. This would suggest that inhibiting the transporter would allow the lantibiotic to penetrate the membrane again. Therefore, a compound specifically targeting the Cpr transporters would be ideal to use as a lead compound ensuring the potent activity of the lantibiotic itself. To achieve this, more knowledge has to be gained about the exact mechanism of these transporters. Although studies have been performed *in vivo*, the understanding of binding affinities of the lantibiotic toward the transporter as well as some structural studies will clearly be needed in future. Structurally, the Cpr transporter appears to be a different class of ABC transporter since none of known ABC transporter structures seems to be an useful template for molecular modeling approaches using available computer tools, which suggest that structural studies will be needed.

The mechanism of the Bce-type transporters is poorly understood. Recently, for the NsrFP system from *S. agalactiae*, an export function was reported using a peptide release assay (Reiners et al., 2017). Nevertheless, also a flippase activity of the target molecule lipid II of the ABC transporters would fit to the published studies, since the amount of the lantibiotic in the supernatant would also increase, if the target of the lantibiotic is not present anymore. This hypothesis is also in line with the studies of the BceAB transporter of *B. subtilis* by Kingston et al. (2014). This flippase activity would also explain why these Bce-type transporters appear to have a large substrate

spectrum and are able to confer resistance against structurally different lantibiotics as well as some antimicrobial peptides. Here a special focus might be present for the uncharacterized ECD_L, the hallmark of BceAB transporters. The function of this ECD_L is unknown, the structure remains elusive so far and further it is not proven that it interacts with the lantibiotic. Therefore, studies revealing function of this ECD_L would likely give a starting point for studies toward the identification of an inhibitor. Remarkable is the complex formation of the BceAB transporter with the TCS. This unusual partnership within the membrane results in a macromolecular complex, which is induced by the presence of the lantibiotic. A pioneering study of the BceAB system from B. subtilis suggests that a bacitracin-UPP complex is recognized by BceAB, recognized by the C-terminal part of the TMD BceB up to helix VIII (Kallenberg et al., 2013). Also the complex with the TCS has been shown to be at least stabilized via the TMD. Therefore, studies on the exact function of the ECD_L, both biochemically and structurally, will be needed to gain a full understanding of the BceAB system.

Both transporters (BceAB and CprABC) have in common that they are upregulated by a specific TCS induced by the peptide in the medium. Inhibiting the histidine kinase would therefore, be an excellent target for novel drugs, which then in combination with lantibiotics would be a treatment procedure.

Since lantibiotics are active in the low nanomolar range against strains without resistance mechanisms, their potential is clearly demonstrated. If the resistance mechanisms of both transporter families are understood, the first step to inhibit these has been taken, lantibiotics and its variants thereof will be able to fulfill their whole antimicrobial potential.

With novel lantibiotics being identified in new sequenced genomes, the full potential of these antimicrobial peptides has likely not been explored. Probably, for every new lantibiotic discovered a specific resistance system may be present in some human pathogens. Since all lantibiotics target a similar molecule within the target membrane, it is plausible that these resistance mechanisms will be similar to the Cpr and Bce systems, therefore they serve as model systems for lantibiotic resistance.

AUTHOR CONTRIBUTIONS

RC, JZ-K, and SS wrote the manuscript. RC and SK prepared the figures. RC, JZ-K, SK, and SS finalized the manuscript.

FUNDING

We gratefully acknowledge funding of the graduate school 2158 (GRK2158) of the Deutsche Forschungsgesellschaft (DFG).

ACKNOWLEDGMENTS

The authors would like to thank Lutz Schmitt and the Institute of Biochemistry for fruitful discussions and their support. We would like to thank Till Harrar for database searches.

REFERENCES

Alkhatib, Z., Abts, A., Mavaro, A., Schmitt, L., and Smits, S. H. (2012). Lantibiotics: how do producers become self-protected? *J. Biotechnol.* 159, 145–154. doi: 10.1016/j.jbiotec.2012.01.032

AlKhatib, Z., Lagedroste, M., Fey, I., Kleinschrodt, D., Abts, A., and Smits, S. H. (2014a). Lantibiotic immunity: inhibition of nisin mediated pore formation by NisI. *PLoS ONE* 9:e102246. doi: 10.1371/journal.pone.0102246

AlKhatib, Z., Lagedroste, M., Zaschke, J., Wagner, M., Abts, A., Fey, I., et al. (2014b). The C-terminus of nisin is important for the ABC transporter NisFEG to confer immunity in *Lactococcus lactis*. *Microbiologyopen* 3, 752–763. doi: 10.1002/mbo3.205

Alvarez-Sieiro, P., Montalban-Lopez, M., Mu, D., and Kuipers, O. P. (2016). Bacteriocins of lactic acid bacteria: extending the family. *Appl. Microbiol. Biotechnol.* 100, 2939–2951. doi: 10.1007/s00253-016-7343-9

Bernard, R., Guiseppi, A., Chippaux, M., Foglino, M., and Denizot, F. (2007). Resistance to bacitracin in *Bacillus subtilis*: unexpected requirement of the BceAB ABC transporter in the control of expression of its own structural genes. *J. Bacteriol.* 189, 8636–8642. doi: 10.1128/JB.01132-07

Bierbaum, G., and Sahl, H. G. (2009). Lantibiotics: mode of action, biosynthesis and bioengineering. *Curr. Pharm. Biotechnol.* 10, 2–18. doi: 10.2174/138920109787048616

Brumfitt, W., Salton, M. R., and Hamilton-Miller, J. M. (2002). Nisin, alone and combined with peptidoglycan-modulating antibiotics: activity against methicillin-resistant *Staphylococcus aureus* and vancomycin-resistant enterococci. *J. Antimicrob. Chemother.* 50, 731–734. doi: 10.1093/jac/dkf190

Chatterjee, C., Paul, M., Xie, L., and van der Donk, W. A. (2005). Biosynthesis and mode of action of lantibiotics. *Chem. Rev.* 105, 633–684. doi: 10.1021/cr030105v

Cleveland, J., Montville, T. J., Nes, I. F., and Chikindas, M. L. (2001). Bacteriocins: safe, natural antimicrobials for food preservation. *Int. J. Food Microbiol.* 71, 1–20. doi: 10.1016/S0168-1605(01)00560-8

Cotter, P. D., Hill, C., and Ross, R. P. (2005a). Bacterial lantibiotics: strategies to improve therapeutic potential. *Curr. Protein Pept. Sci.* 6, 61–75. doi: 10.2174/1389203053027584

Cotter, P. D., Hill, C., and Ross, R. P. (2005b). Bacteriocins: developing innate immunity for food. *Nat. Rev. Microbiol.* 3, 777–788. doi: 10.1038/nrmicro1273

Cotter, P. D., Ross, R. P., and Hill, C. (2012). Bacteriocins—a viable alternative to antibiotics? *Nat. Rev. Microbiol.* 11, 95–105. doi: 10.1038/nrmicro2937

Delves-Broughton, J., Blackburn, P., Evans, R., and Hugenholtz, J. (1996). Applications of the bacteriocin, nisin. *Antonie Van Leeuwenhoek* 69, 193–202. doi: 10.1007/BF00399424

Dintner, S., Heermann, R., Fang, C., Jung, K., and Gebhard, S. (2014). A sensory complex consisting of an ATP-binding cassette transporter and a two-component regulatory system controls Bacitracin resistance in *Bacillus subtilis*. *J. Biol. Chem.* 289, 27899–27910. doi: 10.1074/jbc.M114.596221

Dintner, S., Staron, A., Berchtold, E., Petri, T., Mascher, T., and Gebhard, S. (2011). Coevolution of ABC transporters and two-component regulatory systems as resistance modules against antimicrobial peptides in Firmicutes Bacteria. *J. Bacteriol.* 193, 3851–3862. doi: 10.1128/JB.05175-11

Draper, L. A., Cotter, P. D., Hill, C., and Ross, R. P. (2015). Lantibiotic resistance. *Microbiol. Mol. Biol. Rev.* 79, 171–191. doi: 10.1128/MMBR.00051-14

Draper, L. A., Ross, R. P., Hill, C., and Cotter, P. D. (2008). Lantibiotic immunity. *Curr. Protein Pept. Sci.* 9, 39–49. doi: 10.2174/138920308783565750

Falord, M., Karimova, G., Hiron, A., and Msadek, T. (2012). GraXSR proteins interact with the VraFG ABC transporter to form a five-component system required for cationic antimicrobial peptide sensing and resistance in *Staphylococcus aureus*. *Antimicrob. Agents Chemother.* 56, 1047–1058. doi: 10.1128/AAC.05054-11

Fritz, G., Dintner, S., Treichel, N. S., Radeck, J., Gerland, U., Mascher, T., et al. (2015). A new way of sensing: need-based activation of antibiotic resistance by a flux-sensing mechanism. *mBio* 6:e00975. doi: 10.1128/mBio.00975-15

Gebhard, S. (2012). ABC transporters of antimicrobial peptides in Firmicutes bacteria–phylogeny, function and regulation. *Mol. Microbiol.* 86, 1295–1317. doi: 10.1111/mmi.12078

Gebhard, S., and Mascher, T. (2011). Antimicrobial peptide sensing and detoxification modules: unravelling the regulatory circuitry of *Staphylococcus aureus*. *Mol. Microbiol.* 81, 581–587. doi: 10.1111/j.1365-2958.2011.07747.x

Héchard, Y., and Sahl, H.-G. (2002). Mode of action of modified and unmodified bacteriocins from Gram-positive bacteria. *Biochimie* 84, 545–557. doi: 10.1016/S0300-9084(02)01417-7

Heijenoort, J. V. (1994). Biosynthesis of the bacterial peptidoglycan unit. *New Compr. Biochem.* 27, 39–54. doi: 10.1016/S0167-7306(08)60406-8

Hiron, A., Falord, M., Valle, J., Débarbouillé, M., and Msadek, T. (2011). Bacitracin and nisin resistance in *Staphylococcus aureus*: a novel pathway involving the BraS/BraR two-component system (SA2417/SA2418) and both the BraD/BraE and VraD/VraE ABC transporters. *Mol. Microbiol.* 81, 602–622. doi: 10.1111/j.1365-2958.2011.07735.x

Jung, G. (1991). Lantibiotics-ribosomally sythesized biologically acve polypeptides containing sulfide bridges and α,β-didehyroamino acids. *Angew. Chem. Int. Edn. English* 30, 1051–1068. doi: 10.1002/anie.199110513

Kallenberg, F., Dintner, S., Schmitz, R., and Gebhard, S. (2013). Identification of regions important for resistance and signalling within the antimicrobial peptide transporter BceAB of *Bacillus subtilis*. *J. Bacteriol.* 195, 3287–3297. doi: 10.1128/JB.00419-13

Kawada-Matsuo, M., Oogai, Y., Zendo, T., Nagao, J., Shibata, Y., Yamashita, Y., et al. (2013a). Involvement of the novel two-component NsrRS and LcrRS systems in distinct resistance pathways against Nisin A and Nukacin ISK-1 in *Streptococcus mutans*. *Appl. Environ. Microbiol.* 79, 4751–4755. doi: 10.1128/AEM.00780-13

Kawada-Matsuo, M., Yoshida, Y., Zendo, T., Nagao, J., Oogai, Y., Nakamura, Y., et al. (2013b). Three distinct two-component systems are involved in resistance to the class I bacteriocins, nukacin ISK-1 and nisin A, in *Staphylococcus aureus*. *PLoS ONE* 8:e69455. doi: 10.1371/journal.pone.0069455

Khosa, S., Alkhatib, Z., and Smits, S. H. (2013). NSR from *Streptococcus agalactiae* confers resistance against nisin and is encoded by a conserved nsr operon. *Biol. Chem.* 394, 1543–1549. doi: 10.1515/hsz-2013-0167

Khosa, S., Frieg, B., Mulnaes, D., Kleinschrodt, D., Hoeppner, A., Gohlke, H., et al. (2016a). Structural basis of lantibiotic recognition by the nisin resistance protein from *Streptococcus agalactiae*. *Sci. Rep.* 6:18679. doi: 10.1038/srep18679

Khosa, S., Hoeppner, A., Gohlke, H., Schmitt, L., and Smits, S. H. (2016b). Structure of the response regulator NsrR from *Streptococcus agalactiae*, which is involved in lantibiotic resistance. *PLoS ONE* 11:e0149903. doi: 10.1371/journal.pone.0149903

Kingston, A. W., Zhao, H., Cook, G. M., and Helmann, J. D. (2014). Accumulation of heptaprenyl diphosphate sensitizes *Bacillus subtilis* to bacitracin: implications for the mechanism of resistance mediated by the BceAB transporter. *Mol. Microbiol.* 93, 37–49. doi: 10.1111/mmi.12637

Kuipers, O. P., Beerthuyzen, M. M., de Ruyter, P. G., Luesink, E. J., and de Vos, W. M. (1995). Autoregulation of nisin biosynthesis in *Lactococcus lactis* by signal transduction. *J. Biol. Chem.* 270, 27299–27304. doi: 10.1074/jbc.270.45.27299

Mascher, T. (2006). Intramembrane-sensing histidine kinases: a new family of cell envelope stress sensors in Firmicutes bacteria. *FEMS Microbiol. Lett.* 264, 133–144. doi: 10.1111/j.1574-6968.2006.00444.x

Mascher, T., Margulis, N. G., Wang, T., Ye, R. W., and Helmann, J. D. (2003). Cell wall stress responses in *Bacillus subtilis*: the regulatory network of the bacitracin stimulon. *Mol. Microbiol.* 50, 1591–1604. doi: 10.1046/j.1365-2958.2003.03786.x

McBride, S. M., and Sonenshein, A. L. (2011). The dlt operon confers resistance to cationic antimicrobial peptides in *Clostridium difficile*. *Microbiology* 157, 1457–1465. doi: 10.1099/mic.0.045997-0

Meehl, M., Herbert, S., Götz, F., and Cheung, A. (2007). Interaction of the GraRS two-component system with the VraFG ABC transporter to support vancomycin-intermediate resistance in *Staphylococcus aureus*. *Antimicrob. Agents Chemother.* 51, 2679–2689. doi: 10.1128/AAC.00209-07

Ohki, R., Giyanto, Tateno, K., Masuyama, W., Moriya, S., Kobayashi, K., et al. (2003). The BceRS two-component regulatory system induces expression of the bacitracin transporter, BceAB, in *Bacillus subtilis*. *Mol. Microbiol.* 49, 1135–1144. doi: 10.1046/j.1365-2958.2003.03653.x

Popella, P., Krauss, S., Ebner, P., Nega, M., Deibert, J., and Gotz, F. (2016). VraH Is the third component of the *Staphylococcus aureus* VraDEH system involved in gallidermin and daptomycin resistance and pathogenicity. *Antimicrob. Agents Chemother.* 60, 2391–2401. doi: 10.1128/AAC.02865-15

Qiao, M., Ye, S., Koponen, O., Ra, R., Usabiaga, M., Immonen, T., et al. (1996). Regulation of the nisin operons in *Lactococcus lactis* N8. *J. Appl. Bacteriol.* 80, 626–634. doi: 10.1111/j.1365-2672.1996.tb03267.x

Reiners, J., Lagedroste, M., Ehlen, K., Leusch, S., Zaschke-Kriesche, J., and Smits, S. H. (2017). The N–terminal region of nisin is important for the BceAB-type ABC transporter NsrFP from *Streptococcus agalactiae* COH1. *Front. Microbiol.* 8:1643. doi: 10.3389/fmicb.2017.01643

Rietkötter, E., Hoyer, D., and Mascher, T. (2008). Bacitracin sensing in *Bacillus subtilis*. *Mol. Microbiol.* 68, 768–785. doi: 10.1111/j.1365-2958.2008.06194.x

Saier, M. H. Jr., Yen, M. R., Noto, K., Tamang, D. G., and Elkan, C. (2009). The transporter classification database: recent advances. *Nucleic Acids Res.* 37, D274–D278. doi: 10.1093/nar/gkn862

Siegers, K., and Entian, K. (1995). Genes involved in immunity to the lantibiotic nisin produced by *Lactococcus lactis* 6F3. *Appl. Environ. Microbiol.* 61, 1082–1089.

Singh, M., and Sareen, D. (2014). Novel LanT associated lantibiotic clusters identified by genome database mining. *PLoS ONE* 9:e91352. doi: 10.1371/journal.pone.0091352

Staron, A., Finkeisen, D. E., and Mascher, T. (2011). Peptide antibiotic sensing and detoxification modules of *Bacillus subtilis*. *Antimicrob. Agents Chemother.* 55, 515–525. doi: 10.1128/AAC.00352-10

Stein, T., Heinzmann, S., Düsterhus, S., Borchert, S., and Entian, K.-D. (2005). Expression and functional analysis of the subtilin immunity genes spaIFEG in the subtilin-sensitive host *Bacillus subtilis* MO1099. *J. Bacteriol.* 187, 822–828. doi: 10.1128/JB.187.3.822-828.2005

Stein, T., Heinzmann, S., Solovieva, I., and Entian, K.-D. (2003). Function of *Lactococcus lactis* nisin immunity genes nisI and nisFEG after coordinated expression in the surrogate host *Bacillus subtilis*. *J. Biol. Chem.* 278, 89–94. doi: 10.1074/jbc.M207237200

Suárez, J. M., Edwards, A. N., and McBride, S. M. (2013). The *Clostridium difficile* cpr locus is regulated by a noncontiguous two-component system in response to type A and B lantibiotics. *J. Bacteriol.* 195, 2621–2631. doi: 10.1128/JB.00166-13

Sun, Z., Zhong, J., Liang, X., Liu, J., Chen, X., and Huan, L. (2009). Novel mechanism for nisin resistance via proteolytic degradation of nisin by the nisin resistance protein NSR. *Antimicrob. Agents Chemother.* 53, 1964–1973. doi: 10.1128/AAC.01382-08

Tagg, J. R., Dajani, A. S., and Wannamaker, L. W. (1976). Bacteriocins of gram-positive bacteria. *Bacteriol. Rev.* 40, 722–756.

Tracanna, V., de Jong, A., Medema, M. H., and Kuipers, O. P. (2017). Mining prokaryotes for antimicrobial compounds: from diversity to function. *FEMS Microbiol. Rev.* 41, 417–429. doi: 10.1093/femsre/fux014

van Heel, A. J., de Jong, A., Montalban-Lopez, M., Kok, J., and Kuipers, O. P. (2013a). BAGEL3: automated identification of genes encoding bacteriocins and (non-)bactericidal posttranslationally modified peptides. *Nucleic Acids Res.* 41, W448–W453. doi: 10.1093/nar/gkt391

van Heel, A. J., Mu, D., Montalban-Lopez, M., Hendriks, D., and Kuipers, O. P. (2013b). Designing and producing modified, new-to-nature peptides with antimicrobial activity by use of a combination of various lantibiotic modification enzymes. *ACS Synth. Biol.* 2, 397–404. doi: 10.1021/sb3001084

Willey, J. M., and van der Donk, W. A. (2007). Lantibiotics: peptides of diverse structure and function. *Annu. Rev. Microbiol.* 61, 477–501. doi: 10.1146/annurev.micro.61.080706.093501

Conflict of Interest Statement: The authors declare that the research was conducted in the absence of any commercial or financial relationships that could be construed as a potential conflict of interest.

The reviewer CC and handling Editor declared their shared affiliation.

3.2. Chapter II - Lantibiotic maturation complex

Published in: Scientific reports

Impact factor: 4.847

Own work: 15 %

Protein purification

Interaction studies with ring mutations

SDS-PAGE analysis

Stoichiometry and structure of a lantibiotic maturation complex

Jens Reiners, Andrè Abts, **Rebecca Clemens,** Sander H. J. Smits and Lutz Schmitt

www.nature.com/scientificreports

SCIENTIFIC REPORTS

OPEN

Stoichiometry and structure of a lantibiotic maturation complex

Jens Reiners, André Abts, Rebecca Clemens, Sander H. J. Smits & Lutz Schmitt

Received: 24 June 2016
Accepted: 06 January 2017
Published: 07 February 2017

Lantibiotics are ribosomally synthesized antimicrobial peptides secreted by mainly Gram-positive bacteria. Class 1 lantibiotics mature via two modification steps introduced by a modification LanBC complex. For the lantibiotic nisin, the dehydratase NisB catalyzes the dehydration of serine and threonine residues in the so-called core peptide. Second, five (methyl)-lanthionine rings are introduced in a regio- and stereospecific manner by the cyclase NisC. Here, we characterized the assembly of the NisBC complex *in vitro*, which is only formed in the presence of the substrate. The complex is composed of a NisB dimer, a monomer of NisC and one prenisin molecule. Interestingly, the presence of the last lanthionine ring prevented complex formation. This stoichiometry was verified by small-angle X-ray scattering measurements, which revealed the first structural glimpse of a LanBC complex in solution.

Bacteriocins are a group of antimicrobial peptides produced by Gram-positive as well as Gram-negative bacteria and some of them undergo posttranslational modifications (PTM(s))[1,2]. Within bacteria they mostly remain inactive and are secreted via dedicated transport systems. So far, more than 750 different bacteriocins have been isolated from natural sources[1] and the number constantly rises. Within the group of bacteriocins, a subfamily consists of ribosomally synthesized and posttranslational modified peptides, which are called lantibiotics. Here, non-natural amino acids and specific structures, which have an essential role on activity (e.g. lanthionine rings, dehydrated amino acids, heterocycles or head to tail cyclization of the peptide) are posttranslationally introduced. Common to all class I lantibiotics is a N-terminal leader sequence, which is crucial for the recognition by the PTM enzymes, secretion and for keeping the peptide in an inactive state within the cell. This leader sequence, which is often also called leader peptide, is fused to the so-called core peptide, in which all modifications occur.

Lanthipeptides contain the non-natural amino acids lanthionine or (methyl)-lanthionine and in case that they also display antimicrobial activity, these peptides are consequently called lantibiotics[3,4]. They are classified in four different classes (Type I-IV) depending on the enzymes involved in the PTM(s)[3,4]. Up to now, however, antimicrobial activities have only been reported for members of class I and II. Type I lantibiotics are modified by two different PTM enzymes, a lantibiotic dehydratase, LanB, and a lantibiotic cyclase, LanC. The enzyme LanB dehydrates specifically serine or threonine residues, whereas LanC catalyzes the thioether ring formation of the dehydrated amino acid and a C-terminally located cysteine residue within the core peptide via a Michael addition reaction[5]. This results in the formation of lanthionine (from Ser) or (methyl)-lanthionine (from Thr) rings, which are crucial for the activity as well as stability[6–12]. Type II lantibiotics are modified by a single enzyme called LanM, which catalyzes both, the dehydration and cyclization reaction, respectively[13]. In all cases the genes encoding the lantibiotic as well as the PTM enzymes are localized within in a single gene cluster and are valuable probes to identify lantibiotic operons in newly sequenced genomes[14].

Nisin is a class I lantibiotic produced by several *Lactococcus lactis* (*L. lactis*) strains[15–17]. It contains characteristic dehydrated amino acids and five (methyl)-lanthionine rings, named rings A to E[18,19]. These rings are essential for the antimicrobial activity displayed against numerous Gram-positive bacteria[8,20,21]. The leader peptide as elaborated above is responsible for the recognition by the PTM enzymes, here called NisB and NisC, and furthermore is essential for the subsequent secretion by the ABC transporter, here called NisT[22–28].

In detail, NisB dehydrates serine and threonine residues in the core peptide after ribosomal synthesis of nisin[29–32]. Seminal work on the mechanism of the dehydration reaction has demonstrated that a glutamate is transferred from glutamyl-$tRNA^{Glu}$ to specific Ser/Thr side chains within the nisin core peptide introducing glutamylated intermediates[29,33]. After glutamate elimination, these Ser/Thr residues are converted to dehydroalanine and dehydrobutyrine with absolute stereoselectivity. Subsequently, NisC catalyzes a Michael addition of a C-terminal cysteine residue with the corresponding dehydrated amino acids to form thioether rings, the characteristic (methyl)-lanthionine rings[5,30,34,35]. The entire maturation process is schematically summarized in

Institute of Biochemistry, Heinrich-Heine-University Duesseldorf, Universitaetsstraße 1, 40225 Duesseldorf, Germany. Correspondence and requests for materials should be addressed to L.S. (email: Lutz.Schmitt@hhu.de)

Supplementary Fig. 1. Although the activity of the single enzymes, NisB and NisC, has been demonstrated[29,33–35], the assembly of a lantibiotic PTM complex has so far not been described *in vitro*.

In 1996, the first study revealed an interaction between NisC and NisB as well as between NisC and the ABC transporter NisT[36]. Furthermore, information about the directionality of the modification reaction was obtained suggesting a N- to C-terminal modification mechanism[9]. This is apparently in contrast to the PTM complex involved in NAI-107 maturation where an opposite directionality (C- to N-terminal) was discussed, which still is not fully understood[37].

The PTM complex consisting of NisB-NisC-NisA was observed using a system that employed a His-tag fused to prenisin[38]. This allowed the isolation of the PTM complex from the cytosol of *L. lactis*. These associated proteins were identified as NisB and NisC, although in sub-stoichiometric amounts[38].

Structural information is available for both PTM enzymes, NisB and NisC. However, this information is restricted to the isolated states of both enzymes. Two structures of lantibiotic dehydratases have been published[33,37]. The structure of NisB in complex with its substrate from *L. lactis*[33] as well as the apo structure of MibB involved in NAI-107 biosynthesis from *Actinobacteria*[37] were reported. Despite the low sequence homology (approximately 20%), the topology and fold of both proteins were very similar[37]. Interestingly, the amino acids involved in glutamylation and glutamate elimination are structurally highly conserved in both enzymes, which obviously suggests a fundamental similar mechanism of dehydration. The structure of NisC in the apo state has been solved with the catalytically important Zn^{2+} ion[34,35].

Despite our increased knowledge of the nisin maturation reaction, little if any information about the complex stoichiometry of the PTM NisBC complex is available. Furthermore, the complex assembling process remains unclear. The nisin maturation machinery has been successfully explored to install PTMs in therapeutic peptides[39–41]. This substrate spectrum can be even further extended if the PTM complex could be employed *in vitro*.

Here, we describe for the first time an *in vitro* study revealing the formation of the nisin maturation complex composed of NisB, NisC and either unmodified or dehydrated prenisin peptide. Prenisin presents the essential trigger to initiate the *in vitro* formation of the maturation complex. Here, the -FNLD- box located within the leader sequence was identified as the crucial part in triggering complex assembly. Furthermore, our data demonstrated that the nisin PTM machinery consists of a functional dimer of NisB, a monomer of NisC and a single prenisin peptide. Once all rings are installed, as in fully modified prenisin peptide, the complex cannot assemble anymore suggesting a releasing factor upon formation of the last ring. Finally, structural information of the nisin modification complex was obtained by small-angle X-ray scattering (SAXS). Here, the same stoichiometry of the PTM complex was determined and revealed a tunnel located at the interface of NisB and NisC harboring the prenisin substrate. This result supports our *in vitro* studies and provides the first molecular picture of a class I lantibiotic maturation complex.

Results

Characterization of the modification enzymes NisB, NisC and the prenisin variants. Nisin contains several PTMs introduced by a proposed complex of NisB and NisC in an alternating manner[9]. To investigate the assembly of such a complex, we purified NisB and NisC to homogeneity. Previously, it was shown for NisC that the N-terminal His_6-tag interfered with substrate binding and was therefore removed by thrombine cleavage prior to complex formation[22]. Both proteins were purified to a highly pure state as judged from SDS-PAGE analysis (Supplementary Fig. 2A and B). The oligomeric state of isolated NisB or NisC was analyzed via a combination of multi-angle light scattering and size exclusion chromatography (MALS-SEC)[22,25]. NisB is a dimer with a molecular weight of 237.5 ± 0.3 kDa (Supplementary Fig. 2C) and NisC is a monomer with a molecular weight of 48.1 ± 0.5 kDa. (Supplementary Fig. 2D) as previously reported[22,25]. The prenisin peptide and its variants were expressed and secreted by *L. lactis* NZ9000 and isolated via cation exchange chromatography as described[22,25] (Supplementary Fig. 3).

Prior to the complex formation studies, the ability of the single proteins to bind prenisin was tested using MALS-SEC. Here, a dimer of NisB binds one unmodified prenisin molecule[25] and the monomer of NisC binds also one unmodified prenisin molecule[22] (Supplementary Fig. 4A and B) resulting in an increase of the observed molecular masses to 54.5 ± 0.6 kDa for NisC and 241.9 ± 0.4 kDa for NisB, respectively. Thus, purified NisB and NisC are capable to binding unmodified prenisin peptide. Higher amounts of prenisin did not result in higher molecular masses suggesting that both protein can only bind one prenisin molecule.

PTM complex assembly. To assemble the nisin PTM complex *in vitro* we incubated NisB and NisC in different molar ratios ranging from 1:1 to 1:8 for 1 h at 25 °C and analyzed a potential complex formation by MALS-SEC. This resulted in two clearly separated elution peaks occurring at 7.4 min and 9.0 min. The first peak contained dimeric NisB with a theoretical molecular mass of 236.6 kDa (Fig. 1, black dashed line) and the second peak contained only NisC with a theoretical molecular weight of 48.5 kDa (not shown). To analyze this further we subjected single elution fractions of the SEC experiment to SDS-PAGE analysis (Supplementary Fig. 5) combined with Western blotting (Fig. 2A) using polyclonal antibodies against NisB and NisC, respectively. This revealed that NisB, even in the presence of a high excess of NisC, formed no complex with NisC (Fig. 1, black dashed line, Fig. 2A).

Next PTM complex formation was analyzed under conditions, in which either of the two enzymes, NisB or NisC, was preloaded with unmodified prenisin peptide. Upon saturation of NisB with unmodified prenisin peptide and subsequent incubation with 20 μM NisC prior to complex formation, a molecular mass of 263.8 ± 0.3 kDa was observed. This indicated formation of a NisB-NisC-NisA complex. When NisC was first saturated with unmodified prenisin peptide and subsequently incubated with 20 μM NisB, a molecular weight of 247.1 ± 0.4 kDa was observed for NisB (Supplementary Fig. 6).

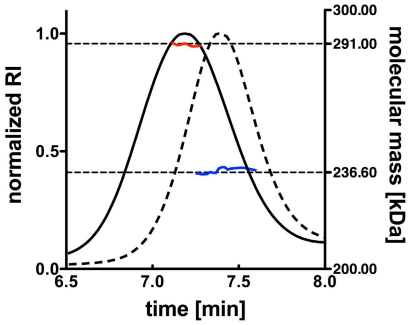

Figure 1. MALS-SEC analysis of the mixed protein samples consisting of NisB and NisC, in the presence or absence of the dehydrated prenisin peptide. The dashed black graph shows the elution profile of a mixture of 20 μM NisB and 160 μM NisC resulting in a molecular weight of 237.5 ± 0.3 kDa (blue line). The analysis of 20 μM NisB, 160 μM NisC and 200 μM dehydrated prenisin peptide is shown by the black graph, revealing an apparent molecular weight of 291.2 ± 0.9 kDa (red line) of the formed complex. The two black dotted lines indicate the theoretical molecular weight of an isolated NisB (236.6 kDa) dimer and of a complex consisting of a NisB dimer, a monomer of NisC and one prenisin peptide molecule (291 kDa).

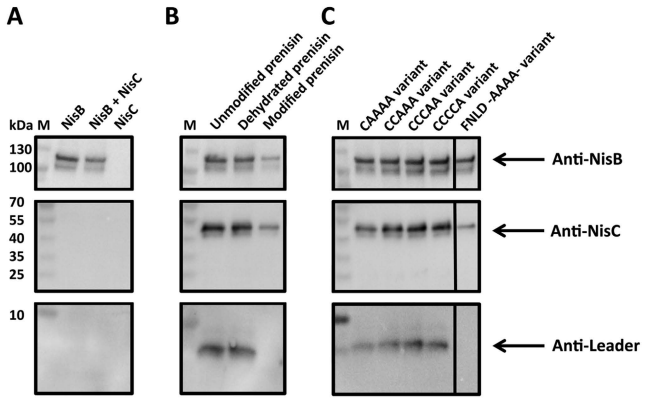

Figure 2. Western blot analysis of the PTM complex containing fraction. Elution fractions marked with a red box in the corresponding SDS-PAGE gels (Supplementary Figs 5, 7 and 8) were used for further analysis. The antibodies used are indicated with an arrow. (**A**) **M**: protein marker. **NisB**: The fraction resulting of the analytical SEC of 20 μM NisB. NisB and NisC: This sample represents the interaction analysis of 20 μM NisB and 160 μM NisC. **NisC**: The fraction resulting of the analytical SEC of 160 μM NisC. (**B**,**C**) In the following lanes the results of the complex formation for the different prenisin peptide variants are shown. PTM complex is formed and consists of NisB, NisC and prenisin peptide.

This demonstrates that the presence of unmodified prenisin peptide triggers complex formation. However, the molecular mass determined in both experiments did not fit to any theoretically combination of the three components (1: 1: 1 or 2: 1: 1 or 2: 2: 2 or any other ratio) (Supplementary Table 2). This suggested that a fully assembled NisB-NisC-NisA complex with equimolar concentrations of NisB and NisC and an excess of unmodified prenisin peptide was not obtained under these experimental conditions.

To obtain a fully assembled complex, we kept the concentration of NisB constant at 20 μM as well as the 10 fold-excess of unmodified prenisin peptide (200 μM). We increased the concentration of NisC stepwise from 10 μM to 160 μM and analyzed the molecular weights of the formed complexes via MALS-SEC. Here, we observed a gradual increase of the molecular weight at NisC concentrations of up to 80 μM (Fig. 3 and Supplementary Table 1). Further increase of the NisC concentrations to 160 μM did not change the observed molecular weight of 293.6 ± 1.2 kDa any further (Fig. 3, Table 1 and for a detailed view Supplementary Table 1). This suggested the presence of a stable complex of NisC/NisB/unmodified prenisin peptide at NisC

NisB	NisC	NisA variants	Molekular weight [kDa]
+	–	—	237.5 ± 0.3
+	–	unmodified	241.9 ± 0.4
–	+	—	48.1 ± 0.5
–	+	unmodified	54.5 ± 0.6
+	+	unmodified	293.6 ± 1.2
+	+	dehydrated	291.2 ± 0.9
+	+	modified	250.4 ± 0.7
+	+	FNLD-Box	248.0 ± 0.9

Table 1. MALS-SEC data summarizing the molecular weight of the complex forming analysis for the different prenisin peptide variants and without any prenisin peptide. The theoretical molecular weight of a NisB dimer is calculated to 236.6 kDa, 48.5 kDa for a cleaved NisC monomer and 5.9 kDa for the unmodified prenisin peptide.

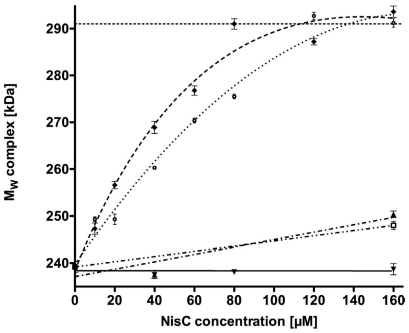

Figure 3. Assembly of the nisin maturation complex visualized via MALS-SEC. The molecular weight of the protein within the elution fraction was determined using MALS-SEC. The concentration of NisB (20 μM) and the different prenisin peptide variants (200 μM) were kept constant and the NisC concentration was varied (indicated on the X-axis). The upper dotted line shows the molecular weight of the theoretical PTM complex of 291 kDa. The molecular weight of NisB incubated with NisC is shown in ▼. With ♦, the molecular weight dependency of the complex with the unmodified prenisin peptide is shown. The dehydrated prenisin peptide profile corresponds to ○. The molecular weight of the complex in the presence of the modified prenisin peptide is indicated by ▲. □ represents the dependency of the molecular weight of the complex in the presence of the -FNLD- box (-AAAA-) variant.

concentrations of 80 μM or higher. The corresponding SDS-PAGE and Western blot analysis demonstrated the presence of both NisB and NisC in the elution fraction, together with the unmodified prenisin peptide (Fig. 2B and Supplementary Fig. 7A). After calculation of all possible stoichiometry's, the nisin PTM machinery possessed a stoichiometry of 2:1:1 (see Supplementary Table 2).

The modification state of nisin dictates complex formation. The unmodified prenisin peptide initiated complex formation between NisB and NisC (Figs 2 and 3). This raised the question whether the modification state within the prenisin core peptide modulates complex formation? We therefore repeated the experiment employing dehydrated or fully modified prenisin peptide. In the latter case, all (methyl)-lanthionine rings are present, while in the dehydrated prenisin core peptide all serine residues and threonine residues are dehydrated[31], but due to the lack of NisC during expression of prenisin, no (methyl)-lanthionine rings were introduced. We incubated the dehydrated and the fully modified prenisin peptide (200 μM) with 20 μM NisB and up to 160 μM NisC. We observed a complex of the PTM machinery after incubation of NisB and NisC with dehydrated prenisin peptide resulting in a molecular weight of 291.2 ± 0.9 kDa employing MALS-SEC analysis (Fig. 1 black line; Figs 2B and 3). This mass is identical within experimental error with the molecular weight determined for the unmodified prenisin peptide PTM enzyme complex. Importantly, an increase of the NisC concentration above 120 μM did not result in higher molecular weights indicating that no higher molecular weight PTM complex was formed (Figs 2B and 3, Table 1 and Supplementary Table 1). The corresponding SDS-PAGE analysis revealed the presence of NisB, NisC and dehydrated prenisin peptide in the elution fraction of the PTM enzyme complex (Supplementary Fig. 7B).

Incubating the fully modified prenisin peptide with NisB and NisC, resulted only in a small shift in the elution profile indicating that the modified prenisin peptide did not trigger complex formation (Figs 2B and 3, Table 1 and Supplementary Table 1 and Supplementary Fig. 7C). In MALS-SEC, a molecular weight of 250.4 ± 0.7 kDa was determined, which supported the idea of a weak interaction and reflects the lack of a stable PTM complex. Altogether, this demonstrated that fully modified prenisin peptide is not capable of inducing the formation of the completely assembled PTM complex, while unmodified and dehydrated prenisin peptide can do.

The role of the (methyl)-lanthionine rings in complex formation. Only the presence of unmodified and dehydrated prenisin peptide triggered complex formation (see above). To investigate whether one or more of the five rings inhibits complex formation, four prenisin peptide variants were produced only differing in the number of (methyl)-lanthionine rings within the core peptide. The native prenisin core peptide contains five cysteine residues giving rise to the five (methyl)-lanthionine rings A-E after modification (Supplementary Fig. 1). By exchanging these cysteine residues subsequently to alanine, prenisin peptide variants were created which vary in the number of (methyl)-lanthionine rings. The CAAAA variant contains only ring A, CCAAA rings A and B, CCCAA rings A-C and CCCCA rings A-D. Here the variants are expressed in the presence of NisB and NisC, which ensures that these variants are dehydrated and the lanthionine rings are present when a cysteine residue is still available. After purification, we incubated 20 μM NisB, 160 μM NisC and 200 μM of these different ring variants of the prenisin peptide for 1 h at 25 °C and analyzed the reaction mixtures by analytical SEC. The corresponding SDS-PAGE analysis is shown in Supplementary Fig. 8A–D. The analysis demonstrated that all ring deficient prenisin peptide variants are capable to form the PTM complex. In all cases, a co-elution of NisB, NisC and the prenisin peptide was observed. The co-elution fraction was furthermore analyzed by Western blot (Fig. 2C) to visualize the presence of NisB, NisC and the prenisin peptide variant used. This result demonstrates that the PTM complex is obtained, in the presence of at least one up to four (methyl)-lanthionine rings. Only when the last (methyl)-lanthionine ring (ring E) was present, i.e. fully modified prenisin peptide, no complex formation was detected. This suggests that coming to the last ring or dehydratable residue at the C-terminus might stimulate the dissociation of the entire PTM complex.

The recognition motive within the leader peptide: the -FNLD- box. We showed above that the modification state of the core peptide has a profound influence on complex formation. Next, we concentrated on the role of the N-terminal leader peptide in the assembly of the modification complex. The single NisB and NisC enzymes recognize the highly conserved -FNLD- box motif within the leader peptide[22,25]. MALS-SEC analysis using the -FNLD- to -AAAA- mutant resulted in a molecular weight of 248.0 ± 0.9 kDa, which indicated low efficiency of PTM complex formation (Figs 2C and 3, Table 1 and Supplementary Fig. 7D). The SDS-PAGE analysis of the analytical SEC revealed a minor shift of NisC and only low amounts of NisC co-eluted with NisB (Supplementary Fig. 7D). This suggests that the -FNLD- box has an important role during complex formation and demonstrated that both, the leader and the core peptide, are essential for the assembly of the nisin PTM complex. This is in line with the observations that this prenisin peptide variant is poorly modified *in vivo*[23,26,27,38].

Visualization of the nisin modification complex with small-angle x-ray scattering (SAXS). We used SAXS to obtain a structural glimpse of the fully assembled PTM complex. Here, we applied 200 μl of each enzyme, NisB (200 μM) and NisC (470 μM), respectively, on a Superdex 200 column and measured the X-ray scatter (Supplementary Fig. 9). We estimated the molecular weight from the POROD volumes[42] (Supplementary Table 3). This resulted in a molecular mass of 239.26 kDa for the NisB sample corresponding to a dimer, and in a molecular mass of 51.56 kDa for NisC, which corresponds to the monomeric state. These results fitted to the theoretically calculated masses deduced from the corresponding sequences (Supplementary Table 3) and were in-line with our MALS-SEC results (Table 1). Next we applied the same method to a NisB sample saturated with dehydrated prenisin peptide (200 μM NisB, 2 mM prenisin). Here, we incubated NisB with prenisin peptide, which should result in saturation of the enzyme. The calculated molecular weight of 256.54 kDa indicated that dehydrated prenisin peptide bound to NisB. The volumetric envelope was calculated from the background-subtracted scattering curves using DAMMIF[43] (Fig. 4).

The structure of NisB (PDB code 4WD9) and NisC (PDB code 2GOD), which were solved previously by X-ray crystallography, were superimposed into the volumetric envelopes using the program SUPCOMB[44] (Fig. 4), demonstrating that the envelope of the enzymes in solution nicely fitted to the published X-ray structures (Fig. 4). Interestingly in the map of the apo-NisB a tunnel on only one site of the envelope was observed (Fig. 5A), which might serve as an entrance to the binding site of prenisin. The leader sequence was visible in the X-ray structure of NisB and after fitting the model into the volumetric envelope obtained by SAXS, it was localized in close vicinity of the observed tunnel (highlighted in red in Fig. 5A). This further strengthens the suggestion that the tunnel might be the binding site for the prenisin molecule. This tunnel however appears to be closed in the volumetric envelope derived from our SAXS measurements of NisB saturated with dehydrated prenisin peptide. An overlay of both envelopes revealed that the tunnel is blocked in the NisB-dehydrated prenisin peptide map (Fig. 5B). Please note that the measurement of both samples were performed at similar concentrations and resulted in volumetric envelopes of comparable resolution. This suggests that the tunnel represents an opening for prenisin, which is blocked once prenisin is bound. Furthermore, this tunnel points into the active site of NisB and to the residues involved in the dehydration reaction as well as glutamylation[23,33,38].

Next we also measured the fully assembled PTM complex. This revealed a molecular weight of 275.1 kDa as deduced from the POROD volume indicating that the PTM complex was not fully assembled, which is likely due to the dilution effect occurring during SEC. Even after increasing the concentration of the PTM complex, the amount of formed complex did not increase. The different molecular weights from the POROD Volume were

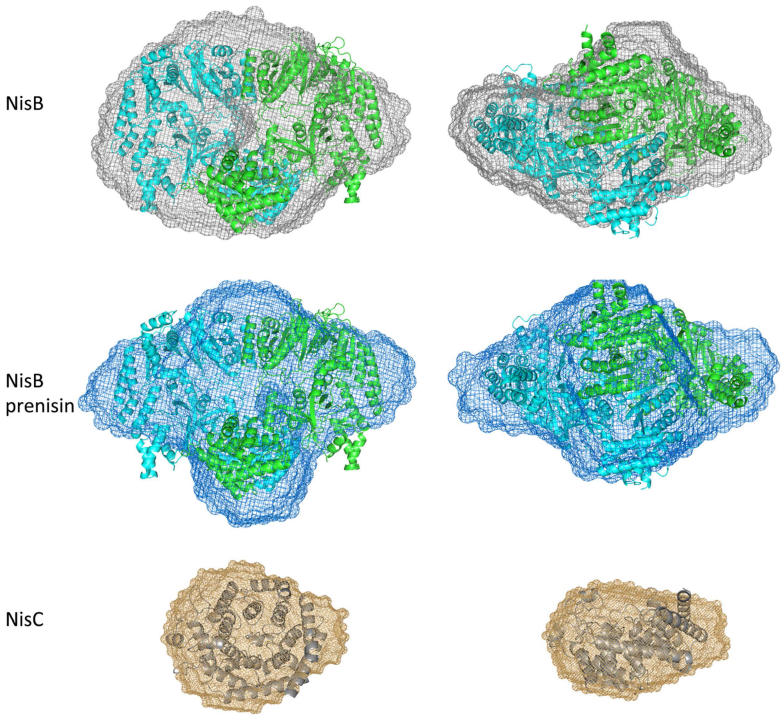

Figure 4. SAXS analysis of apo-NisB, NisB-prenisin and NisC. The volumetric envelopes are shown for NisB (grey mesh), NisB-prenisin (blue mesh) and NisC (orange mesh) as calculated from the scattering data using DAMMIF[43]. The structure of NisB (PDB code: 4WD9) and NisC (PDB code: 2GOD) were docked into the volumetric envelopes using SUPCOMB[44].

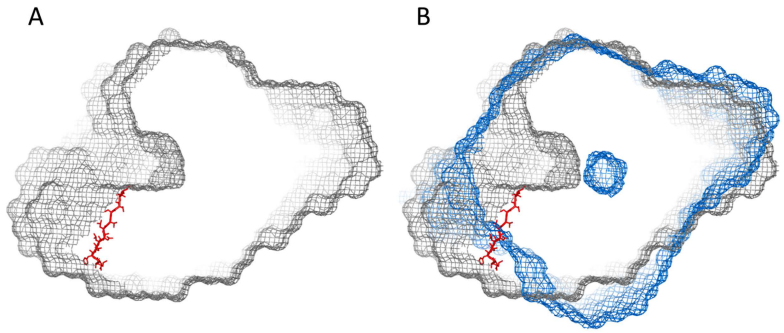

Figure 5. Comparison of the NisB and NisB-prenisin peptide volumetric envelopes as obtained by SAXS. (**A**) The volumetric envelope of NisB is shown as a grey mesh. A 30 Å clip was calculated around the leader peptide as derived from the fitted NisB structure (highlighted in red stick representation) (**B**) An overlay of the NisB envelope (grey mesh) and the NisB-dehydrated prenisin peptide envelope (blue mesh) highlighted that the observed tunnel is closed once dehydrated prenisin peptide is bound to NisB.

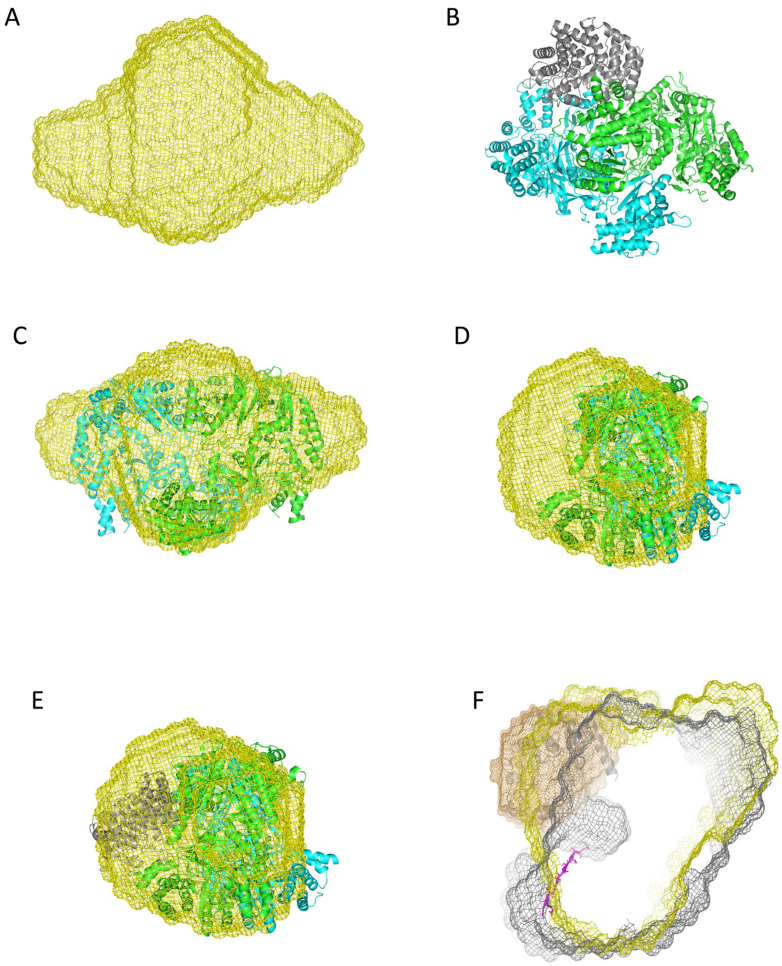

Figure 6. SAXS analysis of the fully assembled PTM complex. (**A**) The volumetric envelope of the fully assembled complex is shown as a yellow mesh. (**B**) The assembled PTM complex as deduced from the program SASREF[54] (The monomers of NisB are colored in blue and green, NisC in dark orange). (**C**) Front view of the PTM complex with only NisB highlighted, (**D**) side view of the PTM complex with only NisB highlighted, (**E**) fully assembled PTM complex with the complex aligned to the volumetric envelope. (**F**) Zoom in into the PTM complex identical to Fig. 5. The observed tunnel in NisB is occupied by dehydrated prenisin peptide and also NisC is located at the same interface of the protein.

also supported by the calculated Radius of Gyration (R_g) as well as estimated D_{max}. We could observe an increase for the PTM complex in comparison to isolated NisB (Supplementary Table 3). The overall shape of the obtained volumetric envelope revealed additional density on top of the NisB volume near the tunnel observed in the NisB experiment (Fig. 6A–D), suggesting that NisC is localized at that position. Furthermore, no additional volume large enough to accommodate another NisC molecule was observed. This demonstrates that the stoichiometry obtained by SAXS was identical to the stoichiometry deduced by SEC-MALS. Independently, we used the program SASREF to calculate the shape of the PTM complex using the structures of NisB and NisC and the experimental scattering data. Here a similar location of NisC was observed. NisC is again localized on top of the tunnel suggesting that this represents the stable conformation of the PTM complex *in vitro* (Fig. 6D–F). NisC has a bowl

like structure and the active site points again towards the tunnel (Fig. 6F). This suggests that NisC is localized next to the prenisin binding site observed for NisB within the PTM complex.

Discussion

Bacteriocins are peptides produced by bacteria and there is one specific class, called lanthipeptides, contains PTMs introduced by specific enzymes, which can be either a single protein (LanM) or two proteins (LanB and LanC, respectively)[3,13,16,17]. In the case of systems containing LanB and LanC, a complex of both enzymes is proposed to be the catalytically active species, but direct experimental evidence of its existence is rare. Here, we provide the first *in vitro* data on the assembly of the nisin PTM complex consisting of the dehydratase NisB and the cyclase NisC. The enzyme NisB and NisC are proposed to work in an alternating fashion to introduce the PTMs in the core section of the prenisin peptide[9]. We only observe the assembly of the PTM complex in the presence of unmodified and dehydrated prenisin peptide (Figs 2 and 3). This is in line with *in vivo* and *in vitro* data, in which direct interaction(s) between NisB and NisC was never observed without the presence of the substrate[3,17,36,38,45]. Purification of the prenisin peptide via an affinity tag directly from the cytosol of *L. lactis* resulted in elution fractions containing both, NisB as well as NisC[38]. This strongly suggested that a fully assembled maturation complex was present within the cytosol. The data presented here provides the first *in vitro* reconstitution of a lantibiotic PTM complex using the three separately purified components.

The stoichiometry of the PTM complex was determined to be 2:1:1 (NisB: NisC: prenisin peptide) by two independent approaches, SEC-MALS as well as SAXS.

The structure of NisB also revealed a dimeric organization with prenisin bound although electron density only for the region surrounding the -FNLD-box within the leader peptide was clearly visible[33]. Within this NisB structure the leader was detected in both monomers, which might be due to the simultaneous overexpression of both, NisB and prenisin, respectively, in combination with the lack of NisC. In the recently published structure of MibB, no substrate was observed[37]. While comparing the binding site of both enzymes, it became obvious that this particular region is rather flexible. This suggests that upon substrate binding NisB undergoes a conformational change as observed in the SAXS experiment. The differences are however subtle.

Interaction between NisB, NisC and the prenisin core peptide. Here, we demonstrated that complex formation between NisB and NisC strictly relies on the presence of prenisin, i.e. either the unmodified or the dehydrated peptide variant. When the cyclization reactions are completed and five (methyl)-lanthionine rings are present in the prenisin peptide, only a very minor amount of PTM complex can be obtained. This might reflect the *in vivo* situation, in which fully modified prenisin peptide is released from the PTM complex as soon as the (methyl)-lanthionine rings are formed and handed over to the dedicated transport system NisT. Since all three components were apparently localized at the membrane of *L. lactis*[36], it seems plausible that an even larger complex consisting of the PTM enzymes and the ABC transporter exists within the bacterial cell. Installing the lantibiotic PTMs and the subsequent secretion benefits from an efficient coupling of lantibiotic biosynthesis, maturation and secretion.

Within the leader peptide of class I lantibiotics, the -FNLD- box is highly conserved[26] and was identified as the recognition motif for the isolated enzymes NisB and NisC, respectively[22,25,38]. With the exchange of the -FNLD- motif against four alanines (-AAAA-), the formation of the PTM complex was drastically reduced (Figs 2 and 3 and Table 1). This is in contrast to *in vitro* results with isolated proteins, where no binding was observed[22,25]. But we have to stress that in these *in vitro* studies only low concentrations of the -AAAA- mutant of prenisin peptide were used and that the concentrations used in this study were several times higher. Nevertheless, our result clearly support that this highly conserved motif possesses a strong effect on complex formation as exemplified by the -AAAA- mutant. This was previously also highlighted by *in vivo* studies, which demonstrated that this variant is poorly modified and contains almost no dehydrations or cyclisation within its core peptide[23,26,27,38].

SAXS analysis revealed that in the apo-NisB structure a tunnel is present in close proximity of the binding site of the leader sequence. This tunnel is not observed within the NisB-dehydrated prenisin peptide complex. This suggested that the dehydrated prenisin peptide occupies this space. Interestingly, only one tunnel is observed indicating that one prenisin molecule can bind to NisB in solution. The other possible binding site appears to be closed. Furthermore, we observed that NisC is localized next to this tunnel with its active site pointing towards the prenisin binding site as well as the region of NisB, which contains the residues important for the dehydration and glutamylation reactions[29,33].

Taken all data together the dehydration reaction within the core peptide likely changes the conformation of prenisin such that the active site of NisC becomes accessible, which is capable to cyclize the first ring. This would be inline with the model proposed that nisin is modified via a ping-pong mechanism[9,46] were dehydration and cyclization occur in an alternate fashion. Due to (methyl)-lanthionine ring formation, the peptide shifts forward and the second dehydration step can occur. It remains unclear whether the position of the leader peptide is also shifted during this process and consequently moves out of the PTM complex. *In vivo* this might be favorable since the leader sequence needs to be recruited by the ABC transporter NisT. Finally, the presence of ring E prevented complex formation, or stimulate the dissociation. Apparently, the conformation of the core peptide is different in comparison to the conformation of nisin that contains rings A-D. This likely is ensured by the more bulky intertwined conformation of ring D and E[19].

In summary, the data obtained in this study identified two factors influencing complex formation of the maturation enzymes NisB and NisC, respectively. First the core peptide, it can be dehydrated and also particular modified. *In vitro* the presence of the last (methyl)-lanthionine ring, ring E, abolished complex formation. Second, the N-terminal leader peptide plays an important role. The highly conserved -FNLD- box is an essential recognition factor for the modification enzymes NisB and NisC. Finally, the MALS-SEC analysis revealed the first quantitative

data elucidating the stoichiometry of the nisin maturation complex. This complex revealed a molecular weight of approximately 291 kDa corresponding to a stoichiometry of 2:1:1 (NisB/NisC/prenisin peptide) *in vitro*.

Materials and Methods

Cloning the prenisin ring deficient variants. For producing ring deficient prenisin peptides, a shuttle vector accessible for the bacteria *L. lactis* and *E. coli* was created[47]. The correctness of the obtained plasmids was successfully verified by sequencing.

Purification of NisB, NisC and the prenisin peptide variants. NisB was expressed in *L. lactis* and purified as previously described[25]. The expression and purification of NisC was performed as described in ref. 22. Briefly, the dehydratase NisB was homologously expressed in *L. lactis* NZ9000 and purified to homogeneity via immobilized metal ion affinity chromatography (IMAC) followed by SEC. NisC was heterologously expressed in *E. coli* BL21 and isolated via a three-step purification strategy. The first step was again IMAC chromatography using a TALON® Superflow Cartage Colum, followed by a SEC purification step. The N-terminal His_6-tag of NisC was cleaved off by thrombin treatment. Non-digested NisC was removed via a second IMAC step.

The prenisin peptide purification was performed as described in ref. 22. For the determination of the prenisin concentration and the variants a RP-18 HPLC column was used[22]. In general prenisin is expressed via a two plasmid system. On the first plasmid wildtype prenisin or the cysteine variants of core nisin or the FNLD variants of the leader part of nisin is expressed. The second plasmid contains the PTM complex consisting of NisB, NisC and NisT. By varying the latter plasmid, the modification status of prenisin can be varied. Here, the deletion of NisC leads to a prenisin peptide variant, which is dehydrated but no lanthionine rings are installed. Similarly, the deletion of both, NisB and NisC, on the plasmid results in a prenisin peptide varians where no dehydration and no cyclization are present. The differences in modification are highlighted in Supplementary Figure S1.

Analysis of complex formation. To determine the molecular weight and stoichiometry of the NisB/NisC/prenisin peptide complex, a combination of multi-angle light scattering and size exclusion (MALS-SEC) was used to visualize complex formation. The analyses were performed on an Agilent 1260 HPLC System in combination with a triple-angle light scatter detector (miniDAWN TREOS) and a differential refractive index detector (Optilab rEX – both Wyatt Technology Europe).

Analysis of isolated NisB and NisC were performed by injection of 200 μL of a 20 μM solution of each protein. The second step was the analysis of prenisin peptide bound proteins. We used 20 μM NisC, respectively 20 μM NisB and incubate it with 200 μM prenisin peptide for 1 h at 25 °C.

For the initial complex analysis we saturated NisB with the unmodified prenisin peptide and analyzed the mixture by MALS-SEC. Here, we used 20 μM unmodified prenisin peptide saturated NisB and incubate it with 20 μM NisC for 1 h at 25 °C. The same analysis was performed with 20 μM unmodified prenisin peptide saturated NisC and subsequent incubation with 20 μM NisB. A Volume of 200 μL was applied on an Agilent BioSEC-5 colum (300 Å, 7.8 × 300 mm) pre-equilibrated with MALS buffer (50 mM HEPES-NaOH, pH 7.5, 500 mM NaCl) at a flow rate of 1.0 mL/min or on a Superdex 200 10/300 increase colum (GE Healthcare) at a flow rate of 0.75 mL/min. Data-analysis was performed with the ASTRA software package (Astra V 5.3.4.20) (Wyatt Technology).

To visualize complex formation, we kept the concentrations of NisB (20 μM) and of the prenisin peptide variants (200 μM) constant in the different samples. We used only different concentrations of NisC from 10 μM to 160 μM.

Analytical co-elution studies. The co-elution studies were performed on a Äkta Micro system using a Superdex 200 PC 3.2 column (GE Healthcare) equilibrated with 50 mM HEPES-NaOH, pH 7.5, 500 mM NaCl with a flow rate of 0.05 mL/min.

A 50 μL reaction mixture consisting of 20 μM NisB, 160 μM NisC and 200 μM prenisin peptide variant was incubated for 1 h at 25 °C and subsequently applied to SEC analysis. Elution was observed at 280 nm. After co-elution, the corresponding fractions were analyzed by a 4–20% gradient Tris-Glycine SDS-PAGE (Biorad) gel stained with Page-Blue (Thermo Fisher).

Immunoblotting and SDS-PAGE analysis. All SDS-PAGE and Western blotting experiments were performed with standard laboratory techniques[48–50]. The antibodies for NisB[38], NisC[38] and the nisin leader peptide[26] were kindly provided by Dr. Moll, LanthioPharma, Groningen (Netherlands).

Visualization of the nisin modification complex by small-angle X-ray scattering (SAXS). SAXS data were collected at ESRF Grenoble on beamline BM29 equipped with a PILATUS 1 M detector (Dectris). The sample to detector distance was kept fixed at 2.867 m. The achievable q-range under these conditions was 0.025–5 nm^{-1}. The maximum measurable R_g (radius of gyration) of the investigated particles were 20 nm. All measurements were performed at 4 °C and the system was coupled to a size exclusion chromatography.

For analysis of the nisin modification complex, a mixture of 40 μM NisB, 320 μM NisC and 400 μM dehydrated prenisin peptide was incubated for 1 h at 25 °C. Analysis of isolated NisB was performed with a 200 μM solution and for NisC with a 470 μM solution. A volume of 200 μL was applied on a Superdex 200 10/300 increase colum (GE Healthcare) pre-equilibrated with SAXS-buffer (50 mM HEPES-NaOH, pH 7.5, 500 mM NaCl, 5% Glycerol) at a flow rate of 0.75 mL/min. For data processing we used the ATSAS Software package (Version 2.7.1)[51]. Primary data reduction were performed using the program PRIMUS[42]. The forward scattering $I(0)$ as well as the radius of gyration (R_g) were calculated with the Guinier approximation[52], which is implemented in PRIMUS[42]. We calculated the pair-distribution function $p(r)$ and estimate the maximum particle dimension (D_{max}) employing the program GNOM[53]. The low resultion *ab initio* models were calculated with DAMMIF[43] (10 runs for each sample)

and used to perform the docking of the NisB-NisC dehydrated prenisin peptide complex, which was calculated with SASREF[54]. For superimposing of the models, we used SUPCOMB[44]. These programs are all part of the ATSAS program package available on the EMBL website (http://www.embl-hamburg.de/biosaxs/software.html).

References

1. Alvarez-Sieiro, P., Montalban-Lopez, M., Mu, D. D. & Kuipers, O. P. Bacteriocins of lactic acid bacteria: extending the family. *Appl. Microbiol. Biot.* **100,** 2939–2951 (2016).
2. Cotter, P. D., Hill, C. & Ross, R. P. Bacteriocins: developing innate immunity for food. *Nature Rev. Microbiol.* **3,** 777–88 (2005).
3. Chatterjee, C., Paul, M., Xie, L. & van der Donk, W. A. Biosynthesis and mode of action of lantibiotics. *Chem. Rev.* **105,** 633–84 (2005).
4. Zhang, Q., Yu, Y., Velasquez, J. E. & van der Donk, W. A. Evolution of lanthipeptide synthetases. *Proc. Natl. Acad. Sci. USA* **109,** 18361–6 (2012).
5. Okeley, N. M., Paul, M., Stasser, J. P., Blackburn, N. & van der Donk, W. A. SpaC and NisC, the cyclases involved in subtilin and nisin biosynthesis, are zinc proteins. *Biochemistry* **42,** 13613–24 (2003).
6. AlKhatib, Z. *et al.* The C-terminus of nisin is important for the ABC transporter NisFEG to confer immunity in *Lactococcus lactis*. *Microbiology open* **3,** 752–63 (2014).
7. Chan, W. C. *et al.* Structure-activity relationships in the peptide antibiotic nisin: Antibacterial activity of fragments of nisin. *Febs Letters* **390,** 129–132 (1996).
8. Hasper, H. E., de Kruijff, B. & Breukink, E. Assembly and stability of nisin-lipid II pores. *Biochemistry* **43,** 11567–75 (2004).
9. Lubelski, J., Khusainov, R. & Kuipers, O. P. Directionality and coordination of dehydration and ring formation during biosynthesis of the lantibiotic nisin. *J. Biol. Chem.* **284,** 25962–72 (2009).
10. Rink, R. *et al.* Dissection and modulation of the four distinct activities of nisin by mutagenesis of rings A and B and by C-terminal truncation. *Appl. Environ. Microbiol.* **73,** 5809–5816 (2007).
11. van Heusden, H. E., de Kruijff, B. & Breukink, E. Lipid II induces a transmembrane orientation of the pore-forming peptide lantibiotic nisin. *Biochemistry* **41,** 12171–12178 (2002).
12. Wiedemann, I. *et al.* Specific binding of nisin to the peptidoglycan precursor lipid II combines pore formation and inhibition of cell wall biosynthesis for potent antibiotic activity. *J. Biol. Chem.* **276,** 1772–1779 (2001).
13. Knerr, P. J. & van der Donk, W. A. Discovery, Biosynthesis, and Engineering of Lantipeptides. *Annu. Rev. Biochem.* **81,** 479–505 (2012).
14. van Heel, A. J., de Jong, A., Montalban-Lopez, M., Kok, J. & Kuipers, O. P. BAGEL3: automated identification of genes encoding bacteriocins and (non-)bactericidal posttranslationally modified peptides. *Nucleic Acids Res.* **41,** W448–W453 (2013).
15. Breukink, E. *et al.* Use of the cell wall precursor lipid II by a pore-forming peptide antibiotic. *Science* **286,** 2361–4 (1999).
16. Lubelski, J., Rink, R., Khusainov, R., Moll, G. N. & Kuipers, O. P. Biosynthesis, immunity, regulation, mode of action and engineering of the model lantibiotic nisin. *Cell. Mol. Life Sci.* **65,** 455–76 (2008).
17. Arnison, P. G. *et al.* Ribosomally synthesized and post-translationally modified peptide natural products: overview and recommendations for a universal nomenclature. *Nat. Prod. Rep.* **30,** 108–60 (2013).
18. Rogers, L. A. The Inhibiting Effect of *Streptococcus Lactis* on *Lactobacillus Bulgaricus*. *J. Bacteriol.* **16,** 321–5 (1928).
19. Van de Ven, F. J., Van den Hooven, H. W., Konings, R. N.& Hilbers, C. W. NMR studies of lantibiotics. The structure of nisin in aqueous solution. *Eur. J. Biochem.* **202,** 1181–8 (1991).
20. Severina, E., Severin, A. & Tomasz, A. Antibacterial efficacy of nisin against multidrug-resistant Gram-positive pathogens. *J. Antimicrob. Chemother.* **41,** 341–7 (1998).
21. Brumfitt, W., Salton, M. R. & Hamilton-Miller, J. M. Nisin, alone and combined with peptidoglycan-modulating antibiotics: activity against methicillin-resistant *Staphylococcus aureus* and vancomycin-resistant *enterococci*. *J. Antimicrob. Chemother.* **50,** 731–4 (2002).
22. Abts, A., Montalban-Lopez, M., Kuipers, O. P., Smits, S. H. & Schmitt, L. NisC binds the FxLx motif of the nisin leader peptide. *Biochemistry* **52,** 5387–95 (2013).
23. Khusainov, R., Moll, G. N. & Kuipers, O. P. Identification of distinct nisin leader peptide regions that determine interactions with the modification enzymes NisB and NisC. *FEBS Open Bio* **3,** 237–42 (2013).
24. Kuipers, A. *et al.* NisT, the transporter of the lantibiotic nisin, can transport fully modified, dehydrated, and unmodified prenisin and fusions of the leader peptide with non-lantibiotic peptides. *J. Biol. Chem.* **279,** 22176–82 (2004).
25. Mavaro, A. *et al.* Substrate recognition and specificity of the NisB protein, the lantibiotic dehydratase involved in nisin biosynthesis. *J. Biol. Chem.* **286,** 30552–60 (2011).
26. Plat, A., Kluskens, L. D., Kuipers, A., Rink, R. & Moll, G. N. Requirements of the engineered leader peptide of nisin for inducing modification, export, and cleavage. *Appl. Environ. Microbiol.* **77,** 604–11 (2011).
27. Plat, A., Kuipers, A., Rink, R. & Moll, G. N. Mechanistic aspects of lanthipeptide leaders. *Curr. Protein Pept Sci.* **14,** 85–96 (2013).
28. Qiao, M. & Saris, P. E. Evidence for a role of NisT in transport of the lantibiotic nisin produced by *Lactococcus lactis N8*. *FEMS Microbiol. Lett.* **144,** 89–93 (1996).
29. Garg, N., Salazar-Ocampo, L. M. & van der Donk, W. A. *In vitro* activity of the nisin dehydratase NisB. *Proc. Natl. Acad. Sci. USA* **110,** 7258–63 (2013).
30. Koponen, O. *et al.* NisB is required for the dehydration and NisC for the lanthionine formation in the post-translational modification of nisin. *Microbiology* **148,** 3561–8 (2002).
31. Karakas Sen, A. *et al.* Post-translational modification of nisin. The involvement of NisB in the dehydration process. *Eur. J. Biochem.* **261,** 524–32 (1999).
32. Qiao, M. *et al.* Regulation of the nisin operons in *Lactococcus lactis N8*. *J. Appl. Bacteriol.* **80,** 626–34 (1996).
33. Ortega, M. A. *et al.* Structure and mechanism of the tRNA-dependent lantibiotic dehydratase NisB. *Nature* **517,** 509–12 (2015).
34. Li, B. & van der Donk, W. A. Identification of essential catalytic residues of the cyclase NisC involved in the biosynthesis of nisin. *J. Biol. Chem.* **282,** 21169–75 (2007).
35. Li, B. *et al.* Structure and mechanism of the lantibiotic cyclase involved in nisin biosynthesis. *Science* **311,** 1464–7 (2006).
36. Siegers, K., Heinzmann, S. & Entian, K. D. Biosynthesis of lantibiotic nisin. Posttranslational modification of its prepeptide occurs at a multimeric membrane-associated lanthionine synthetase complex. *J. Biol. Chem.* **271,** 12294–301 (1996).
37. Ortega, M. A. *et al.* Structure and tRNA Specificity of MibB, a Lantibiotic Dehydratase from Actinobacteria Involved in NAI-107 Biosynthesis. *Cell. chemical. biology* **23,** 370–80 (2016).
38. Khusainov, R., Heils, R., Lubelski, J., Moll, G. N. & Kuipers, O. P. Determining sites of interaction between prenisin and its modification enzymes NisB and NisC. *Mol. Microbiol.* **82,** 706–18 (2011).
39. Kluskens, L. D. *et al.* Post-translational modification of therapeutic peptides by NisB, the dehydratase of the lantibiotic nisin. *Biochemistry* **44,** 12827–34 (2005).
40. Rink, R. *et al.* NisC, the cyclase of the lantibiotic nisin, can catalyze cyclization of designed nonlantibiotic peptides. *Biochemistry* **46,** 13179–89 (2007).
41. Rink, R. *et al.* Lantibiotic structures as guidelines for the design of peptides that can be modified by lantibiotic enzymes. *Biochemistry* **44,** 8873–82 (2005).

42. Konarev, P. V., Volkov, V. V., Sokolova, A. V., Koch, M. H. J. & Svergun, D. I. PRIMUS: a Windows PC-based system for small-angle scattering data analysis. *J. Appl. Crystallogr.* **36,** 1277–1282 (2003).
43. Franke, D. & Svergun, D. I. DAMMIF, a program for rapid *ab-initio* shape determination in small-angle scattering. *J. Appl. Crystallogr.* **42,** 342–346 (2009).
44. Kozin, M. B. & Svergun, D. I. Automated matching of high- and low-resolution structural models. *J. Appl. Crystallogr.* **34,** 33–41 (2001).
45. Khusainov, R. & Kuipers, O. P. When the leader gets loose: *in vivo* biosynthesis of a leaderless prenisin is stimulated by a trans-acting leader peptide. *Chembiochem* **13,** 2433–8 (2012).
46. Kuipers, A., Meijer-Wierenga, J., Rink, R., Kluskens, L. D. & Moll, G. N. Mechanistic dissection of the enzyme complexes involved in biosynthesis of lacticin 3147 and nisin. *Appl. Environ. Microbiol.* **74,** 6591–7 (2008).
47. AlKhatib, Z. *et al.* Lantibiotic immunity: inhibition of nisin mediated pore formation by NisI. *PLoS One* **9,** e102246 (2014).
48. Laemmli, U. K. Cleavage of structural proteins during the assembly of the head of bacteriophage *T4*. *Nature* **227,** 680–5 (1970).
49. Towbin, H., Staehelin, T. & Gordon, J. Electrophoretic transfer of proteins from polyacrylamide gels to nitrocellulose sheets: procedure and some applications. *Proc. Natl. Acad. Sci. USA* **76,** 4350–4 (1979).
50. Burnette, W. N. "Western blotting": electrophoretic transfer of proteins from sodium dodecyl sulfate–polyacrylamide gels to unmodified nitrocellulose and radiographic detection with antibody and radioiodinated protein A. *Anal. Biochem.* **112,** 195–203 (1981).
51. Petoukhov, M. V. *et al.* New developments in the ATSAS program package for small-angle scattering data analysis. *J. Appl. Crystallogr.* **45,** 342–350 (2012).
52. Guinier, A. Diffraction of x-rays of very small angles-application to the study of ultramicroscopic phenomenon. *Annales de Physique* **12,** 161–237 (1939).
53. Svergun, D. I. Determination of the Regularization Parameter in Indirect-Transform Methods Using Perceptual Criteria. *J. Appl. Crystallogr.* **25,** 495–503 (1992).
54. Petoukhov, M. V. & Svergun, D. I. Global rigid body modeling of macromolecular complexes against small-angle scattering data. *Biophys. J.* **89,** 1237–1250 (2005).

Acknowledgements

We thank the EMBL-Lab Outstation Grenoble for the local support as well as the whole team of BM-29 beamline at the ESRF (Grenoble). We also thank Christine Tölzer (Institute of Biochemistry, University of Cologne, Germany) for helping with the SAXS evaluation and Dr. Gert Moll (Lanthiopharma, Groningen, The Netherlands) for his kind gift of antibodies. The Crystal and X-ray facility of the Heinrich Heine University is acknowledged for their support throughout the project. This work was supported by the DFG (grant Schm1279/13-1) to L.S.

Author Contributions

J.R., A.A. and R.C. performed the experiments, J.R., A.A., S.H.J.S. and L.S. designed the experiments, J.R., S.H.J.S. and L.S. evaluated the data and J.R., S.H.J.S. and L.S. wrote the manuscript.

Additional Information

Supplementary information accompanies this paper at http://www.nature.com/srep

Competing financial interests: The authors declare no competing financial interests.

How to cite this article: Reiners, J. *et al.* Stoichiometry and structure of a lantibiotic maturation complex. *Sci. Rep.* **7**, 42163; doi: 10.1038/srep42163 (2017).

Publisher's note: Springer Nature remains neutral with regard to jurisdictional claims in published maps and institutional affiliations.

Supplementary material

Stoichiometry and structure of a lantibiotic maturation complex

Jens Reiners, André Abts, Rebecca Clemens, Sander H. J. Smits and Lutz Schmitt*

Institute of Biochemistry, Heinrich-Heine-University Duesseldorf, Universitaetsstraße 1, 40225 Duesseldorf, Germany

Figure S1: **Schematic overview of the nisin maturation process. I)** The leader peptide is shown on the top and the highly conserved -FNLD- box is highlighted by a red box. The unmodified prenisin peptide represents the ribosomally synthesized peptide. **II)** NisB dehydrates specific serine and threonine residues (grey) in the core peptide. The final peptide is called dehydrated prenisin peptide, which contains the dehydrated amino acids dehydroalanine (dha) and dehydrobutyrine (dhb). **III)** These dehydrated amino acid residues get linked via NisC to C-terminal located cysteine residues (brown), resulting in the modified prenisin peptide. In the core peptide one lanthionine ring A (orange) and four (methyl)-lanthionine rings B-E (red) are present. **IV)** After introduction of the post-translational modifications the modified prenisin peptide is secreted via NisT across the cytoplasmic membrane and processed by the serine protease NisP. The modified prenisin peptide is cleaved into the leader peptide and mature nisin. Modified from [1].

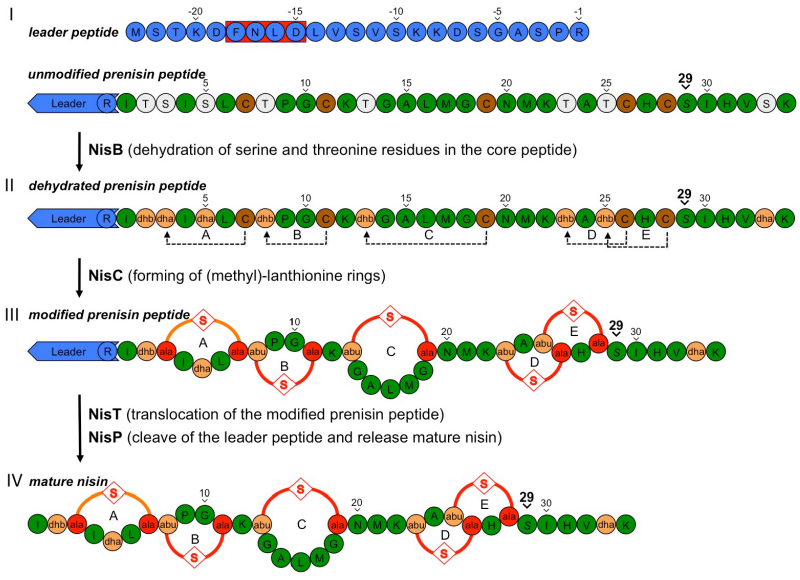

Figure S2: **SDS-PAGE analysis of the purification process of NisC and NisB, respectively**. **(A) NisB purification:** Lane M: protein marker. Lane 1: Crude extract of *L. lactis* cells expressing NisB-His_6. Lane 2: Flow through of the IMAC column. Lane 3: Combined IMAC elution fractions containing NisB-His_6. Lane 4: NisB-His_6 elution fraction after SEC. **(B) NisC purification:** Lane M: protein marker. Lane 1: Crude extract of His_6-NisC expressing *E. coli* cells. Lane 2: IMAC flow through. Lane 3: Combined His_6-NisC IMAC elution fractions. Lane 4: His_6-NisC elution fraction after SEC. Lane 5: Tag-free NisC after thrombin treatment. **(C)** Molecular weight determination of NisB using MALS-SEC: In black the elution profile of a purified NisB sample analyzed with MALS-SEC is shown. The observed molecular weight of 237.5 ± 0.3 kDa fits very well with the theoretical molecular weight of a NisB dimer 236.6 kDa (www.expasy.org). **(D)** The black elution profile represents the MALS-SEC analysis of a purified NisC sample. A molecular weight of 48.1 ± 0.5 kDa was determined, which is in-line with the theoretical calculated molecular weight of a cleaved NisC monomer of 48.5 kDa (www.expasy.org).

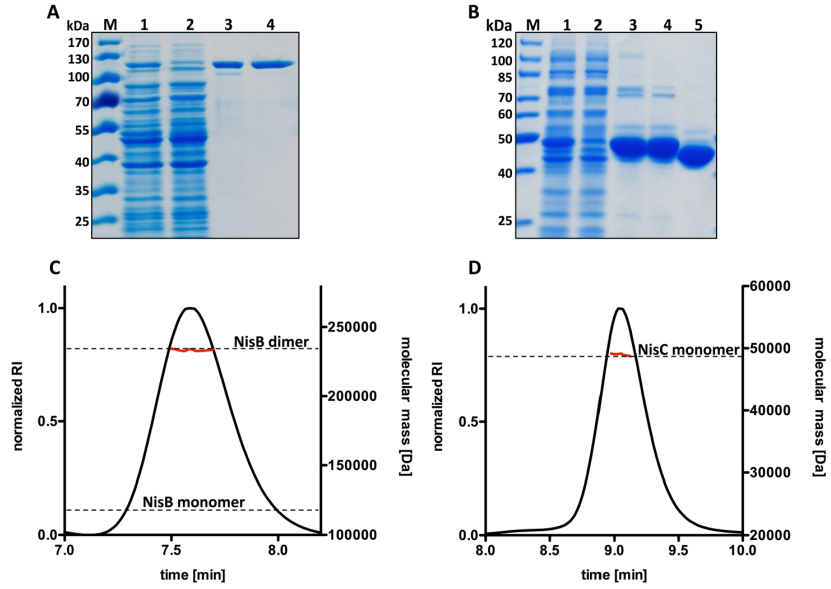

Figure S3: **Page-Blue (Thermo Fischer) stained Tricine SDS-PAGE [2] analysis of the purified prenisin peptide variants**: All variants were purified using cation exchange chromatography as previously described [1,3]. The final concentration of the purified peptide variants was determined by subjecting the prenisin peptide variants to HPLC analysis [3]. Due to space limitation several gels have been made, which are indicated by black boxes and vertical lines.

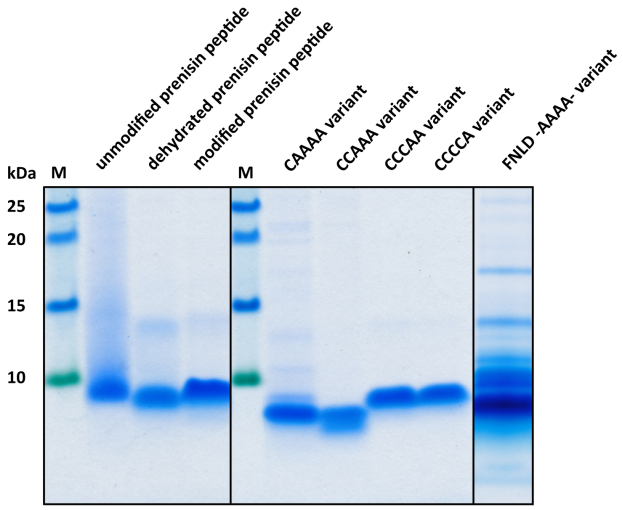

NisB and NisC substrate binding

With the MALS-SEC analysis we could show the substrate binding from NisB and NisC. The prenisin binding to NisC resulted in a changes elution time due to a change in the hydrodynamic radius (Figure S4 A, black line) in comparison to ligand-free NisC (Figure S4 A, dashed line). The observed molecular weight of ligand-free NisC was 48.1 ± 0.5 kDa. After incubation of unmodified prenisin peptide with NisC, we observed a molecular weight of 54.5 ± 0.6 kDa, which fits to NisC with one prenisin bound (theoretical molecular weight of 54.3 kDa). NisB showed no difference in the elution profile, but MALS-SEC analysis highlighted a molecular weight of 237.5 ± 0.3 kDa (Figure S4 B, blue line) for NisB and 241.9 ± 0.4 kDa for the NisB-NisA bound complex. This indicated that one unmodified prenisin peptide molecule was bound to a NisB dimer (theoretical molecular weight of 242.2 kDa). Thus, these results demonstrate a 1:1 stoichiometry for a monomer of NisC with one prenisin molecule, and also that a dimer of NisB binds one prenisin molecule. The results are in-line with previous *in vitro* studies [1,3], but in contrast to the NisB structure [4], which showed two leader peptide fragments bound within the NisB dimer.

Figure S4: **MALS-SEC analysis of the mixed protein samples consisting of NisB or NisC, in the presence and absence of prenisin peptide**. **(A)** The dashed black graph shows the elution profile of 20 µM NisC resulting in a molecular weight of 48.1 ± 0.5 kDa (blue line). The analysis of 20 µM NisC and 200 µM unmodified prenisin peptide is shown as the black graph, revealing an apparent molecular weight of 54.5 ± 0.6 kDa (red line) of the formed complex. **(B)** The dashed black graph represents the elution profile of 20 µM NisB resulting in a molecular weight of 237.5 ± 0.3 kDa (blue line). The analysis of 20 µM NisB and 200 µM unmodified prenisin peptide is shown as the black graph revealing an apparent molecular weight of 241.9 ± 0.4 kDa (red line) of the formed complex.

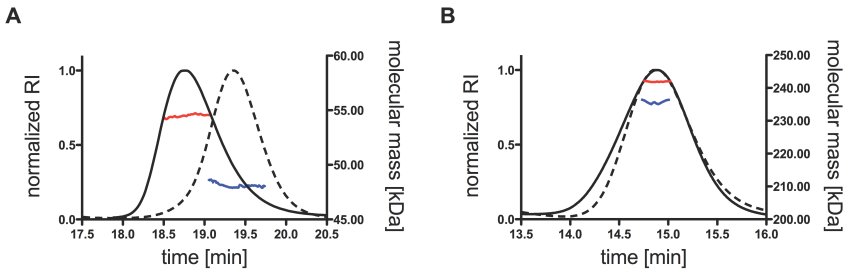

Figure S5**: SDS-PAGE analysis of fractions of size exclusion chromatograms of NisB or NisC sample as well as a NisB / NisC sample**.

The corresponding SDS gels from the size exclusion chromatography (Superdex 200 PC 3.2) fractions are shown in **(A)** 20 µM NisB (blue profile). **(B)** 160 µM NisC (red profile) **(C)** 20 µM NisB and 160 µM NisC (black profile). As observed, NisB and NisC are detected in different fractions of the SEC elution profile. The elution profiles of NisB and NisC remain unchanged in the case of the simultaneous injection of both proteins (C) indicating no complex formation. For the analysis of complex formation the fraction highlighted by a red box was used in SDS page analysis and subsequent Western blot analysis (Figure 2a).

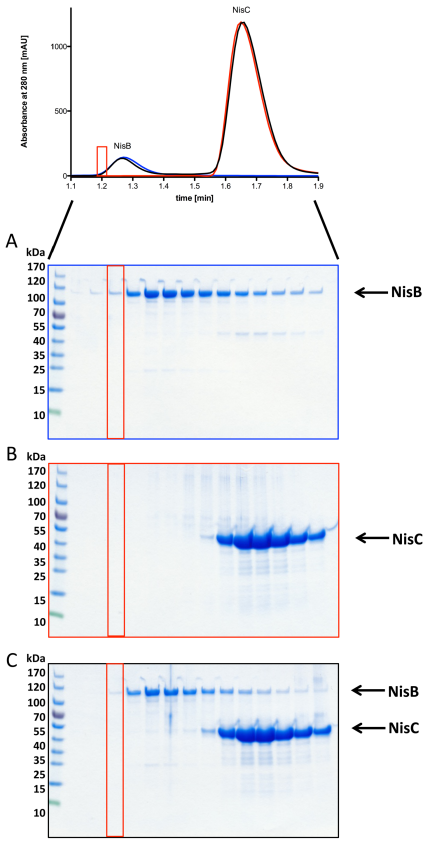

Figure S6: **MALS-SEC analysis of the pre-saturated protein samples consisting of NisB or NisC, in the presence of prenisin peptide**. **(A)** The black graph shows the elution profile of 20 µM NisB saturated with unmodified prenisin peptide and incubated with 20 µM NisC, Resulting in a molecular weight of 263.8 ± 0.3 kDa (red line). **(B)** The analysis of 20 µM NisC saturated with unmodified prenisin peptide and incubated with 20 µM NisB is shown with the black graph, revealing an apparent molecular weight of 247.1 ± 0.4 kDa (red line).

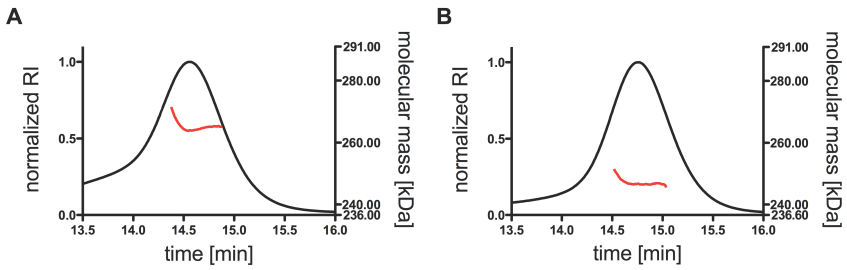

Figure S7: **SDS-PAGE analysis showing the results of the dependency of the leader and core peptides on complex formation**. The corresponding SDS gels from the size exclusion chromatography (Superdex 200 PC 3.2) fractions are shown. **(A)** 20 µM NisB and 160 µM NisC in the presence of 200 µM of the unmodified prenisin peptide. **(B)** 20 µM NisB and 160 µM NisC in the presence of 200 µM of the dehydrated prenisin peptide. **(C)** 20 µM NisB and 160 µM NisC in the presence of 200 µM of the modified prenisin peptide. **(D)** 20 µM NisB and 160 µM NisC in the presence of 200 µM of the –FNLD- box variant (-AAAA-) mutant prenisin. Red-boxed elution fractions were used for Western blot analysis (Fig. 2b-c).

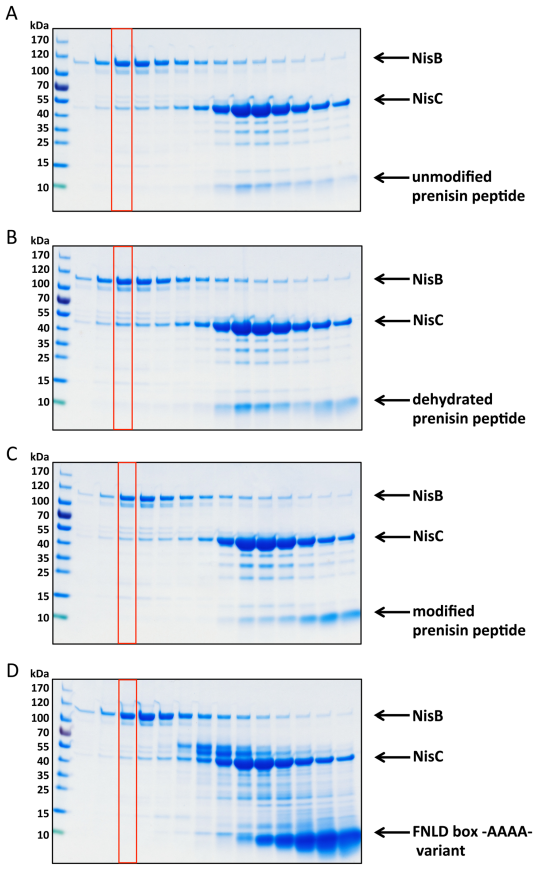

Figure S8: **SDS-PAGE analysis showing the influence in varying the number of installed (methyl)-lanthionine rings**. The corresponding SDS gels from the size exclusion chromatography (Superdex 200 PC 3.2) fractions are shown. **(A)** 20 µM NisB and 160 µM NisC in the presence of 200 µM of the CAAAA variant. **(B)** 20 µM NisB and 160 µM NisC in the presence of 200 µM of the CCAAA variant. **(C)** 20 µM NisB and 160 µM NisC in the presence of 200 µM of the CCCAA variant. **(D)** 20 µM NisB and 160 µM NisC in the presence of 200 µM of the CCCCA variant. Red-boxed elution fractions were used for the Western blot analysis (Fig. 2c).

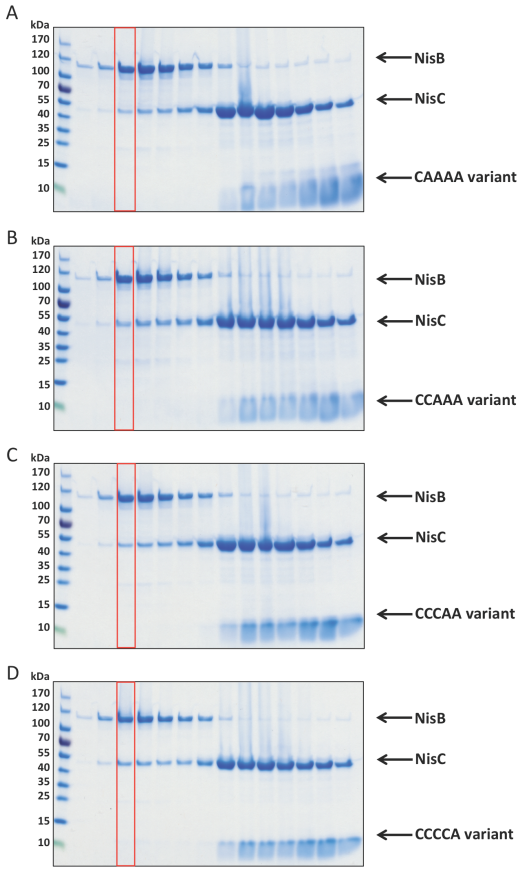

Figure S9: **SAXS plots of the different Proteins.** Experimental curves are shown in black dots and the *ab-initio* model fit as red line. Displayed is the intensity as a function of momentum transfer s. **(A)** Plot NisB, DAMMIF fit. **(B)** NisB saturated with dehydrated prenisin peptide, DAMMIF fit. **(C)** NisC, DAMMIF fit. **(D)** NisBCA complex, DAMMIF fit. **(E)** NisBCA complex, SASREF fit.

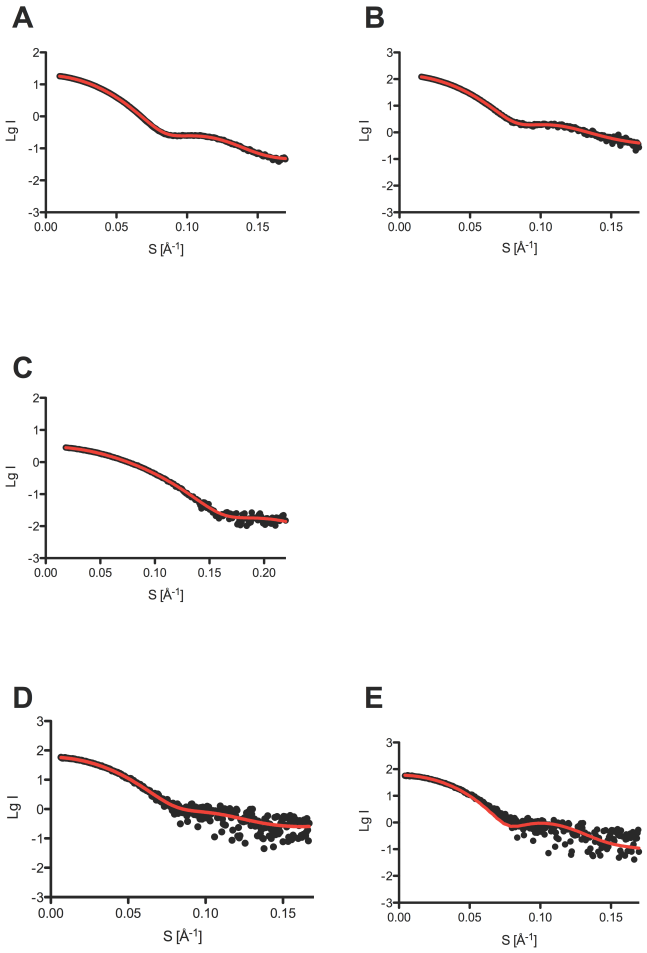

Table S1: **MALS-SEC data summarizing the molecular weight (M_w) of the analysis of complex forming for the different prenisin peptide variants.** For the analysis, we kept the concentration of NisB (20 µM) and the different prenisin peptides (200µM) constant. We only changed the concentration of NisC from 0 µM up to 160 µM. The theoretical molecular weight of a NisB dimer is calculated to 236.6 kDa, 48.5 kDa for a tag-free NisC monomer and 5.9 kDa for the unmodified prenisin peptide. All measurements were done at least in triplicate. n.d. = not determined.

NisC concentration [µM]	without prenisin peptide	M_W nisin maturation complex [kDa]			
		unmodified	dehydrated	modified	FNLD Variant
0	236.4 ± 0.3	n. d.	241.9 ± 0.4	n.d.	n.d.
10	n.d.	247.3 ± 1.2	249.3 ± 0.5	n.d.	n.d.
20	n.d.	256.6 ± 0.8	249.3 ± 1.1	n.d.	n.d.
40	237.5 ± 0.3	268.9 ± 1.3	260.3 ± 0.3	237.5 ± 0.8	n.d.
60	n.d.	276.8 ± 1.0	270.4 ± 0.5	n.d.	n.d.
80	238.1 ± 0.3	291.2 ± 1.1	275.5 ± 0.5	n.d.	n.d.
120	n.d.	287.2 ± 0.7	292.7 ± 0.8	n.d.	n.d.
160	238.7 ± 1.2	293.6 ± 1.2	291.2 ± 0.9	250.4 ± 0.7	248.0 ± 0.9

Table S2: **Theoretical Molecular weight from different ratios of NisB, NisC and NisA.**

The theoretical molecular weight of a NisB dimer is calculated to 236.6 kDa, 48.5 kDa for a tag-free NisC monomer and 5.9 kDa for the unmodified prenisin peptide

Ratio			
NisB	NisC	NisA	Molecular weight [kDa]
1	1	1	172.7
1	2	1	221.2
1	1	2	178.6
1	2	2	227.1
2	1	2	296.9
2	1	1	291.0
2	2	1	339.5
2	2	2	345.4

Table S3: **Overall SAXS Data**

Data collection parameters				
Detector	PILATUS 1 M			
Detector distance (m)	2.867			
Beam size (µm x µm)	700 x 700			
Wavelength (Å)	0.99			
Sample environment	Quartz glass capillary, 1 mm ø			
s range (nm^{-1})‡	0.025–5.0			
Temperature (°C)	4			
Exposure time per frame (s)	1.5 s continuously*			
Mode of measurement	online SEC			
Sample	**NisB**	**NisBA**	**NisC**	**NisBCA**
Structural parameters				
I(0) from P(r)	19.07	141.10	3.0	58.79
R_g (real-space from P(r)) (nm)	4.29	4.33	2.41	4.42
I(0) from Guinier fit	19.20	142.14	3.00	58.94
s-range for Guinier fit (nm^{-1})	0.12 - 0.30	0.16 - 0.33	0.21 - 0.54	0.14 - 0.32
R_g (from Guinier fit, AutoR_g) (nm)	4.37	4.39	2.42	4.45
D_{max} (nm)	13.44	15.06	8.16	15.66
POROD volume estimate (nm^3)	382.82	410.47	82.5	440.17
Molecular mass (kDa)				
From POROD volume [kDa]	239.26	256.54	51.56	275.1
From I(0)	n.a.			
From sequence	236.6	242.4	48.5	291
Software				
Primary data reduction	PRIMUS [5]			
Data processing	GNOM [6]			
Ab initio modelling	DAMMIF [7]			DAMMIF[7]/SASREF[8]
Evaluation, averaging of models	DAMAVER [9]			
Superimposing	SUPCOMB [10]			
Model visualization	PyMOL			

‡s = $4\pi\sin(\theta)/\lambda$, 2θ – scattering angle, λ – Xray-wavelength.* 0.5 s dead time between frames, n.a. not applicable.

Literature

1. Mavaro, A. et al. Substrate recognition and specificity of the NisB protein, the lantibiotic dehydratase involved in nisin biosynthesis. *J. Biol. Chem.* **286**, 30552-60 (2011).
2. Schagger, H. Tricine-SDS-PAGE. *Nat Protoc.* **1**, 16-22 (2006).
3. Abts, A., Montalban-Lopez, M., Kuipers, O.P., Smits, S.H. & Schmitt, L. NisC binds the FxLx motif of the nisin leader peptide. *Biochemistry* **52**, 5387-95 (2013).
4. Ortega, M.A. et al. Structure and mechanism of the tRNA-dependent lantibiotic dehydratase NisB. *Nature* **517**, 509-12 (2015).
5. Konarev, P.V., Volkov, V.V., Sokolova, A.V., Koch, M.H.J. & Svergun, D.I. PRIMUS: a Windows PC-based system for small-angle scattering data analysis. *J. Appl. Crystallogr.* **36**, 1277-1282 (2003).
6. Svergun, D.I. Determination of the Regularization Parameter in Indirect-Transform Methods Using Perceptual Criteria. *J. Appl. Crystallogr.* **25**, 495-503 (1992).
7. Franke, D. & Svergun, D.I. DAMMIF, a program for rapid *ab-initio* shape determination in small-angle scattering. *J. Appl. Crystallogr.* **42**, 342-346 (2009).
8. Petoukhov, M.V. & Svergun, D.I. Global rigid body modeling of macromolecular complexes against small-angle scattering data. *Biophys. J.* **89**, 1237-1250 (2005).
9. Volkov, V.V. & Svergun, D.I. Uniqueness of ab initio shape determination in small-angle scattering. *J. Appl. Crystallogr.* **36**, 860-864 (2003).
10. Kozin, M.B. & Svergun, D.I. Automated matching of high- and low-resolution structural models. *J. Appl. Crystallogr.* **34**, 33-41 (2001).

3.3. Chapter III - CD1348 lipoprotein from *Clostridium difficile*

Published in: in Preparation

Own work: 50 %
Expression and Purification
Double labelling of CD1348 protein for NMR
Interaction studies *in vitro* and *in vivo*
Writing the Manuscript

Characterization of CD1348 of the CprABC operon: Purification and interaction studies with different lantibiotics

Rebecca Clemens, Jens Reiners, Daniel Mulnaes, Wolfgang Hoyer, Philipp Neudecker, Holger Gohlke and Sander H. J. Smits

Characterization of CD1348 of the CprABC operon: Purification and interaction studies with different lantibiotics

Rebecca Clemens, Jens Reiners, Daniel Mulnaes, Wolfgang Hoyer, Philipp Neudecker, Holger Gohlke and Sander H. J. Smits

Abstract

Bacteriocins are small ribosomally synthesized peptides and some of them are showing antimicrobial activity against Gram-positive bacteria. One large group are the lanthionine containing antibiotics (lantibiotics). They are post-translational modified by dehydration serine and threonine residues followed by an intramolecular addition of a neighboured cysteine residue. This modification is performed by different modification enzymes depending on which class the lantibiotic are belonging to. Lantibiotics are used since decades in the food industry. Some human pathogenic bacteria express resistance proteins which counteract with the lantibiotic [1; 2; 3; 4; 5]. In *Clostridium difficile* such resistance proteins have been identified. The resistance system consists of an ABC-transporter, the CprABC and a two-component system, containing a response regulator (CprR) and a histidine kinase (CprK), which are encoded on one operon. The Cpr system confers resistance against nisin, gallidermin and subtilin [1]. The present study focuses on the CD1348 lipoprotein encoded directly in front of the CprABC operon. The purification of the so far uncharacterized lipoprotein was established and first interaction studies were performed with different lantibiotics, nisin and gallidermin using *in vitro* studies and *in vivo* studies in *Lactococcus lactis*. It was determined that the CD1348 does not generate a resistance to the lantibiotics nisin and gallidermin and also no real interaction could be observed. Reason for missing observed interactions might be that the correct substrate was not found or it is a protein generating heat stability to the cell, which could be a reason of the high heat stability of the CD1348 up to 90 °C.

Introduction

The urgency of novel antibiotics generation has put the focus on possible alternatives like the antimicrobial peptides (AMPs). One large group of this AMPs are bacteriocins. They are small ribosomal- synthesized peptides, of which some display high antimicrobial activity [6; 7]. This bacteriocins are used since decades as food preservatives and recently as antibiotic alternatives [8; 9]. One large group of this bacteriocins are the lanthionine containing antibiotics, called lantibiotics. These lantibiotics are antimicrobial peptides which are post-translational modified [10]. Mostly they are produced by Gram-positive bacteria and consist of 19-38 amino acids [10; 11; 12]. The post-translational modification involves the dehydration of serine and threonine, resulting in the lantibiotic typical 2,3-didehydroalanine (Dha) and 2,3- didehydrobutyrine (Dhb). This is followed by the intramolecular addition of a neighboured cysteine residue onto Dha or Dhb to form the lanthionine or methyllanthionine rings [10; 13]. It is already known, that lantibiotics are able to inhibit multi-drug resistant pathogens like *Staphylococci*, *Enterococci*, *Streptococci* and *Clostridia* species [14]. They are classified in four different classes depending on which enzyme types are involved in the post-translational modification [13; 15; 16].

Nisin is till date the best characterized lantibiotic and was first described in 1928 [17]. It belongs to the class I lantibiotics which are post-translational modified via the dehydratase NisB and the cyclase NisC. Nisin is produced by some *Lactococcus lactis* and *Streptococcus uberis* strains [11; 13]. Nisin is able to perform at least a dual mode of action. First it is able to bind to the pyrophosphate group of the precursor molecule of peptidoglycan, the lipid II and inhibits the cell wall synthesis [18; 19; 20; 21]. Second, after binding to lipid II it is able to form pores through the membrane, which leads to cell death [22]. Nisin is highly active, it leads to cell death even in a nanomolar range [13; 23].

Some bacteria show resistance against lantibiotic, nisin, even if they are non-producer strains, they express protein systems which protect them from the lantibiotic around. This systems and mechanisms are in detail reviewed in Draper et al. (2015) [24].

Understanding the resistance mechanism of these lantibiotic resistance in bacteria is needed as the aim is the use of lantibiotics in medicine.

In former studies resistance systems have been identified and characterized, e.g. BceAB in *Bacillus subtilis* [25; 26], BraAB [5], VraDE in *Staphylococcus aureus* [4; 5], LctFEG, $NsrFE_1E_2G$ in *Streptococcus mutans* [27], the NsrFP in *Streptococcus agalactiae* [3], and the CprABC system of *Clostridium difficile* [1; 2].

The resistance system of *S. agalactiae* contains an ABC-transporter NsrFP and a two-component system, containing a histidine kinase NsrK and a response regulator NsrR (Figure 1). Directly in front of the NsrFP ABC-transporter a membrane associated serine protease is encoded, Nsr. This protease is characterized and the structure is figured out in detail. Nsr cleaves of the last six amino acids of nisin and shows a 20-fold higher resistance expressed in *L. lactis* against nisin [3; 28; 29]. Also, the NsrFP transporter has been characterized recently. This transporter is not only able to transport nisin (17-fold of resistance), but also gallidermin seems to be one substrate (13-fold of resistance) of the ABC transporter as well [30].

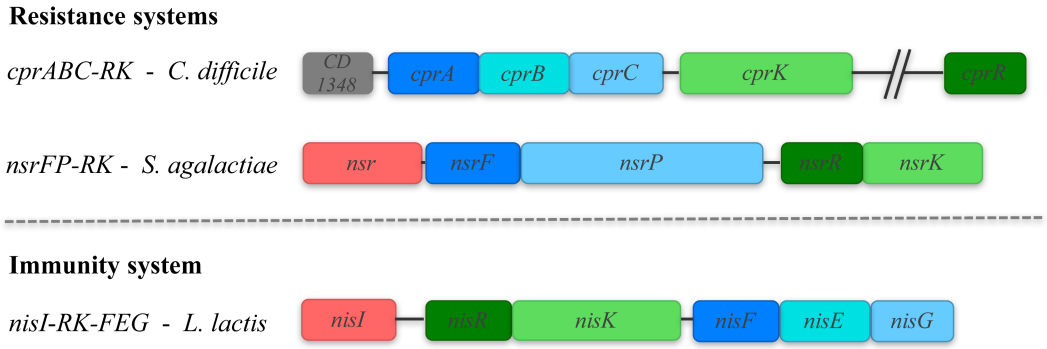

Figure 1: Resistance and immunity systems of Gram-positive bacteria. Shown in blue are the ABC-transporter of the resistance and immunity systems. The nucleotide binding domain is depicted in dark blue. The transmembrane domains are depicted in light blue and cyan. In green the two-component system consisting of the histidine kinase (light green) and response regulator (dark green) is depicted. The lipoprotein NisI and the Nsr, membrane associated serine protease are depicted in red, belonging to the corresponding resistance and immunity system. The CD1348 lipoprotein is depicted in grey which is till date uncharacterized. Based on [31] (Chapter I).

The resistance system of *C. difficile* also contains an ABC-transporter (CprABC) and a two-component system (CprK and CprR). Former studies are showing, that the system is also recognizing different lantibiotics and is able to provide resistance against all of them [1; 2]. *C. difficile* is a Gram-positive, spore forming bacteria, which causes intestinal diseases, mostly chronical [32]. The spores are resistant against cell death and even against heat [33; 34]. The vegetative cells, once in the human colon, can survive there. The normal flora provides colonization of the *C. difficile*. Antimicrobial treatment accelerated the overgrowth of *C. difficile*, this leads to clinical diseases. These diseases are often chronical and can be diarrheal to fatal colitis [32; 35; 36]. The symptoms of the disease are caused by two toxins, TcdA and TcdB. *C. difficile* is able to secret the two toxins in the gastrointestinal tract of mammals [37].

Because of the CprABC system *C. difficile* is also resistant against several lantibiotics so that the treatment of *C. difficile* is difficult [1].

In this study, we focused on the CD1348 lipoprotein [1; 2], which is encoded directly in front of the CprABC transporter. This protein is till date uncharacterized. To investigate the function of the CD1348 protein the first step was to purify it in high quality to do *in vitro* analysis. Two different constructs were purified, a none codon optimized and a codon optimized one. For *in vitro* interaction studies, analytical co-elution studies and tryptophan measurements were chosen. To investigate, whether the CD1348 lipoprotein is a resistance protein, *in vivo* studies in *L. lactis* were performed as well. An expression test in *L. lactis* NZ9000 was performed to be certain, that the protein is expressed in the growth inhibition studies with nisin and gallidermin (Figure 2).

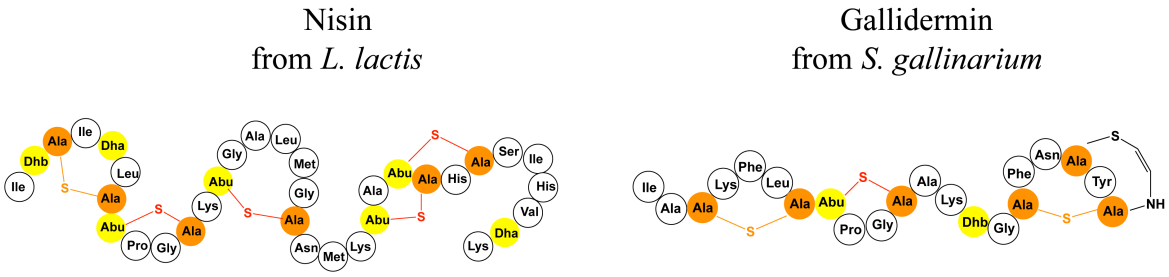

Figure 2: Schematic representation of lantibiotics nisin and gallidermin. The dehydrated amino acids and the cysteines of the lantibiotics are depicted in yellow and orange. The (methyl-) lanthionine rings are highlighted in orange and red. Based on [10].

The hypothesis was, that the CD1348 lipoprotein is able to perform resistance against lantibiotics. Like other proteins directly encoded in front of an ABC-transporter which perform resistance or immunity. Examples are the serine protease, mentioned before, Nsr [3] and the immunity protein of *L. lactis*, NisI [38].

Material and Methods

Cloning. The gene for the lipoprotein was synthesized from GeneArt (Thermo Fisher Scientific) as a none codon optimized and as an optimized gene for *E. coli.* The different genes were cloned in pMAT. The plasmid pET16-NHis-Lipo(opt) was cloned with the Gibson Assembly Cloning Kit (New England BioLabs) according to the manufacturer's protocol. Therefore, plasmid pET16b was linearized by PCR using the primers pET16-NHis-for and pET16-NHis-rev. The primer pair LipoEcoli-Gibs-F and LipoEcoli-Gibs-R was used to amplify the sequence of the lipoprotein without the first 19 amino acids and changing the twentieth amino acid C20A. The new plasmid was verified with sequence analysis.
To insert a TEV cleavage site a site directed mutagenizes was performed with the TEV LIPO for and TEV LIPO rev primer pair. The new plasmid was verified with sequence analysis.
The gene for CD1348 lipoprotein was synthesized from GeneArt (Thermo Fisher Scientific) and cloned in pIL-SV. The plasmid pIL-SV-Lipo was cloned with the Gibson Assembly Cloning Kit (New England BioLabs) according to the manufacturer´s protocol. Therefore, plasmid pIL-SV was linearized by PCR using the primers pIL-SV-C-lipo-for and pIL-SV-C-lipo-rev. The primer pair pIL-SV-Del-C for and pIL-SV-Del-C rev was used to delete the C-terminal His-tag. The new plasmid was verified with sequence analysis.

Table 1: Oligonucleotide used for cloning.

Oligonucleotide	Sequence
pET16-NHis-for	GAAATTTATTACAACGGTAAACTGATCGAACTGCGTTAACTAGCATAACCCC TTGGGGC
pET16-NHis-rev	GTTCAACCGCAGAAATGCTGTAATCCATGGCGCCGCTGCTGTGATGATGATG
LipoEcoli-Gibs-F	GCCATGGATTACAGCATTTCTGCG
LipoEcoli-Gibs-R	ACGCAGTTCGATCAGTTTACC
TEV LIPO for	GCCATGGATTACAGCATTTCTGCG
TEV LIPO rev	GCCCTGAAAATAAAGATTCTCGCCGCTGCTGTGATGATGATG
pIL-SV-C-lipo for	GATATACTACAATGGAAAATTAATAGAATTAAGACACCACCACCACCACTAA AAAG
pIL-SV-C-lipo rev	CAATTATTAAAAAACTTACTGCTATTTTATTCATATAATTCTCCTTTATTTATT ATACCCGCG
pIL-SV-Del-C-for	TCTTAATTCTATTAATTTTCCATTGTAGTATATC
pIL-SV-Del-C-rev	TAAAAAGGATTGGTTATTTTACCAATC

Test expression of CD1348. *E. coli* BL21 (DE3) cells transformed with the pET-16b-Lipo plasmid were used for a 5 mL lysogeny broth (LB) preculture containing 100 µg/mL ampicillin. For test expression 300 mL flasks with baffles were used. 8 x 50 mL LB media containing 100 µg/mL ampicillin was inoculated to an optical density (OD_{600}) of 0.1. Four cultures were grown at 37 °C and 180 rpm. At an OD_{600} of 0.8 two cultures were induced with 1 mM Isopropyl-ß-D-thiogalactopyranoside (IPTG) and two with 0.1 mM IPTG.
Four cultures had a decreased temperature curve during culture from 37 °C to 18 °C at an OD_{600} of 0.5 and induced with 1 mM IPTG (two flasks) and 0.1 mM IPTG (two flasks) at an OD_{600} of 0.8. Every hour a sample was taken and the cells were centrifuged 2 min at 14,000g at 4 °C. The harvested cells were diluted to an OD_{600} of 1 and further analysed via Western blot with a Penta-His Antibody.

Overexpression of CD1348 and the CD1348 codon optimized. *E. coli* BL21 (DE3) cells containing the pET-16b-Lipo opti. Plasmid/ pET-16b-Lipo-TEV opti. were used for 100 mL LB preculture containing 100 µg/mL ampicillin. Two litres LB medium with 100 µg/mL ampicillin was inoculated to an OD_{600} of 0.1, and grown at 37 °C and 180 rpm shaking to an OD_{600} of 0.5. The temperature was degraded to 18 °C and till the OD_{600} of 0.8 was reached. The culture was induced with 0.1 mM IPTG and grown overnight. After 20 h cells were harvested at 6,000g and stored at -20 °C.

Purification tests of CD1348 non-codon optimized. Cells were thawed on ice and resuspended in 50 mM Tris-HCl pH 8, 50 mM NaCl and 10% glycerol. Cells were lysed with a cell disruptor (Microfluidics M-110P, 1500 bar) 5-6 cycles and centrifuged at 4 °C for 45 min at 200,000 g. The supernatant was supplemented with imidazole (pH 8) in a final concentration of 20 mM imidazole. The supernatant was loaded on an immobilized metal-ion affinity chromatography (IMAC) column (Chelating HP column 5mL preloaded with Ni^{2+} GE Healthcare) with 1 mL/min. After washing the loaded column till baseline using the washing buffer (20 mM Tris-HCl pH 8, 500 mM NaCl and 20 mM imidazole) the CD1348 was eluted with the elution buffer (20 mM Tris-HCl pH 8, 500 mM NaCl and 400 mM imidazole) in gradient step 100% in 100 min.
Different elution steps were tested as well. The stepwise elution was performed in 5 steps of different imidazole concentrations 40 mM, 60 mM, 80 mM, 150 mM and 400 mM. The eluted protein was monitored via NanoDrop and SDS-PAGE. Fractions containing the CD1348 protein were pooled. Via size-exclusion chromatography (SEC) the concentrated

protein was further purified. The column was equilibrated with the SEC buffer (25 mM MES pH 6.5, 150 mM NaCl) and the protein was purified with a Superdex 75 10/300 GL column with a flow rate of 0.3 mL/min. All fractions containing the CD1348 were pooled and concentrated with an Amicon ultracentrifugation unit (10 kDa MWCO).

Purification of CD1348 with His-tag codon optimized. Cells were thawed on ice and resuspended in 50 mM Tris-HCl pH 8, 50 mM NaCl and 10% glycerol. Cells were lysed with a cell disruptor (Microfluidics M-110P, 1500 bar) 5-6 cycles and centrifuged at 4 °C for 45 min at 200,000 g. The supernatant was supplemented with imidazole (pH 8) in a final concentration of 20 mM imidazole. The supernatant was loaded on an IMAC column (Chelating HP column 5mL preloaded with Ni^{2+} GE Healthcare) with 1 mL/min. After washing the loaded column till baseline with the washing buffer (20 mM Tris-HCl pH 8, 500 mM NaCl and 20 mM imidazole) the CD1348 was eluted with the elution buffer (20 mM Tris-HCl pH 8, 500 mM NaCl and 400 mM imidazole) in one step. The eluted protein was monitored via NanoDrop and SDS-PAGE and the fractions containing the CD1348 protein were pooled. Via size-exclusion chromatography (SEC) the concentrated protein was further purified. The column was equilibrated with the SEC buffer (25 mM MES pH 6.5, 250 mM NaCl and 10% glycerol) and the protein was purified with a HighLoad 16/600 Superdex 200 pg with a flow rate of 0.5 mL/min. All fractions containing the CD1348 were pooled and concentrated with an Amicon ultracentrifugation unit (10 kDa MWCO). The CD1348 was concentrated to 10 mg/mL, flash frozen in liquid nitrogen and stored at -80 °C. To determine the concentration the absorbance at 280 nm with a NanoDrop ND-1000 spectrophotometer using the theoretical extinction coefficient of CD1348 of 21.43 L mol^{-1} cm^{-1} and the molecular weight 20.18 kDa was used (Calculated via EXPASY ProtParam).

Determination of the oligomeric state of CD1348. To determine the oligomeric state of the CD1348 a multi- angel light scattering and size exclusion (MALS-SEC) was used. The analyses were performed on an Agilent 1260 HPLC system in combination with a triple-angle light scatter detector (miniDawn treos) and a differential refractive index detector (Optilab rEX- both Wyatt Technology Europe). The purified CD1348 was analysed on a Superdex 200 10/300 increase column (GE Healthcare) with a MALS buffer containing 25 mM MES pH 6.5 and 250 mM NaCl. The used protein concentration was 300 µM and the Data analysis was performed with the ASTRA software (Wyatt Technology).

Purification of CD1348 without His-tag codon optimized. Cells were thawed on ice and resuspended in 50 mM Tris-HCl pH 8, 50 mM NaCl and 10% glycerol. Cells were lysed with a cell disruptor (Microfluidics M-110P, 1500 bar) 5-6 cycles and centrifuged at 4 °C for 45 min at 200,000 g. The supernatant was supplemented with imidazole (pH 8) with a final concentration of 20 mM imidazole. The supernatant was loaded on an IMAC column (Chelating HP column 5mL preloaded with Ni^{2+} GE Healthcare) with 1 mL/min. After washing the loaded column till baseline with the washing buffer (20 mM Tris-HCl pH 8, 500 mM NaCl and 20 mM imidazole) the CD1348 was eluted with the elution buffer (20 mM Tris-HCl pH 8, 500 mM NaCl and 400 mM imidazole) in one step. The eluted protein was monitored via NanoDrop and SDS-PAGE and the fractions containing the lipoprotein were pooled.

The protein was diluted with Dilution buffer (20 mM Tris-HCl pH 8, 250 mM NaCl) to a concentration to 2 mg/mL and 1:200 TEV Protease (Sigma) was added and the His-tag was cleaved over night at 4 °C.

To purify the cleaved protein, a second IMAC was performed. The whole solution was loaded on an IMAC column (Chelating HP column 5mL preloaded with Ni^{2+} GE Healthcare) with 1 mL/min and the load was fractionated to get the protein without His-tag eluted. After washing till base line with wash buffer (20 mM Tris-HCl pH 8, 250 mM NaCl) the none cleaved CD1348 was eluted like mentioned before. The load fractions with the cleaved CD1348 protein were pooled and concentrated with an Amicon ultracentrifugation unit (10 kDa MWCO) and further purified via SEC.

The column was equilibrated with the SEC buffer (25 mM MES pH 6.5, 250 mM NaCl and 10% glycerol) and the protein was purified with a HighLoad 16/600 Superdex 200 pg with a flow rate of 0.5 mL/min. All fractions containing the CD1348 were pooled and concentrated with an Amicon ultracentrifugation unit (10 kDa MWCO). The CD1348 was concentrated to 10 mg/mL, flash frozen in liquid nitrogen and stored at -80 °C. To determine the concentration, the absorbance at 280 nm via NanoDrop ND-1000 spectrophotometer using the theoretical extinction coefficient of CD1348 of 21.43 L mol^{-1} cm^{-1} and the molecular weight 18.63 kDa was measured (calculated via EXPASY ProtParam).

Expression and purification of CD1348 for NMR measurements. *E. coli* BL21 (DE3) cells containing the pET-16b-Lipo opti plasmid were used for 100 mL LB preculture containing 100 µg/mL ampicillin. Two litres M9 minimal medium containing ^{15}N ammonium chloride (Cambridge Isotope Laboratories, Inc.) /and ^{13}C-D-glucose (Cambridge Isotope Laboratories, Inc.) and 100 µg/mL ampicillin were used. The medium was inoculated to an OD_{600} of 0.1, grown at 37 °C and 180 rpm shaking to an OD_{600} of 0.5. The temperature was degraded to 18 °C and till the OD_{600} of 0.8 was reached. The culture was induced with 0.1 mM IPTG and grown overnight. After 20h cells were harvested at 6,000g and stored at -20 °C.

Cells were thawed on ice and resuspended in 50 mM Tris-HCl pH 8, 50 mM NaCl and 10% glycerol. Cells were lysed with a cell disruptor (Microfluidics M-110P, 1500 bar) 5-6 cycles and centrifuged at 4 °C for 45 min at 200,000 g. The supernatant was supplemented with imidazole (pH 8) in a final concentration of 20 mM imidazole. The supernatant was loaded on an IMAC column (Chelating HP column 5mL preloaded with Ni^{2+} GE Healthcare) with 1 mL/min. After washing the loaded column till baseline with the washing buffer (20 mM Tris-HCl pH 8, 500 mM NaCl and 20 mM imidazole) the CD1348 was eluted with the elution buffer (20 mM Tris-HCl pH 8, 500 mM NaCl and 400 mM imidazole) in one step. The eluted protein was monitored via NanoDrop and SDS-PAGE and the fractions containing the CD1348 were pooled. Via size-exclusion chromatography (SEC) the concentrated protein was further purified. The column was equilibrated with the SEC buffer (25 mM MES pH 6.5 and 100 mM NaCl) and the protein was purified with a HighLoad 16/600 Superdex 200 pg with a flow rate of 0.5 mL/min. All fractions containing the CD1348 were pooled and concentrated with an Amicon ultracentrifugation unit (10 kDa MWCO). The CD1348 was concentrated to 14 mg/mL and 5 mM sodium azide was added to the sample. To determine the concentration, the absorbance at 280 nm with a NanoDrop ND-1000 spectrophotometer using the theoretical extinction coefficient of CD1348 of 21.43 L mol^{-1} cm^{-1} and the molecular weight 20.18 kDa was used (Calculated via EXPASY ProtParam).

Visualization of CD1348 from *C. difficile* by small-angle X-ray scattering (SAXS).
At the EMBL-Lab outstation Grenoble, the protein was freshly purified with a Superdex 200 10/300 column (GE Healthcare) pre-equilibrated with SAXS-buffer (25 mM MES pH 6.5, 250 mM NaCl, 5 % glycerol) at a flow rate of 0.5 mL/min.
All SAXS data were collected on beamline BM29 at the ESRF Grenoble [39; 40], equipped with a PILATUS 1M detector (Dectris) with a fixed distance of 2.867 m. The achievable q-range under these conditions was 0.025 - 5 nm^{-1} and the maximum measurable R_g (radius of gyration) of the investigated particles were 20 nm. All measurements were performed at 4 °C with protein concentrations between 0.51 and 7.68 mg/mL. For each sample, ten frames with an exposer time of one second were collected. By comparing these frames, the possibility of radiation damage during the measurement was excluded.
All used programs for data processing were part of the ATSAS Software package (Version 2.8.1) [41], available on the EMBL website (http://www.embl-hamburg.de/biosaxs/software.html). The primary data reduction was performed with the program PRIMUS [42]. With the Guinier approximation [43] (implemented in PRIMUS [42]) the forward scattering *I(0)* and the radius of gyration (R_g) was determined. The maximum particle dimension (D_{max}) with the pair-distribution function *p(r)* was estimated, computed with the program GNOM [44]. Low resolution *ab initio* models were calculated with GASBOR [45]. Superimposing of the predicted model was done with the program SUPCOMB [46]. A reference solution of bovine serum albumin (66 kDa) was used to determine the molecular weight of the lipoprotein from the forward scattering.

Circular dichroism spectroscopy measurements. Far-UV circular dichroism (CD) spectra were measured on a JASCO J-815 spectropolarimeter in a 1 mm Quartz cuvette (Hellma) using protein samples at a concentration of 10 µM. The buffer was 25 mM MES pH 6.5, 250 mM NaCl and 25 mM MES pH 6.5, 100 mM NaCl. Melting curves were recorded at 220 nm with a heating rate of 1 °C min^{-1}.

Crystallization. The screening for protein crystals was performed at 12 °C with a NT8robot (Formulatrix) and the sitting-drop vapour-diffusion method. Initial screens were performed with several of commercial crystallization screens. The used purified protein concentration was between 7 mg/mL and 15 mg/mL. The drop consisting of 0.1 µL protein solution and 0.1 µL reservoir solution were placed on a sitting drop plate and equilibrated against 50 µL of the reservoir solution. If an initial crystal was grown the prepared plates were observed

after 2 days and till 1 month. Some quasi micro crystals could be observed in the PACT plate with the conditions 0.2 M Sodium/ potassium phosphate and 0.1 M Bis Tris propane pH 8.5 20% (w/v) PEG 3350 and the 0.2 M sodium iodide and 20% (w/v) PEG 3350. Two optimization plates containing 250 mM-100 mM Sodium/ potassium phosphate (50 mM steps) and 5%-30% (w/v) PEG 3350 (5% steps) in a sitting drop plate were performed, containing 1 µL protein (8 mg/mL or 14 mg/mL) and 1 µL the reservoir buffer was placed and equilibrated against 300 µL buffer. Another two optimization plates containing 300 mM-150 mM Sodium iodide (50 mM steps) and 5%-30% (w/v) PEG 3350 (5% steps) in a sitting drop plate were performed, containing 1 µL protein (8 mg/mL or 14 mg/mL) and 1 µL the reservoir buffer was placed and equilibrated against 300 µL buffer.

Nuclear magnetic resonance (NMR)-measurements. The NMR samples contained 0.63 mM [U-^{15}N] or 0.63 mM [U-^{13}C,^{15}N] CD1348, 100 mM NaCl, 5 mM NaN_3, 25 mM MES (pH 6.5) in 10% (v/v) D2O. NMR experiments were recorded at 30 °C on Bruker AVANCE III HD 600 MHz, Bruker AVANCE III HD 700 MHz, Varian VNMRS 800 MHz, or Varian VNMRS 900 MHz NMR spectrometers, equipped with room temperature (900 MHz) or cryogenically cooled (600 MHz, 700 MHz, 800 MHz) triple or quadruple resonance probes with z-axis pulsed field gradient capabilities. The sample temperature was calibrated using methanol-d4 [47]. Sequence-specific assignments for the backbone resonances were obtained from TROSY [48; 49; 50] versions of the following 2D and 3D triple-resonance experiments [51]: [^{1}H,^{15}N] TROSY [50], [^{1}H,^{13}C] CT-HSQC [52], [^{1}H,^{15}N] TOCSY-HSQC [53] with a 10.0 kHz DIPSI-2rc mixing scheme [54] (60 ms mixing time), [^{1}H,^{15}N] NOESY-TROSY [53] (120 ms mixing time), TROSY-HNCO [49], TROSY-HN(CO)CA [55], TROSY-HN(CO)CACB [49], TROSY-HNCA [55], TROSY-HN(CA)CO [55], TROSY-HNCACB [55], and H(CCO)NH-TROSY and C(CO)NH-TROSY [56] with a 16.7 kHz FLOPSY-16 mixing scheme [57] (14 ms mixing time). The $1H_2O$ resonance was suppressed by gradient coherence selection, with quadrature detection in the indirect dimensions achieved by States-TPPI [58] and the echo-antiecho method [59; 60]. All NMR spectra were processed with NMRPipe [61] software and analysed with NMRViewJ [62]. ^{1}H chemical shifts were referenced with respect to external DSS in D_2O, ^{13}C and ^{15}N chemical shifts were referenced indirectly [63]. ^{1}HN and ^{15}N amide group chemical shifts were obtained from the peak positions of the TROSY multiplet components by subtracting out the scalar coupling contribution of -|1JNH|/2 and +|1JNH|/2, respectively, assuming a uniform scalar coupling constant of 1JNH = -93 Hz. Random Coil Index (RCI) [64]

backbone order parameters, SRCI2, and confidence levels for helical (H) or extended/strand (E) secondary structure, PH or PE, respectively, were calculated from the backbone chemical shifts using TALOS-N [65] with the default parameters.

Purification of Nisin. Nisin was purified as described in Abts et al. (2011) [66]. To determine the nisin concentration, nisin was measured by using RP-HPLC as previously described in Abts et al. (2013) [67].

Analytical co-elution studies of CD1348 with nisin. To see interaction between the CD1348 protein and nisin, a Äkta micro system and a Superdex 75 PC 3.2 column (GE Healthcare) were used. The column was preequilibrated with 25 mM MES pH 6.5, 250 mM NaCl buffer with a flow of 0.05 mL/min. 50 µL of a protein mixture of 15 µM purified His-tag CD1348 and 150 µM purified nisin was incubated 1h at 20 °C and analysed via size exclusion. The corresponding fraction were analysed via 15% SDS-PAGE.

Tryptophan fluorescence measurements. To determine the tryptophan fluorescence of the CD1348 protein in interaction with different lantibiotics, 1 µM CD1348 protein, purified as described, the fluorescence with an excitation at 280 nm with an emission of 300-400 nm was measured (FluorEssence V3.5, Horiba Scientific Slits both 4 nm) at 30 °C. Then the lantibiotic was added in 10 µL steps after every 2min and the fluorescence was measured. As a control, the used buffer (25 mM MES pH 6.5, 250 mM NaCl) was measured with 1 µM Protein and 10 µL buffer was stepwise added. Also, the buffer and the lantibiotic was measured stepwise to be sure that the fluorescence change is no artefact from the used lantibiotic or buffer. The control protein buffer was subtracted from the protein lantibiotic measurements to be sure that just the changes of binding are observed.

Expression of CD1348 in *L. lactis*. The NZ9000CD1348 strain was grown in GM17 media supplemented with 5 µg/mL chloramphenicol. To induce the expression of the lipoprotein 1 ng/mL nisin was added and the cells were grown at 30 °C overnight. The cells were harvested at OD_{600} of 2.5 by centrifuging at 5,000g for 30min. With a 50 mM HEPES pH 8, 150 mM NaCl and 10% (v/v) glycerol buffer the cells were resuspended to an OD_{600} of 200 and 1/3 (w/v) glass beads (0.3 mm) were added. To lyses the cells were 1 min disrupted and 2 min storing on ice, this cycle was repeated six times and the lysed cells were centrifuged. The low centrifugation step at 10,000g at 4 °C for 20 min were performed to collect the

cytoplasmic part. The high centrifugation step for 1 h at 100,000g at 4 °C were performed to harvest the membranes. To analyse the membrane, fraction SDS Loading dye was added and the samples were used for an SDS-PAGE and Western blot analysis.

Determination of the resistance of the *L. lactis* NZ9000 CD1348 strain by Growth Inhibition (IC_{50}). *L. lactis* NZ9000 and NZ9000CD1348 cells were grown overnight in GM17 containing 5 µg/µl chloramphenicol and 1 ng/mL nisin at 30 °C. The cells were diluted to an OD_{600} of 0.1 and then incubated with a serial dilution of the analysed lantibiotic in a 96-well plate. Each well contain 50 µL of the respective lantibiotic and 150 µL GM17 with the corresponding strain, so in total the volume of each well contains 200 µL. The 96-well plate was incubated at 30 °C for 5 h. The optical density was determined via plate reader BMG at 584 nm. The optical density was normalized and plotted against the logarithm of the corresponding antibiotic concentration. The IC_{50} value was calculated using the following equation

$$y = OD_{min} + \frac{OD_{max} - OD_{min}}{1 + 10^{(\log(IC50) - x) * p}}$$

OD_{max} stands for the normalized OD value, at which the lowest concentration of the antibiotic was added and the strains grew without inhibition. The OD_{min} corresponds to the normalized OD were the highest lantibiotic concentration was added and the cell growth was inhibited the most. x is the logarithmic of the antibiotic/ lantibiotic concentration with was added and y represents the calculated normalized OD value. In general, the IC_{50} value is the concentration of one lantibiotic where the growth of cells is inhibited by 50%.

Results

Test expression of CD1348. To find the best expression conditions of the CD1348 protein expression tests were performed. The cloning was successful so *E. coli* BL21 (DE3) cells containing the pET16b-Lipo plasmid could be used for test expression. Four different conditions were tested. First different temperatures 37 °C and 37 °C followed 18 °C were tested. Different Isopropyl-ß-D-thiogalactopyranoside (IPTG) concentrations, 1 mM IPTG and 0.1 mM IPTG were also tested. LB media containing 100 µg/mL ampicillin was inoculated to an OD_{600} of 0.1 and the cells were grown at 37 °C and 180 rpm. At an OD_{600} of 0.5 two cultures the temperature was decreased to 18 °C. The other cultures were still grown at 37 °C. At an OD_{600} of 0.8 the cells were induced with 1 mM IPTG or 0.1 mM IPTG. Every hour samples were taken adjusted to an OD_{600} of 1 and analysed via Western blot (Penta-His antibody) (Figure 3). The molecular mass was compared with the calculated weight 20.18 kDa (calculated via EXPASY ProtParam).

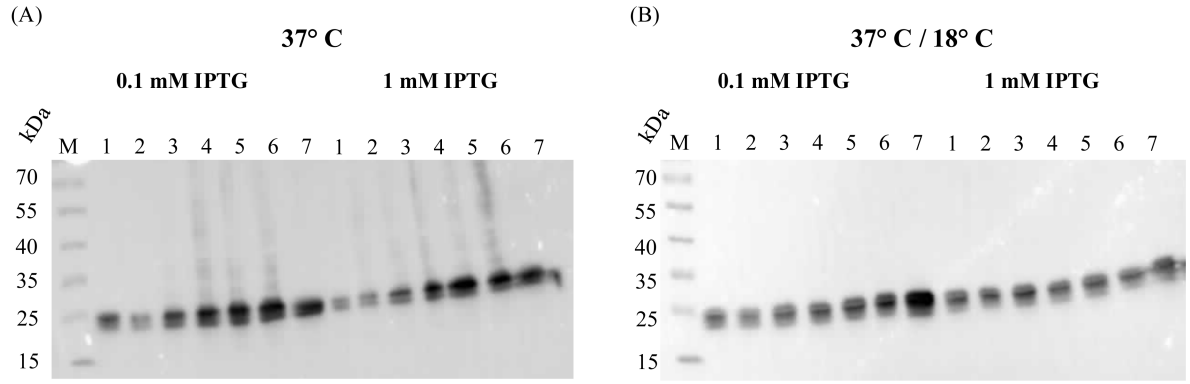

Figure 3: Expression tests of the CD1348 protein. A) The test expression at 37 °C was sampled after every hour and detected via Western blot (Penta-His Antibody). 10% SDS-PAGE gel was used. 1 is the sample after the first hour of expression till 7 overnight. The different IPTG concentrations are shown. B) The test expression at 37 °C / 18 °C was sampled after every hour and detected via Western blot (Penta-His Antibody). 10% SDS-PAGE gel was used. 1 is the sample after the first hour of expression till 7 overnight. The different IPTG concentrations are shown. M is the protein ladder (PageRuler prestained protein ladder (Thermo Fisher Scientific)).

The best observed condition was the expression at 37 °C followed by 18 °C induced with 0.1 mM IPTG grown over night (Figure 3). This condition was used for following purifications, codon optimized and non-codon optimized plasmids.

Purification tests of the CD1348. To establish the purification of the CD1348 a two-step protocol out of 2 L cell culture was tested. First a nickel affinity chromatography was performed to determine at which concentration of imidazole the CD1348 elute, a gradient elution was tested. The gradient was chosen 100% (400mM imidazole) in 100 min (Figure

4). Here could be shown that the CD1348 elute in an inhomogeneous peak at an imidazole concentration over the whole gradient (Figure 4).

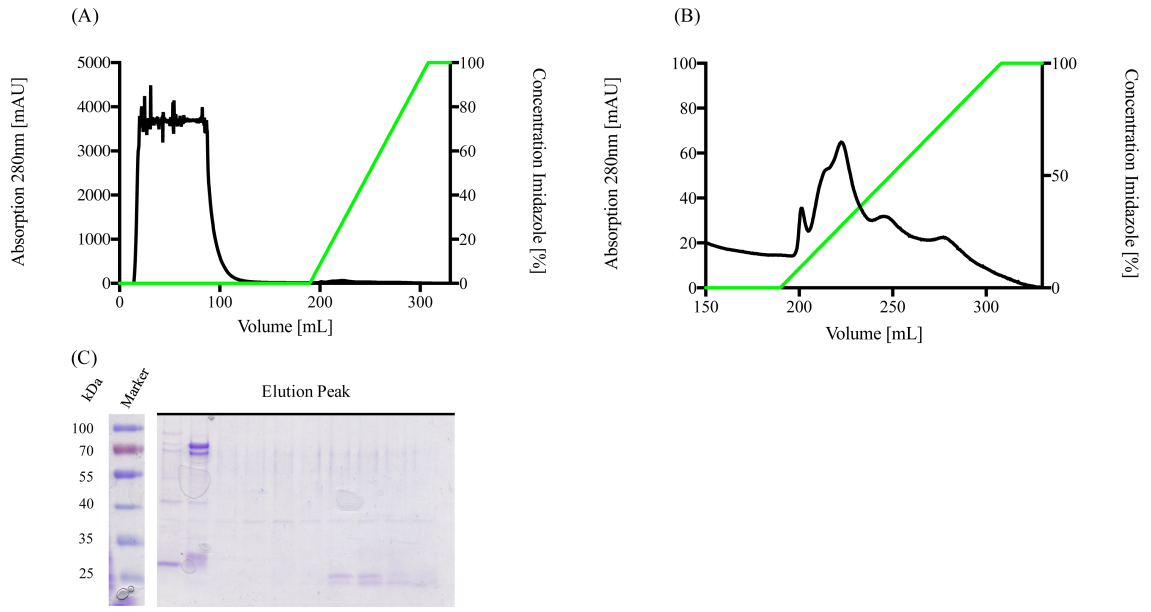

Figure 4: IMAC chromatogram and SDS-PAGE gel of the first CD1348 purification. A) Shows the IMAC chromatogram with the gradient elution step 100% imidazole concentration (400 mM Imidazole, depicted in green) in 100 min. Here the absorption at 280 nm [mAU] against the volume [mL] is shown. B) Shows the zoom in of the elution peak of A) the peak is inhomogeneous and is eluting nearly over the whole chromatogram. Here the absorption at 280 nm [mAU] against the volume [mL] is shown. (C) Shows the 10% SDS-PAGE analysis of the whole elution peak of (B). It is shown that the peak consists of a lot of impurities and some CD1348 protein shown in the last three lines. M is the protein ladder (PageRuler prestained protein ladder (Thermo Fisher Scientific)).

The protein was concentrated and a size exclusion chromatography was performed. Here a small inhomogeneous peak could be seen (data not shown). To optimize the purification the protein was purified again out of 6 L cell culture. A nickel affinity chromatography was performed now with a stepwise elution. The steps were chosen at 40 mM, 60 mM, 80 mM, 150 mM and 400 mM imidazole (chromatogram not shown). As a control, a sample of every elution step was analysed via SDS-PAGE (Figure 5).

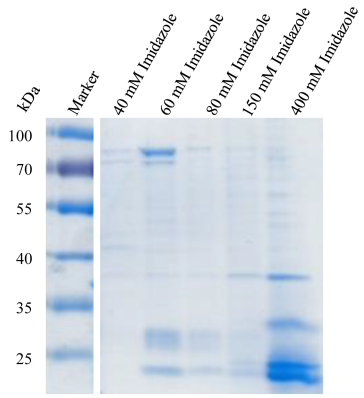

Figure 5: Stepwise IMAC Elution SDS-PAGE of CD1348 purification. 10% Gel of the taken samples of the step elution IMAC fractions. The sample was taken from the main peak of the elution peak. The different steps were taken at 40 mM, 60 mM, 80 mM 150 mM and 400 mM imidazole concentration. The gel shows that the impurities are getting lesser but the protein is not pure. Marker is protein ladder (PageRuler prestained protein ladder (Thermo Fisher Scientific)).

Although, the stepwise elution produced better results than the gradient elution still some impurities were found. After this purification protocol, impurities were still detected and the yield was not good enough, therefore the *E. coli* codon optimized gene was ordered and it was tried to purify the protein again.

Expression and Purification of CD1348 codon optimized protein. The cloning and the overexpression in *E. coli* BL21 (DE3) cells of the CD1348 lipoprotein was successfully. The protein was purified via two-step protocol with His-tag and via three-step protocol with the His-tag cleaved out of 2 L cell culture. A nickel affinity chromatography was the first step in both purifications followed by a size exclusion chromatography for the His tagged protein or a second nickel affinity chromatography after TEV cleavage followed by a size exclusion chromatography. The CD1348 protein eluted in three (none cleaved) (Figure 6) or two peaks (cleaved one) (Figure 8) from the size exclusion. The yield of the non-cleaved protein was around 15 mg/L and for the cleaved one the yield was around 4 mg/L of cell culture. The purity of the protein was checked via SDS-PAGE and Western blot. The molecular mass was compared with the calculated weight 18.63 kDa and 20.18 kDa (calculated via EXPASY ProtParam). Interestingly the none-cleaved protein appears as a double band in SDS-PAGE analysis, while the cleaved protein shows a single band (Figure 6, Figure 8). To be sure, that the seen double bands are both the CD1348 protein, the Western blot was performed with an anti CD1348 antibody (Figure 6) so it was sure that it is the CD1348 protein.

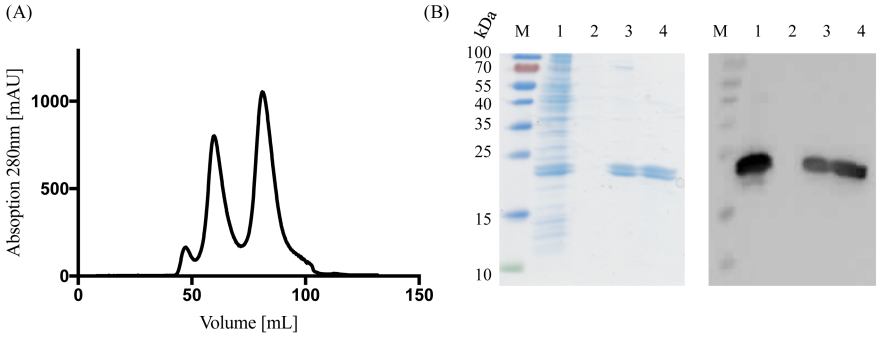

Figure 6: CD1348 purification without cleaving the His-tag. A) The size exclusion using a HighLoad 16/600 Superdex 200 pg. The third peak is the CD1348 protein in high purity. Here the absorption at 280 nm [mAU] against the volume [mL] is shown. B) 15% SDS-PAGE showing the purification steps and the purity of the CD1348 protein. The Western blot shows, that the protein is highly pure. M is the used protein ladder (PageRuler prestained protein ladder (Thermo Fisher Scientific)) 1 is the load of the IMAC, 2 the flow through and 3 the IMAC elution. 4 is the SEC elution and shows the highly pure CD1348 protein. The used Antibody was an anti-CD1348 polyclonal antibody from rabbit (DavidsBiotechnologie GmbH).

To determine the oligomeric state of the CD1348 a multi-angle light scattering and size exclusion (MALS-SEC) measurement was performed. The purified CD1348 protein was measured on a Superdex 200 10/300 increase (GE Healthcare) column and the molar mass was calculated (Figure 7). The calculated molar mass of 21.19 ± 0.19 kDa in comparison to the molar mass of 20.18 kDa indicated that the CD1348 is a monomer in solution.

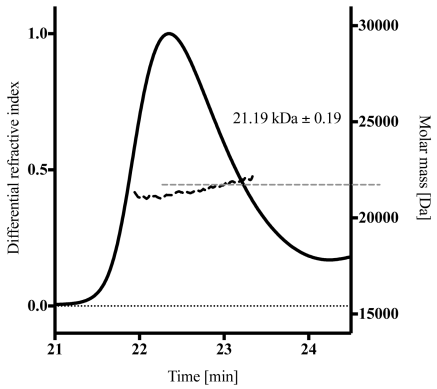

Figure 7: MALS measurements of CD1348 with His-tag. To obtain the oligomeric state of the CD1348 protein a MALS measurement was performed. A Superdex 200 column was used. The differential reflective index and the molecular mass was plotted against the time. The calculated molecular mass of 21.19 ± 0.19 kDa in comparison to the 20.18 kDa is showing that the CD1348 has an oligomeric state of a monomer.

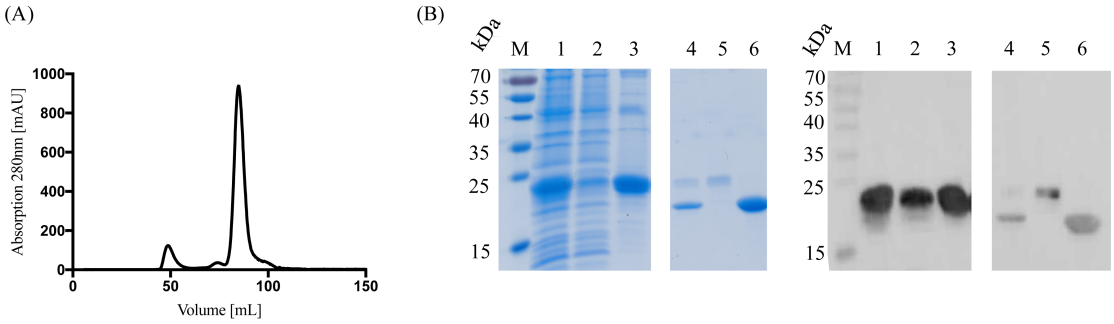

Figure 8: Purification CD1348 without His-tag. A) The size exclusion using a HighLoad 16/600 Superdex 200 pg. The second peak is the CD1348 protein in high purity. Here the absorption at 280 nm [mAU] against the volume [mL] is shown. B) 15% SDS-PAGE showing the purification steps and the purity of the CD1348 protein. The Western blot shows as well, that the protein is highly pure. M is the used protein ladder, PageRuler prestained protein ladder (Thermo Fisher Scientific), 1 the IMAC load, 2 the flow through, 3 the IMAC elution. 4 is the load of the SEC, 5 the first peak at 50 mL and 6 the high pure cleaved CD1348 in the SEC elution peak. The used Antibody was an anti-CD1348 polyclonal antibody from rabbit (Davids Biotechnologie GmbH).

CD measurements melting curves. The Far-UV circular dichroism (CD) spectra were measured on a JASCO J-815 spectropolarimeter in a 1 mm Quartz cuvette (Hellma) using protein samples at a concentration of 10 µM CD1348 with His-tag. The buffer was 25 mM MES pH 6.5, 250 mM NaCl and 25 mM MES pH 6.5, 100 mM NaCl. Melting curves were recorded at 220 nm with a heating rate of 1 °C min^{-1}. To observe the stability of the CD1348 protein we performed melting curves to get an idea how heat stable the protein is with different salt concentrations. CD 1348 is stable even until 90 °C based on the melting curves (Figure 9). Salt concentration is not significant influencing the behaviour of the protein.

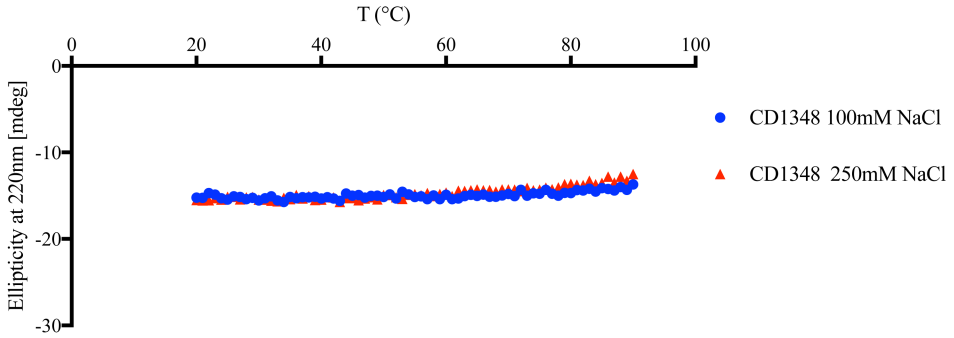

Figure 9: CD Measurement melting curves. The CD1348 protein concentration was 10 µM and the melting curves were recorded at 220 nm with a 1 °C min^{-1} heating rate. Blue shows the curve of CD1348 protein in a 25 mM MES pH 6.5, 100 mM NaCl and red the protein in a 25 mM MES pH 6.5, 250 mM NaCl buffer.

Crystallography. To characterize the structure of the CD1348 lipoprotein crystallography was chosen. The yield and the quality of the CD1348 was high enough to try crystallography tests. These tests were performed with and without the His-tag, to check, if the His-tag has an influence on the crystallization of the CD1348. Initial screenings were performed with commercial available screens using the sitting drop method. No initial diamond- shaped crystal could be observed in one of the initial plates. Only some quasi micro crystals could be observed in the PACT plate with the conditions 0.2 M Sodium/ potassium phosphate and 0.1 M Bis Tris propane pH 8.5 20% (w/v) PEG 3350 and the 0.2 M sodium iodide and 20% (w/v) PEG3350 (Figure 10).

(A) (B)

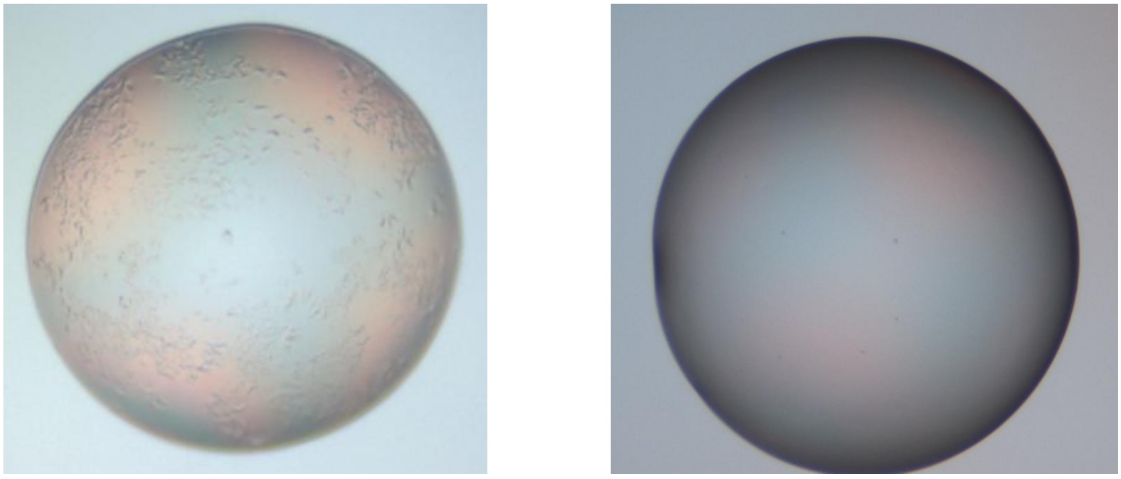

Figure 10: Crystallization initial drops with quasi micro crystals. A) The drop containing 0.1 µL CD1348 protein and 0.1 µL reservoir solution (0.2 M Sodium/ potassium phosphate and 0.1 M Bis Tris propane pH 8.5, 20% (w/v) PEG 3350) after 10 days. Some micro crystals could be observed. B) The drop containing 0.1 µL CD1348 protein and 0.1 µL reservoir solution (0.2 M sodium iodide and 20% (w/v) PEG3350) after 10 days. Two micro crystals could be observed.

An optimization 24-well plate containing 250 mM-100 mM Sodium/ potassium phosphate (50 mM steps) and 5%-30% (w/v) PEG 3350 (5% steps) in two sitting drop plates were performed. The drops contain 1 µL protein (8 mg/mL or 14 mg/mL) and 1 µL buffer. 300 µL buffer were placed in the reservoir for equilibration. Another optimization 24-well plate containing 300 mM-150 mM Sodium iodide (50 mM steps) and 5%-30% (w/v) PEG 3350 (5% steps) in two sitting drop plates were performed. The plates were prepared as mentioned before with a protein concentration of 8 mg/mL or 14 mg/mL. The optimized plates do not show any crystals at all.

NMR-Measurements. Beside the crystallography NMR measurements are a method to determine the structure of the CD1348 protein. The CD1348 protein is a small protein with 20 kDa. NMR spectroscopy is an option to determine the structure of such small proteins. Purified CD1348 protein with His-tag was used for the first NMR measurement. The 1D ^{1}H spectrum (Figure 11) was used to control if the CD1348 protein is a good candidate for NMR measurements and to analyse if the combination of protein and buffer are good for further analyses.

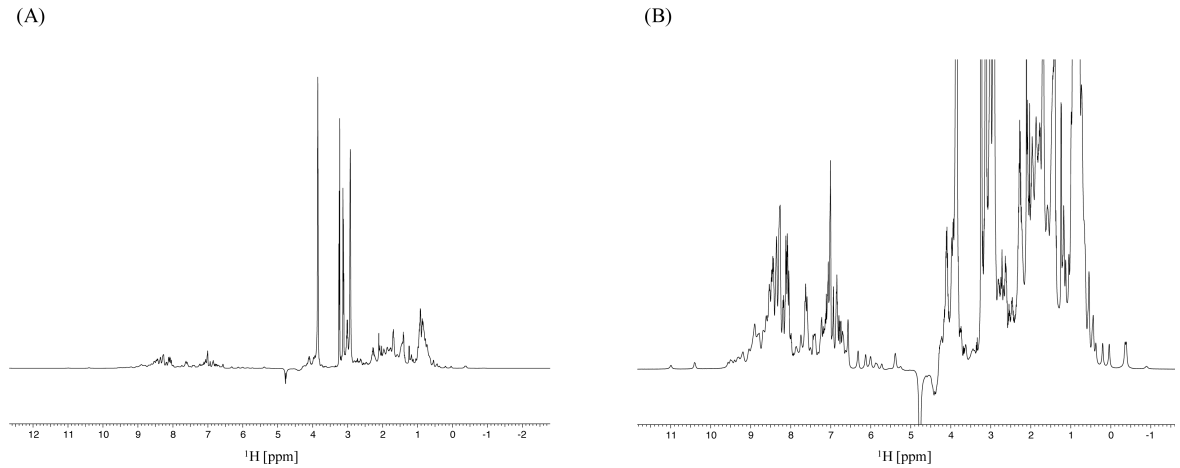

Figure 11: 1D ^{1}H spectrum of the CD1348 protein. A) The whole 1D ^{1}H spectrum of the CD1348 protein. The resonance between 2 ppm and 4 ppm is the spectrum of the used MES buffer. B) A zoom in of the CD1348 protein spectrum. A 1D ^{1}H spectrum is too complex to determine the structure. Therefore, 2D spectra like the [^{1}H,^{15}N] TROSY was measured.

The 1D ^{1}H spectrum confirms that the used conditions and concentration of the CD1348 are useable for NMR measurements with ^{15}N and ^{13}C labelled protein. The CD1348 protein was labelled with a M9 minimal media containing ^{15}N ammonium chloride /and ^{13}C-D-glucose. Different NMR spectra were measured to determine the structure. One of the measured NMR spectra is shown in Figure 12. It is a [^{1}H, ^{15}N] TROSY measured at 600 MHz. 630 µM of [U- ^{15}N] CD1348 protein was measured in a 25 mM MES pH 6.5, 100 mM NaCl, 5 mM NaN_3 buffer containing 10 % D_2O. The sample was measured at 30 °C in a Bruker AVANCE III HD 600 MHz.

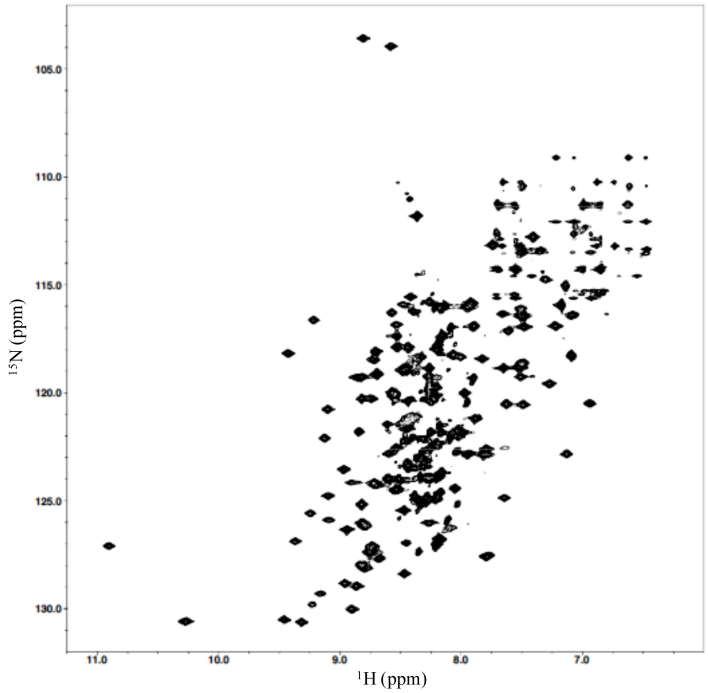

Figure 12: [^{1}H, ^{15}N] TROSY spectrum of 630 µM [U-^{15}N] CD1348 protein. The protein was measured in 25 mM MES pH 6.5, 100 mM NaCl, 5 mM sodium azide and 10% D_2O. The spectrum was recorded at 30 °C at 600 MHz on a Bruker AVANCE III HD.

To calculate the structure, additionally [^{1}H,^{13}C] CT-HSQC, [^{1}H,^{15}N] TOCSY-HSQC with a 10.0 kHz DIPSI-2rc mixing scheme, [^{1}H,^{15}N] NOESY-TROSY, TROSY-HNCO, TROSY-HN(CO)CA, TROSY-HN(CO)CACB, TROSY-HNCA, TROSY-HN(CA)CO, TROSY-HNCACB, H(CCO)NH-TROSY and C(CO)NH-TROSY with a 16.7 kHz FLOPSY-16 mixing scheme were measured (data not shown). NMR structure calculation is still in progress.

SAXS-Measurements. To determine the overall shape of a protein SAXS is an easy and fast way. In the ESRF Grenoble at Beamline 29 with a PILATUS detector the measurements with freshly purified CD1348 protein SAXS measurements were performed. The protein was purified with a Superdex 200 10/300 column (GE Healthcare) at a flow rate of 0.5 mL/min. The used buffer was a MES pH 6.5 buffer (25 mM MES pH 6.5, 250 mM NaCl, 5 % glycerol). The protein concentration range of the SAXS measurement was between 0.51 mg/mL and 7.68 mg/mL. For each sample ten different frames with an exposer time of one second were measured, resulting in a scattering curve (Figure 13).

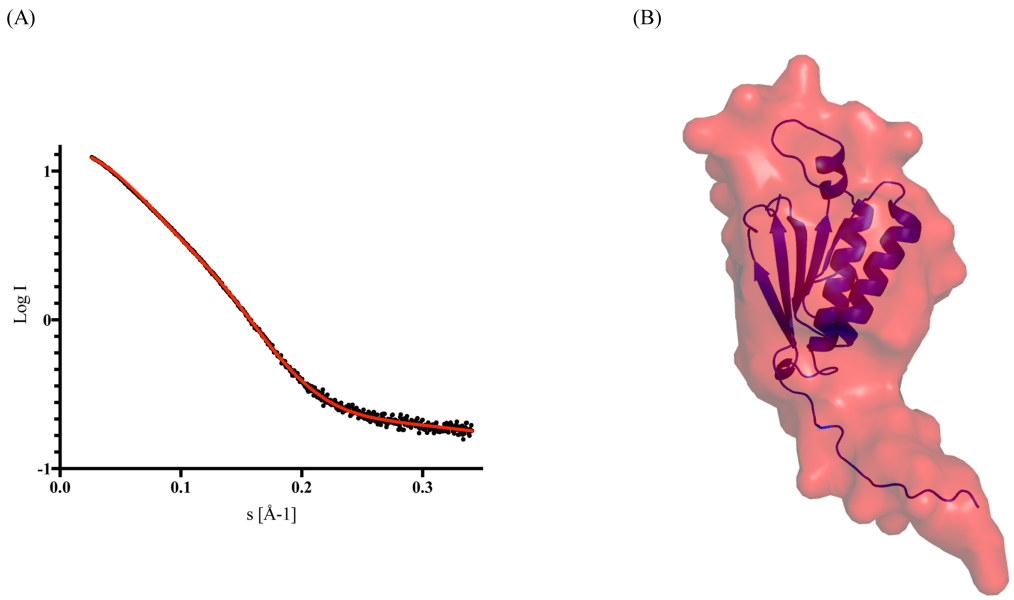

Figure 13: SAXS plot and analysis of the CD1348 protein. A) Experimental curve is shown in black dots and the *ab-initio* model fit as red line. The intensity is displayed as a function of momentum transfers. B)The volumetric envelope from the CD1348 lipoprotein, as calculated from the scattering data using GASBOR [45], is shown in red surface. The predicted model of the lipoprotein (shown in blue) was docked into the volumetric envelope using SUPCOMB [46].

With the measured scattering curve a low resolution *ab initio* model was calculated with GASBOR [45]. The *ab initio* model shows a volumetric envelope with a long flexible N-terminal domain and a compact C-terminal domain (Figure 13, Table 2). With the TOP model program (D. Mulnaes et al., unpublished) a model structure of the CD1348 was calculated. The model contains a long flexible N-terminal loop domain, five ß-sheets and two major α-helices. This calculated model was fitted in the SAXS low-resolution model. In Figure 13 B the fit is shown. The independent calculation of the structure of CD1348 and the *ab initio* model of CD1348 are showing high similarity and both models are fitting perfectly together.

Table 2: Overall SAXS data of CD1348.

Beamline	BM29, ESRF Grenoble [39; 40]
Data collection parameters	
Detector	PILATUS 1 M
Detector distance (m)	2.867
Beam size (µm x µm)	700 x 700
Wavelength (Å)	0.99
Sample environment	Quartz glass capillary, 1 mm ø
s range (nm^{-1})‡	0.025–5.0
Temperature (°C)	4
Exposure time per frame (s)	10 x 1s
Mode of measurement	static
Protein concentration range (mg/mL)	0.51 – 7.68
Sample	**CD1348 from *C. difficile***
Structural parameters	
I(0) from P(r)	14.31
R_g (real-space from P(r)) (nm)	2.54
$I(0)$ from Guinier fit	14.25
s-range for Guinier fit (nm^{-1})	0.154 – 0.453
R_g (from Guinier fit) (nm)	2.43
D_{max} (nm)	10.14
POROD volume estimate (nm^3)	35.12
Molecular mass (kDa)	
From POROD volume	20.66
From I(0)	14.28
From sequence	18.63
Software	
Primary data reduction	PRIMUS [42]
Data processing	GNOM [44]
Ab initio modelling	GASBOR [45]
Superimposing	SUPCOMB [46]
Model visualization	PyMOL

Interaction tests *in vivo* and *in vitro*. To get an answer, whether the CD1348 is a lipoprotein which provides resistance against lantibiotics or is able to interact with them analytical co-elution studies, tryptophan measurements and growth inhibition (IC_{50}) were performed.

To see if there is an interaction between the CD1348 and the lantibiotics *in vitro* analytical co-elution and tryptophan measurements were performed. For the co-elution studies the purified lipoprotein (His-tag) and the purified nisin were incubated at 20 °C for 1 h and added on a Äkta micro with an Superdex 75 3.2 column. A shift in the chromatogram would support the theory of interaction as the interacting protein complex is bigger and this will influence the elution volume. A SDS-PAGE for analysis was done to see if the nisin elute in a different fraction when the lipoprotein is present (Figure 14). Here the lipoprotein corresponds to the band of 20.18 kDa, where nisin is the lower band in the SDS-PAGE. In the control measurement, the same amount of CD1348 and nisin were run on the same column to see the difference.

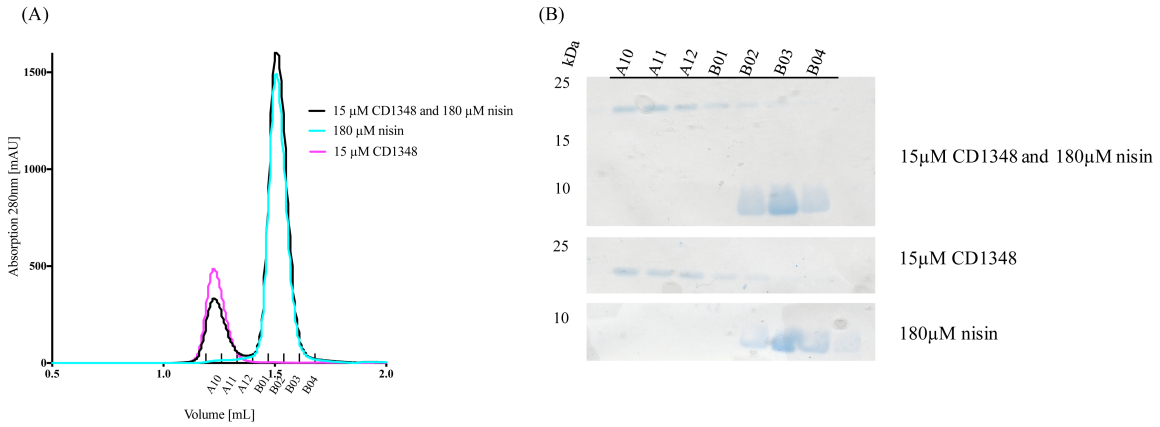

Figure 14: Co-elution studies of CD1348 and nisin. A) Co-elution chromatograms black 15 µM CD1348 and 180 µM nisin incubated for one hour. Cyan 180 µM nisin as control, and magenta as control 15 µM CD1348. There is no shift in the chromatogram observed. B) 15% SDS-PAGE of the corresponding fractions. First CD1348 and nisin incubated, second CD1348 control and third the nisin control. There are no differences in the elution. The CD1348 is elution alone and with nisin in the fractions A10-B02.

As shown in Figure 14 the chromatogram of the CD1348 with nisin does not show any difference to the control measurement of CD1348 and nisin alone. Also, the SDS-PAGE analysis does not show a shift in the elution fractions. The CD1348 is eluting alone and with nisin in the fractions A10-B02 as well. Nisin is eluting in both cases (control measurement and with CD1348) in the fractions B02-B04. Analytical co-elution studies do not show interaction of nisin and CD1348.

Tryptophan fluorescence measurement is a more sensitive method to detect interactions. This method was used, as the results before have shown no interaction and to exclude a missing sensitivity. The lipoprotein with nisin and gallidermin were measured with different lantibiotic concentrations to see an interaction and a saturation. The tryptophan quenching measurements were performed with 1 µM purified cleaved lipoprotein and purified nisin and gallidermin. If the protein binds to the lantibiotics a tryptophan quenching should be observed. With higher lantibiotic concentration the quenching should be more as a saturation is reached. The curves can be analysed with Prism (One site-Total and nonspecific binding) and a K_D value could be calculated (Table 3).

Table 3: Tryptophan quenching measurements with One site-Total and nonspecific binding analysis

CD1348	Gallidermin	Nisin
K_D value [µM]	2.4	9.6

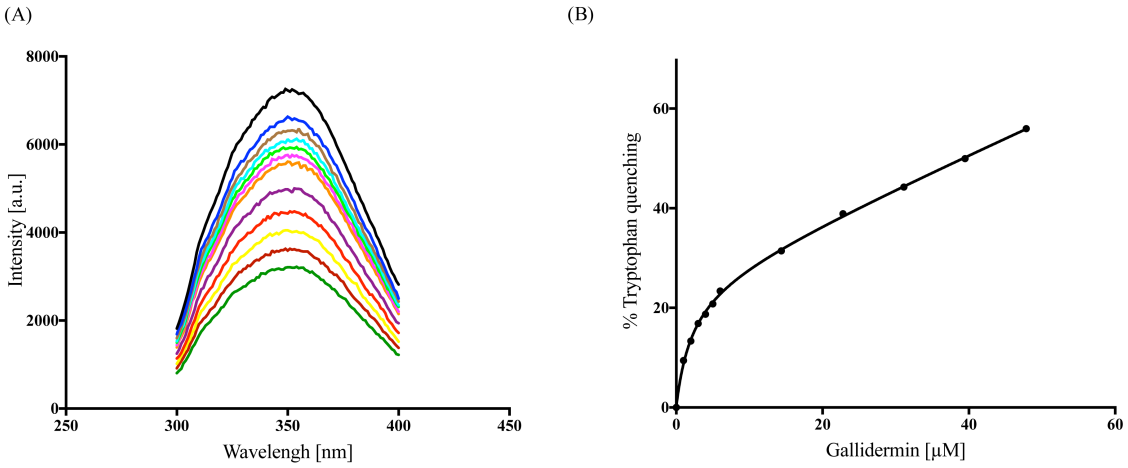

Figure 15: Tryptophan quenching 1 µM CD1348 with gallidermin. A) The intensity against the wavelength is shown. The different colours are presenting the different used gallidermin concentrations, starting with black 0 µM till dark green 47.85 µM gallidermin. A tryptophan quenching can be observed by using higher concentrations of gallidermin. B) The relative tryptophan quenching is plotted against the gallidermin concentration [µM]. A One site-Total and nonspecific binding is the best fitting parameter and results in a K_D value of 2.4 µM for gallidermin.

In the tryptophan quenching measurements (Figure 15) a decreasing fluorescence signal could be observed. With increasing gallidermin concentration (0-47.85 µM) the calculated K_D value of 2.4 µM gallidermin (9.6 µM nisin) shows an interaction. These experiments are two times single measurements for both lantibiotics. The measurements of nisin was influenced by the low solubility of nisin in the used buffer. This measurement was a first try to have an impression if interactions take place. To determine if the observed interaction results in resistance of Gram-positive cells IC_{50} measurements were performed.

The IC_{50} measurements were performed in *L. lactis* NZ9000 cells containing the pIL-SV-Lipo plasmid and an empty pIL-SV as control. This control was used to assure the observed results are based on expressed CD1348 protein. To control the functionality of the expression of the lipoprotein in the NZ9000 cells, a membrane preparation was performed and the membrane was analysed via Western blot analysis. The expression level of the CD1348 lipoprotein was successful (Figure 16) and the IC_{50} measurements could be performed.

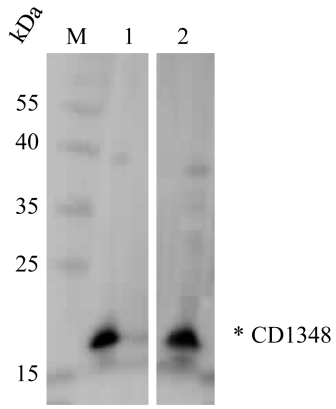

Figure 16: Western blot membrane preparation NZ9000CD1348. M is the PageRuler prestained protein ladder (Thermo Fisher Scientific) 1 is the cell pellet and 2 is the prepared membrane with the containing CD1348 lipoprotein. The CD1348 is expressed and located in the membrane. The used antibody was an anti-CD1348 polyclonal antibody from rabbit (Davids Biotechnologie GmbH).

The IC_{50} measurements were performed in a 96-well plate for 5h with a serial dilution of nisin and gallidermin. The CD1348 was cloned in a pIL-SV shuttle vector for induction 1 ng/mL nisin was used. As a control, a strain containing just the empty shuttle vector was used and treated the same way. This control vector is also used in former studies Reiners et al. (2017) and it is known that this strain is not resistant to nisin. The IC_{50} value of this strain is in a low nanomolar range (4.9 ± 0.4 nM) [30]. An already established expression system was used to identify the behaviour of nisin resistance or immunity proteins [28; 30; 38]. To determine if the CD1348 protein has a resistance function growth inhibition experiments were performed with the two mentioned strains.

Nisin is highly active against the control strain (5.2 ± 0.5 nM) but also the NZ9000CD1348 strain is highly sensitive to nisin and does not show any resistance towards the lantibiotic (Table 4; Figure 17). The same setup was performed with gallidermin in literature the control strain has an IC_{50} value of 67.1 ± 9.1 nM gallidermin [30]. Also in this study, the control strain is in the same value (34.7 ± 3.3 nM). The NZ9000CD1348 strain has nearly the same IC_{50} value and also shows no resistance against gallidermin (Table 4).

Table 4 : IC_{50} values of nisin and gallidermin against NZ9000Cm and NZ9000CD1348 strains.

	NZ9000Cm	NZ9000CD1348
Lantibiotic	IC_{50} [nM]	IC_{50} [nM]
Nisin	5.2 ± 0.5	4.9 ± 0.4
Gallidermin	34.7 ± 3.3	20.9 ± 1.9

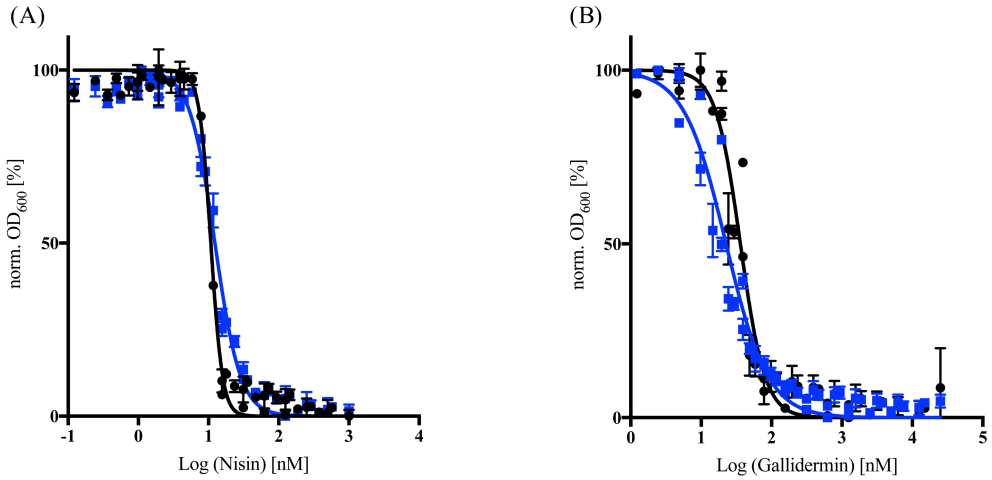

Figure 17: Activity of nisin and gallidermin against the NZ9000Cm and the NZ9000CD1348 strain. A) The IC_{50} of nisin against NZ9000 (black) and NZ9000CD1348 (blue) was determined. As observed the curves do not shift significant, so the two strains are equal resistance against nisin. B) The IC_{50} of gallidermin against NZ9000 (black) and NZ9000CD1348 (blue) was determined. As observed the curves do not shift significant, so the two strains are equal resistance against gallidermin.

As the control strain and the NZ9000 strain expressing the CD1348 protein are showing the same IC_{50} values, the CD1348 lipoprotein seems not protecting cells from the mode of action of nisin and gallidermin.

Discussion

The urgency of developing new antibiotics is the reason for focusing on the lantibiotics in treatment of Gram-positive bacteria. Lantibiotic are one possible answer of the development of new treatments. They are used in food industry since decades and some are also already tested in medical studies to treat diseases [8; 9; 68]. They are antimicrobial active against a lot of Gram-positive bacteria already in a nanomolar range [6; 7; 13; 23]. But already there are some bacteria and especially human pathogens showing inherently resistance against some lantibiotics [24].

The known resistance systems are mostly similar structured all have a two-component system, containing a histidine kinase and a response regulator [24] and an ABC-transporter. The CprABC system of *C. difficile*, a spore forming Gram-positive bacteria, contains also all these components even it is not known yet how the CprABC transporter works, transport or efflux. This described system shows resistance against nisin, gallidermin, subtilin and mersacidin [1; 2].

These different lantibiotics containing one thing in common the second ring [1]. To characterize the CD1348 lipoprotein directly encoded in front of the ABC transporter (CprABC) was the aim of this study.

The hypothesis that this lipoprotein is a resistance protein could not be proven. It does not show resistance in the experimental set up in NZ9000 cells. Also, the *in vitro* interaction studies do not show a result to get a clear answer of the functionality of this protein. The co-elution studies show no interaction. In the tryptophan measurements a quenching could be observed, but no saturation was reached and the best fitting result were observed in One site-Total and nonspecific binding. Missing resistance in the NZ9000 cells is more sensing to say that the *in vitro* interaction is just because of the negatively charged regions in the protein and the positively charged lantibiotics. The tryptophan measurements are more sensible than the co-elution studies, so that the observed charge interaction is not strong enough to be seen in a stable complex. As a control for these results, obtained by tryptophan fluorescence measurements, another positively charged molecule like Pep5 would give an idea about it [69]. A different reason of the missing resistance could be that nisin and gallidermin are not substrates of the CD1348. In other systems, it has been shown that these resistance proteins can be highly specific to one substrate [28; 38]. It might be possible that CD1348 protein does not recognize the N-terminal part of the lantibiotics. But maybe some specific C-terminal region has to be part of the lantibiotic which we do not know yet.

Another reason could be that the lipoprotein is not involved in the lantibiotic resistance. Maybe because of this it shows no overexpression with the CprABC transporter like described in previously studies [2]. A structure model was calculated with the TOP model program (D. Mulnaes, unpublished). Via SAXS the model could be determined as correct. A fitting of both models shows that the independent calculated model and the measured results are showing a high similarity. Via MALS and SAXS measurements it could be determined that CD1348 is present in a monomeric state. The NMR measurements results in a first secondary structure which could be compared with the TOP model structure. Here it could be shown that the NMR secondary structure and the secondary structure of the model are highly similar (Figure 18).

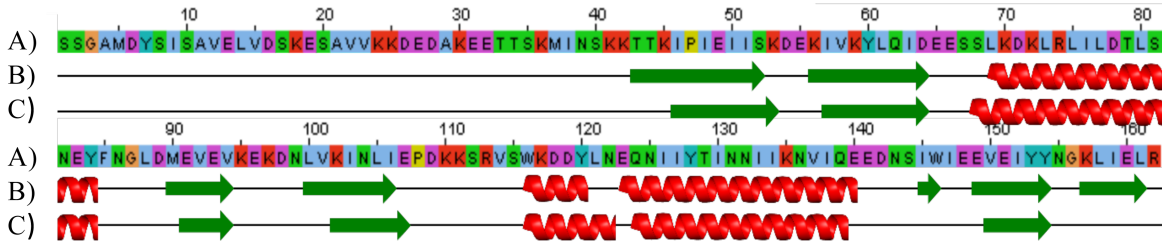

Figure 18: Comparison of the secondary structures of NMR measurement and model of CD1348. A) Amino acid sequence of the CD1348. B) Secondary structure as measured by NMR. C) Predicted secondary structure determined from the model using DSSP [70].

So, with this knowledge the model of CD1348 could be used as the structure of CD1348 till the NMR calculation is finished and the structure is solved.

One of the interesting result of this study is the thermostability of the CD1348 up to 90 °C. This could be one hint about the function of the protein. To get an idea how the protein is able to be heat stable a closer look to the structure model of the CD1348 protein could help. Hydrophobic regions and hydrogen bonds are known to be necessary for heat stable proteins [71]. The model structure of the CD1348 protein is containing three major parts a long loop region on the N-terminus, a α-helices region and a ß-sheet region (Figure 19).

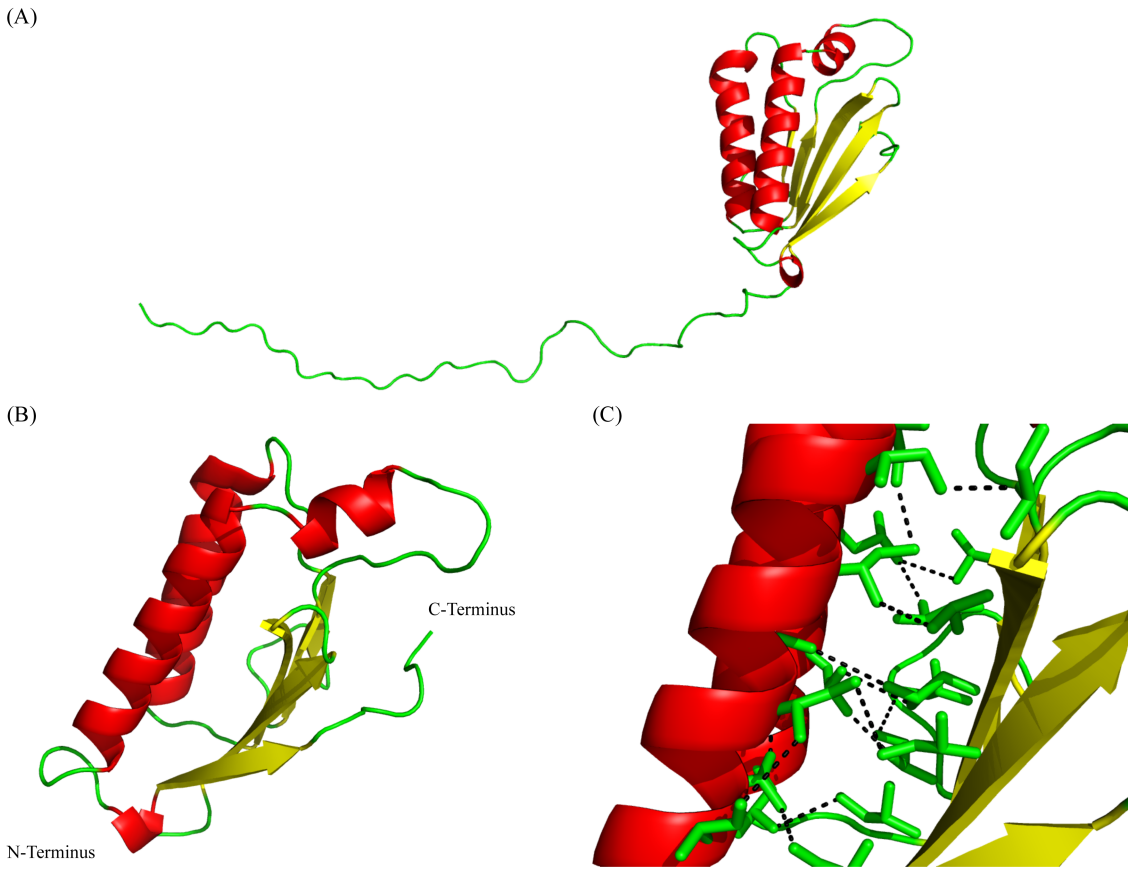

Figure 19: Model structure of the CD1348. A) The structure of CD1348. In green the loop region is depicted. In red, the α-helices are shown and in yellow the ß-sheets are shown. B) A zoom in of the CD1348 structure lacking the N-terminal loop. In green the loop region is depicted. In red, the α-helices are shown and in yellow the ß-sheets are shown. C) A zoom in in the centre of the structure. In green are the hydrophobic amino acids isoleucine, leucine and valine depicted. The distance between the amino acids of the α-helical region and the ß-sheet region is depicted in black. There are a lot of distances between 3 and 4 Å so these amino acids can interact with each other and this could be a reason for the heat stability of the CD1348 protein.

Because of the hydrophobic amino acids isoleucine, leucine and valine, which are more or less all located in the centre of the structure the α-helices and the ß-sheets can interact with each other and the structure is stabilised. Nearly all amino acids have a distance between 3 and 4 Å so they are able to interact with each other. This can be one reason for the heat stability of the protein. If the heat stability has an influence of the function of the CD1348 is not yet known. In *C. difficile* is a regulator lipoprotein, gerS, known which is necessary for heat resistance of the germination of the spore [72]. If the CD1348 lipoprotein is potentially important for heat resistance of spores is not determined until know. The CD1348 protein does not show a sequence similarity to any other protein known yet. A NCBI blast of the CD1348 supports this (Table 5).

Table 5: Examples of NCBI protein blast of the CD1348 (UniProt code Q18BL3) amino acid sequence. The *Clostridium difficile* was excluded.

Description	Identity
Hypothetical protein (*Romboutsia maritimum*)	45%
Hypothetical protein (*Romboutsia lituseburensis*)	44%
Hypothetical protein (*Romboutsia* sp. MT17)	43%
Hypothetical protein (*Asaccharospora irregularis*)	42%
Hypothetical protein (*Clostridium dakarense*)	40%
Lipoprotein (*Romboutsia ilealis*)	37%
Hypothetical protein (*Clostridium baratii*)	29%

Characterization of CD1348 might be easier if other similar proteins are found. The position and the surrounding proteins can then give an idea about the function of this kind of proteins. Genome studies could be helpful to see in which condition the protein is overexpressed. This also can be a step closer to characterize CD1348 more in detail. In this study first steps in characterization are done with purification and exclusion of first substrates.

Acknowledgements

We thank Diana Kleinschrodt and Iris Fey of the Protein Production Facility for excellent support during the initial stages of this project. We thank all the members of the institute of Biochemistry for fruitful discussions.

References

[1] J.M. Suarez, A.N. Edwards, and S.M. McBride, The *Clostridium difficile cpr* locus is regulated by a noncontiguous two-component system in response to type A and B lantibiotics. J Bacteriol 195 (2013) 2621-31.

[2] S.M. McBride, and A.L. Sonenshein, Identification of a genetic locus responsible for antimicrobial peptide resistance in *Clostridium difficile*. Infect Immun 79 (2011) 167-76.

[3] S. Khosa, Z. AlKhatib, and S.H. Smits, NSR from *Streptococcus agalactiae* confers resistance against nisin and is encoded by a conserved *nsr* operon. Biol Chem 394 (2013) 1543-9.

[4] Y. Yoshida, M. Matsuo, Y. Oogai, F. Kato, N. Nakamura, M. Sugai, and H. Komatsuzawa, Bacitracin sensing and resistance in *Staphylococcus aureus*. FEMS Microbiol Lett 320 (2011) 33-9.

[5] M. Kawada-Matsuo, Y. Yoshida, T. Zendo, J. Nagao, Y. Oogai, Y. Nakamura, K. Sonomoto, N. Nakamura, and H. Komatsuzawa, Three distinct two-component systems are involved in resistance to the class I bacteriocins, Nukacin ISK-1 and nisin A, in *Staphylococcus aureus*. PLoS One 8 (2013) e69455.

[6] J.R. Tagg, A.S. Dajani, and L.W. Wannamaker, Bacteriocins of Gram-positive bacteria. Bacteriol Rev 40 (1976) 722-56.

[7] P.D. Cotter, C. Hill, and R.P. Ross, Bacteriocins: developing innate immunity for food. Nat Rev Microbiol 3 (2005) 777-88.

[8] J. Cleveland, T.J. Montville, I.F. Nes, and M.L. Chikindas, Bacteriocins: safe, natural antimicrobials for food preservation. Int J Food Microbiol 71 (2001) 1-20.

[9] P.D. Cotter, R.P. Ross, and C. Hill, Bacteriocins - a viable alternative to antibiotics? Nat Rev Microbiol 11 (2013) 95-105.

[10] J.M. Willey, and W.A. van der Donk, Lantibiotics: peptides of diverse structure and function. Annu Rev Microbiol 61 (2007) 477-501.

[11] T.R. Klaenhammer, Genetics of bacteriocins produced by lactic acid bacteria. FEMS Microbiol Rev 12 (1993) 39-85.

[12] G. Bierbaum, and H.G. Sahl, Lantibiotics: mode of action, biosynthesis and bioengineering. Curr Pharm Biotechnol 10 (2009) 2-18.

[13] C. Chatterjee, M. Paul, L. Xie, and W.A. van der Donk, Biosynthesis and mode of action of lantibiotics. Chem Rev 105 (2005) 633-84.

[14] J. Dischinger, S. Basi Chipalu, and G. Bierbaum, Lantibiotics: promising candidates for future applications in health care. Int J Med Microbiol 304 (2014) 51-62.

[15] Q. Zhang, Y. Yu, J.E. Velasquez, and W.A. van der Donk, Evolution of lanthipeptide synthetases. Proc Natl Acad Sci U S A 109 (2012) 18361-6.

[16] P.J. Knerr, and W.A. van der Donk, Discovery, biosynthesis, and engineering of lantipeptides. Annu Rev Biochem 81 (2012) 479-505.

[17] L.A. Rogers, The Inhibiting Effect of *Streptococcus Lactis* on *Lactobacillus Bulgaricus*. J Bacteriol 16 (1928) 321-5.

[18] I. Wiedemann, E. Breukink, C. van Kraaij, O.P. Kuipers, G. Bierbaum, B. de Kruijff, and H.G. Sahl, Specific binding of nisin to the peptidoglycan precursor lipid II combines pore formation and inhibition of cell wall biosynthesis for potent antibiotic activity. J Biol Chem 276 (2001) 1772-9.

[19] E. Breukink, Use of the Cell Wall Precursor Lipid II by a Pore-Forming Peptide Antibiotic. Science 286 (1999) 2361-2364.

[20] H. Brotz, M. Josten, I. Wiedemann, U. Schneider, F. Gotz, G. Bierbaum, and H.G. Sahl, Role of lipid-bound peptidoglycan precursors in the formation of pores by nisin, epidermin and other lantibiotics. Mol Microbiol 30 (1998) 317-27.

[21] H.E. Hasper, N.E. Kramer, J.L. Smith, J.D. Hillman, C. Zachariah, O.P. Kuipers, B. de Kruijff, and E. Breukink, An alternative bactericidal mechanism of action for lantibiotic peptides that target lipid II. Science 313 (2006) 1636-7.
[22] H.E. Hasper, B. de Kruijff, and E. Breukink, Assembly and stability of nisin-lipid II pores. Biochemistry 43 (2004) 11567-75.
[23] J. Delves-Broughton, P. Blackburn, R.J. Evans, and J. Hugenholtz, Applications of the bacteriocin, nisin. Antonie Van Leeuwenhoek 69 (1996) 193-202.
[24] L.A. Draper, P.D. Cotter, C. Hill, and R.P. Ross, Lantibiotic resistance. Microbiol Mol Biol Rev 79 (2015) 171-91.
[25] E. Rietkotter, D. Hoyer, and T. Mascher, Bacitracin sensing in *Bacillus subtilis*. Mol Microbiol 68 (2008) 768-85.
[26] R. Ohki, Giyanto, K. Tateno, W. Masuyama, S. Moriya, K. Kobayashi, and N. Ogasawara, The BceRS two-component regulatory system induces expression of the bacitracin transporter, BceAB, in *Bacillus subtilis*. Molecular Microbiology 49 (2003) 1135-1144.
[27] M. Kawada-Matsuo, Y. Oogai, T. Zendo, J. Nagao, Y. Shibata, Y. Yamashita, Y. Ogura, T. Hayashi, K. Sonomoto, and H. Komatsuzawa, Involvement of the novel two-component NsrRS and LcrRS systems in distinct resistance pathways against nisin A and nukacin ISK-1 in *Streptococcus mutans*. Appl Environ Microbiol 79 (2013) 4751-5.
[28] S. Khosa, B. Frieg, D. Mulnaes, D. Kleinschrodt, A. Hoeppner, H. Gohlke, and S.H. Smits, Structural basis of lantibiotic recognition by the nisin resistance protein from *Streptococcus agalactiae*. Sci Rep 6 (2016) 18679.
[29] Z. Sun, J. Zhong, X. Liang, J. Liu, X. Chen, and L. Huan, Novel mechanism for nisin resistance via proteolytic degradation of nisin by the nisin resistance protein NSR. Antimicrob Agents Chemother 53 (2009) 1964-73.
[30] J. Reiners, M. Lagedroste, K. Ehlen, S. Leusch, J. Zaschke-Kriesche, and S.H.J. Smits, The N-terminal Region of Nisin Is Important for the BceAB-Type ABC Transporter NsrFP from *Streptococcus agalactiae* COH1. Front Microbiol 8 (2017) 1643.
[31] R. Clemens, J. Zaschke-Kriesche, S. Khosa, and S.H.J. Smits, Insight into Two ABC Transporter Families Involved in Lantibiotic Resistance. Front Mol Biosci 4 (2017) 91.
[32] J.G. Bartlett, Narrative review: the new epidemic of *Clostridium difficile*-associated enteric disease. Ann Intern Med 145 (2006) 758-64.
[33] S. Nakamura, K. Yamakawa, J. Izumi, S. Nakashio, and S. Nishida, Germinability and heat resistance of spores of *Clostridium difficile* strains. Microbiol Immunol 29 (1985) 113-8.
[34] R.P. Vonberg, E.J. Kuijper, M.H. Wilcox, F. Barbut, P. Tull, P. Gastmeier, C.d.-I.C.G. European, P. European Centre for Disease, Control, P.J. van den Broek, A. Colville, B. Coignard, T. Daha, S. Debast, B.I. Duerden, S. van den Hof, T. van der Kooi, H.J. Maarleveld, E. Nagy, D.W. Notermans, J. O'Driscoll, B. Patel, S. Stone, and C. Wiuff, Infection control measures to limit the spread of *Clostridium difficile*. Clin Microbiol Infect 14 Suppl 5 (2008) 2-20.
[35] S.P. Borriello, Pathogenesis of *Clostridium difficile* infection. J Antimicrob Chemother 41 Suppl C (1998) 13-9.
[36] J.S. Brazier, *Clostridium difficile*: from obscurity to superbug. Br J Biomed Sci 65 (2008) 39-44.
[37] D.E. Voth, and J.D. Ballard, *Clostridium difficile* toxins: mechanism of action and role in disease. Clin Microbiol Rev 18 (2005) 247-63.

[38] Z. AlKhatib, M. Lagedroste, I. Fey, D. Kleinschrodt, A. Abts, and S.H. Smits, Lantibiotic immunity: inhibition of nisin mediated pore formation by NisI. PLoS One 9 (2014) e102246.

[39] P. Pernot, P. Theveneau, T. Giraud, R.N. Fernandes, D. Nurizzo, D. Spruce, J. Surr, S. McSweeney, A. Round, F. Felisaz, L. Foedinger, A. Gobbo, J. Huet, C. Villard, and F. Cipriani, New beamline dedicated to solution scattering from biological macromolecules at the ESRF. Journal of Physics: Conference Series 247 (2010) 012009.

[40] P. Pernot, A. Round, R. Barrett, A. De Maria Antolinos, A. Gobbo, E. Gordon, J. Huet, J. Kieffer, M. Lentini, M. Mattenet, C. Morawe, C. Mueller-Dieckmann, S. Ohlsson, W. Schmid, J. Surr, P. Theveneau, L. Zerrad, and S. McSweeney, Upgraded ESRF BM29 beamline for SAXS on macromolecules in solution. Journal of synchrotron radiation 20 (2013) 660-4.

[41] M.V. Petoukhov, D. Franke, A.V. Shkumatov, G. Tria, A.G. Kikhney, M. Gajda, C. Gorba, H.D.T. Mertens, P.V. Konarev, and D.I. Svergun, New developments in the ATSAS program package for small-angle scattering data analysis. J Appl Crystallogr 45 (2012) 342-350.

[42] P.V. Konarev, V.V. Volkov, A.V. Sokolova, M.H.J. Koch, and D.I. Svergun, PRIMUS: a Windows PC-based system for small-angle scattering data analysis. J Appl Crystallogr 36 (2003) 1277-1282.

[43] A. Guinier, Diffraction of X-rays of very small angles-application to the study of ultramicroscopic phenomenon. Annales de Physique 12 (1939) 161-237.

[44] D.I. Svergun, Determination of the Regularization Parameter in Indirect-Transform Methods Using Perceptual Criteria. J Appl Crystallogr 25 (1992) 495-503.

[45] D.I. Svergun, M.V. Petoukhov, and M.H. Koch, Determination of domain structure of proteins from X-ray solution scattering. Biophys J 80 (2001) 2946-53.

[46] M.B. Kozin, and D.I. Svergun, Automated matching of high- and low-resolution structural models. J Appl Crystallogr 34 (2001) 33-41.

[47] M. Findeisen, T. Brand, and S. Berger, A ^{1}H-NMR thermometer suitable for cryoprobes. Magn Reson Chem 45 (2007) 175-8.

[48] M. Salzmann, G. Wider, K. Pervushin, and K. Wuthrich, Improved sensitivity and coherence selection for [^{15}N,^{1}H]-TROSY elements in triple resonance experiments. J Biomol NMR 15 (1999) 181-4.

[49] D. Yang, and L.E. Kay, Improved ^{1}HN-detected triple resonance TROSY-based experiments. J Biomol NMR 13 (1999) 3-10.

[50] D. Nietlispach, Suppression of anti-TROSY lines in a sensitivity enhanced gradient selection TROSY scheme. J Biomol NMR 31 (2005) 161-6.

[51] M. Sattler, Heteronuclear multidimensional NMR experiments for the structure determination of proteins in solution employing pulsed field gradients. Progress in Nuclear Magnetic Resonance Spectroscopy 34 (1999) 93-158.

[52] G.W. Vuister, and A. Bax, Resolution enhancement and spectral editing of uniformly ^{13}C-enriched proteins by homonuclear broadband ^{13}C decoupling. Journal of Magnetic Resonance (1969) 98 (1992) 428-435.

[53] O. Zhang, L.E. Kay, J.P. Olivier, and J.D. Forman-Kay, Backbone ^{1}H and ^{15}N resonance assignments of the N-terminal SH_3 domain of drk in folded and unfolded states using enhanced-sensitivity pulsed field gradient NMR techniques. Journal of Biomolecular NMR 4 (1994) 845-858.

[54] J. Cavanagh, and M. Rance, Suppression of cross-relaxation effects in TOCSY spectra via a modified DIPSI-2 mixing sequence. Journal of Magnetic Resonance (1969) 96 (1992) 670-678.

[55] D. Yang, and L.E. Kay, TROSY Triple-Resonance Four-Dimensional NMR Spectroscopy of a 46 ns Tumbling Protein. Journal of the American Chemical Society 121 (1999) 2571-2575.

[56] H. Kovacs, and A. Gossert, Improved NMR experiments with ^{13}C-isotropic mixing for assignment of aromatic and aliphatic side chains in labeled proteins. J Biomol NMR 58 (2014) 101-12.

[57] M. Kadkhodaie, O. Rivas, M. Tan, A. Mohebbi, and A.J. Shaka, Broadband homonuclear cross polarization using flip-flop spectroscopy. Journal of Magnetic Resonance (1969) 91 (1991) 437-443.

[58] D. Marion, M. Ikura, R. Tschudin, and A. Bax, Rapid recording of 2D NMR spectra without phase cycling. Application to the study of hydrogen exchange in proteins. Journal of Magnetic Resonance (1969) 85 (1989) 393-399.

[59] L. Kay, P. Keifer, and T. Saarinen, Pure absorption gradient enhanced heteronuclear single quantum correlation spectroscopy with improved sensitivity. Journal of the American Chemical Society 114 (1992) 10663-10665.

[60] J.r. Schleucher, M. Sattler, and C. Griesinger, Coherence Selection by Gradients without Signal Attenuation: Application to the Three-Dimensional HNCO Experiment. Angewandte Chemie International Edition in English 32 (1993) 1489-1491.

[61] F. Delaglio, S. Grzesiek, G. Vuister, G. Zhu, J. Pfeifer, and A. Bax, NMRPipe: A multidimensional spectral processing system based on UNIX pipes. Journal of Biomolecular NMR 6 (1995).

[62] B.A. Johnson, and R.A. Blevins, NMR View: A computer program for the visualization and analysis of NMR data. J Biomol NMR 4 (1994) 603-14.

[63] J.L. Markley, A. Bax, Y. Arata, C.W. Hilbers, R. Kaptein, B.D. Sykes, P.E. Wright, and K. Wuthrich, Recommendations for the presentation of NMR structures of proteins and nucleic acids. J Mol Biol 280 (1998) 933-52.

[64] M.V. Berjanskii, and D.S. Wishart, A simple method to predict protein flexibility using secondary chemical shifts. J Am Chem Soc 127 (2005) 14970-1.

[65] Y. Shen, and A. Bax, Protein backbone and sidechain torsion angles predicted from NMR chemical shifts using artificial neural networks. J Biomol NMR 56 (2013) 227-41.

[66] A. Abts, A. Mavaro, J. Stindt, P.J. Bakkes, S. Metzger, A.J. Driessen, S.H. Smits, and L. Schmitt, Easy and rapid purification of highly active nisin. Int J Pept 2011 (2011) 175145.

[67] A. Abts, M. Montalban-Lopez, O.P. Kuipers, S.H. Smits, and L. Schmitt, NisC binds the FxLx motif of the nisin leader peptide. Biochemistry 52 (2013) 5387-95.

[68] S.C. Yang, C.H. Lin, C.T. Sung, and J.Y. Fang, Antibacterial activities of bacteriocins: application in foods and pharmaceuticals. Front Microbiol 5 (2014) 241.

[69] M. Kordel, F. Schüller, and H.-G. Sahl, Interaction of the pore forming-peptide antibiotics Pep 5, nisin and subtilin with non-energized liposomes. FEBS Letters 244 (1989) 99-102.

[70] W. Kabsch, and C. Sander, Dictionary of protein secondary structure: pattern recognition of hydrogen-bonded and geometrical features. Biopolymers 22 (1983) 2577-2637.

[71] B. Folch, M. Rooman, and Y. Dehouck, Thermostability of salt bridges versus hydrophobic interactions in proteins probed by statistical potentials. J Chem Inf Model 48 (2008) 119-27.

[72] K.A. Fimlaid, O. Jensen, M.L. Donnelly, M.B. Francis, J.A. Sorg, and A. Shen, Identification of a Novel Lipoprotein Regulator of *Clostridium difficile* Spore Germination. PLoS Pathog 11 (2015) e1005239.

3.4. Chapter IV - Lipid composition of *Lactococcus lactis*

Published in: in preparation

Own work: 40 %
Growth inhibition measurements
Growth curves
Genome preparation and genome analysis
Lipid extraction, purification and characterization
Writing the manuscript

Lantibiotic resistant *L. lactis* has an altered lipid composition

Rebecca Clemens, Thomas Zobel, Diran Herebian, Julia Zaschke-Kriesche, Hans Klose and Sander H. J. Smits

Lantibiotic resistant *L. lactis* has an altered lipid composition

Rebecca Clemens, Thomas Zobel, Diran Herebian, Julia Zaschke-Kriesche, Hans Klose and Sander H. J. Smits

Abstract

In this study, we characterized a lantibiotic and antibiotic resistant *Lactococcus lactis subsp. cremoris* NZ9000 strain, called NZ9000Pseudo. This strain shows resistance against nisin, gallidermin, vancomycin and penicillin G, which all target the cell wall synthesis machinery of Gram-positive bacteria. Although nearly all tested anti- and lantibiotics are targeting the peptidoglycan precursor lipid II, the binding sides of the anti- and lantibiotics are located at different positions of lipid II. Only penicillin binds to the penicillin-binding protein and inhibits transpeptidation. To determine the cause of resistance in the *Lactococcus lactis* strain, we performed different tests with the resistant strain and the control strain NZ9000. Via growth curves and IC_{50} measurements, we determined the resistance of NZ9000Pseudo strain. Since it shows resistance against nisin, a Sytox green assay was performed, to determine whether the pore formation of nisin is inhibited by the resistant strain. Peptidoglycan and phospholipid analyses were performed to find the reason of the resistance. Also, microscopy analyses of the living cells were performed to visualize the cells and to see differences between the cells of NZ9000Pseudo and the control strains.
We were able to analyse the lipid composition of the original *L. lactis* strain, which is not available till date and compare it with the resistant strain. This comparison shows difference in the lipid composition. The living cells of the NZ9000Pseudo strain are not clustered like the control strain and the resistant strain is able to inhibit the pore formation of nisin. With the help of genome sequencing, we want to determine the reason of the different lipid composition, but till date it was not able to find the exact reason of the resistance in the genome.

Introduction

Antibiotics became important for human life expectancy since the discovery of penicillin by Alexander Flemming [1; 2]. There are a lot of different classes of antibiotics based on the mode of action of the antibiotic and the target they have [3]. While some antibiotics target the nucleic acid synthesis like quinolones, some target the protein synthesis or the metabolic pathways, chloramphenicol and sulfonamides are examples of this kind of antibiotics [4; 5]. In this study, we would like to focus on the antibiotics that target the cell wall synthesis [3; 6]. These antibiotics are ß-lactam (such as penicillin G), glycopeptides (e.g. vancomycin and lipodepsiglycopeptides (such as ramoplanin A2) (Figure 1) [7; 8; 9].

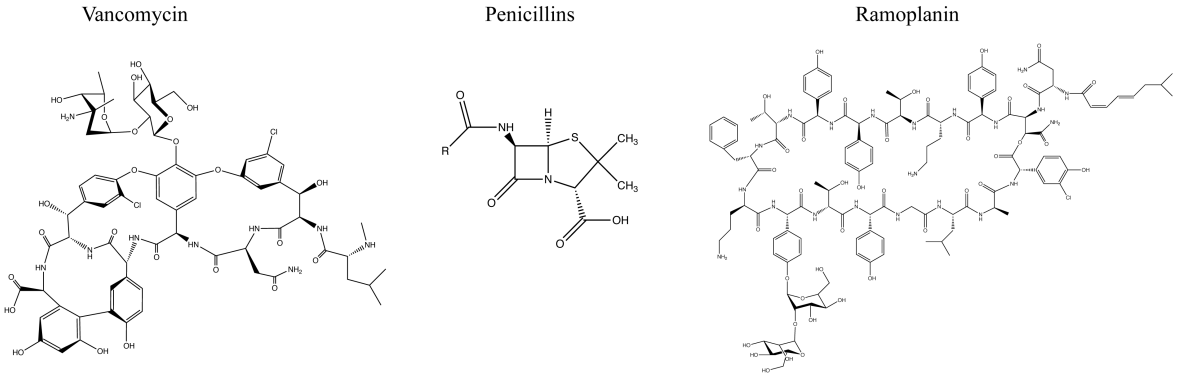

Figure 1: Members of three different classes of antibiotics. Vancomycin is the first discovered glycopeptide antibiotic, while penicillin is the first ß-lactam antibiotic and ramoplanin A2 is a lipodepsiglycopeptide antibiotic. Based on [10; 11].

All these antibiotics target the cell wall synthesis of Gram-positive bacteria. Vancomycin is targeting the D-Ala-D-Ala part of the pentapeptide of lipid II and binding via 5 hydrogen bonds [8; 12]. Ramoplanin is also interacting with the lipid II via the MurNAc-(GlcNAc)-Ala-γ-D-Glu pyrophosphate region [6]. Penicillin G is inhibiting the transpeptidation via binding to the penicillin binding protein (PBP) (Figure 2) [2].

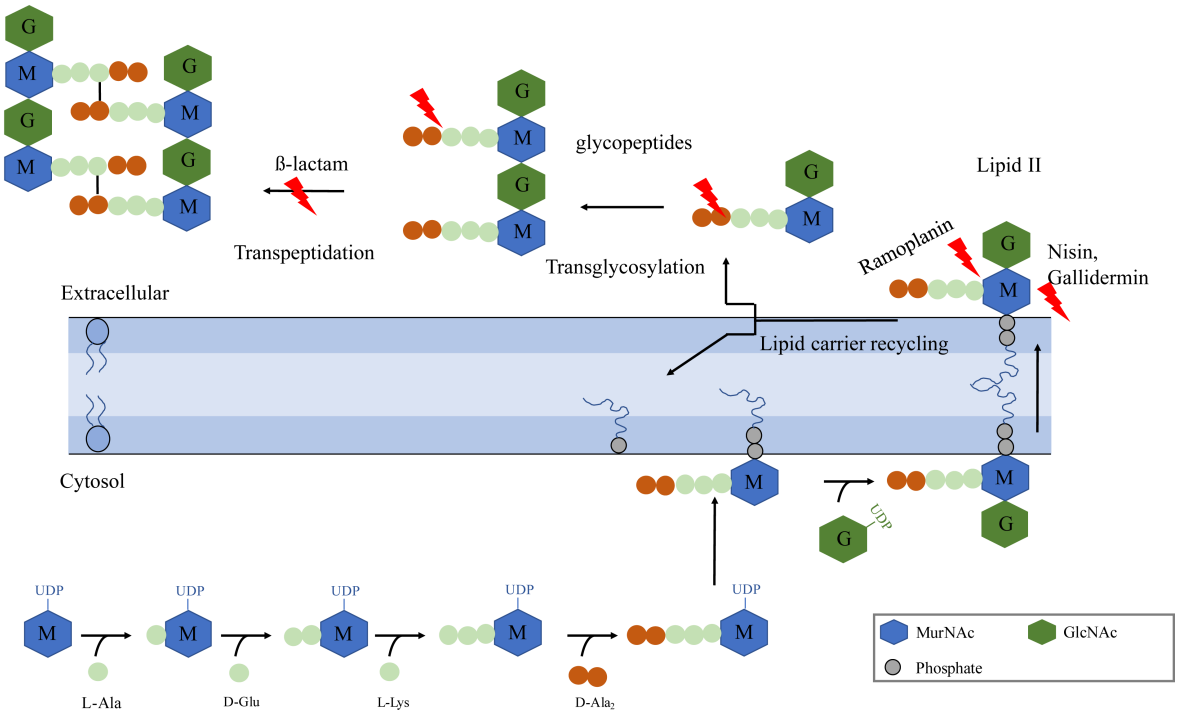

Figure 2: Cells wall synthesis and target of selected antibiotics and lantibiotics. Depicted is the cell wall synthesis starting with the first muramic acid. The red flashes show the target positions of the different anti- and lantibiotics. Based on [13; 14].

Some resistance mechanisms against these antibiotics have already been discovered, such as example the vancomycin resistant bacteria. There are different ways of conferring to perform resistance. First some cells are able to develop an alternative depsipeptide D-Ala-D-Lac instead of the original D-Ala-D-Ala peptide, for example here the vancomycin resistance (*van*) operon is responsible for the alternative depsipeptide production [10; 15; 16]. Due to the modification to a D-Ala-D-Lac depsipeptide the vancomycin loses one hydrogen bond to the precursor molecule lipid II and the binding is 1000-fold reduced in comparison to the original D-Ala-D-Ala peptide [6; 12; 15]. Another route of vancomycin resistance is trough production of a thicker cell wall with a lesser degree of cross-linked peptidoglycan compared to non-resistant strains. *Staphylococcus aureus* strain Mu50 is one example of Gram-positive bacteria performing such a resistance [17; 18]. Via microscopy and peptidoglycan analyses, the resistance mechanism thicker cell wall was determined [17; 18]. With the thicker cell wall and lesser cross-linked peptidoglycan molecules, the binding capacity of vancomycin is increased. Vancomycin binds to the D-Ala-D-Ala molecules in the peptidoglycan layer and does not reach the original target molecule, lipid II. So, with the help of the `false´ binding the transglycosylation and transpeptidation is not inhibited and the cell can still grow [16; 17; 18]. Strains like the methicillin-resistant *Staphylococcus aureus* (MRSA), one main reason for hospital-acquired infections [19], contain a modified penicillin-binding protein

(PBP) which results in resistance against the penicillin, methicillin. With the modification of the PBP, the penicillin has a lower affinity towards the PBP and does not inhibit the transpeptidation anymore [20; 21; 22].

Antibiotics are not the only antimicrobial reagents which target cell wall synthesis. There are so called antimicrobial peptides (AMPs) which display antimicrobial activity against Gram-positive bacteria [23; 24]. One main subgroup of AMPs is called lantibiotics.

Some lantibiotics such as nisin and gallidermin are active in the nanomolar range [25; 26]. The best characterized lantibiotic is nisin (Figure 3). This lantibiotic has at least a dual mode of action. First it is able to bind to lipid II, a peptidoglycan precursor and thereby inhibits cell growth [27; 28; 29; 30]. Second, nisin is able to form pores with the lipid II in the membrane which leads to cell death [31]. Nisin binds via the first two rings to the diphosphate moiety of lipid II, which inhibits cell growth. With increased nisin concentration, a complex of eight nisin and four lipid II molecules is formed and nisin can flip into the membrane via the flexible hinge region [27; 32; 33]. Another lantibiotic is gallidermin from *Staphylococcus gallinarium* (Figure 3) which is also able to interact with the lipid II and inhibits cell growth [34]. Like for antibiotics, also against lantibiotics different resistance mechanisms have been described.

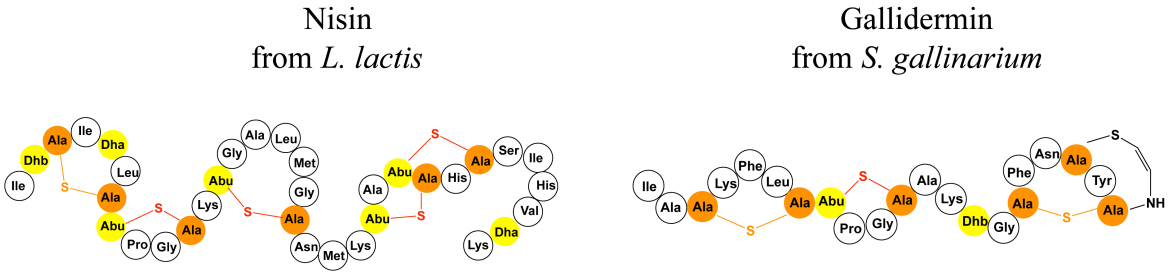

Figure 3: Schematic representation of two examples of lantibiotics, nisin and gallidermin. The dehydrated amino acids and the cysteines of the lantibiotics are highlighted in yellow and orange. The (methyl-) lanthionine rings are depicted in orange and red. Based on [35].

The *dltABCD* operon is responsible for the D-alanylation of lipoteichoic acids (LTAs) and the wall teichoic acids (WTAs). This alanylation confers a positive charge to the LTAs and WTAs and therefore, the positively-charged lantibiotics are not able to interact with the cell membrane anymore [36; 37; 38]. Also changes in the phospholipid composition and the membrane fatty acid composition are known to provide resistance against nisin. Here the charge of the membrane is one reason how resistance could arise. If the changes results in a more positively-charged membrane, the lantibiotics are not able to interact with the

membrane as efficiently as in the wild type [36; 39; 40; 41]. The composition of the fatty acids is changing the fluidity of the membrane and it is more rigid [36; 42; 43].

All these mentioned anti- and lantibiotics have common mode of interaction with the cell wall. The targets of this anti- and lantibiotics are different and to observe a resistance against nearly all of the used substances was really surprisingly.

In this study, we have a closer look on an antibiotic and lantibiotic resistant *L. lactis* NZ9000 strain, named here as NZ9000Pseudo strain. It exhibits resistance against nisin, gallidermin, penicillin G and vancomycin. To characterize the NZ9000Pseudo strain in detail and to analyse the resistance against the different substances, various analyses were performed. First, growth curves and growth inhibition assays were performed to determine the resistance against different antibiotics and compared with the sensitive *L. lactis* NZ9000 strain. Next step was to analyse via Sytox analysis with nisin if the pore formation is inhibited. To determine the resistance mechanism of the NZ9000Pseudo strain, lipid analyses of both strains were performed. Via LC-MS/MS analysis it was analysed if there are differences in the membrane lipid composition. To visualize the bacterial cells, microscopy measurements were performed using both strains, NZ9000Pseudo and NZ9000Cm and the cells were compared.

Material and Methods

Determination of the resistance of the *L. lactis* NZ9000Pseudo strain by Growth Inhibition (IC_{50}). *L. lactis* NZ9000Cm and NZ9000Pseudo cells were grown overnight in GM17 media containing 5 µg/µl chloramphenicol and 1 ng/mL nisin at 30 °C. The cells were diluted to an OD_{600} of 0.1 and then incubated with a serial dilution of the analysed antibiotic or lantibiotic in a 96-well plate. Each well contained 50 µL of the respective antibiotic/ lantibiotic and 150 µL GM17 with the corresponding strain, thus, a total the volume of 200 µL in each well. The 96-well plate was incubated at 30 °C over 5 h. The optical density was determined via plate reader BMG at 584 nm. The optical density was normalized and plotted against the logarithm of the corresponding antibiotic. The IC_{50} value was calculated using the following equation:

$$y = OD_{min} + \frac{OD_{max} - OD_{min}}{1 + 10^{(\log(IC50) - x) * p}}$$

Here, OD_{max} stands for the normalized OD value where the lowest concentration of the antibiotic was added and the strains grew without inhibition. The OD_{min} corresponds to the normalized OD were the highest antibiotic/ lantibiotic concentration was added and the cell growth was inhibited the most. x is the logarithmic of the antibiotic/ lantibiotic concentration which was added and y represents the calculated normalized OD value. In general, the IC_{50} value is the concentration of an antibiotic or a lantibiotic where the growth of cells is inhibited by 50% [44].

Calculation of the fold of resistance. In order to compare the different antibiotics/ lantibiotics and the corresponding IC_{50} values, the IC_{50} value of the NZ9000Pseudo strain was divided by the IC_{50} value of the control strain resulting in the fold of resistance [44].

$$\text{Fold of resistance} = \frac{\text{IC}_{50}(\text{NZ9000Pseudo})}{\text{IC}_{50}(\text{control strain})}$$

Determination of the growth curves with the different antibiotics. To determine the growth curves of *L. lactis* NZ9000Cm and the NZ9000Pseudo strains, the optical density was measured over 18 h every hour in presence of different concentrations of the corresponding antibiotic/ lantibiotic. Therefore, a preculture of the corresponding strain in GM17 media containing 5 µg/mL chloramphenicol and 1 ng/mL nisin was prepared and grown over night at 30 °C. A 96-well plate was prepared with a serial dilution of the

antibiotic, where each well contained 50 µL of the antibiotic. The cells were diluted to an OD_{600} of 0.1 in freshly prepared GM17 and then 150 µL of the cells were added in the 96-well plate. Then the plate was measured over 18 h at 30 °C via the plate reader BMG at a wavelength of 584 nm. The measured optical densities were added in one data file separated in the different used antibiotic/ lantibiotic concentration to see at which concentration the NZ9000Cm and NZ9000Pseudo begin growing and to see the different behaviour of the strains.

Purification of nisin. Nisin was purified as described in Abts et al. (2011) [45]. To determine the nisin concentration, nisin was measured by using RP-HPLC as previously described in Abts et al. (2013) [46].

Lipid extraction. To extract the membrane lipids of both NZ9000Cm and the NZ9000Pseudo strains. A membrane preparation was performed. Cells were grown in GM17 media containing 5 µg/mL chloramphenicol and were inoculated to an OD_{600} to 0.1 with a preculture. The cells were grown at 30 °C for 6 h. The cells were harvested at 8,000 rpm for 30 min and resuspended in HEPES buffer (50 mM HEPES pH 8, 150 mM NaCl and 10% (v/v) glycerol), the OD_{600} in each prepared cell sample was inoculated to an OD_{600} of 200. The cells were flash frozen in liquid nitrogen and stored at -80 °C.
The cells were thawed on ice and 10 mg/mL lysozyme was added. The cells were incubated for 30 min at 30 °C. A pinch of DNAse I was added to the cells and incubated again for 15 min on ice. The cell suspension with an OD_{600} of 200 were lysed using cell disruptor (Microfluidics M-110P, 1500 bar) in 5-6 cycles and then centrifuged at 27,000g x 2 for 15 min. The supernatant was centrifuged again at 55,000 rpm for 1 h 15 min to sediment the membranes.
The pellet was solubilized in 10 mL of 20 mM HEPES pH 7. 20 mL chloroform and 40 mL methanol were added to the membranes and it was incubated for 24 h at 4 °C. The supernatant was taken and additionally 20 mL chloroform and water each was added and everything was mixed for 3 h at room temperature. To separate the different phases the solution was incubated over night at 4 °C. The next day the chloroform phase was taken and the lipids were separated from chloroform with the help of a rotary evaporator. The lipids were solved in a 50 mM HEPES pH 7.4, 150 mM NaCl and 10% (v/v) glycerol to a concentration of 20 mg/mL.

Thin layer chromatography (TLC). To perform the thin layer chromatography (TLC) a TLC Silica plate was prepared with 10 µL spots of the NZ9000Cm and the NZ9000Pseudo lipids (20 mg/mL). As solvent, a 90:54:5.5:5.5 mixture of chloroform, methanol, ammonia and water was added in a TLC chamber. The plate was put in the chamber and running for 2h 30min. The endpoint of the solvent was marked and the plate was stained with iodide.
Also, a staining with ninhydrin (2 g/L in butanol) [47] and Dragendorff´s reagent 3.5 mL water, 1 mL solution A and 0.25 mL solution B; solution A: 25 g/L bismuth nitrate in 20 % acetic acid; solution B: 400 g/L potassium iodide was performed.
With these different staining methods, the different amines were stained. The iodide is capable of staining all amines, while the ninhydrin stains the primary and secondary amines and the Dragendorff´s reagent stains the tertiary amines.

LC-MS/MS analyses of lipids. Lipid extraction was performed as previously described. Tandem mass spectrometric analyses were conducted on a QTRAP 5500 mass spectrometer coupled with an UHPLC-system ExionLC AD (Sciex). Flow injection analysis was used for all experiments. Identification and quantification of lipid species were performed by using different scan techniques (neutral loss, precursor ion scan, multiple reaction monitoring and full scan) in positive or negative electrospray ionization mode. Cardiolipin molecular species were measured by coupling SelexIon-QTRAP-MS/MS (Sciex) based on differential mobility spectrometry technology (DMS). All data were then processed by LipidView (Sciex) software. Standards and internal standards were purchased from Avanti Polar Lipids.

Microscopy. To prepare the cells for microscopy analysis, the coverslips were prepared in a 24-well plate. The coverslips were coated with poly-L-lysin for 10 min. Afterwards the coverslips were washed two times with PBS buffer and one time with GM17 media containing 5 µg/mL chloramphenicol and 1 ng/mL nisin. Different dilutions (1:500 / 1:50 / 1:5) of prepared overnight culture (see above) were prepared in 500 µL. The prepared dilutions were added to the coverslips and the 24-well plate was centrifuged for 5 min at 3,000 rpm. The cells were fixed with 4% PFA and washed three times. The mounted coverslips were visualized under a microscope. 63x oil was used in a NA1.46 and DIC and Z-stacks were made.

Sytox binding assay. The cells of NZ9000Cm and NZ9000Pseudo were grown over night in GM17 media containing 5 µg/mL chloramphenicol and 1ng/mL nisin.
The grown cells were diluted to an OD_{600} of 0.1 in freshly prepared GM17 media containing 5 µg/mL chloramphenicol. The cultures were grown until an OD_{600} of 0.4-0.5 and SYTOX green dye (Invitrogen) was added to a final concentration of 2.5 µM and incubated for 5 min. The fluorescence was measured at an excitation of 504 nm and an emission of 523 nm, and was monitored for 500 sec. When a stable baseline was reached nisin in different concentrations was added and the signal was monitored for additional 10 min.

Genome Preparation. To isolate the genome DNA of NZ9000Cm and NZ9000Pseudo the cells were grown over night in 50 mL GM17 media containing 5 µg/µl chloramphenicol at 30 °C. The cells were harvested at 4,000 rpm for 15 min at 4 °C. The genomic DNA was isolated with the ZR Fungal/Bacterial DNA MiniPrep™ (ZYMO RESEARCH) kit according to the manufacturer´s protocol. The quality of the genomic DNA was determined via NanoDrop and via an agarose gel (1%). The genome sequencing was performed by GATC BIOTECH NextGenSequencing.

Results

Determination of antibiotic and lantibiotic resistance. To determine the resistance of the resistant strain NZ9000Pseudo, IC_{50} measurements were performed. The measurements were performed with a NZ9000 strain transformed with a pIL-SV empty vector as a control, because this strain is sensitive against the different lantibiotics and antibiotics. To compare the different strains to each other the NZ9000Pseudo strain was transformed with a pIL-SV empty vector. Nisin was purified as previously described [45]. The other tested antibiotics and lantibiotics were bought in the highest purity (vancomycin by Sigma Aldrich; ramoplanin by Sigma Aldrich, penicillin by Fluka BioChemica and gallidermin by Enzo Life science). To address the activity of the antibiotics against the NZ9000Pseudo strain growth experiments and growth curves were performed with increasing antibiotic concentrations. The calculated IC_{50} values (Table 1) display that the lantibiotics are highly active against the NZ9000Cm and also the antibiotics are active against this strain. The NZ9000Pseudo is more resistant to nearly all tested lantibiotics and antibiotics. The IC_{50} values of the NZ9000Pseudo strain are higher as compared to the NZ9000Cm. For nisin the NZ9000Pseudo strain has a IC_{50} value of 47.1 ± 3.7 nM, while the NZ9000Cm has a value of 8.8 ± 0.6 nM. For gallidermin the values are 42.7 ± 3.5 nM (NZ9000Cm) and 134.4 ± 18.7 nM (NZ9000Pseudo). For vancomycin and penicillin G the values are 285.9 ± 14.7 nM (NZ9000Cm), 594.4 ± 30.9 nM (NZ9000Cm) and 706.8 ± 32.3 nM (NZ9000Pseudo), 2697 ± 153.5 nM (NZ9000Pseudo), respectively (Table 1). Only the ramoplanin shows no resistance in the NZ9000Pseudo strain. The IC_{50} values of ramoplanin are 116.5 ± 4.1 nM (NZ9000Cm) and 141.7 ± 6.1 nM (NZ9000Pseudo), nearly the same (Table 1).

Table 1: IC_{50} values of the used antibiotics and lantibiotics against NZ9000Cm and NZ9000Pseudo strains.

	NZ9000Cm	NZ9000Pseudo	
Antibiotic/Lantibiotic	**IC_{50} (nM)**	**IC_{50} (nM)**	**Fold of resistance**
Nisin	8.8 ± 0.6	47.1 ± 3.7	5.3
Gallidermin	42.7 ± 3.5	134.4 ± 18.7	3.2
Vancomycin	285.9 ±14.7	709.8 ± 32.3	2.5
Ramoplanin	116.5 ± 4.1	141.7 ± 6.1	1.2
Penicillin G	594.4 ± 30.9	2697 ± 153.5	4.5

By dividing the two IC_{50} values, the fold of resistance (Table 1; Figure 4) was determined. This fold of resistance makes it easier to compare the different antibiotics and the lantibiotics to each other. Against nisin the NZ9000Pseudo is most resistant with a fold of resistance of 5.3, which means that it needs 5 times more nisin to kill 50 % of the cells compared to the NZ9000Cm strain. As mentioned before, the NZ9000Pseudo strain is not resistant against ramoplanin as seen from the fold of resistance of 1.2. The other antibiotics are in a range of 2.5-5.3 fold of resistance (Table 1, Figure 4). This displays that the NZ9000Pseudo raises resistance against several antibiotics and lantibiotics.

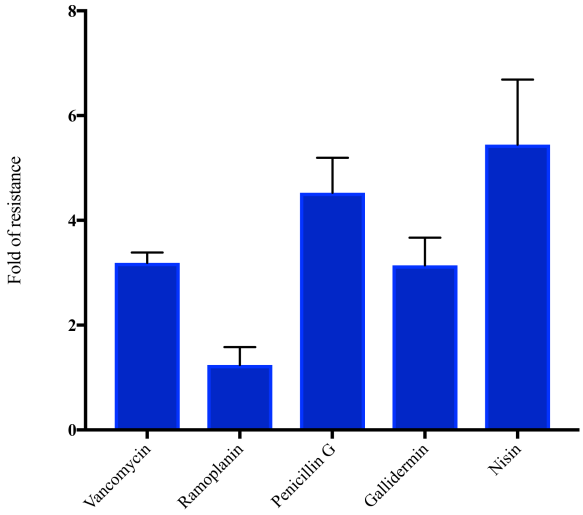

Figure 4: Fold of resistance of NZ9000Pseudo. The fold of resistance is calculated by dividing the IC_{50} value of NZ9000Pseudo strain by the IC_{50} value of the NZ9000Cm strain. The NZ9000Pseudo strain shows higher resistance against nisin, while there is nearly no resistance against ramoplanin.

Determination of the growth behaviour of the NZ9000Pseudo strain. To determine if the growth of the NZ9000Pseudo strain is different to the control NZ9000Cm strain growth curves were performed. The cells were grown for 18 h at 30 °C in GM17 media containing 5 µg/mL chloramphenicol. OD_{600} was measured hourly in the plate reader (Fluostar BMG). To prevent variance in the measurements for every experimental set up the NZ9000Cm and the NZ9000Pseudo were measured together on one 96-well plate with serially diluted antibiotics or lantibiotics. It could be observed that the NZ9000Pseudo strain grows faster in the presence of higher concentrations of antibiotics and lantibiotics than the NZ9000Cm. The NZ9000Pseudo strain is able to survive in higher concentrations and regrow after hours to a high OD_{600} while the NZ9000Cm is not growing at all. These growth curves were performed with every antibiotic and lantibiotic tested. As the IC_{50} measurements before proves, the ramoplanin does not show a difference in the growth curves of the NZ9000Pseudo and NZ9000Cm. The NZ9000Pseudo maybe starts to grow one hour before

the NZ9000Cm strain but in comparison with the other tested reagents here, this is not a significant resistance. The other substances the NZ9000Pseudo grows one or two concentrations higher than the NZ9000Cm strain (Figure 5).

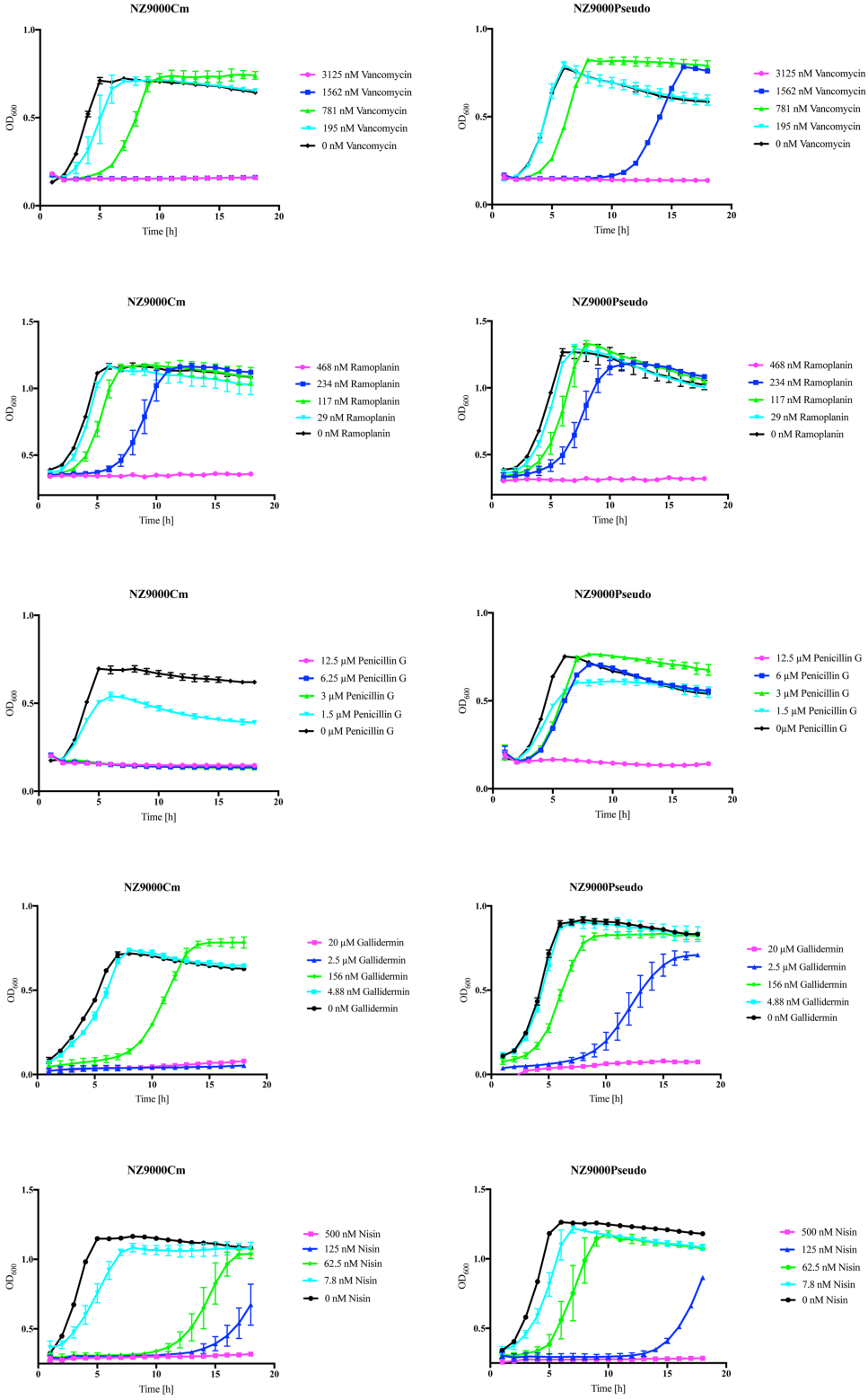

Figure 5: Growth curves of NZ9000Cm and NZ9000Pseudo strains with the different tested antibiotics and lantibiotics. The growth curves amplify the results of the IC_{50} measurements where the NZ9000Pseudo starts growing at higher concentrations compared with the NZ9000Cm strain. With ramoplanin nearly the same growth pattern of the two strains could be observed, so the sensitivity of strains is the same towards ramoplanin. With nisin and penicillin it can be observed that the NZ9000Pseudo grow faster to a high OD_{600} in presence of high concentrations of these substances.

Determination of the pore forming behaviour of NZ9000Pseudo. To determine if the NZ9000Pseudo strain is able to prevent the *L. lactis* strain from the mode of action of nisin, a Sytox green assay was performed. Nisin is able to form pores in the membranes of Gram-positive bacteria via binding to the precursor molecule lipid II [31]. Sytox green nucleid acid dye is an established method to monitor the pore formation [44; 48]. The dye binds to the DNA, enters the cell through the built pores and the fluorescence signal increases. With the determined IC_{50} values (see above) different nisin concentrations were calculated to monitor the pore formation on the two different strains. It could be observed that the NZ9000Pseudo strain does not form pores as fast as the NZ9000Cm strains (Figure 6). In the slope of the fluorescence measurements, the pore formation is visualized. If the pores are formed fast, with a concentration higher than the IC_{50} value, the measured slope is steep and the saturation is reached in a short time resulting in direct death of the bacterial cells upon addition of nisin. If the cells are inhibiting pore formation, the same nisin concentration results in a flatter slope and a longer time is needed till saturation.

With the help of the lag-phase, the time till the slope starts to increase, the two strains could be compared. An explanation for the different used values, lag-phase and k-value is depicted in Figure 6 A. Comparing both strains, the NZ9000Pseudo strain has a longer lag-phase than the NZ9000Cm strain at the same nisin concentrations. The pore formation is inhibited by the NZ9000Pseudo. The slope of the Sytox measurements were determined as k-value (Figure 6) and shows for the NZ9000Cm strain that the slope is getting steeper with higher nisin concentrations till a saturation is reached, meaning it is not able to form the pores faster anymore. Comparing these results with the NZ9000Pseudo, the k-value of the NZ9000Pseudo measurements is lower. The slope of these measurements is constant upon addition of higher concentrations of nisin.

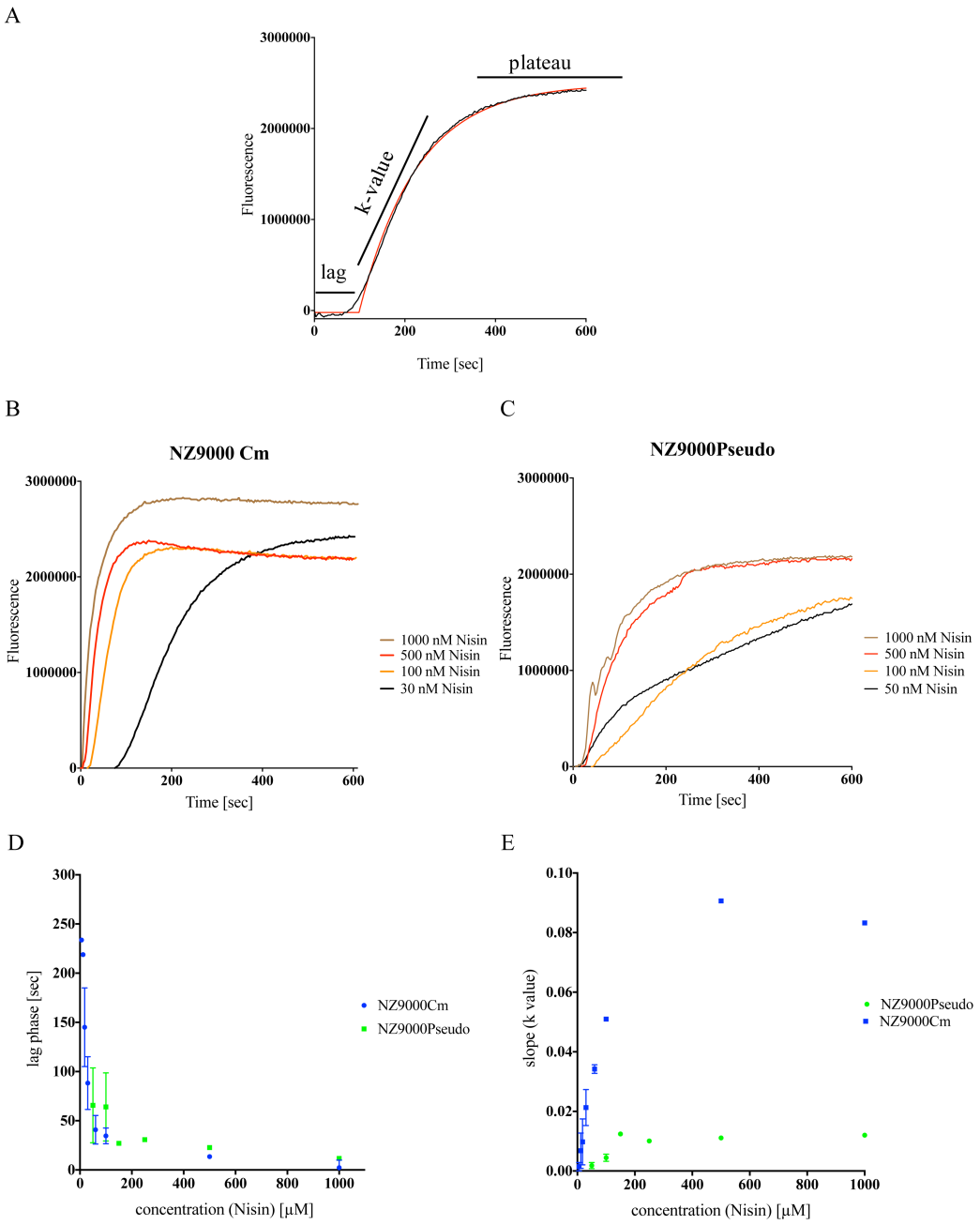

Figure 6: Determination of pore formation in NZ9000Cm and NZ9000Pseudo. A) Example of the different values of the Sytox green assay. In black the measurement is depicted in red the fit to determine the different values. B-C) The measurements of the Sytox green assay. The fluorescence plotted against the time. 0 is the point of addition of nisin. The difference of the two strains in the time and increase of fluorescence is shown. D) The lag-phase of the NZ9000Cm and NZ9000Pseudo Sytox measurements are shown. The lag-phase of different nisin concentrations is depicted and, in the diagram, it is shown that the NZ9000Pseudo cells have a longer lag-phase until the pore formation is started. E) The slope of the Sytox curve is plotted against the nisin concentration. With a higher concentration of nisin the slope of the NZ9000Cm is increased. The slope of the NZ9000Pseudo is mostly the same at all concentrations.

The NZ9000Pseudo cells are able to inhibit pore formation. The lag-phase is increased and the k-value is constant at mostly all nisin concentrations. All in all, it could be said that the NZ9000Pseudo strain is able to prevent nisin to form a pore with the lipid II molecules. It could be a hint that just the same amount of nisin is able to get to the membrane and is able to bind, no matter how high the concentration is. Because nisin binds to the lipid II

peptidoglycan precursor the next step is to figure out why the NZ9000Pseudo strain is more resistant against the different antibiotics and lantibiotics and is able to inhibit the pore formation of nisin. Thus, a peptidoglycan analysis of the purified peptidoglycan was performed via HPLC-MS in cooperation with University of Tuebingen (PD Dr. Evi Stegmann). The HPLC-MS data of the peptidoglycan does not show any difference upon comparing the NZ9000Pseudo and the NZ9000Cm (data not shown). The peptidoglycan was not modified or somehow changed in the composition. If some differences could be observed here, then the modification of the peptidoglycan could be the cause of resistance. However, the results of the peptidoglycan analysis did not show any differences.

Thus, the peptidoglycan could be excluded as reason for the determined resistance in the NZ9000Pseudo strain and there is a different cause. All of the tested antibiotics and lantibiotics are targeting the cell wall synthesis. The membrane lipids can have an influence on the binding and the charge of the membrane so that the antibiotics cannot bind anymore or the membrane is more rigid [36; 39; 40; 41; 42]. To analyse whether the membrane lipids are changed, a lipid extraction was performed. Via thin layer chromatography and LC-MS/MS the membrane lipids were further analysed. Analyses were performed with the NZ9000Cm and the NZ9000Pseudo strains because there are so far, no available data of the membrane lipid composition of *L. lactis*. To see differences, analyses of the original has to be performed first to compare the strains.

The thin layer chromatography was performed for 2 h 30 min, 10 µL of NZ9000Pseudo lipids (20 mg/mL) and NZ9000Cm lipids (20 mg/mL) were spotted on a thin layer silica plate and run in a thin layer chamber with a solvent, a 90:54:5.5:5.5 chloroform, methanol, ammonia and water mixture. Afterwards the plate was stained with iodide, ninhydrin and the Dragendorff´s reagent. To stain the different amines, primary and secondary are stained via ninhydrin and tertiary via Dragendorff´s reagent. Iodide is used to stain all amines.

In the thin layer chromatogram stained with the ninhydrin a difference in the lipid band could be observed as one band was running lower in the NZ9000Pseudo strain compared to the NZ9000Cm (Figure 7). While the iodide staining of the two strains looked similar to each other (Figure 7). Because of the ninhydrin staining it could be said that the lipid composition is different. To determine the lipid composition in detail a LC-MS/MS analysis was performed to get the exact lipid compositions of both strains.

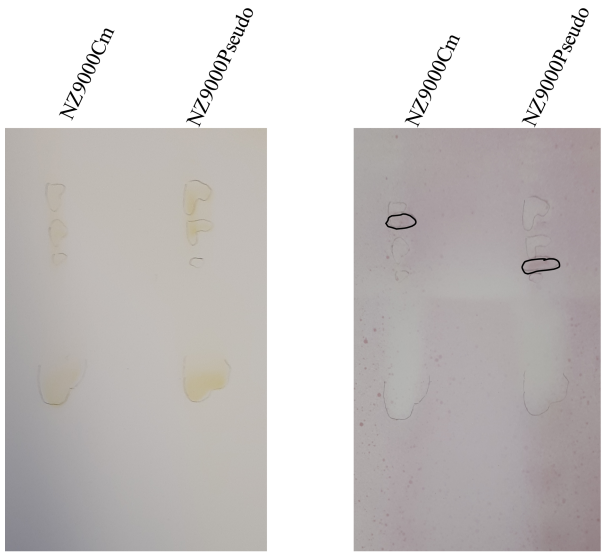

Figure 7: Thin layer chromatography of NZ9000Cm and NZ9000Pseudo lipids. A TLC was performed with 90:54:5.5:5.5 chloroform methanol ammonia and water mixture. 10 µL of 20 mg/mL lipids solution of NZ9000Cm and NZ9000Pseudo was stained with iodide and ninhydrin. The iodide stained plate does not show differences in the two different strains. The ninhydrin stained shows a band running lower in the NZ9000Pseudo than in the NZ9000Cm marked with black in the figure.

As a control to identify the different lipids, standards were purchased from Avanti Polar Lipids. The lipids could be identified and the composition of the lipids in the NZ9000Cm and the NZ9000Pseudo could be determined. The fraction of the different lipids is shown in Figure 8. Here difference between the two strains, NZ900Cm and NZ9000Pseudo could be observed. The phosphatidylcholine (PC) and phosphatidylethanolamine (PE) are more present in the control strain (NZ9000Cm). Therefore, the cardiolipin (CL) and phosphatidylglycerol (PG) is increased in the NZ9000Pseudo strain. The lipid compositions of the strains are different which could be a reason for the determined resistance in the NZ9000Pseudo strain. The distribution of the lipids is changed and so the membrane components are different.

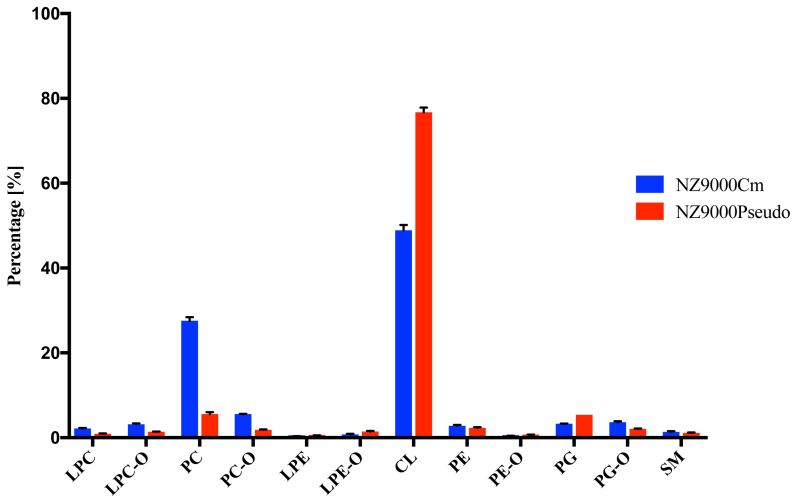

Figure 8: Composition of the lipids of NZ9000Cm and the NZ9000Pseudo strains. The NZ9000Pseudo (red coloured columns) shows more PC and PE concentrations. The CL and the PG concentrations are increased in comparison to the NZ900Cm strain (blue coloured columns). This is a two-time experiment. Data Supplementary table 1.

Visualization of the NZ9000Pseudo cells. To determine if the living cells are behaving differently, not only in the growing behaviour but also in the accumulation of the cells, microscopy was performed. For microscopy, overnight cultures of the NZ9000Cm and the NZ9000Pseudo strain were prepared. On the next day, they were inoculated to an OD_{600} of 0.1 and grown till an OD_{600} of 0.3.

To prepare the cells for microscopy analysis, the coverslips were prepared in a 24-well plate. The coverslips were coated with poly-L-lysin for 10 min. To wash the coverslips PBS buffer was used and in the last washing step GM17 media containing 5 µg/mL chloramphenicol and 1 ng/mL nisin. Different dilutions (1:500 / 1:50 / 1:5) of prepared cultures were prepared in 500 µL. The prepared dilutions were added to the coverslips and the 24-well plate was centrifuged for 5 min at 3,000 rpm. The cells were fixed with 4 % PFA and washed again. With the microscopy, it was possible to determine the different length of the cells and how the cells accumulate. In Figure 10, the percentage of the observed length of the NZ9000Cm and NZ9000Pseudo cells are shown. It could be observed that the NZ9000Pseudo strain shows more 1 µm cells (41.28% 1 nM; 55.5 % 10 nM) in comparison with the NZ9000Cm (23.45% 1 nM). The control strain contains more 2 µm (33.67%) and 15 µm (27.54%) cells. The NZ9000Pseudo strain contains 29.43% (1 nM) and 25.61% (10 nM) of the 2 µm and only 14.20% (1 nM) and 9.7% (10 nM) of the 15 µm cells (Figure 10).

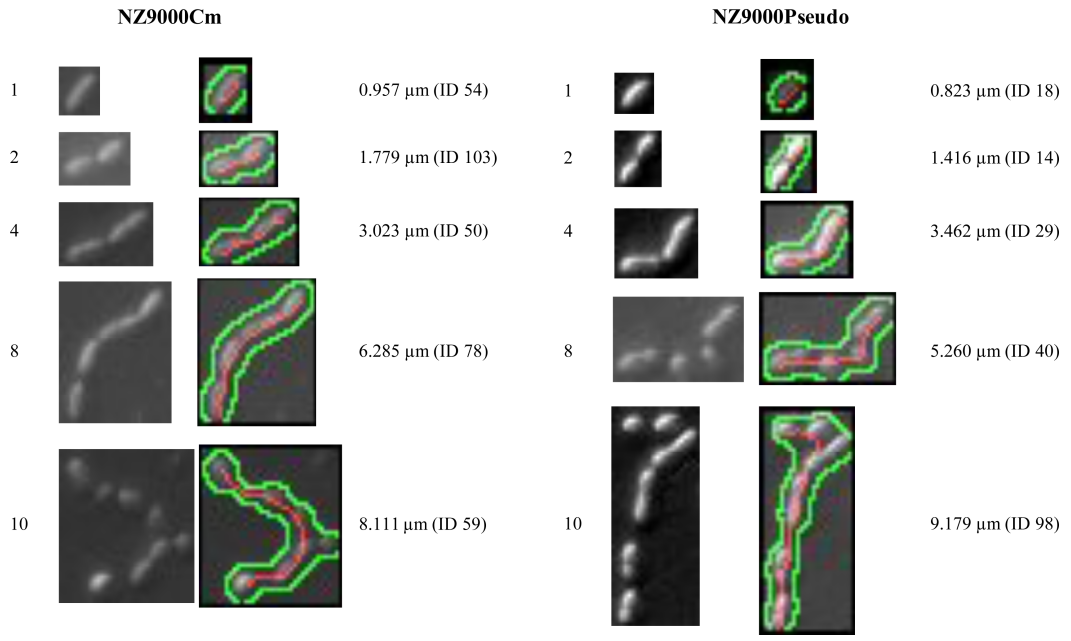

Figure 9: Microscopy of the NZ9000Cm and the NZ9000Pseudo. With the microscope, it was able to determine the length of the different accumulation states of the cells. The length of the different cell types is also different. A single cell of the NZ9000Cm is 0.957 µm in size, while a single cell of the NZ9000Pseudo is just 0.823 µm in size. Also, the various accumulation states of the different cell numbers are depending in the two strains.

The length which could be observed stands for how many cells are accumulated (Figure 9). A single cell is 1 µm in length. So, the NZ9000Pseudo cells does not accumulate like the NZ9000Cm cells. The observed behaviour shows that the strains are not only different in the resistance and lipid composition, they also behave different in the accumulation, which is also an interesting behaviour and could be a reason for the observed resistance of the NZ9000Pseudo strain. This may also be an outcome of the different lipid composition.

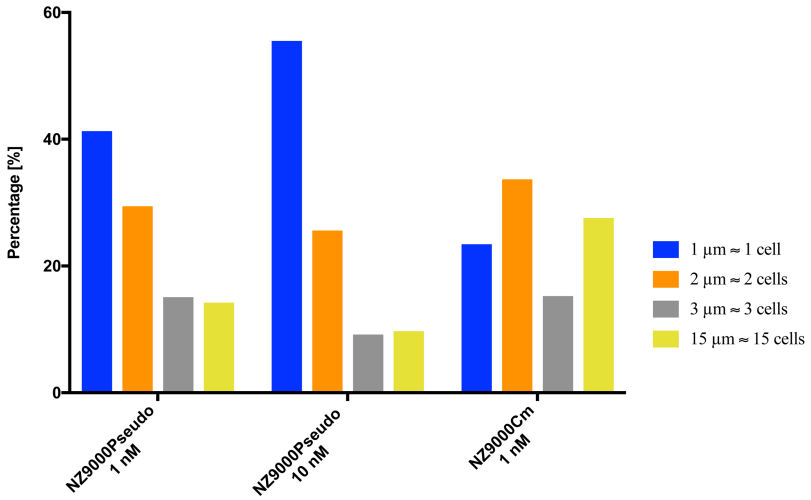

Figure 10: Microscopy analysis of the appearance of the NZ9000Pseudo and the NZ9000Cm strains. There are two different amounts of NZ9000Pseudo cells depicted (1 nM, 10 nM) and 1 nM NZ9000Cm as a control. It is obvious that the NZ9000Pseudo has a higher percentage of 1 µm length than the NZ9000Cm strain.

Determination of the reason behind the resistance via genome sequencing. The genome sequencing of the NZ9000Cm and the NZ9000Pseudo strain was performed by GATC BIOTECH NextGenSequencing. The genome preparation was performed with the ZR Fungal/Bacterial DNA MiniPrep™ (ZYMO RESEARCH) kit. The analysis of the NZ9000Cm was showing nearly no difference to the genome of *Lactococcus lactis subsp. cremoris* NZ9000 strain (GenBank Number CP002094.1) and thus, the NZ9000Cm strain is the original *Lactococcus lactis subsp. cremoris* NZ9000 strain. The genome sequencing of the NZ9000Pseudo strain shows different mutations, which were more in comparison to the NZ9000Cm. Just 50% of the sequencing frames could be mapped to the control genome of the *Lactococcus lactis subsp. cremoris* NZ9000. Even though there were many changes in the genome sequence of the NZ9000Pseudo strain, some just occurred only once in the sequencing frames and even more occurred in 50% of the sequencing frames. Hence, it was not obvious to determine which mutation results in a significant change in the genome. Because of the less mapping efficiency, a contamination in the bacterial sample had to be excluded. To identify if the used cells were contaminated IC_{50} tests were performed with different NZ9000Pseudo colonies of a GM17 agar plate containing 5 µg/mL chloramphenicol. Seven colonies were tested and all showed nearly the same IC_{50} curve (Figure 11).

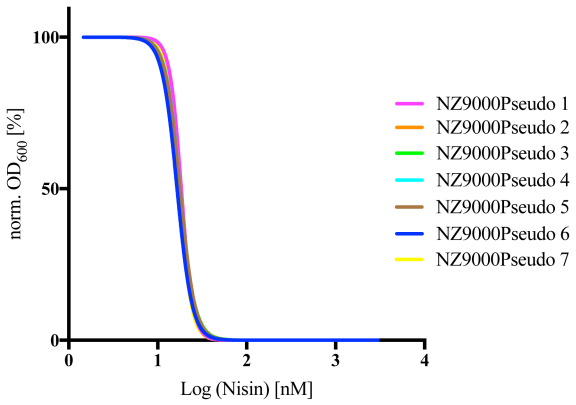

Figure 11: IC_{50} measurements with seven different NZ9000Pseudo colonies. It is shown that the seven tested colonies have the same IC_{50} curves (colonies 1-7). It is a one-time experiment.

Since the IC_{50} measurements of the single colonies showed no difference in behaviour, it can be excluded that the cells are containing any impurity. This cannot be the reason for the low alignment percentage of the genome sequencing. Three proteins which had many mutations in the DNA sequence are shown in Table 2. The whole mutation list is mentioned in the supplemental part.

Table 2: Three examples of the genome sequencing. These proteins showed mutations in the genome sequencing, which are less than 50%.

Protein	**Gen-Position**	**Reference**	**Observed**
23S ribosomal RNA	2524827	T	TA
	2524829	C	A
	2524837	T	A
	2524881	C	T
	2524904	T	C
	2524910	C	A
	2524911	G	A
	2524915	T	C
	2524917	C	T
	2524922	G	A
	2524978	A	C
	2524991	A	T
	2524994	T	A
pstA – phosphate transporter ATP binding protein	1876050	C	T
	1876065	T	C
	1876120	A	T
atpA and atpB F_0F_1-type ATP synthase	1929139	T	A
	1929151	C	A
	1929152	C	T
	1929157	A	C
	1929163	A	G
	1929175	A	T
	1929178	A	C
	1929184	C	A
	1929193	T	A
	1929199	T	G
	1929202	A	G
	1929208	A	C
	1929211	A	T
	1929214	G	A

	1929232	G	A
	1929238	C	T
	1929247	G	A
	1929250	A	T
	1929252	G	A
	1931512	A	T
	1931518	A	G
	1931525	T	A
	1931529	C	T
	1931532	C	T
	1931533	C	T
	1931545	A	G
	1931557	A	G

Nevertheless, the observed mutations appeared in several different proteins (Table 2) which are not directly involved in the lipid synthesis or the cell wall synthesis. At this moment, it is not possible to determine which mutation is a real one and which one has an influence on the lipid composition. However, there are some mutations in the genome of the NZ9000Pseudo strain. In Uniprot the amino acid sequence of the proteins, containing a mutation, was checked. The known activity sites and binding sites of this proteins are not directly affected by the mutations. That does not mean that the mutation is not important but the closer look to the genome do not give the answer to the resistance behaviour of the NZ9000Pseudo strain yet.

Discussion

There are already some mechanisms known of lantibiotic resistance and also against antibiotic resistance. Vancomycin resistant bacteria have developed different resistance strategies. They can develop a new amino acid D-Ala-D-Lac combination in comparison to the original D-Ala-D-Ala. The *van* operon is responsible for the alternative depsipeptide [10; 15; 16]. Because of this alternative depsipeptide formation, the vancomycin loses one hydrogen bond to the precursor molecule lipid II and the binding is 1000-fold reduced in comparison to the wild type bonds [6; 12; 15]. Also, a thicker cell wall formation is known to perform resistance against vancomycin. Vancomycin resistance in *Staphylococci* are known to be performed due to a thicker cell wall and an increased peptidoglycan synthesis. So that the vancomycin still binds to the D-Ala-D-Ala but there is much more peptidoglycan and thus the cells are still alive [16]. Also, there are resistant strains against penicillin known that contain mutations in the penicillin binding protein (PBP). Thereby, the penicillin has a lower binding affinity and is not inhibiting the transpeptidation anymore [20; 21; 22].
Also, nisin resistance can have several different reasons like resistance proteins, like ABC-transporters, positively charged LTAs and WTAs, both due to the *dltABCD* operon, cell wall thickness and a different membrane composition of phospholipids and fatty acids [36]. The strain in this study shows resistance against nearly all tested antibiotics. Via different analysis it could not be determined directly the cause of the resistance of the cells. But one difference was observed in the lipid composition of the NZ9000Cm and the NZ9000Pseudo strains. Here, it was not only interesting to analyse the lipid composition of the NZ9000Pseudo strain but also the NZ9000Cm strain was interesting because till date the exact lipid composition of the *L. lactis* is not published. Here the major phospholipid is the cardiolipin (CL) different to *Bacillus cereus* (*B. cereus*) which contains PE as major phospholipid. Also, *Bacillus subtilis* (*B. subtilis*) and *Staphylococcus aureus* (*S. aureus*) contain a different major phospholipid, here the phosphatidylglycerol (PG) is the major one. In the *L. lactis* strains, measured in this study, the percentage of PG and CL are different to the other strains. The most prominent phospholipid in both strains is the cardiolipin with 48.9% and 76.7% in the NZ9000Cm and NZ9000Pseudo strains. In the *L. lactis* are lysolipids detectable with 6.5% in the NZ9000Cm and 4.3% in the NZ9000Pseudo. The lipid composition of bacteria can vary a lot. While *B. subtilis* has PG as major phospholipid (70%) [49], *B. cereus* has PE as major phospholipid (43%-70% depending the growth temperature) [50]. In contrast *S. aureus* with 58% PG and 42% CL [51]. So, the original *L. lactis* has

different to all strains CL (48.9%) as major phospholipid and contains 33.1% PC as second most present lipid. With the known phospholipid composition of the *L. lactis* strain it was possible to compare the resistant NZ9000Pseudo strain with the original strain. The phospholipids of the NZ9000Pseudo are different in the composition. The strain contains more CL (76.7%) than the NZ9000Cm, original, strain (Table 3).

Table 3: Major phospholipid components of different Gram-positive bacteria [51].

Phospholipid (% total membrane)	*L. lactis* NZ9000	*L. lactis* NZ9000Pseudo	*B. cereus* (a)	*B. subtilis* [49]	*S. aureus* [52]
PE (-O)	3.2	2.9	43	12	-
PG (-O)	6.9	7.5	40	70	58
CL	48.9	76.7	17	4	42
PC (-O)	33.1	7.4	-	-	-
SM	1.4	1.1	-	-	-
LPE (-O)	1	2	-	-	-
LPC (-O)	5.4	2.3	-	-	-

a) Growing at 37 °C a higher value up to 70% PE is found at 15 °C growth conditions. The PG is then reduced to 17%, the CL is nearly the same [50].

In the *L. lactis* NZ9000 strain PC and SM was detectable which is not mentioned in the different compared Gram-positive bacteria (Table 3). Here the two *L. lactis* strains also show differences. The NZ9000Cm contains 33.1% PC (PC+PC-O) and 1.4% SM while the NZ9000Pseudo contains 7.4% PC (PC+PC-O) and 1.1% SM.

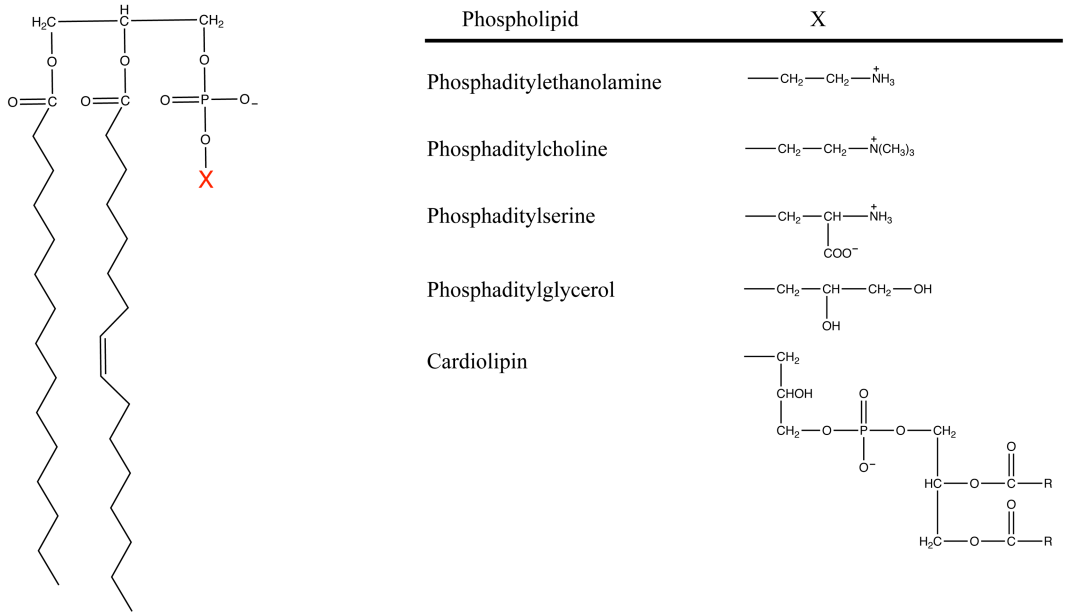

Figure 12: Phospholipids and their head groups. Based on [53].

PC is a neutrally charged phospholipid like the PE. The NZ9000Cm strain consists of more neutrally charged PC and PE but lesser negatively charged CL and PG (Figure 8, Table 3, Figure 12). That was surprising because it is published that a decrease in negatively charged could lead to nisin resistance in the cell [36]. But here the NZ9000Pseudo the resistant strain contains more negatively charged CL. So maybe it is not the phospholipids itself, but fatty acids of the phospholipids could be the reason. The composition of the phospholipids with the different fatty acids, is shown in the supplementary part. So, the membrane fluidity can also be another reason for the observed resistance.

In general, at the moment the cause of the resistance in the NZ9000Pseudo strain against nisin, gallidermin, penicillin and vancomycin could not be determined in detail. At the moment, it seems that a different composition of the phospholipid or fatty acids could be the reason. The diversification of the lipids compared to the NZ9000Cm strain is different as there are less PC lipids and PE but more of the CL and PG lipids. The reason behind the different composition cannot be determined. The genome sequencing does not show a reason for this. If it is a mixture of the different mutations or if one mutation is the reason for all cannot be said. If the composition of the lipids is the only reason behind this resistance would be really interesting to know, because then a strain used in a lab could mutate suddenly and be highly resistant. The reason behind this would be really interesting to analyse the evolution of the cells. This could appear in patients as well and could result in a new multi resistant bacteria.

The living cells were analysed via microscopy and it could be observed that the NZ9000Pseudo cells do not accumulate like the NZ9000Cm cells. This could also be a reason of the different cell membrane composition. The cells are not able to cluster anymore and are present as single cells with a length of 1 µm. The cells have to be analysed again to be sure of the reason behind the observed resistance. It seems to be the different lipid composition but the WTAs and LTAs have not been analysed yet, and it is also known that the different charged WTAs are able to generate resistance against nisin [36; 37]. Also, a thicker cell wall could be a reason for the resistance. Although the peptidoglycan was analysed it has not been quantified. Maybe the peptidoglycan is not modified but the amount of peptidoglycan is different. This could also answer the resistance. It could also be all together and not only the lipid composition, as also the peptidoglycan amount is different. We can definitely say that the strain described here is a lantibiotic and antibiotic resistant strain which develops this resistance due to a self-mutation. The *L. lactis* phospholipid

composition has been solved, so that any difference in the phospholipids of *L. lactis* can now be compared.

Author contributions

SS conceived and directed this study. RC performed the growth inhibition measurements, the growth curve studies, the lipid extraction, thin layer chromatography and the genome preparation. TZ performed the Microscopy measurements. DH did the lipid MS analysis. HK performed the Sytox measurements. RC and SS wrote the manuscript. All the authors read and approved the manuscript.

Acknowledgements

We thank all the members of the Institute of Biochemistry for fruitful discussions.

References

[1] A. Fleming, On the antibacterial action of cultures of a penicillium, with special reference to their use in the isolation of *B. influenzae*. 1929. Bull World Health Organ 79 (2001) 780-90.

[2] A.H. van Hoek, D. Mevius, B. Guerra, P. Mullany, A.P. Roberts, and H.J. Aarts, Acquired antibiotic resistance genes: an overview. Front Microbiol 2 (2011) 203.

[3] H.C. Neu, The crisis in antibiotic resistance. Science 257 (1992) 1064-73.

[4] G.S. Bbosa, N. Mwebaza, J. Odda, D.B. Kyegombe, and M. Ntale, Antibiotics/antibacterial drug use, their marketing and promotion during the post-antibiotic golden age and their role in emergence of bacterial resistance. Health 06 (2014) 410-425.

[5] G. Kapoor, S. Saigal, and A. Elongavan, Action and resistance mechanisms of antibiotics: A guide for clinicians. J Anaesthesiol Clin Pharmacol 33 (2017) 300-305.

[6] D.G. McCafferty, P. Cudic, B.A. Frankel, S. Barkallah, R.G. Kruger, and W. Li, Chemistry and biology of the ramoplanin family of peptide antibiotics. Biopolymers 66 (2002) 261-84.

[7] K.F. Kong, L. Schneper, and K. Mathee, Beta-lactam antibiotics: from antibiosis to resistance and bacteriology. APMIS 118 (2010) 1-36.

[8] M.S. Butler, K.A. Hansford, M.A. Blaskovich, R. Halai, and M.A. Cooper, Glycopeptide antibiotics: back to the future. J Antibiot (Tokyo) 67 (2014) 631-44.

[9] D.K. Farver, D.D. Hedge, and S.C. Lee, Ramoplanin: a lipoglycodepsipeptide antibiotic. Ann Pharmacother 39 (2005) 863-8.

[10] A. Muller, A. Klockner, and T. Schneider, Targeting a cell wall biosynthesis hot spot. Nat Prod Rep 34 (2017) 909-932.

[11] A. Coates, Y. Hu, R. Bax, and C. Page, The future challenges facing the development of new antimicrobial drugs. Nat Rev Drug Discov 1 (2002) 895-910.

[12] D.H. Williams, The glycopeptide story--how to kill the deadly 'superbugs'. Nat Prod Rep 13 (1996) 469-77.

[13] N. McCallum, P.S. Meier, R. Heusser, and B. Berger-Bachi, Mutational analyses of open reading frames within the *vraSR* operon and their roles in the cell wall stress response of *Staphylococcus aureus*. Antimicrob Agents Chemother 55 (2011) 1391-402.

[14] E. Breukink, and B. de Kruijff, Lipid II as a target for antibiotics. Nat Rev Drug Discov 5 (2006) 321-32.

[15] C.T. Walsh, S.L. Fisher, I.S. Park, M. Prahalad, and Z. Wu, Bacterial resistance to vancomycin: five genes and one missing hydrogen bond tell the story. Chem Biol 3 (1996) 21-8.

[16] J. Pootoolal, J. Neu, and G.D. Wright, Glycopeptide antibiotic resistance. Annu Rev Pharmacol Toxicol 42 (2002) 381-408.

[17] H. Hanaki, H. Labischinski, Y. Inaba, N. Kondo, H. Murakami, and K. Hiramatsu, Increase in glutamine-non-amidated muropeptides in the peptidoglycan of vancomycin-resistant *Staphylococcus aureus* strain Mu50. J Antimicrob Chemother 42 (1998) 315-20.

[18] L. Cui, X. Ma, K. Sato, K. Okuma, F.C. Tenover, E.M. Mamizuka, C.G. Gemmell, M.N. Kim, M.C. Ploy, N. El Solh, V. Ferraz, and K. Hiramatsu, Cell Wall Thickening Is a Common Feature of Vancomycin Resistance in *Staphylococcus aureus*. Journal of Clinical Microbiology 41 (2003) 5-14.

[19] E. Binda, F. Marinelli, and G.L. Marcone, Old and New Glycopeptide Antibiotics: Action and Resistance. Antibiotics (Basel) 3 (2014) 572-94.

[20] P.D. Stapleton, and P.W. Taylor, Methicillin resistance in *Staphylococcus aureus*: mechanisms and modulation. Sci Prog 85 (2002) 57-72.
[21] C.G. Dowson, T.J. Coffey, C. Kell, and R.A. Whiley, Evolution of penicillin resistance in *Streptococcus pneumoniae*; the role of *Streptococcus mitis* in the formation of a low affinity PBP2B in *S. pneumoniae*. Molecular Microbiology 9 (1993) 635-643.
[22] J. Fishovitz, J.A. Hermoso, M. Chang, and S. Mobashery, Penicillin-binding protein 2a of methicillin-resistant *Staphylococcus aureus*. IUBMB Life 66 (2014) 572-7.
[23] P.D. Cotter, C. Hill, and R.P. Ross, Bacteriocins: developing innate immunity for food. Nat Rev Microbiol 3 (2005) 777-88.
[24] P.D. Cotter, R.P. Ross, and C. Hill, Bacteriocins - a viable alternative to antibiotics? Nat Rev Microbiol 11 (2013) 95-105.
[25] C. Chatterjee, M. Paul, L. Xie, and W.A. van der Donk, Biosynthesis and mode of action of lantibiotics. Chem Rev 105 (2005) 633-84.
[26] J. Delves-Broughton, P. Blackburn, R.J. Evans, and J. Hugenholtz, Applications of the bacteriocin, nisin. Antonie Van Leeuwenhoek 69 (1996) 193-202.
[27] I. Wiedemann, E. Breukink, C. van Kraaij, O.P. Kuipers, G. Bierbaum, B. de Kruijff, and H.G. Sahl, Specific binding of nisin to the peptidoglycan precursor lipid II combines pore formation and inhibition of cell wall biosynthesis for potent antibiotic activity. J Biol Chem 276 (2001) 1772-9.
[28] E. Breukink, Use of the Cell Wall Precursor Lipid II by a Pore-Forming Peptide Antibiotic. Science 286 (1999) 2361-2364.
[29] H. Brotz, M. Josten, I. Wiedemann, U. Schneider, F. Gotz, G. Bierbaum, and H.G. Sahl, Role of lipid-bound peptidoglycan precursors in the formation of pores by nisin, epidermin and other lantibiotics. Mol Microbiol 30 (1998) 317-27.
[30] H.E. Hasper, N.E. Kramer, J.L. Smith, J.D. Hillman, C. Zachariah, O.P. Kuipers, B. de Kruijff, and E. Breukink, An alternative bactericidal mechanism of action for lantibiotic peptides that target lipid II. Science 313 (2006) 1636-7.
[31] H.E. Hasper, B. de Kruijff, and E. Breukink, Assembly and stability of nisin-lipid II pores. Biochemistry 43 (2004) 11567-75.
[32] S.T. Hsu, E. Breukink, E. Tischenko, M.A. Lutters, B. de Kruijff, R. Kaptein, A.M. Bonvin, and N.A. van Nuland, The nisin-lipid II complex reveals a pyrophosphate cage that provides a blueprint for novel antibiotics. Nat Struct Mol Biol 11 (2004) 963-7.
[33] E. Breukink, C. van Kraaij, R.A. Demel, R.J. Siezen, O.P. Kuipers, and B. de Kruijff, The C-terminal region of nisin is responsible for the initial interaction of nisin with the target membrane. Biochemistry 36 (1997) 6968-76.
[34] F. Gotz, S. Perconti, P. Popella, R. Werner, and M. Schlag, Epidermin and gallidermin: *Staphylococcal* lantibiotics. Int J Med Microbiol 304 (2014) 63-71.
[35] J.M. Willey, and W.A. van der Donk, Lantibiotics: peptides of diverse structure and function. Annu Rev Microbiol 61 (2007) 477-501.
[36] L.A. Draper, P.D. Cotter, C. Hill, and R.P. Ross, Lantibiotic resistance. Microbiol Mol Biol Rev 79 (2015) 171-91.
[37] A. Peschel, M. Otto, R.W. Jack, H. Kalbacher, G. Jung, and F. Gotz, Inactivation of the *dlt* operon in *Staphylococcus aureus* confers sensitivity to defensins, protegrins, and other antimicrobial peptides. J Biol Chem 274 (1999) 8405-10.
[38] N.E. Kramer, S.A. van Hijum, J. Knol, J. Kok, and O.P. Kuipers, Transcriptome analysis reveals mechanisms by which *Lactococcus lactis* acquires nisin resistance. Antimicrob Agents Chemother 50 (2006) 1753-61.
[39] A. Verheul, N.J. Russell, T.H.R. Van, F.M. Rombouts, and T. Abee, Modifications of membrane phospholipid composition in nisin-resistant *Listeria monocytogenes* Scott A. Appl Environ Microbiol 63 (1997) 3451-7.

[40] A.D. Crandall, and T.J. Montville, Nisin resistance in *Listeria monocytogenes* ATCC 700302 is a complex phenotype. Appl Environ Microbiol 64 (1998) 231-7.
[41] X. Ming, and M.A. Daeschel, Correlation of Cellular Phospholipid Content with Nisin Resistance of *Listeria monocytogenes* Scott A. Journal of Food Protection 58 (1995) 416-420.
[42] A.S. Mazzotta, and T.J. Montville, Nisin induces changes in membrane fatty acid composition of *Listeria monocytogenes* nisin-resistant strains at 10 °C and 30 °C. J Appl Microbiol 82 (1997) 32-8.
[43] X. Ming, and M.A. Daeschel, Nisin Resistance of Foodborne Bacteria and the Specific Resistance Responses of *Listeria monocytogenes* Scott A. Journal of Food Protection 56 (1993) 944-948.
[44] J. Reiners, M. Lagedroste, K. Ehlen, S. Leusch, J. Zaschke-Kriesche, and S.H.J. Smits, The N-terminal Region of Nisin Is Important for the BceAB-Type ABC Transporter NsrFP from *Streptococcus agalactiae* COH1. Front Microbiol 8 (2017) 1643.
[45] A. Abts, A. Mavaro, J. Stindt, P.J. Bakkes, S. Metzger, A.J. Driessen, S.H. Smits, and L. Schmitt, Easy and rapid purification of highly active nisin. Int J Pept 2011 (2011) 175145.
[46] A. Abts, M. Montalban-Lopez, O.P. Kuipers, S.H. Smits, and L. Schmitt, NisC binds the FxLx motif of the nisin leader peptide. Biochemistry 52 (2013) 5387-95.
[47] R. West, Siegfried Ruhemann and the discovery of ninhydrin. Journal of Chemical Education 42 (1965) 386.
[48] B.L. Roth, M. Poot, S.T. Yue, and P.J. Millard, Bacterial viability and antibiotic susceptibility testing with SYTOX green nucleic acid stain. Appl Environ Microbiol 63 (1997) 2421-31.
[49] S. Clejan, T.A. Krulwich, K.R. Mondrus, and D. Seto-Young, Membrane lipid composition of obligately and facultatively alkalophilic strains of *Bacillus spp*. J Bacteriol 168 (1986) 334-40.
[50] M.A. Haque, and N.J. Russell, Strains of *Bacillus cereus* vary in the phenotypic adaptation of their membrane lipid composition in response to low water activity, reduced temperature and growth in rice starch. Microbiology 150 (2004) 1397-404.
[51] R.F. Epand, P.B. Savage, and R.M. Epand, Bacterial lipid composition and the antimicrobial efficacy of cationic steroid compounds (Ceragenins). Biochim Biophys Acta 1768 (2007) 2500-9.
[52] P.R. Beining, E. Huff, B. Prescott, and T.S. Theodore, Characterization of the lipids of mesosomal vesicles and plasma membranes from *Staphylococcus aureus*. J Bacteriol 121 (1975) 137-43.
[53] M. Aktas, L. Danne, P. Moller, and F. Narberhaus, Membrane lipids in *Agrobacterium tumefaciens*: biosynthetic pathways and importance for pathogenesis. Front Plant Sci 5 (2014) 109.

Supplementary part

Supplementary table 1: Phospholipid composition of NZ9000Cm and NZ9000Pseudo.

Phospholipid (% total membrane)	NZ9000Cm	NZ9000Pseudo
LPC	2.2	0.9
LPC-O	3.2	1.4
PC	27.6	5.6
PC-O	5.6	1.8
LPE	0.3	0.5
LPE-O	0.8	1.46
PE	2.8	2.3
PE-O	0.4	0.7
PG	3.29	5.4
PG-O	3.7	2.1
CL	48.9	76.7
SM	1.4	1.1

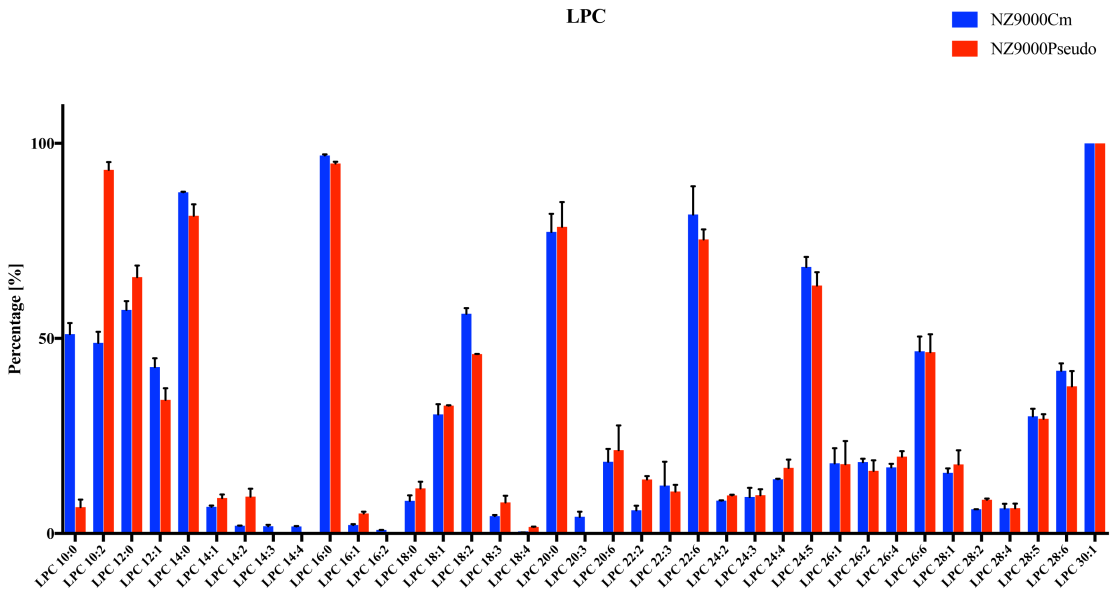

Supplementary figure 1: LPC fatty acid composition of NZ9000Cm and NZ9000Pseudo.

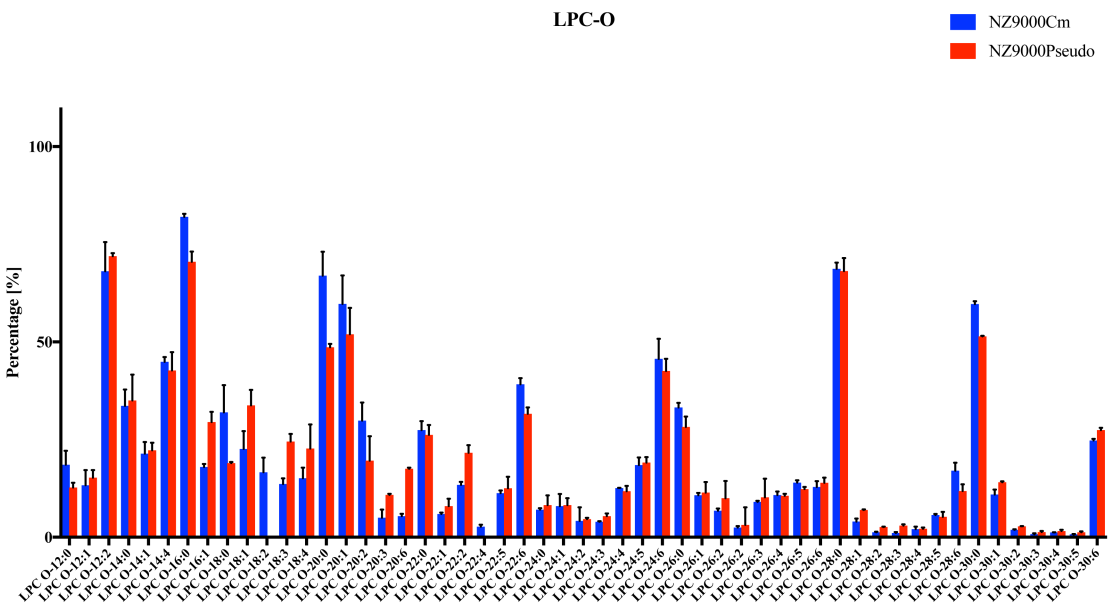

Supplementary figure 2: LPC-O fatty acid composition of NZ9000Cm and NZ9000Pseudo.

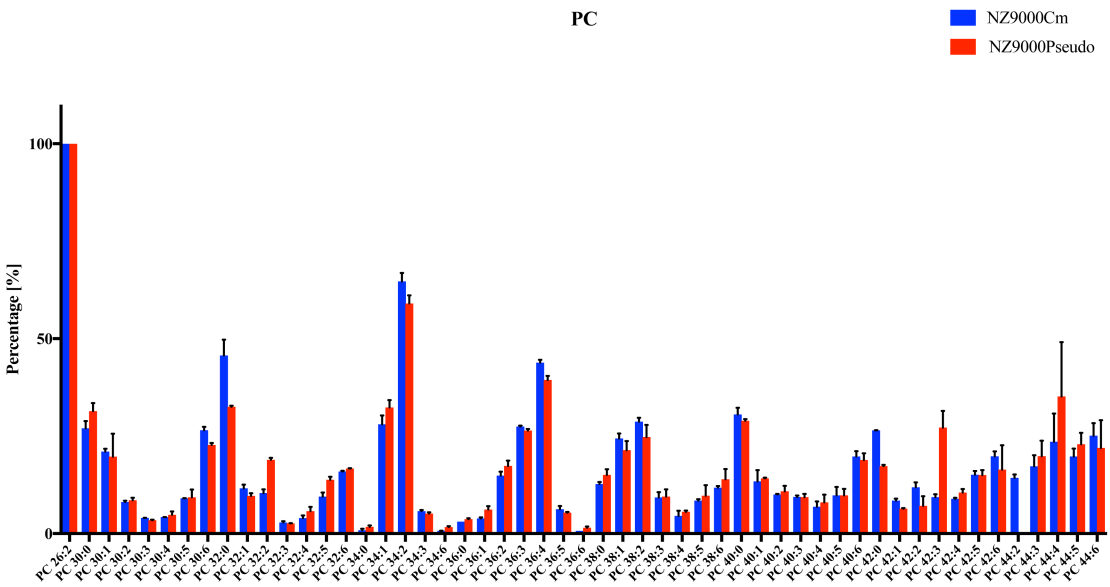

Supplementary figure 3: PC fatty acid composition of NZ9000Cm and NZ9000Pseudo.

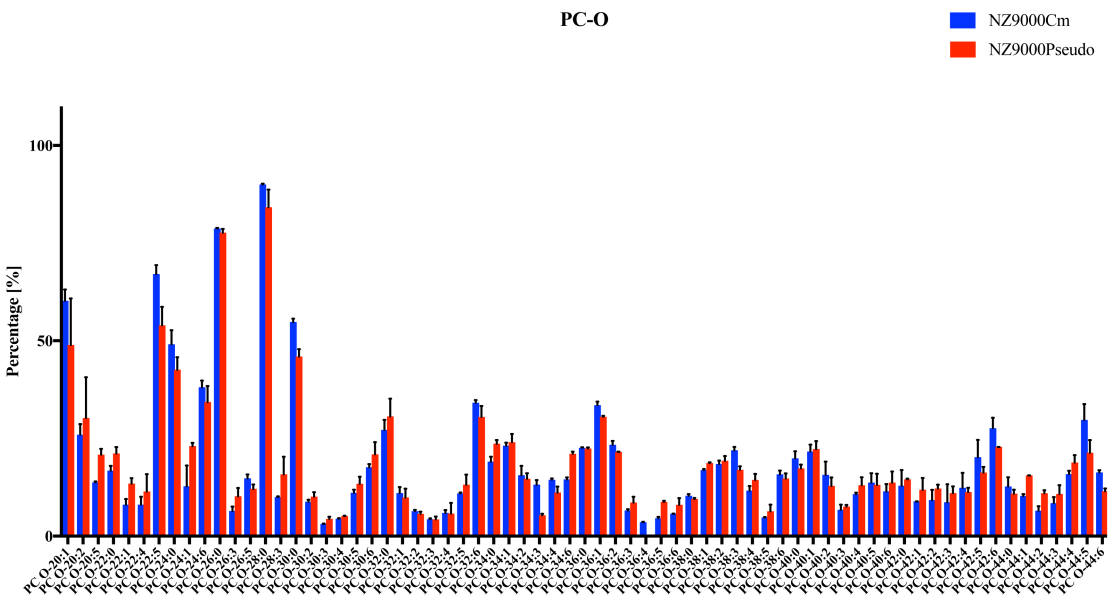

Supplementary figure 4: PC-O fatty acid composition of NZ9000Cm and NZ9000Pseudo.

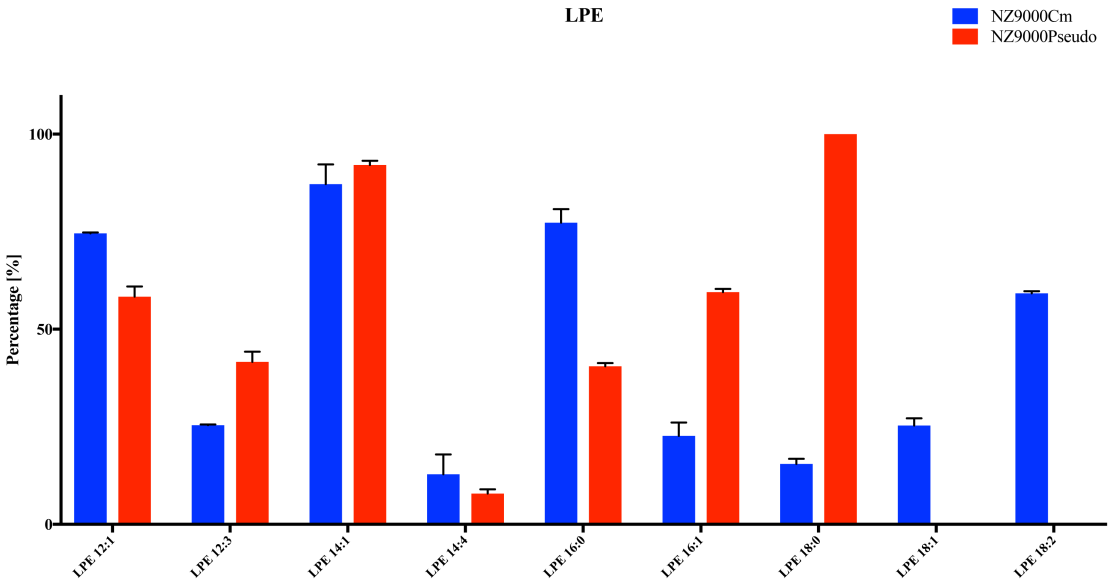

Supplementary figure 5: LPE fatty acid composition of NZ9000Cm and NZ9000Pseudo.

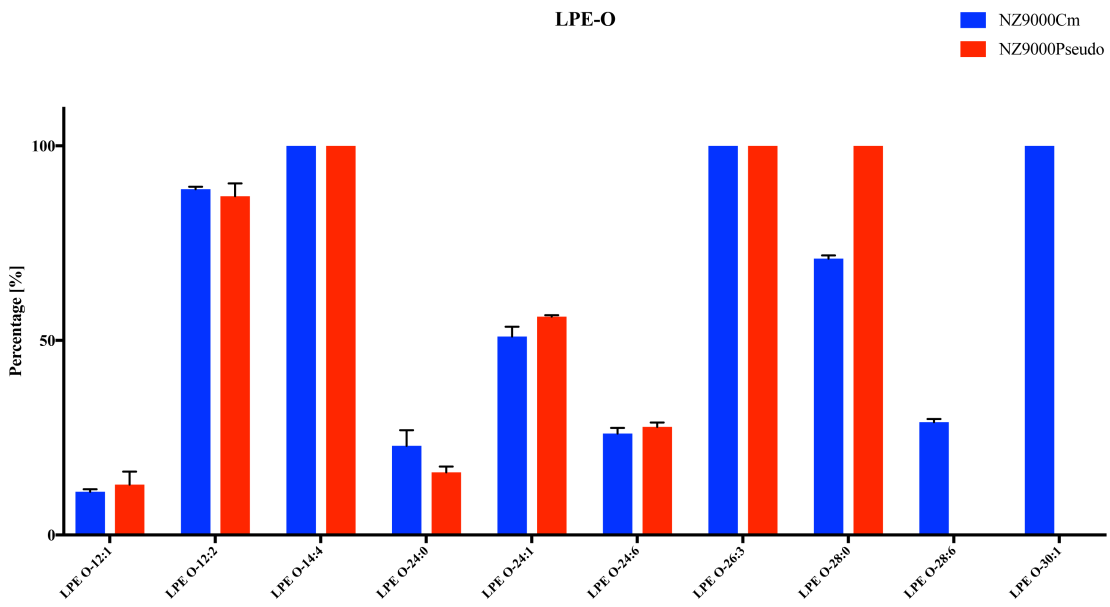

Supplementary figure 6: LPE-O fatty acid composition of NZ9000Cm and NZ9000Pseudo.

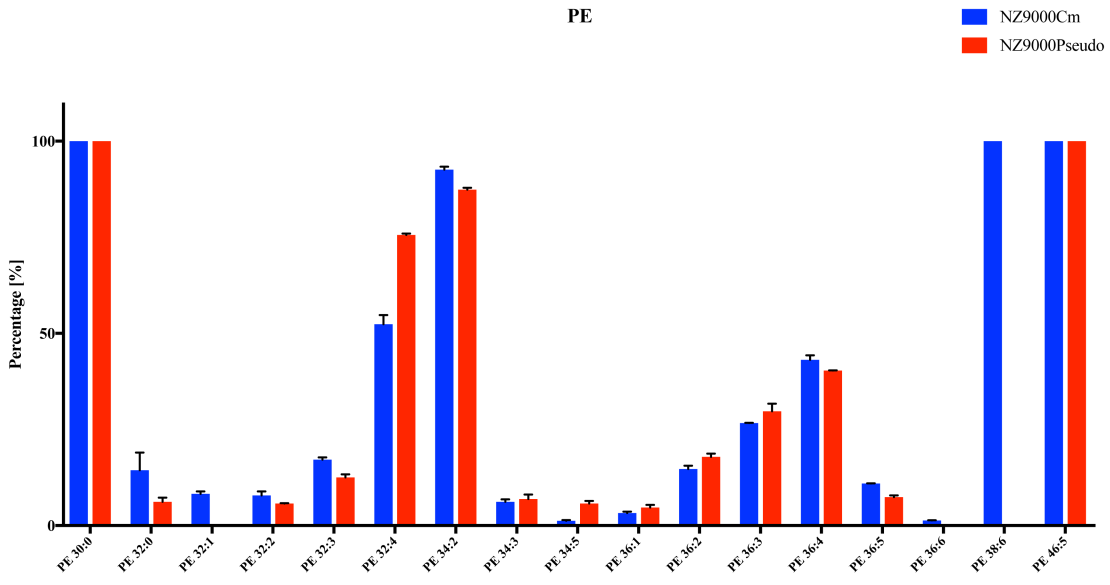

Supplementary figure 7: PE fatty acid composition of NZ9000Cm and NZ9000Pseudo.

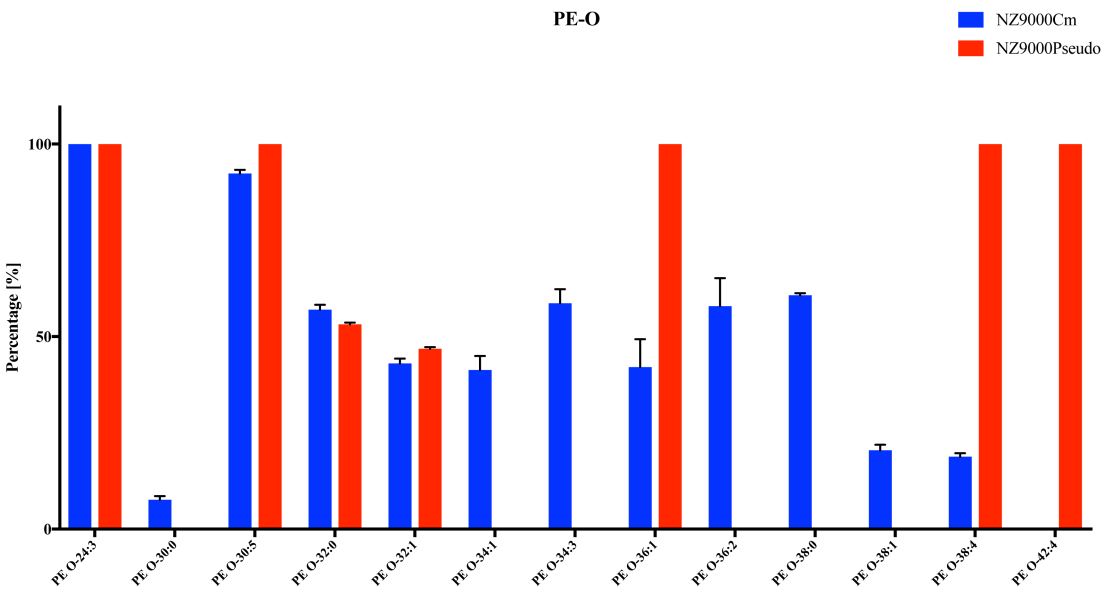

Supplementary figure 8: PE-O fatty acid composition of NZ9000Cm and NZ9000Pseudo.

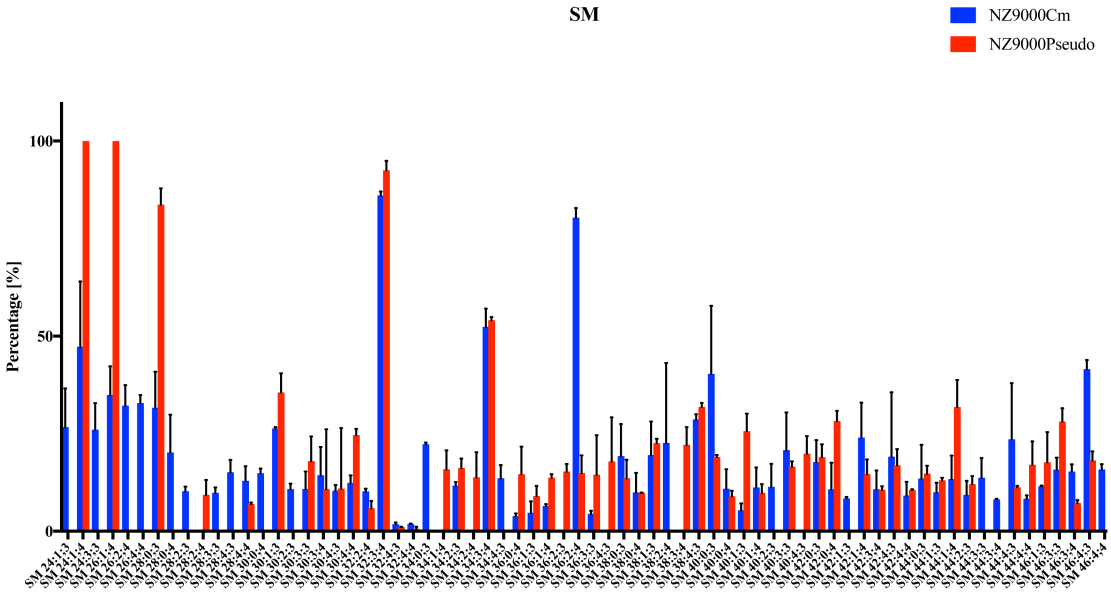

Supplementary figure 9: SM fatty acid composition of NZ9000Cm and NZ9000Pseudo.

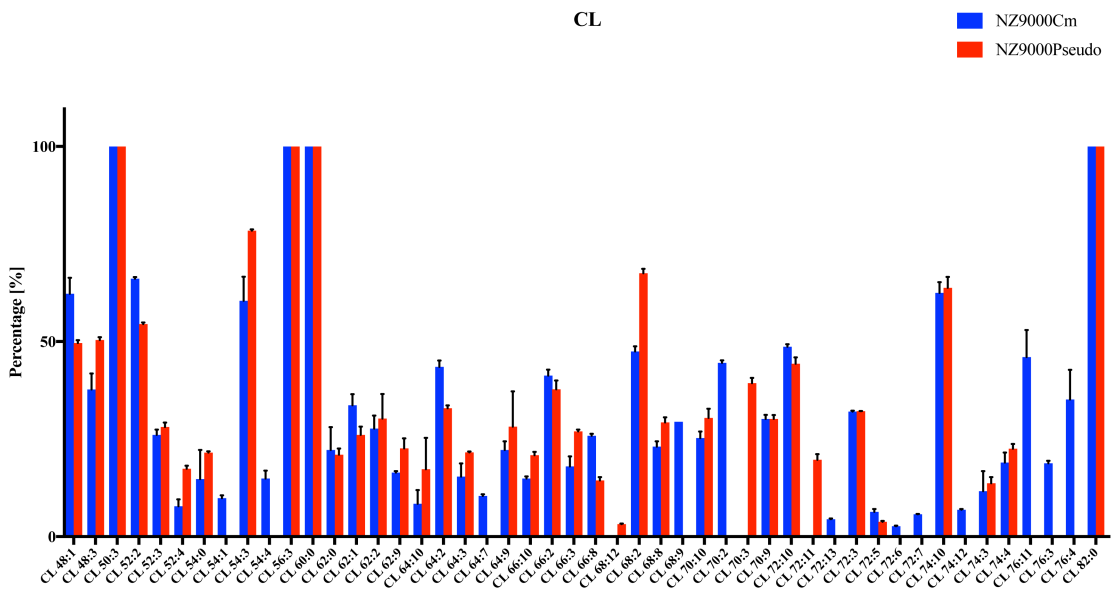

Supplementary figure 10: CL fatty acid composition of NZ9000Cm and NZ9000Pseudo.

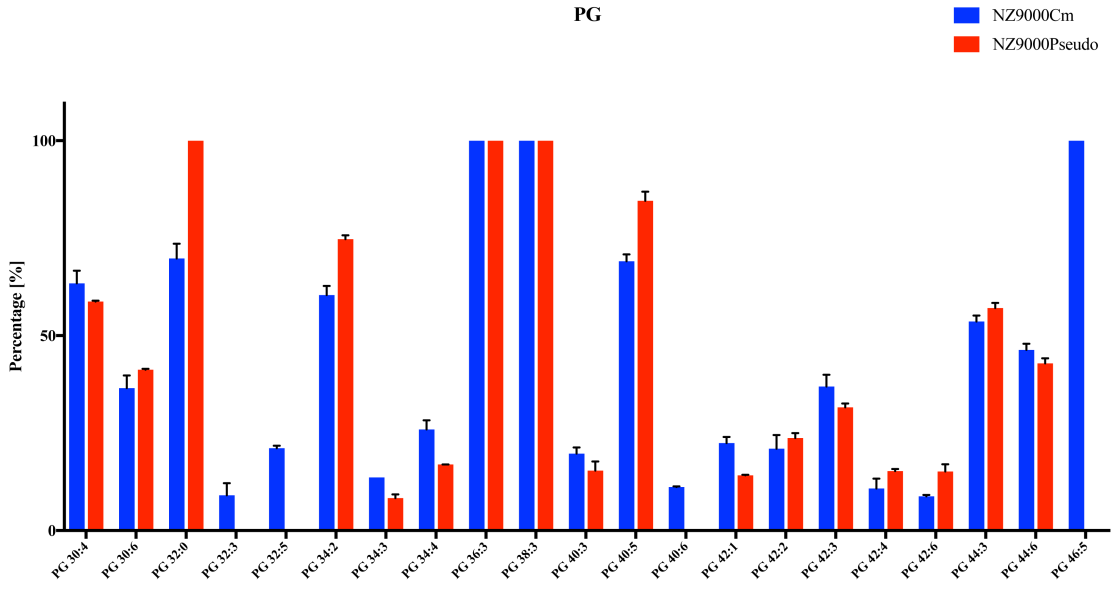

Supplementary figure 11: PG fatty acid composition of NZ9000Cm and NZ9000Pseudo.

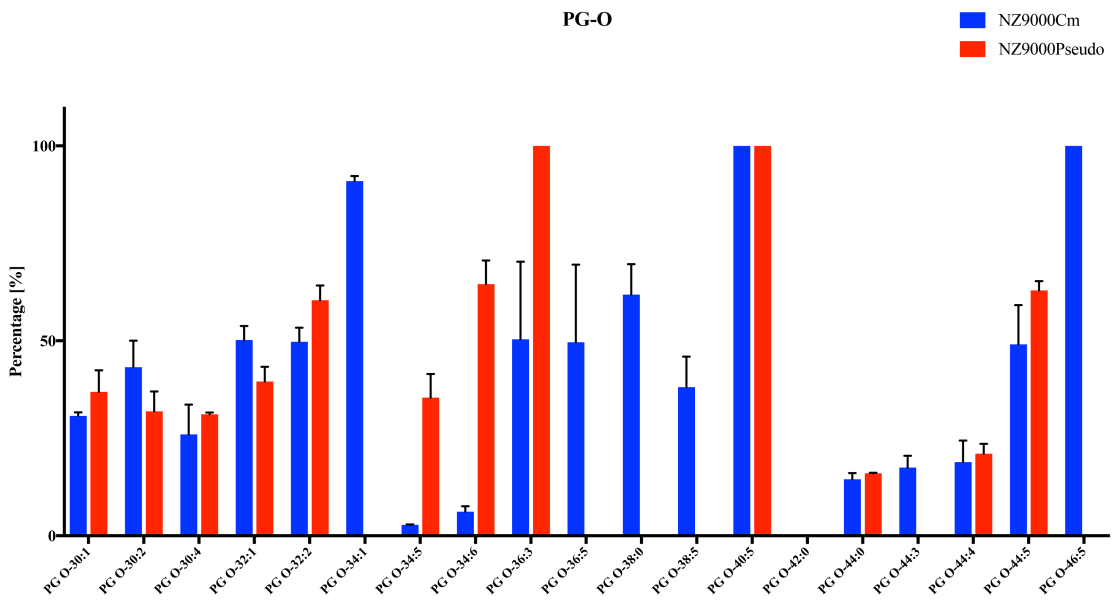

Supplementary figure 12: PG-O fatty acid composition of NZ9000Cm and NZ9000Pseudo.

Supplementary table 2: All mutations found in the genome analysis of NZ9000Pseudo genome and the corresponding proteins. Reference was the Genbank Genome of *Lactococcus lactis subsp. cremoris* NZ9000 strain (GenBank Number CP002094.1).

Name	Gen-Position	Reference	Observed
tRNASer, tRNAMet	25777	T	G
	25784	G	C
	25790	G	A
	25791	T	A
	25805	A	T
	25806	C	T
	25831	A	G
	25840	C	T
	25841	T	C
	25874	A	G
	25815	T	TTC
	25818	A	AGGAATT AAGTTTC CTTAGTC T
tRNAPro	517908	T	G
eno	608204	ACT	A
	608210	A	AGC
LLNZ_05175	970028	T	C
	970124	G	T
	970125	T	A
pstA – phosphate transporter ATP binding protein	1876050	C	T
	1876065	T	C
	1876120	A	T
atpA and atpB F_0F_1-type ATP synthase	1931622	CTGA	C
	1929139	T	A
	1929151	C	A

	1929152	C	T
	1929157	A	C
	1929163	A	G
	1929175	A	T
	1929178	A	C
	1929184	C	A
	1929193	T	A
	1929199	T	G
	1929202	A	G
	1929208	A	C
	1929211	A	T
	1929214	G	A
	1929232	G	A
	1929238	C	T
	1929247	G	A
	1929250	A	T
	1929252	G	A
	1931512	A	T
	1931518	A	G
	1931525	T	A
	1931529	C	T
	1931532	C	T
	1931533	C	T
	1931545	A	G
	1931557	A	G
rpoC	1966101	TAGC	T
	1964917	A	T
	1964931	A	T
	1964932	G	A
	1964941	C	T
	1966165	C	T
	1966168	C	T
	1966185	G	T

	1966240	T	A
	1966264	A	T
	1966285	T	A
LLNZ_t13347	2131340	T	C
	2131363	A	G
	2131347	AT	A
LLNZ_t13349	2131349	AACCTAG	A
pheS	2163381	G	GGA
	2163309	T	C
	2163325	C	A
	2163454	C	A
Val S	2409209	G	T
	2409210	T	A
	2409212	T	A
rpsI	2506521	G	GC
	2506524	AC	A
	2506432	G	A
	2506452	C	G
	2506453	T	A
	2506477	G	A
	2506513	C	A
23S ribosomal RNA	2524827	T	TA
	2524829	C	A
	2524837	T	A
	2524881	C	T
	2524904	T	C
	2524910	C	A
	2524911	G	A
	2524915	T	C
	2524917	C	T

	2524922	G	A
	2524978	A	C
	2524991	A	T
	2524994	T	A
elongation factor G	2515898	G	A
	2515913	G	A

3.5. Chapter V - Viral infectivity factor of HIV

Published in: in Preparation

Own work: 70 %
Secretion tests of Vif variants
Purification tests
Interaction studies *in vitro*
Writing the Manuscript

Purification and interaction studies of the viral infectivity factor of HIV

Rebecca Clemens, Carsten Münk and Sander H. J. Smits

Purification and interaction studies of the viral infectivity factor of HIV

Rebecca Clemens, Carsten Münk and Sander H. J. Smits

Abstract

Human immunodeficiency virus (HIV) is a lentivirus, a retrovirus belonging to the RNA viruses. Viral infectivity factor (Vif) protein is one of six known accessory proteins of HIV-1 and known to be necessary for the HIV replication in the host cells. Vif forms a complex with the human apolipoprotein B mRNA editing enzyme catalytic polypeptide-like 3 (APOBEC3) proteins and inhibits by this the effect of APOBEC3 proteins. These proteins have antiviral properties and negatively affect the virus replication. APOBEC3 proteins get ubiquitinated and degraded because of the formed Vif complex. The HI-virus is able to replicate in the host cell without hindrance based of the formed complex. To develop new treatments of HIV the Vif protein became one of the most interesting target proteins.
In this study, we try to purify Vif in high yield and monodispersity to perform structural studies. Therefore, we cloned a construct allowing to secret the Vif protein from *Escherichia coli* directly into the media and purify it in a soluble manner.

Keywords: Lentivirus, HIV, accessory protein, Vif, APOBEC, purification, secretion

Introduction

The human immunodeficiency virus (HIV) belongs to the RNA virus family and exploit cellular components for its own replication [1]. More specifically, HIV belongs to the lentiviruses, which are a class of the retroviruses [2; 3]. HIV can be divided in two different subtypes the HIV-1, the most prominent subtype, and the HIV-2 [4; 5; 6]. The used treatments against HIV are combinations of targeting key viral enzymes [7]. These treatments are successful in controlling viral load, but because of the long-time use they become ineffective due to mutations of the virus [8]. So one of the six accessory proteins of HIV becomes an interesting target in the HIV drug development. This protein is the *v*iral *i*nfectivity *f*actor (Vif) [9; 10; 11]. Vif is necessary for the survival of the HIV in the human body [12; 13].

There are proteins in the human body which have antiviral properties and negatively impact on viral replication [1; 14; 15]. In the human body are seven of the apolipoprotein B mRNA editing enzyme catalytic polypeptide- like 3 (APOBEC3) proteins encoded, APOBEC3A, APOBEC3B, APOBEC3C, APOBEC3D, APOBEC3F, APOBEC3G and APOBEC3H [15; 16; 17]. The principal activity of APOBEC3 proteins is the cytidine deamination of single-stranded DNA, shown in biochemical and cell culture assays [18; 19]. Four of these proteins are able to reduce the HIV-1 replication. These proteins are A3D, A3F, A3H and A3G [8].

The Vif protein inhibits the effect of reduced replication and by this no intervention of the HIV-1 replication in the host cell takes place. The Vif protein makes use of the cellular Cullin-Ring ubiquitin ligase and by this leading to the ubiquitination and proteasomal degradation of the APOBEC3 proteins. Based on this degradation the virus can replicate itself without any hindrance [20; 21; 22].

The complex, which degrades the APOBEC3 proteins, is only able to be formed in presence of the Vif protein. Vif is a 23 kDa basic protein and it is well characterized. The function and the corresponding binding sites are already known. The formed complex which is important for the degradation of the APOBEC3 contains the Vif protein, the APOBEC3 protein, the transcription co-factor core-binding factor subunit ß (CBF-ß), the adapter proteins ELONGIN B and C, and the CULLIN-5 (Figure 1) [23].

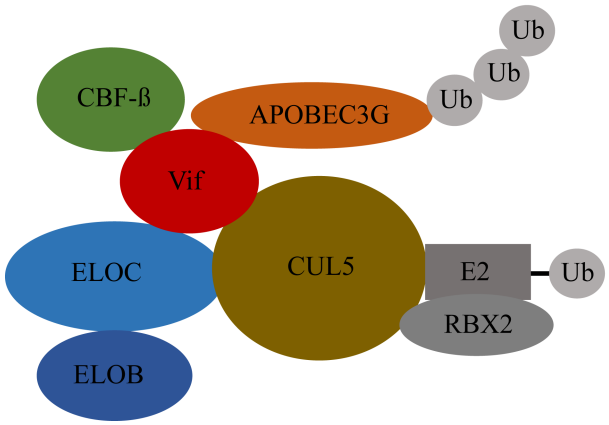

Figure 1: Complex formed by Vif. The complex is formed from the Vif protein to ubiquitinate and degrade the APOBEC3G protein. Vif is recruiting the Cullin 5, CBF-ß and the adapter proteins Elongin C and B. This results in the degradation of the human immunity cytidine deaminase APOBEC3G. The corresponding binding domains are depicted in Figure 2. Modified from [8].

The corresponding binding sites necessary for the complex forming are well characterized. The N-terminal part of the protein is not only necessary for RNA binding also all-important APOBEC3 binding sites are located here [23]. The DRMR domain is known for binding the APOBEC3F, while the YRHHY domain is necessary to bind the APOBEC3G [24; 25]. An additional APOBEC3F domain could be determined at the end of the N-terminal region of Vif. This domain of the protein is necessary for APOBEC3 binding [26].

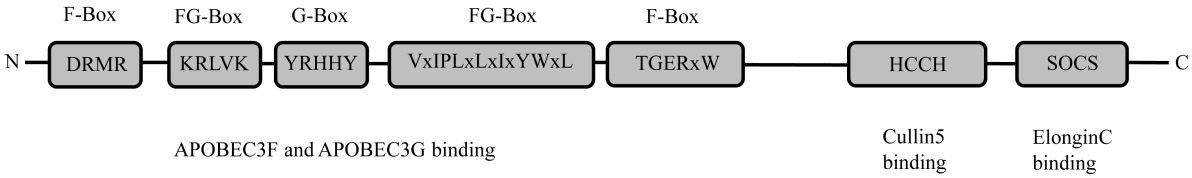

Figure 2: Functional domains of Vif. Shown are the known binding sites of the Vif protein. The N-terminus is known for binding RNA and more important binding the APOBEC3 proteins. Two FG-boxes which are necessary for APOBEC3F and G binding, are determined. Also, two F-boxes are known for APOBEC3F binding and one G-box is known for APOBEC3G binding. After the APOBEC3 binding domains the Cullin 5 binding site is located. The HCCH domain is also a zinc binding site which is important for Cullin 5 binding. The SOCS domain is for ElonginC binding responsible. Modified [4; 27].

Two FG-boxes are identified in this domain. APOBEC3F and APOBEC3G interact with the Vif protein [26; 27]. The HCCH region is known for two different functions. First it is a zinc binding motif but beside this the Cullin 5 interacts with this region [28; 29]. The so called SOCS box was identified as the Elongin C binding side [30].

Although the function and most binding sites are characterized, still not everything is known about the protein. There is no crystal structure of the Vif APOBEC3 protein complex available and it is unknown if there is a conformation change while binding to the different proteins, like APOBEC3F and APOBEC3G. Knowing the structure would be a step forward

in understanding the binding process and developing more specific drugs, which are inhibiting the binding step.

Therefore, we want to establish a purification of Vif with a high yield for co-crystallography with APOBEC3. In this purification, first Vif should be secreted out of *Escherichia coli* to have folding in a native way, without defolding the protein using urea or guanidine. Constructs of different Vif variants from HIV-1 type viruses were cloned. These variants concern a C-terminal secretion signal followed by a TEV-cleavage site and a 6x His-tag. To generate the needed yield, test secretion studies were performed and different purification ways were tested. Also, first interaction studies with A3C protein were performed via pulldown assays.

Material and Methods

Cloning. The plasmid p3S-TEV-Vif (all different variants) was cloned with the In-Fusion Cloning Kit (New England BioLabs) according to the manufacturer`s protocol. Therefore, plasmid p3S was linearized by PCR using the primer pair p3S-rev and p3S-for. The primer pair inf-1-Vif-for and inf-1-Vif-rev was used to amplify the sequence of the viral infectivity factor. Sequence analysis verified the new plasmid.
With a side-directed mutagenesis the construct p3S-TEV-Vif47 was cloned with a 10xHis-tag. Therefore, the primer pair Vif-10H-for and Vif-10H-rev was used. Via Sequence analysis the new plasmid was verified.

Table 1: Oligonucleotides used for cloning.

Oligonucleotide	Sequence
p3S-for	ATTGATGGCCGTCACCACC
p3S-rev	CATTTAATTACCTCTTAACCAGTTAATGAAAAATTAAAATC
inf-1-Vif-for	AGAGGTAATTAAATGGAAAACAGATGGCAGGTGATG
inf-1-Vif-rev	GTGACGGCCATCAATGTGTCCATTCATTGTATGGCTCCC
Vif-10H-for	CATCATCATCATGATTATGATATTCCTACTACTGAGAATTTGTATTTTC AGG
Vif-10H-rev	GTGGTGGTGGTGGTGGTGACG

Secretion of the viral infectivity factor. Chemically competent *E. coli* BL21 (DE3) cells were transformed with the pSJ37 (pK184-HlyBD) and the p3S-TEV-Vif (different variants) plasmids and were grown on a LB agar plate supplemented with 100 µg/mL ampicillin and 30 µg/mL kanamycin at 37 °C. An overnight culture of a single colony was used to inoculate 30 mL 2xYT media supplemented with 100 µg/mL ampicillin, 30 µg/mL kanamycin and 5 mM (final concentration) of $CaCl_2$ to an OD_{600} 0.1. At 37 °C and 180 rpm the cells were grown in flasks with baffles. At an OD_{600} of 0.4-0.6 the cells were induced with 1 mM Isopropyl-ß-D-thiogalactopyranoside (IPTG) and grown for 6 h. After every hour 500 µL aliquots were taken and centrifuged at 14,000 g for 5 min at 4 °C. The cells were adjusted to an OD_{600} of 1 and the supernatant were analysed by SDS-PAGE and Western Blot, the protein was compared with the calculated molecular mass 49 kDa (EXPASY ProtParam). The used antibodies are a polyclonal secretion signal Antibody and HIV-1 Vif Monoclonal Antibody (#319) (Thermo Fisher Scientific).

Purification of the viral infectivity factor. To purify the viral infectivity factor of HIV-1 the protein was secreted like described above. 2 x 30 mL 2xYT media supplemented with 100 µg/mL ampicillin, 30 µg/mL kanamycin and 5 mM (final concentration) of $CaCl_2$ were induced with 1 mM IPTG at an OD_{600} of 0.4-0.6 and were grown for 3h. Afterwards the cells were centrifuged at 8,000 rpm for 40 min at 4 °C. The supernatant was filtered throw a 0.45 µm filter and loaded to two Nickel affinity chromatography columns 2 x 1 ml HiTrap™ IMAC HP (GE Healthcare) with a flow rate of 0.5 mL/min. By washing the column with washing buffer (20 mM Tris-HCl pH 8, 150 mM NaCl and 10% (v/v) glycerol) with a flow rate of 1 mL/min till baseline, non-binding proteins are excluded. To elute the protein a gradient elution was used, 100% elution buffer (100 mM Tris-HCl pH 8, 150 mM NaCl, 10% (v/v) glycerol and 400 mM imidazole) in 50 min. The elution peak containing fractions were analysed via SDS-PAGE and Western blot as control of the purification steps.

Purification with dialyses step. To purify the viral infectivity factor of HIV-1 the protein was secreted like described above. 4 x 50 mL 2xYT media supplemented with 100 µg/mL ampicillin, 30 µg/mL kanamycin and 5 mM (final concentration) of $CaCl_2$ were induced with 1 mM IPTG at an OD_{600} of 0.4-0.6 and were grown for 3 h. Afterwards the cells were centrifuged at 8,000 rpm for 40 min at 4 °C. The supernatant was filtered with a 0.45 µm filter and concentrated to a volume of 40 mL with an Amicon ultracentrifugation unit (30 kDa MWCO). The concentrated supernatant was dialysed in a 12-15 kDa dialysis membrane tube (thermos scientific) overnight in 5 L of dialysis buffer (100 mM Tris-HCl pH 8, 150 mM NaCl and 10% (v/v) glycerol). After dialysis, the supernatant was centrifuged 25 min 45,000 rpm at 4 °C to get rid of aggregate. The supernatant was loaded to a nickel affinity chromatography column 5 mL HiTrap™ IMAC HP (GE Healthcare) with a flow rate of 0.5 mL/min. Also, copper and cobalt affinity chromatography were tested. After a washing step with the washing buffer till baseline a gradient elution 100% elution buffer (100 mM Tris-HCl pH 8, 150 mM NaCl, 10% (v/v) glycerol and 400 mM imidazole) in 50 min was chosen for elution. For tests with TEV cleavage 1 mg TEV was added to the supernatant in the dialysis step. The purification steps were analysed via SDS-PAGE and Western-Blot. Protein bands were compared with the calculated molecular mass of full length 49 kDa and cleaved 23.9 kDa (EXPASY ProtParam).

Purification with Nickel NTA resin. To purify viral infectivity factor of HIV-1 the protein was secreted like described above. 4 x 150 mL 2xYT media supplemented with 100 µg/mL ampicillin, 30 µg/mL kanamycin and 5 mM (final concentration) of $CaCl_2$ were induced with 1 mM IPTG at an OD_{600} of 0.4-0.6 and were grown for 3 h. Afterwards the cells were centrifuged at 8,000rpm for 40 min at 4 °C. The supernatant was filtered with a 0.45 µm filter and concentrated to a volume of 25 mL with an Amicon ultracentrifugation unit (30 kDa MWCO). 2 mL Nickel NTA resin (Qiagen) was added and incubated over night at 4 °C shaking. Next day the resin was loaded in a drip column. To wash the resin 2 x 10 mL washing puffer (20 mM Tris- HCl pH 8, 250 mM NaCl, 5mM $CaCl_2$ and 10 % (v/v) glycerol) was added to the column. After these, two additional washing steps (2 x 10 mL) with a buffer containing 5 mM imidazole were performed. To elute the protein 5 mL of elution buffer (20 mM Tris- HCl pH 8, 250 mM NaCl, 5mM $CaCl_2$, 10 % (v/v) glycerol and 400 mM imidazole) was added. All washing and elution steps were analysed via SDS-PAGE and Western blot to determine the purification steps.

Size exclusion chromatography. For size exclusion chromatography, a Superdex 200 10/300 GL (GE Healthcare) column was used. The column was equilibrated with a 100 mM Tris-HCl pH 8, 150 mM NaCl and 10 % (v/v) glycerol. 500 µL of the protein was injected to the equilibrated column with a flow rate of 0.3 mL/min and fractionated (300 µL).

Purification with cross flow concentration. To increase the volume of the secretion a cross flow system was used. In 5 x 1 L Vif protein was secreted as before and concentrated with a cross flow system. A 10 kDa membrane was used. Washing steps with water and NaOH were performed to clean the membrane. The membrane was equilibrated with 3 L buffer (20 mM Tris-HCl pH 8, 250 mM NaCl 10% (v/v) glycerol and 5 mM $CaCl_2$). 5 L supernatant was concentrated with a flow rate of 2 mL/min and washed with 1 L buffer to a volume of 250 mL. With an Amicon ultracentrifugation unit (30 kDa MWCO) the supernatant was concentrated to a total volume of 40 mL. 10 mL resin was added and incubated overnight. Next day the resin was added in a glass column and washed till baseline with 20 mM Tris-HCl pH 8, 250 mM NaCl, 10% (v/v) glycerol and 5 mM $CaCl_2$. With a gradient of 100% in 100 min the column was eluted with a 20 mM Tris-HCl pH 8, 250 mM NaCl, 10% (v/v) glycerol, 5 mM $CaCl_2$ and 400 mM imidazole.

Inclusion body purification. To purify the Vif protein out of inclusion bodies *E. coli* BL21 (DE3) cells containing the p3S-TEV-Vif47 were used. Cells were grown in 2xYT media containing 100 µg/mL ampicillin and were inoculated to an OD_{600} of 0.1. At 37 °C 180 rpm the cells were grown till an OD_{600} of 0.5 and were induced with 1 mM IPTG. After 3 h the temperature was decreased to 25 °C over night. The next day, the cells were harvested for 30 min at 8,000 rpm. The cells were resuspended in 50 mM Tris-HCl pH 8, 50 mM NaCl and 50 mM EDTA. After a 15 min centrifugation step at 5,000 rpm the cells were flash frozen in liquid nitrogen and stored at -80 °C.

For inclusion body purification cells were thawed on ice with 50 mM Tris-HCl pH 8, 50 mM NaCl and 50 mM EDTA buffer containing DNAse I. After resuspending the cells were lysed via cell disruption (Microfluidics M-110P, 1500 bar) for 5-6 cycles. Then the disrupted cells were centrifuged 30 min for 15,000 rpm. The pellet was resuspended in 50 mM Tris-HCl pH 8 50 mM NaCl, 50 mM EDTA and 1% (v/v) Triton X 100 and centrifuged again for 30 min. The pellet was then resuspended in 50 mM Tris-HCl pH 8 and 1 M NaCl buffer and centrifuged again. The pellet was again resuspended this time in a defolding buffer containing 50 mM Tris-HCl pH 8, 50 mM NaCl and 6 M Guanidine. The solution was incubated for 4 h at 10 °C.

Afterwards the solution was centrifuged again, and the supernatant was used for the refolding buffer test. Here 100 µL of the inclusion body solution was added in dialysis knots and the dialysis takes place in 100 mL of the corresponding buffers overnight.

Table 2: Components for the inclusion body buffer screen.

pH	Buffer	Ionic strength	Amphiphilic	Reducing (10mM)	Additive
4	50 mM NaAc	100 mM NaCl	Glycerol 10% (v/v)	ß-mercaptoethanol	800 mM Arginine
5	50 mM MES	200 mM NaCl			Glucose 500mM
6,5	50 mM MOPS				
7	50 mM TRIS	5 mM $CaCl_2$	PEG 400 0.05% (w/v)		
8	50 mM TRIS				
9	50 mM CHES				

Table 3: Buffer used for the inclusion body refolding.

	pH 4	pH 5	pH 6.5	pH 7	pH 8	pH 9
1	100 mM NaCl Glycerol Arginine $CaCl_2$	100 mM NaCl Glycerol Arginine $CaCl_2$	100 mM NaCl Glycerol Arginine $CaCl_2$	100 mM NaCl Glycerol Arginine $CaCl_2$	100 mM NaCl Glycerol Arginine $CaCl_2$	100 mM NaCl Glycerol Arginine $CaCl_2$
2	100 mM NaCl PEG 400 ß-mercaptoethanol $CaCl_2$	100 mM NaCl PEG 400 ß-mercaptoethanol $CaCl_2$	100 mM NaCl PEG 400 ß-mercaptoethanol $CaCl_2$	100 mM NaCl PEG 400 ß-mercaptoethanol $CaCl_2$	100 mM NaCl PEG 400 ß-mercaptoethanol $CaCl_2$	100 mM NaCl PEG 400 ß-mercaptoethanol $CaCl_2$
3	150 mM NaCl	150 mM NaCl	150 mM NaCl	150 mM NaCl	150 mM NaCl	150 mM NaCl
4	100 mM NaCl PEG 400 Arginine $CaCl_2$	100 mM NaCl PEG 400 Arginine $CaCl_2$	100 mM NaCl PEG 400 Arginine $CaCl_2$	100 mM NaCl PEG 400 Arginine $CaCl_2$	100 mM NaCl PEG 400 Arginine $CaCl_2$	100 mM NaCl PEG 400 Arginine $CaCl_2$
5	200 mM NaCl PEG 400 Glucose $CaCl_2$	200 mM NaCl PEG 400 Glucose $CaCl_2$	200 mM NaCl PEG 400 Glucose $CaCl_2$	200 mM NaCl PEG 400 Glucose $CaCl_2$	200 mM NaCl PEG 400 Glucose $CaCl_2$	200 mM NaCl PEG 400 Glucose $CaCl_2$
6	200 mM NaCl Glycerol ß-mercaptoethanol $CaCl_2$	200 mM NaCl Glycerol ß-mercaptoethanol $CaCl_2$	200 mM NaCl Glycerol ß-mercaptoethanol $CaCl_2$	200 mM NaCl Glycerol ß-mercaptoethanol $CaCl_2$	200 mM NaCl Glycerol ß-mercaptoethanol $CaCl_2$	200 mM NaCl Glycerol ß-mercaptoethanol $CaCl_2$
7	PEG 400 ß-mercaptoethanol Arginine	PEG 400 ß-mercaptoethanol Arginine	PEG 400 ß-mercaptoethanol Arginine	PEG 400 ß-mercaptoethanol Arginine	PEG 400 ß-mercaptoethanol Arginine	PEG 400 ß-mercaptoethanol Arginine

At the next morning, the solution was centrifuged to separate the refolded protein from the aggregate. Afterwards the pellet and the supernatant SDS-PAGE loading dye was added and a Western blot was performed to analyse if Vif protein was refolded and in the supernatant.

Purification of interaction protein APOBEC3C. The GST-tagged APOBEC3C protein was purified as described before [31; 32]. Protein concentration was determined via NanoDrop with the (theoretical) extinction coefficient and molecular mass.

Pulldown of viral infectivity factor and APOBEC3C. For interaction studies of Vif and the APOBEC3C protein Pierce^{TM} gluthathione magnetic agarose beads (ThermosFisher SCIENTIFIC) were used. The concentration of the purified proteins was determined via NANO Drop with the theoretical molecular mass and extinction coefficient. At first the beads were incubated with 60 µg of the GST tagged APOBEC3C and the beads were washed three times with 100 µL washing buffer (50 mM Tris-HCl pH 8, 10 mM $CaCl_2$, 5 mM ß-mercaptoethanol, 500 mM NaCl and 10% (v/v) glycerol) to get rid of not bind protein. After the washing steps 28 µg of Vif protein was added and incubated for 15 min at 25 °C with the beads containing the APOBEC3C protein and softly mixed every 3 min. The beads were again washed 7 times with 100 µL washing buffer to be sure that all protein which was not bind to the APOBEC3C was washed out. In the end 30 µL elution buffer (50 mM Tris-HCl pH 8, 10 mM $CaCl_2$, 5 mM ß-mercaptoethanol, 500 mM NaCl, 40 mM reduced L-glutathione and 10% (v/v) glycerol) was added to elute the APOBEC3C Vif complex. All washing and elution steps were saved for SDS-PAGE and Western blot analysis.

Results

Test secretion of the different Vif variants. To determine if the Vif proteins were secreted in *E. coli* BL21 (DE3) a test secretion was performed. In small scale secretion (30 mL) 2xYT media containing 100 µg/mL ampicillin, 30 µg/mL kanamycin and 5 mM (final concentration) of $CaCl_2$ the test secretion was performed at 37 °C at 180 rpm. The cells were inoculated to an OD_{600} of 0.1 with a preculture of a single colony. At an OD_{600} of 0.4-0.6 the cells were induced with 1 mM IPTG. After every hour 500 µL of cell culture were harvested and centrifuged for 5 min at 14,000 g. 200 µL of the supernatant was mixed with 50 µL SDS-PAGE loading dye. The samples were analyzed via Western blot analysis with a specific antibody for secretion signal (Figure 3). The results of the different variants were compared with the calculated molecular mass 49 kDa (EXPASY ProtParam). Here all different Vif variants were secreted over 6 h. The different variants were secreted in various amounts. The best secreted variants were the Vif 47, 283, 460, 523 and 564, while the variants 221 and 224 showed lower secretion level.

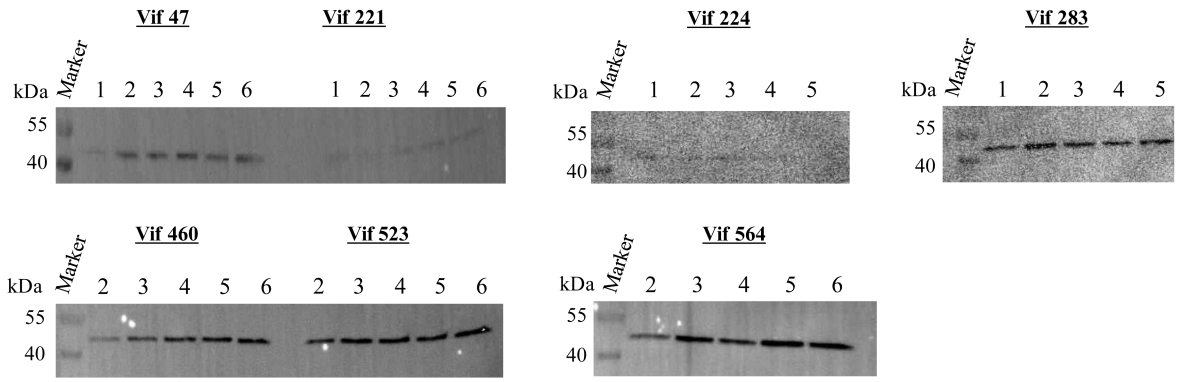

Figure 3: Secretion tests of the different Vif variants. The different samples taken every hour after induction are shown for different variants of Vif proteins. After 1 to 6 hours 200 µL of the media supernatant was loaded on a 10 % SDS-PAGE and analysed via Western blot with the first antibody of the secretion signal. The used marker was the PageRuler^{TM} prestained protein ladder.

Three other variants 222, 330 and 454 did not show any secretion level via Western Blot analysis and were not shown here. The best time of secretion was determined as three hours after induction point.

To determine if the antibody of the secretion signal and the new antibody which is a monoclonal antibody of Vif (Thermo Fisher Scientific) are detecting the same variants and having the same sensitivity, the samples of three hour of all variants were analysed again with both antibodies (Figure 4).

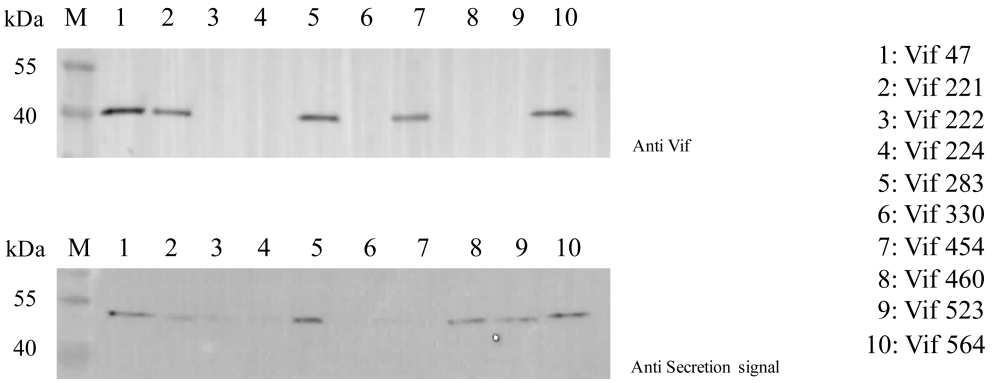

Figure 4: Antibody check against the different variants of Vif proteins. The secretion test sample of every variant after 3 h was tested again with the Anti secretion signal and with the anti-Vif antibody it was obvious that the Vif antibody is giving clearer signals but not for all variants. M is the PageRuler^{TM} prestained protein ladder. See Table 4.

It was determined that the Vif antibody detected just five of the ten different variants. The results of the Western blot using the Vif antibody are showing distinct signals compared to the secretion signal antibody. The secretion signal antibody detected six of the ten variants. Even when the signals are not distinct as the Vif antibody bands, this antibody detects more variants. The different sensitivity of detected Vif variants by the antibodies are listed in Table 4.

Table 4: Overview of the Antibodies and the variants. X is marking for which variant the antibody is working.

Secretion			
Vif	Name	Antibody detection	
		Anti-Vif	Anti-Secretion signal
47	NL4-3 Vif WT	X	X
221	Vif-D-158 (D-2)	X	X
222	Vif-C-564 (C-1)	-	-
224	Vif-C-748 (C-2)	-	X
283	Vif-D-114 (D-1)	X	X
330	Vif-C-MJ4 (C-3)	-	-
454	Vif-F-029 (F-1)	X	-
460	Vif-F-019 (F-2)	-	X
523	Vif-F-020 (F-3)	-	X
564	Vif-B-R01 (B-2)	X	X

Interesting is that some variants are detectable of both antibodies and some just of the secretion signal antibody. The three variants mentioned before (222, 330 and 454) which show no signal in the first secretion test, are showing new results in the second analysis. The samples (222, 330) were also not detectable with the Vif antibody and seem to be not

secreted at all. The variant 454 was not detectable with the secretion signal antibody but with the Vif antibody it became clear that the secretion is working and just the detection in the secretion tests were limiting.

For first purification trails the Vif 47 variant was chosen. Because both antibodies are working with the variant and the high amount of secretion level.

Purification tests of the Vif 47 variant. The first step of the purification tests was a nickel affinity chromatography. The cells were grown in 2 x 30 mL 2xYT media containing 100 µg/mL ampicillin, 30 µg/mL kanamycin and 5 mM (final concentration) $CaCl_2$. At an OD_{600} of 0.4-0.6 the cells were induced with 1 mM IPTG. 3 hours after induction the cells were harvested for 1 h at 8,000 rpm and the supernatant was additionally filtered throw a 0.45 µm filter. The supernatant was loaded on a 2 x 1 mL IMAC HP column (GE Healthcare) with a flow rate of 0.5 mL/min. After washing the column, a gradient elution was chosen to elute the protein (100% are 400 mM imidazole). The first try of purification was not successful. There was nearly no elution peak and via SDS-PAGE analysis no Vif protein bands were detectable. Only the Western blot analysis determined that a lot of the protein was not binding to the column. It was detected in the flow through (Figure 5). The used construct contains a 6 x His-tag at the C-terminus of the Vif protein and after the His-tag a TEV cleavage site and the secretion signal is located.

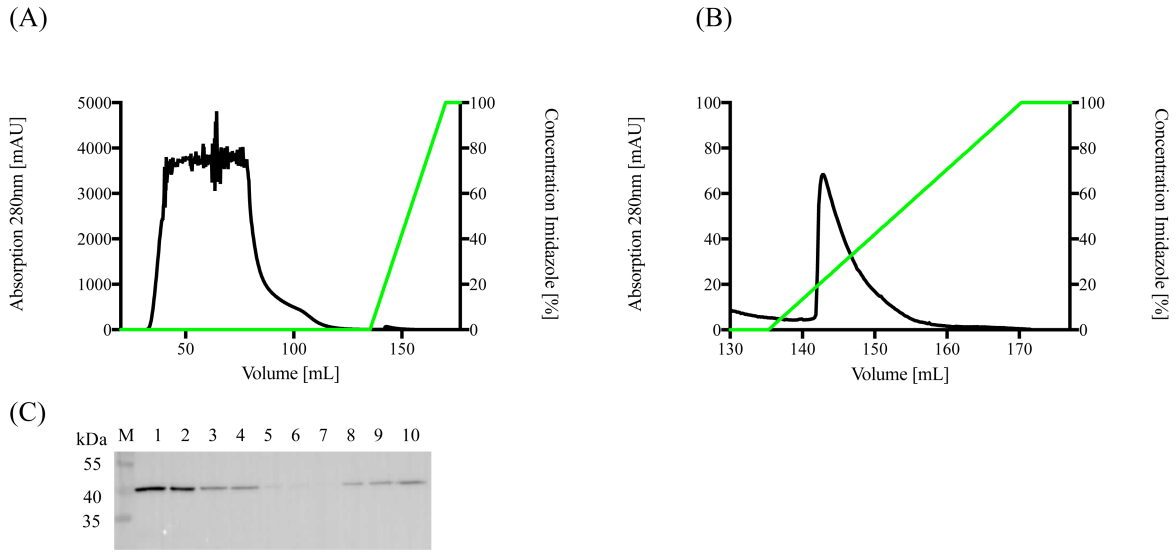

Figure 5 First Nickel affinity chromatography of Vif. A) The IMAC chromatogram of the secreted Vif protein. A small elution peak is shown at the beginning of the gradient elution (green line). In B) a zoom in in the elution peak is shown. C) Here a Western blot analysis was performed to determine in which step the protein get lost. 1 is the supernatant and 2 the load of the IMAC. 3 and 4 are fractions of the main loading peak. 5-7 are the shoulder of the loading peak and 8-10 the elution fractions were loaded. It can be seen that the protein is not binding to the column and a lot of protein was determined in the loading peak. M is the PageRuler^{TM} prestained protein ladder.

Due to the fact that the His-tag is located in the middle of the construct, it could be possible that the His-tag is not available for binding to the column.

To increase the amount of bound protein the volume of the secretion was increased to 200 mL and a bigger column (5 mL HiTrap™ IMAC HP column) was used. Also the elution was changed to a two-step elution. The first step contains 200 mM imidazole and the second step 400 mM imidazole. The changed conditions of this purification compared to the first purification did not show an increased elution peak. The changes had a contradictory effect and no elution peak was detected anymore. One reason for this effect could be that the supernatant with the media components were blocking the binding positions and the protein could not bind anymore. The column becomes brown while loading the supernatant. So, the next step was to concentrate the supernatant of the secretion up to 40 mL (start volume 200 mL) with an Amicon ultracentrifugation unit (30 kDa MWCO) and perform a dialysis to get rid of some media components and to perform a buffer exchange. Also 1 mg TEV protease was added to see if the secretion signal was cleaved and so the amount of Vif protein binding to the column could be increased (Figure 6). The used TEV protease (Sigma Aldrich) is 23 kDa big and contains also a His-tag. So, the used TEV will also bind to the column and has the same size as the cleaved Vif protein (23 kDa). To detect the difference between TEV and Vif a Western blot analysis with penta-His antibody and Vif antibody was performed (Figure 6).

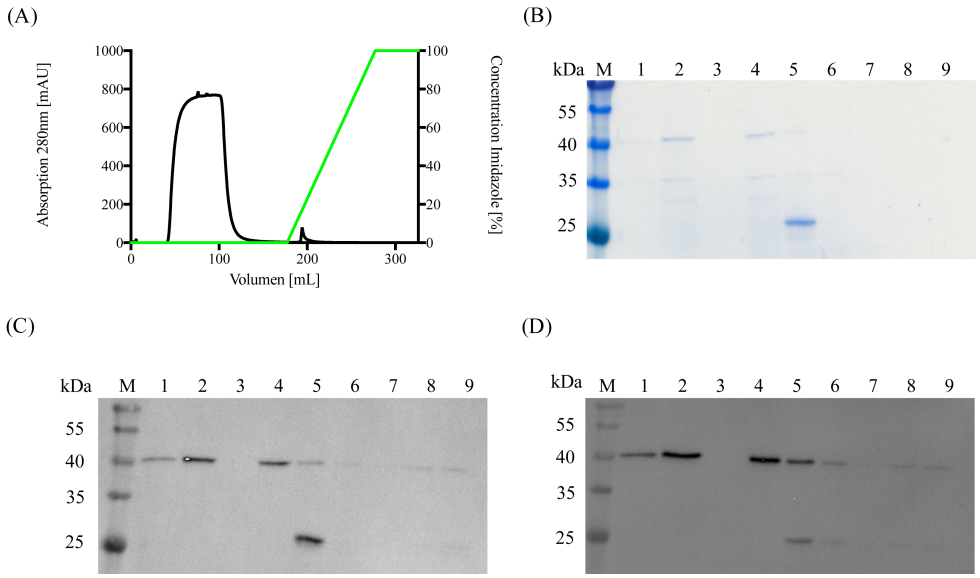

Figure 6: Purification after TEV cleavage. A) Nickel affinity chromatogram of Vif is depicted. A small elution peak is shown in the beginning of the gradient elution (green line). B) SDS-Page analysis of the different purification steps. 1 shows the supernatant and 2 the concentrated supernatant. 3 is the flow through of the concentration step. 4 shows the supernatant before dialysis and TEV cleavage. 5 is the supernatant after overnight dialysis and TEV cleavage. 6 is the flow through of the IMAC and 7-9 are the elution peaks. To determine the steps in a more sensitive way and to analyse whether there is a lot of cleaved protein two Western blots were performed. One with a penta-His-tag antibody C) and one with the Vif antibody D). It became obvious that the cleavage of the TEV did not work correct and that there is more none cleaved protein in the fractions. M is the PageRuler™ prestained protein ladder.

The IMAC looks promising and the elution peak has increased compared to the first purification. Also, the SDS-PAGE shows less impurities but still in the IMAC elution peak there were still no detectable Vif bands visible.

The Western blot analysis determined that there was nearly no cleaved protein and the amount of Vif protein binding to the column was not increased. The affinity of the His-tag to the column was still not high and also the TEV cleavage shows that the region the His-tag is located in could be a problem for purification due to steric hindrance

To determine if different metal ions are solving the problem of binding the column was loaded once with 100 mM copper chloride. Copper is known for a higher binding affinity.

The elution peak of the IMAC performed with copper ions shows a high elution peak. The peak was concentrated and a further size exclusion was performed. Via SDS-PAGE analysis it could be shown that the purification with copper is also not working properly. The huge elution peak consisted mostly of impurities. And the size exclusion peaks were full of impurities too (Figure 7).

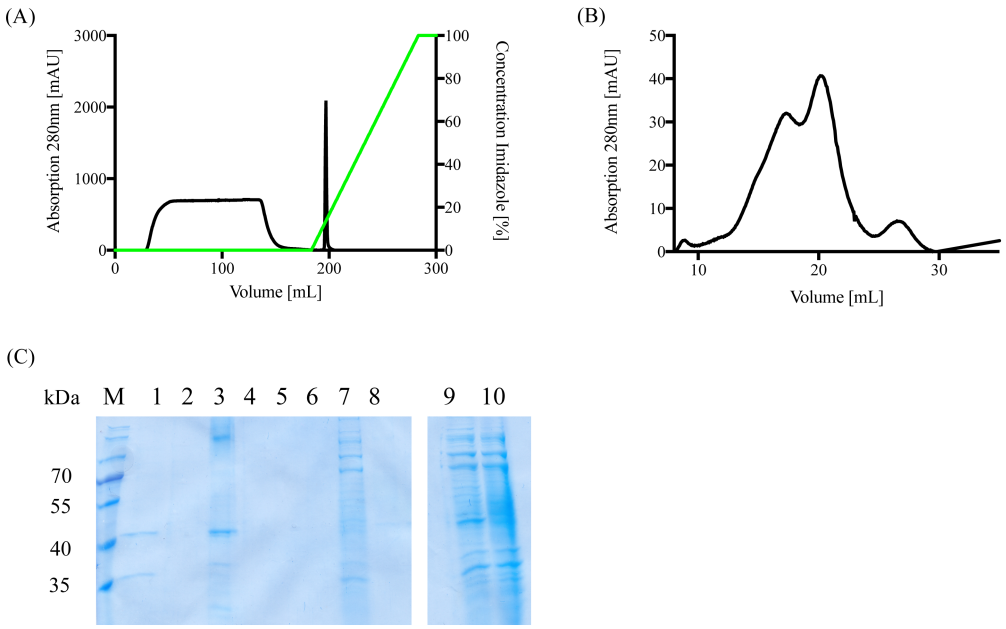

Figure 7: Copper affinity chromatography of Vif. A) In A the IMAC chromatogram is depicted and the elution peak in the gradient elution (green line) is shown. B) Because of the huge elution peak, the elution peak was concentrated and a size exclusion chromatogram with a Superdex 200 10/300 GL (GE Healthcare) was performed. The chromatogram was not homogeneous and there are two different dominant peaks. For analysis, the peaks were concentrated and analysed via SDS-PAGE. C) In C the purification steps are analysed via SDS-PAGE, 1 shows the concentrated supernatant, 2 the flow through of the concentration step. 3 is the supernatant after dialysis. 4 and 5 are the flow through fractions of the IMAC and 6 - 8 are the elution peak fraction. 9 is the concentrated first peak of the size exclusion and 10 the second. It became clear that the protein is still not pure. M is the PageRuler^{TM} prestained protein ladder.

The copper ion increases the elution peak but the Vif protein was not purified in high yield and purity. So the copper ion does not show a better performance in the purification of the

Vif protein. The ion was changed to a more His-tag specific metal ion, cobalt. The affinity of cobalt ions is not as high as the copper ion, but the specifity to a His-tag is better. The IMAC was performed as before. The only change was the used metal ion. The observed elution peak was comparable with the nickel affinity chromatogram (Figure 8). Via SDS-PAGE it could be detected that less impurities in the concentrated elution peak (band 9) are available than in comparison to the purification using copper.

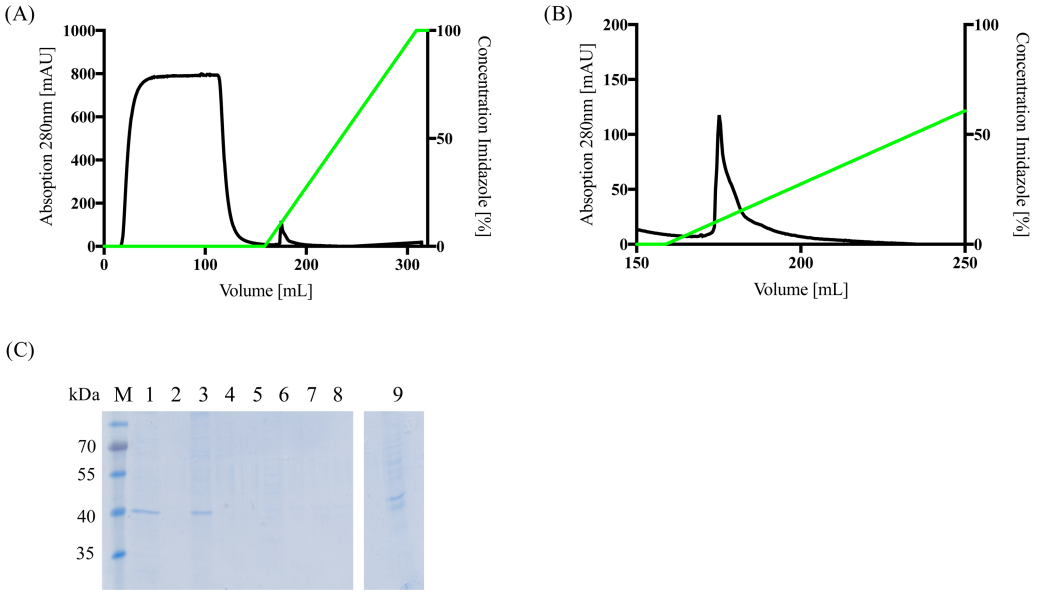

Figure 8: Cobalt affinity chromatography of Vif. A) In A the IMAC chromatogram is depicted and the elution peak in the gradient elution (green line) is shown. B) Zoom in of the elution peak. C) In C the purification steps are analysed via SDS-PAGE. 1 shows the concentrated supernatant, 2 the flow through of the concentration step. 3 is the supernatant after dialysis. 4 and 5 are the flow through fractions of the IMAC and 6 - 8 are the elution peak fraction. To see how high the purity of the elution is, the elution fractions were concentrated and loaded on the gel, lane 9. It became clear that the protein is still not pure. M is the PageRuler^{TM} prestained protein ladder.

The purification with cobalt improved the binding of Vif to the column but the protein was still not pure and the yield was way too low for crystallography. The next try to purify the Vif protein was with 2 mL Nickel NTA agarose resin (Qiagen). The intention was to incubate the supernatant with resin over night at 4 °C and shaking, to increase the binding of Vif. The resin was added to 25 mL concentrated supernatant (start volume 200 mL) and incubated over night at 4 °C. Then the resin and the supernatant were loaded to a drip column. The washing steps were performed 2 times with 10 mL wash buffer and 2 times 10 mL wash buffer containing 5 mM imidazole. The elution step was performed with elution buffer. All steps were analysed via SDS-PAGE and Western blot (Figure 9). The resin seems to work much more efficient in the purification of Vif. In the flow through of the resin was still unbound protein, but with this purification much more Vif protein could be purified compared to the previous ones.

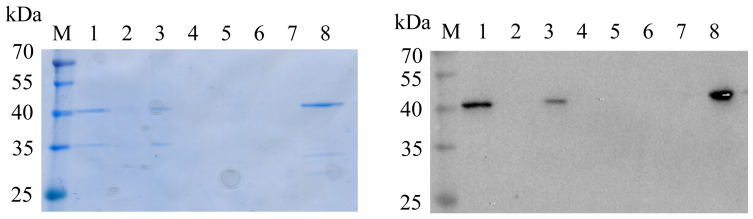

Figure 9: First purification of Vif via Nickel NTA resin. A Nickel NTA agarose resin (Qiagen) was used to purify the Vif protein. 1 is the concentrated supernatant of the secreted media. 2 is the flow through of the concentration step. 3 is the flow through of the resin load, not all Vif protein binds to the resin. 4-7 are the different washing steps, no Vif protein elutes in these steps. 8 the elution step of the Vif purification with resin. The Vif protein elutes in these 5 ml in a concentration of 0.1 mg/mL. M is the PageRuler^{TM} prestained protein ladder, the used antibody was the Vif antibody.

The concentration of the 5 mL elution fraction was determined via NanoDrop containing a concentration of 0.1 mg/mL.

To increase the binding of the Vif protein a construct with a 10 x His-tag was cloned via a side directed mutagenesis. The new plasmid was verified with sequence analysis. The new construct was used with an increased secretion volume 5 L 2xYT media. To concentrate the 5 L of secretion supernatant a cross flow system with a 10 kDa membrane was used. The 5 L were concentrated with a flow rate of 2 mL/min up to 250 mL and then again concentrated via an Amicon ultracentrifugation unit (30 kDa MWCO) to 25 mL. To the concentrated supernatant 10 mL of the Nickel NTA agarose resin was added and incubated over night at 4 °C shaking. The supernatant and resin were added in a glass column and washed with washing buffer till baseline. The elution was performed with 400 mM imidazole. The elution fractions were analysed via SDS-PAGE and Western blot (Figure 10).

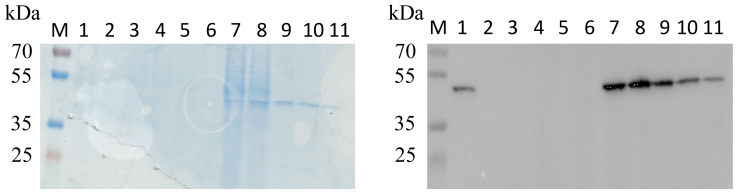

Figure 10 Crossflow purification of Vif. With the cross flow 5 L supernatant could be concentrated and washed with buffer. 1 is the concentrated supernatant after cross flow. 2 is the flow through of the crossflow. 3 is the flow through of the resin load to the glass column and does not contain any Vif protein. This time everything was binding to the resin. 4-6 are the washing steps of the resin and 7-11 are the elution fractions, 7 and 8 still impurities are found but the Vif protein was purified in a better quality than in any purification before. M is the PageRuler^{TM} plus prestained protein ladder, the used antibody was the Vif antibody.

The purification via cross flow and resin purification showed better results than all other purifications. The elution fractions contain Vif protein, but still some impurities were detected. The protein amount achieved with the optimized elution was not useable for

crystallography tests, but first interaction studies of the Vif protein with APOBEC3C protein (see below) could be performed.

To get a higher yield another purification was tested, without secreting the protein. The next tested purification variant was the purification of Vif from inclusion bodies in *E. coli*. Therefore, the plasmid was transformed, without the pSJ37 plasmid, in *E. coli* BL21 (DE) cells. The cells were grown at 37 °C 180 rpm till a OD_{600} 0.5 and induced with 1 mM IPTG. The temperature was decreased to 25 °C and the cells were grown over night. After harvesting the cells, the cells were lysed via cell disruption and the inclusion bodies were purified. With defolding buffer, containing 6 M guanidine, the inclusion bodies were incubated for 4 hours at 4 °C to defold the protein. Afterwards dialysis buffer tests were performed via dialysis knots to determine a refolding buffer. 42 different refold buffers were tested to analyse if the Vif protein is refolded and soluble in the supernatant after dialysis. Just one buffer, buffer 4 (100 mM NaCl, 0.05% (w/v) PEG 400, 400 mM Arginine and 50 mM corresponding pH dependent buffer substance) shows Vif protein in the supernatant (Figure 11).

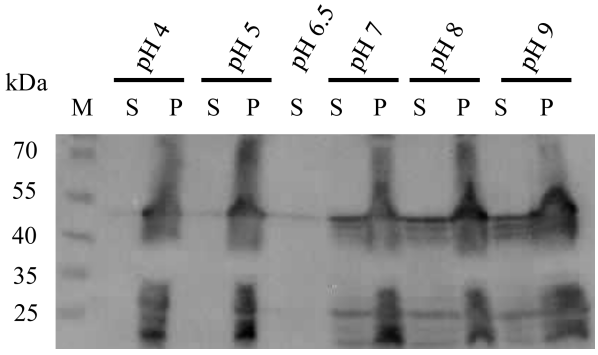

Figure 11: Refolding tests of Vif protein. Shown is buffer 4 with different pH. S is the supernatant after dialysis overnight and P is the pellet after dialysis. The refolded protein should be in the supernatant in a soluble state. It is obvious that the low pH like 4-6.5 the protein is hardly refolded. At pH 7-9 the protein is found in the supernatant and it can be said that the buffer 4 pH 8 is the best refolding buffer which was tested. M is the PageRuler^{TM} prestained protein ladder.

So this buffer, buffer 4 pH 8 (50 mM Tris–HCl pH 8, 100 mM NaCl, 0.05% (w/v) PEG 400 and 400 mM Arginine) was tested to refold the Vif protein and an IMAC was performed afterwards. But this purification does not show a purified and high yielded Vif protein. The purification of Vif protein for crystallography and co-crystallization with APOBEC3C could not be established.

Pulldown assay of APOBEC3C and Vif protein. The quality of the purified Vif protein was not good enough to perform crystallography, but first interaction tests could be performed. A pulldown assay with Pierce™ glutathione magnetic agarose beads (Thermo Fisher Scientific) was performed. Therefore, APOBEC3C was purified and Vif protein was purified as described before. 60 µg APOBEC3C protein was bound to the beads. After three washing steps 28 µg Vif protein was added to the beads and incubated for 15 min at 25 °C. After seven washing steps the bound protein was eluted with 30 µL elution buffer. All steps were analysed via SDS-PAGE and a Western blot (Figure 12).

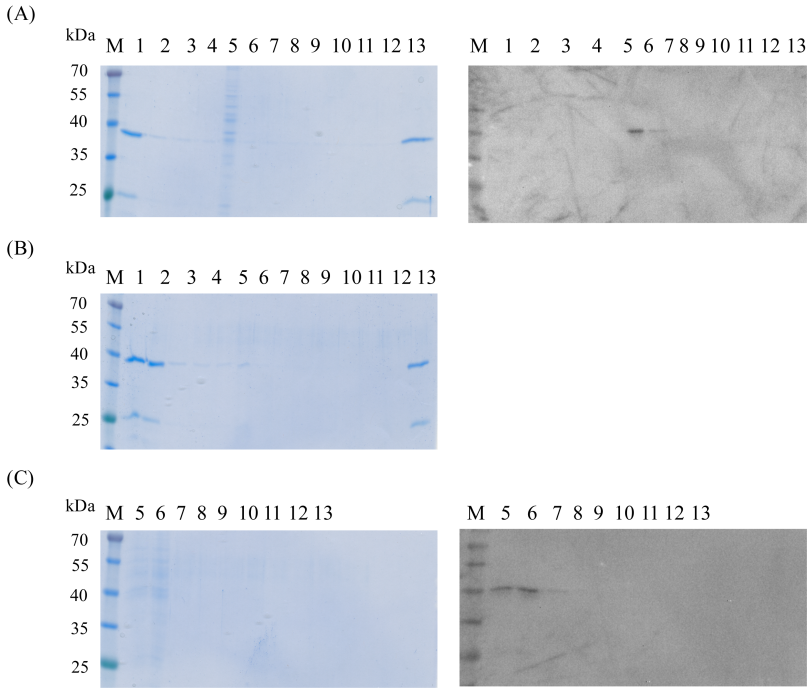

Figure 12: Pulldown and controls of APOBEC3C and Vif. A) Pulldown assay with APOBEC3C and Vif. In 1 the 60 µg APOBEC3C protein was given to the beads but not all of the protein is binding to the beads. In 2-4 the wash of the beads is shown, nearly no APOBEC3C elute in the wash steps of the beads. In 5 the 28 µg Vif, still with some impurities are incubated with the APOBEC3C containing beads. In the western blot, it can be seen that in the supernatant the Vif protein is detected and so it does not bind to the APOBEC3C protein. In 6-12 the wash steps are shown. 13 shows the elution step. Here the bound APOBEC3C is eluting and in the Western blot shows, that no Vif protein is co-eluting. B) In B) the control of APOBEC3C alone is shown. It looks exactly the same like the pulldown assay. C) Vif alone with the GST- magnetic beads. Also, no difference is shown in comparison to the pulldown assay. M is the PageRuler™ prestained protein ladder.

The pulldown assay shows that the APOBEC3C protein binds to the beads and can be eluted from the beads. In Western blot analysis, it became obvious that the Vif protein is not interacting with the APOBEC3C and is not detectable in the elution fraction. The protein is detectable in the load and in the first washing step of the interaction step. So, there is no interaction of the both proteins. It could not be checked if the secretion signal was inhibiting the interaction of both proteins because the TEV cleavage did not work efficient and there was too little cleaved Vif protein.

Discussion

At the moment treatments of the HI-virus are targeting main enzymes of the virus [7]. This leads to successfully control the virus. Nevertheless, the long-time use of these drugs is resulting in mutations of the virus and in ineffectiveness of the drugs [8]. Therefore, one of six accessory proteins of lentiviruses like HIV becomes the main interest of drug development [9; 10; 11]. This viral infectivity factor protein generates a complex of different host cell proteins. This complex results in a degradation of the host cell virus immunity proteins of the APOBEC3 family [12; 13; 20]. The Vif protein is already well characterized. The different binding sites necessary for the complex forming are solved [24; 25; 26; 27; 28; 29]. One big question is still the crystal structure of the Vif protein in combination with APOBEC3 proteins. Therefore, a purification of the Vif protein in high yield and quality has to be established. In this thesis, a new kind of purification in *E. coli* was tested. Therefore, different Vif proteins out of varying HIV-1 types were successfully cloned with a C-terminal secretion signal and a six His-tag. The secretion was successfully determined via Western blot analysis. It was proven that some of the constructs are not detectable with the used antibodies. As a next step, correct antibodies need to be found for some constructs. For first purification tests a variant was used which is detectable with both used antibodies.

Via column nickel affinity chromatography, the first tests were performed. The affinity of the protein out of the secretion supernatant was too low for purification. Therefore, dialysis and a bigger amount of secretion volume was tested. Changing the used metal ions to copper or cobalt also does not show a significant increase of the purified Vif protein. Zinc could also be an option in immobilized metal ion chromatography. It was not tested because it is already known that the zinc binding motif HCCH can lead to increased protein-protein interaction if zinc is available for binding [33]. To increase the binding efficiency a nickel NTA resin was tested but the affinity of the protein binding to the resin was still too low for a high yield purification. For purification of Vif the nickel NTA resin is the best tested purification variant. Vif should be purified in a folded form and not via denaturating and refolding it [33; 34; 35]. Therefore, *E. coli* as a secretion pathway was used to purify Vif out of the media. In the tested purification steps the protein does not aggregate, resulting in two possibilities. First the aggregated protein does not bind to the column or resin and it could be not observed or second Vif shows less aggregation in this way of purification.

To test if the protein is purified in higher yield also purification of denaturated Vif protein were performed. A purification out of inclusion body was tested with the same construct

used before but without additional pSJ37 plasmid, which is only needed for secretion. A refolding of the protein was determined in a 50 mM Tris–HCl pH 8, 100 mM NaCl, 0.05% (w/v) PEG 400 and 400 mM arginine buffer. This was the only buffer of the tested 42 which shows refolded soluble protein. The purification out of inclusion bodies was not as effective as the purification with Nickel NTA resin. The best tested purification of Vif protein in this thesis was to secrete the protein and purify it with a Nickel NTA resin.

Based on the purification issues the increase of Vif protein concentration was not high enough to perform crystallography, but first interaction studies with APOBEC3C protein could be performed. The interaction studies show no interaction between Vif and APOBEC3C. If the secretion signal has an influence on the interaction of the proteins could not be determined, as the cleavage efficiency of the TEV protease was not sufficient. The established purification seems to be the way for purifying Vif protein in big scale. There was no aggregate observed and with an improvement of the used construct it could be possible to increase the yield.

One possible option could be a change of the used tag. The tag has to be reachable for the used column or resin. Therefore, it could be a possibility to use a GST-tag (26 kDa), like in the APOBEC3C protein [31; 32]. In comparison to the 1 kDa big His-tag the GST-tag is bigger and could be increase the probability for binding. Also, one big advantage of a different tag could be the absence of metal ions. Duarte et al. observe even in the presence of nickel ions a higher aggregation of Vif [35]. So, an ion independent purification like glutathione might improve the purification of the secreted Vif protein. A bigger tag can also have an advantage on the TEV cleavage efficiency. So further improvements for the established purification should be made in future in order to purify soluble, folded, high yielded Vif protein with different APOBEC3 proteins for crystallography. This is needed to get information about possible structural changes and by this develop drugs to inhibit the binding.

Author contributions

SS conceived and directed this study. RC performed the test secretion, purification tests and the interaction studies. RC and SS wrote the manuscript. All authors read and approved the manuscript.

Acknowledgements

We thank Diana Kleinschrodt and Iris Fey of the Protein Production Facility for excellent support during the initial stages of this project. We thank all the members of the institute of Biochemistry for fruitful discussions.

References

[1] M. Widera, F. Hillebrand, S. Erkelenz, A.A. Vasudevan, C. Munk, and H. Schaal, A functional conserved intronic G run in HIV-1 intron 3 is critical to counteract APOBEC3G-mediated host restriction. Retrovirology 11 (2014) 72.
[2] A.J. Cann, Principles of molecular virology. (2005).
[3] E. Gomez-Lucia, V.M. Collado, G. Miro, and A. Domenech, Effect of type-I interferon on retroviruses. Viruses 1 (2009) 545-73.
[4] G. Yang, and X. Xiong, Viral infectivity factor: a novel therapeutic strategy to block HIV-1 replication. Mini Rev Med Chem 13 (2013) 1047-55.
[5] P.M. Sharp, and B.H. Hahn, Origins of HIV and the AIDS pandemic. Cold Spring Harb Perspect Med 1 (2011) a006841.
[6] G. Maartens, C. Celum, and S.R. Lewin, HIV infection: epidemiology, pathogenesis, treatment, and prevention. The Lancet 384 (2014) 258-271.
[7] W.C. Greene, Z. Debyser, Y. Ikeda, E.O. Freed, E. Stephens, W. Yonemoto, R.W. Buckheit, J.A. Este, and T. Cihlar, Novel targets for HIV therapy. Antiviral Res 80 (2008) 251-65.
[8] J.M. Binning, A.M. Smith, J.F. Hultquist, C.S. Craik, N. Caretta Cartozo, M.G. Campbell, L. Burton, F. La Greca, M.J. McGregor, H.M. Ta, K. Bartholomeeusen, B.M. Peterlin, N.J. Krogan, N. Sevillano, Y. Cheng, and J.D. Gross, Fab-based inhibitors reveal ubiquitin independent functions for HIV Vif neutralization of APOBEC3 restriction factors. PLoS Pathog 14 (2018) e1006830.
[9] R.H. Miller, and N. Sarver, HIV accessory proteins as therapeutic targets. Nature Medicine 3 (1997) 389-394.
[10] D. Trono, HIV accessory proteins: leading roles for the supporting cast. Cell 82 (1995) 189-92.
[11] M. Emerman, HIV-1 Regulatory/Accessory Genes: Keys to Unraveling Viral and Host Cell Biology. Science 280 (1998) 1880-1884.
[12] R.S. Larue, J. Lengyel, S.R. Jonsson, V. Andresdottir, and R.S. Harris, Lentiviral Vif degrades the APOBEC3Z3/APOBEC3H protein of its mammalian host and is capable of cross-species activity. J Virol 84 (2010) 8193-201.
[13] A.M. Sheehy, N.C. Gaddis, and M.H. Malim, The antiretroviral enzyme APOBEC3G is degraded by the proteasome in response to HIV-1 Vif. Nat Med 9 (2003) 1404-7.
[14] J.F. Arias, T. Koyama, M. Kinomoto, and K. Tokunaga, Retroelements versus APOBEC3 family members: No great escape from the magnificent seven. Front Microbiol 3 (2012) 275.
[15] J.D. Salter, R.P. Bennett, and H.C. Smith, The APOBEC Protein Family: United by Structure, Divergent in Function. Trends Biochem Sci 41 (2016) 578-594.
[16] R.S. LaRue, S.R. Jonsson, K.A. Silverstein, M. Lajoie, D. Bertrand, N. El-Mabrouk, I. Hotzel, V. Andresdottir, T.P. Smith, and R.S. Harris, The artiodactyl APOBEC3 innate immune repertoire shows evidence for a multi-functional domain organization that existed in the ancestor of placental mammals. BMC Mol Biol 9 (2008) 104.
[17] C. Munk, A. Willemsen, and I.G. Bravo, An ancient history of gene duplications, fusions and losses in the evolution of APOBEC3 mutators in mammals. BMC Evol Biol 12 (2012) 71.
[18] H.C. Smith, R.P. Bennett, A. Kizilyer, W.M. McDougall, and K.M. Prohaska, Functions and regulation of the APOBEC family of proteins. Semin Cell Dev Biol 23 (2012) 258-68.
[19] B. Romani, S. Engelbrecht, and R.H. Glashoff, Antiviral roles of APOBEC proteins against HIV-1 and suppression by Vif. Arch Virol 154 (2009) 1579-88.

[20] X. Yu, Y. Yu, B. Liu, K. Luo, W. Kong, P. Mao, and X.F. Yu, Induction of APOBEC3G ubiquitination and degradation by an HIV-1 Vif-Cul5-SCF complex. Science 302 (2003) 1056-60.
[21] A. Mehle, J. Goncalves, M. Santa-Marta, M. McPike, and D. Gabuzda, Phosphorylation of a novel SOCS-box regulates assembly of the HIV-1 Vif-Cul5 complex that promotes APOBEC3G degradation. Genes Dev 18 (2004) 2861-6.
[22] A. Mehle, B. Strack, P. Ancuta, C. Zhang, M. McPike, and D. Gabuzda, Vif overcomes the innate antiviral activity of APOBEC3G by promoting its degradation in the ubiquitin-proteasome pathway. J Biol Chem 279 (2004) 7792-8.
[23] P. Barraud, J.C. Paillart, R. Marquet, and C. Tisne, Advances in the structural understanding of Vif proteins. Curr HIV Res 6 (2008) 91-9.
[24] R.A. Russell, and V.K. Pathak, Identification of two distinct human immunodeficiency virus type 1 Vif determinants critical for interactions with human APOBEC3G and APOBEC3F. J Virol 81 (2007) 8201-10.
[25] A. Mehle, H. Wilson, C. Zhang, A.J. Brazier, M. McPike, E. Pery, and D. Gabuzda, Identification of an APOBEC3G binding site in human immunodeficiency virus type 1 Vif and inhibitors of Vif-APOBEC3G binding. J Virol 81 (2007) 13235-41.
[26] Z. He, W. Zhang, G. Chen, R. Xu, and X.F. Yu, Characterization of conserved motifs in HIV-1 Vif required for APOBEC3G and APOBEC3F interaction. J Mol Biol 381 (2008) 1000-11.
[27] H. Wang, B. Liu, X. Liu, Z. Li, X.F. Yu, and W. Zhang, Identification of HIV-1 Vif regions required for CBF-beta interaction and APOBEC3 suppression. PLoS One 9 (2014) e95738.
[28] Z. Xiao, E. Ehrlich, Y. Yu, K. Luo, T. Wang, C. Tian, and X.F. Yu, Assembly of HIV-1 Vif-Cul5 E3 ubiquitin ligase through a novel zinc-binding domain-stabilized hydrophobic interface in Vif. Virology 349 (2006) 290-9.
[29] A. Mehle, E.R. Thomas, K.S. Rajendran, and D. Gabuzda, A zinc-binding region in Vif binds Cul5 and determines cullin selection. J Biol Chem 281 (2006) 17259-65.
[30] Y. Yu, Z. Xiao, E.S. Ehrlich, X. Yu, and X.F. Yu, Selective assembly of HIV-1 Vif-Cul5-ElonginB-ElonginC E3 ubiquitin ligase complex through a novel SOCS box and upstream cysteines. Genes Dev 18 (2004) 2867-72.
[31] D. Marino, M. Perkovic, A. Hain, A.A. Jaguva Vasudevan, H. Hofmann, K.M. Hanschmann, M.D. Muhlebach, G.G. Schumann, R. Konig, K. Cichutek, D. Haussinger, and C. Munk, APOBEC4 Enhances the Replication of HIV-1. PLoS One 11 (2016) e0155422.
[32] Y. Iwatani, H. Takeuchi, K. Strebel, and J.G. Levin, Biochemical activities of highly purified, catalytically active human APOBEC3G: correlation with antiviral effect. J Virol 80 (2006) 5992-6002.
[33] I. Paul, J. Cui, and E.L. Maynard, Zinc binding to the HCCH motif of HIV-1 virion infectivity factor induces a conformational change that mediates protein-protein interactions. Proc Natl Acad Sci U S A 103 (2006) 18475-80.
[34] X. Yang, J. Goncalves, and D. Gabuzda, Phosphorylation of Vif and its role in HIV-1 replication. J Biol Chem 271 (1996) 10121-9.
[35] C.A. Duarte, and M. Palomino, An improved method for purification and refolding of recombinant HIV Vif expressed in *Escherichia coli*. Biotechnol Appl Biochem (2017).

4. General Discussion

In this thesis, cloning of the CD1348 from *Clostridium difficile* (*C. difficile*) for heterologous expression in *Escherichia coli* (*E. coli*) and for *in vivo* analysis in *L. lactis* was completed. CD1348 purification was established and activity and affinity analyses were performed. Additionally, via multi-angle light scattering (MALS) a further characterization test of CD1348 was achieved. A model of the protein structure was described with Small-angle X-ray scattering (SAXS) and nuclear magnetic resonance (NMR) (Chapter III).
Additionally, the lipid composition of the *Lactococcus lactis* (*L. lactis*) NZ9000 was analysed to compare it with a lantibiotic and antibiotic resistant strain (Chapter IV).

4.1. Potential function of CD1348

CD1348 is a lipoprotein from *C. difficile* encoded directly in front of a known lantibiotic resistance ABC-transporter, CprABC. This resistance operon consists of a two-component system and the mentioned ABC-transporter [157; 158]. These components are known to be involved in immunity or resistance mechanisms of bacteria against lantibiotics. Two different constellations of resistance and immunity systems are known. One constellation is a two-component system with a periplasmic sensing histidine kinase and a response regulator in combination with a LanFEG type immunity transporter or a CprABC resistance transporter. The other one is an intramembrane sensing kinase and a response regulator forming a two-component system in combination with a BceAB type resistance transporter [67; 106; 135; 152]. Some systems contain an additional membrane associated protein performing resistance or immunity [160]. The hypothesis was that CD1348 is a membrane associated protein performing resistance against lantibiotics like the resistance protein Nsr in *S. agalactiae*, or the immunity proteins of lantibiotic producer strains like NisI in *L. lactis* or SpaI in *Bacillus subtilis* (*B. subtilis*) [154; 160; 161; 162; 164] (Chapter I).
In Chapter III the purification of CD1348 was established and first characterization studies were performed. *In vivo* and *in vitro* measurements were performed with gallidermin and nisin, known lantibiotics against which the ABC-transporter CprABC confers resistance [157]. Comparing results of *L. lactis* NZ9000 strain, expressing the CD1348 protein, to a sensitive NZ9000 strain it could be concluded that CD1348 is not conferring resistance in *L. lactis* against nisin and gallidermin. The IC_{50} values are with 4.9 ± 0.4 nM nisin (CD1348) and 5.2 ± 0.5 nM nisin (20.9 ± 1.9 nM and 34.7 ± 3.3 nM gallidermin) nearly the same

(Chapter III, Table 4). *In vitro* analyses determine K_D values of a µM range (2.4 µM gallidermin/ 9.6 µM nisin) (Chapter III, Table 3), a deathly concentration for *in vivo* measurements. The interaction studies do not provide an answer for the possible protein function with the tested lantibiotics, but show that some kind of interaction is possible. Also, an amino acid sequence blast in the NCBI data base does not give an idea of potential functions. Only hypothetical proteins of *C. difficile* were found with a high similarity. In Figure 15 a NCBI amino acid blast is depicted. The highest alignment score results were found in *C. difficile* strains (Figure 15 red). Excluding the *C. difficile* genome results in a homology loss (45%-29%) of hypothetical proteins from *Romboutsia* or *Clostridia* (Chapter III, Table 5) (Figure 15 pink). So, the function of CD1348 remains elusive.

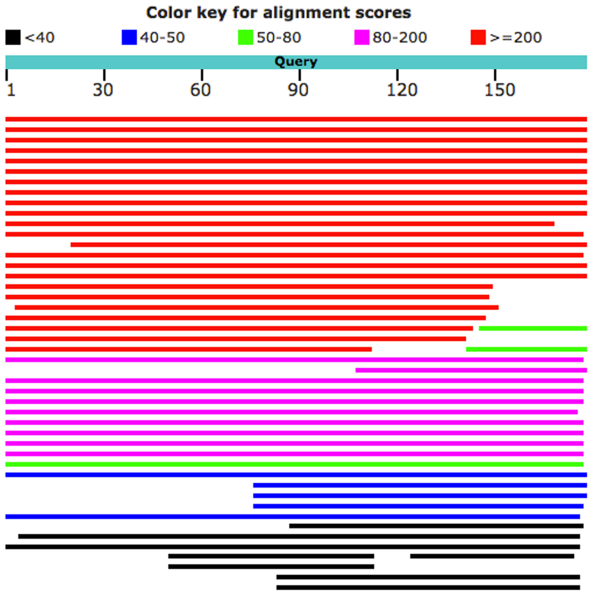

Figure 15: Amino acid NCBI blast of CD1348.
In red, the blast results showing the highest homology are depicted. Here are only *C. difficile* strains mentioned with an identity of 100% - 89%. In pink bacteria with lesser alignment score are depicted. Here also different *Clostridia* strains are shown and also *Romboutsia* strains, like *Romboutsia weinsteini*. In Blue and black the less identity strains are coloured, also here are just *Clostridia* strains, like *Clostridium cadaveris* or *Clostridium baratii* mentioned.

In this thesis, the structure of CD1348 was modelled. A modelling program was used for a protein model and with the help of SAXS and NMR measurements it was able to analyse the protein structure of CD1348 (Chapter III). The SAXS measurements were performed to create a low-resolution model of the protein. A fitting of the calculated model and the SAXS low-resolution model showed that the model structure is highly fitting to the measured SAXS model (Chapter III, Figure 13). Comparing the solved structure with known resistance and immunity proteins like NisI, SpaI or Nsr the uniqueness of the CD1348 structure was detected [171; 218; 219]. The structure of *Sa*Nsr from *Streptococcus agalactiae* (*S. agalactiae*) was solved via X-ray crystallography in 2016 [171] (Figure 16). *Sa*Nsr contains

three domains, an N-terminal helical bundle, the protease cap and a core domain forming a hydrophobic tunnel of 10 Å width [171]. *Sa*Nsr belongs to the S41 family of peptidases and contains a highly conserved TASSAEM motif. This sequence contains the catalytically active serine residue necessary for activity, shown via deletion mutant of this serine [169; 171]. *Sa*Nsr cleaves of the last six amino acids of nisin, therefore *Sa*Nsr needs the C-terminus, the rings D-E and the last serine, of nisin. An absence of these motifs results in a loss of activity of *Sa*Nsr. Based on this known mode of action *Sa*Nsr is highly specific to the C-terminus of nisin [169; 171].

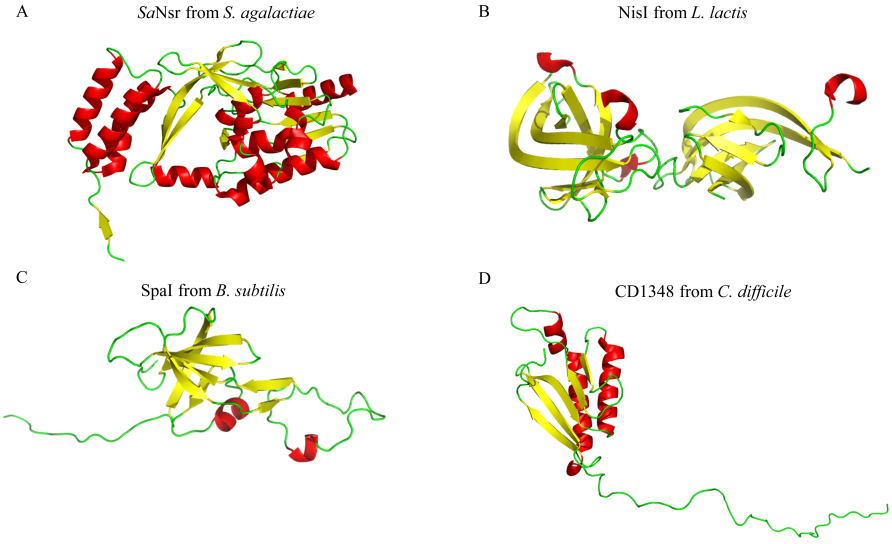

Figure 16: Cartoon representation of crystal structures of NisI and *Sa*Nsr and NMR structures of SpaI and model structure of CD1348.
A) The crystal structures of *Sa*Nsr from *S. agalactiae* (PDB code: 4Y68). B) The crystal structure of NisI from *L. lactis* (PDB code: 5XHB). C) NMR structure of SpaI from *B. subtilis* (PDB code: 2LVL). D) Model structure of CD1348 from *C. difficile*. Depicted in red are the helices, in yellow the sheets and in green the loops.

The structure of lipid-free NisI was also solved via X-ray crystallography in 2018 [219] (Figure 16). NisI is different to *Sa*Nsr a two domain predominantly ß-sheet protein. The N-terminal domain is highly positive charged and is able to bind to the membrane while the C-terminal domain of NisI is negatively charged which is important for the nisin interaction [220]. The interaction of the C-terminal domain and nisin was analysed with deletion mutants and with a hybrid containing the N-terminus of NisI and the C-terminus of SpaI. This hybrid was not able to bind nisin anymore instead it binds to subtilin [221]. This observation was interesting as the original NisI is only able to bind nisin and not subtilin [221]. *In vivo* NisI provides immunity up to a nisin concentration of 60 nM in *L. lactis*. *In vitro* a rather weak affinity was determined in low µM range, perhaps because of the lacking membrane environment [220; 221]. Both domains of NisI contain a similar fold which also

has been observed in the structure of SpaI. SpaI is the immunity protein of *B. subtilis* and is a single domain protein and also a ß-sheet protein. The structure of SpaI was solved via NMR spectroscopy in 2012 (Figure 16) [218]. SpaI is highly specific to subtilin [155; 218]. The CD1348 structure contains three different domains, a large N-terminal loop region, two α-helices and five ß-sheets. The α-helical domain seems to interact via hydrophobic force with the five ß-sheets which could be a reason for the observed heat resistance of the CD1348 protein (Chapter III, Figure 19). There is no dominant positively or negatively charged separation into N-terminus or C-terminus in the protein observed, like in NisI [220]. But still some negatively charged regions could be determined were a positive charged interaction partner could bind. The negative charge in CD1348 is located in the small α-helix at the top of the structure and the C-terminal small α-helical bundle.

Table 1: Result of EBI structure blast of CD1348.
Proteins are ordered due to their RMSD value, representing higher similarity to low.

RMSD (Å)	Gene Name	Organism	Sequence domain	Aligned Amino Acids	Function
2.72	CBFG_00659 (PDB code: 4olo) [222]	*Clostridiales Bacterium* 1_7_47FAA	CcmK-like superfamily	109	Not assigned
2.73	SMU_848 (PDB code: 2g0j)	*Streptococcus mutans*	Cysteine protease Prp	145	Not assigned
2.74	SAOUHSC_01 (PDB code: 4peo)	*Staphylococcus aureus*	Cysteine protease Prp	106	Not assigned
2.89	VC0395_A0969 (PDB code: 4hi2) [223]	*Vibrio cholera* O395	Acylphosphatase-like domain	91	Acylphosphatase activity
2.91	PF1909 (PDB code: 2z8q)	*Pyrococcus furiosus* DSM 3638	3Fe-4S ferredoxin	66	Metal ion binding
2.96	SP_1106 (PDB code: 2idl)	*Streptococcus pneumoniae* TIGR4	Cysteine protease Prp	117	Not assigned
3.04	TRQ2_1395 (PDB code: 2mew)	*Thermotoga Maritima*	Ribosomal protein S10	82	RNA binding
3.13	Pecwa_4094 (PDB code: 4olp) [222]	*Pectobacterium parmentieri* WPP163	Microcompartment protein	107	Not assigned
3.20	TM1457 (PDB code: 1s12) [224]	*Thermotoga Maritima*	Cysteine protease Prp	94	Not assigned
3.38	BSU13900 (PDB code: 1jem) [225]	*Bacillus subtilis*	Phosphocarrier protein	87	Protein binding

To obtain a more general overview of similar proteins and not only focus on possible resistance proteins, the solved structure model was used for a structure blast in the EMBL-EBI Protein Data Bank in Europe to see if any known protein has a similar structure. This search results in a list of several proteins containing a similar structure (Table 1).

Several different Gram-positive bacteria carrying a protein with a somehow similar protein structure could be identified. The proteins were ordered by the Root Mean Square Deviation (RMSD). The RMSD value is calculated between Cα-atoms of matched residues at best 3D superposition of the query and the target structure. Large RMSD values (>3 Å) represent a reduced similarity of the compared protein structures [226]. In Figure 17 depicted are the CD1348 (178 aa) structure and two matched structures with different RMSD values. The SMU.848 has a RMSD value of 2.73 Å and the Pecwa_4094 of 3.13 Å. The similarity of the Pecwa_4094 structure is matching less than for SMU.848. Because there was no protein found with a RMSD value under 2 a second blast was performed, lacking the large N-terminal loop domain, to see if a better match could be found. This blast was performed to figure out whether the N-terminal part influences the outcome. But no changes in RMSD values were detected in this second outcome.

Having a closer look to the structures of the fitting proteins the blast results only show a reduced similarity to CD1348. The detected similar proteins all have a ß-sheet and a α-helical domain like CD1348 but they are all lacking the large N-terminal loop region. One explanation for the lacking N-terminal loop region might be that these proteins are no lipoproteins and are not anchored within the membrane.

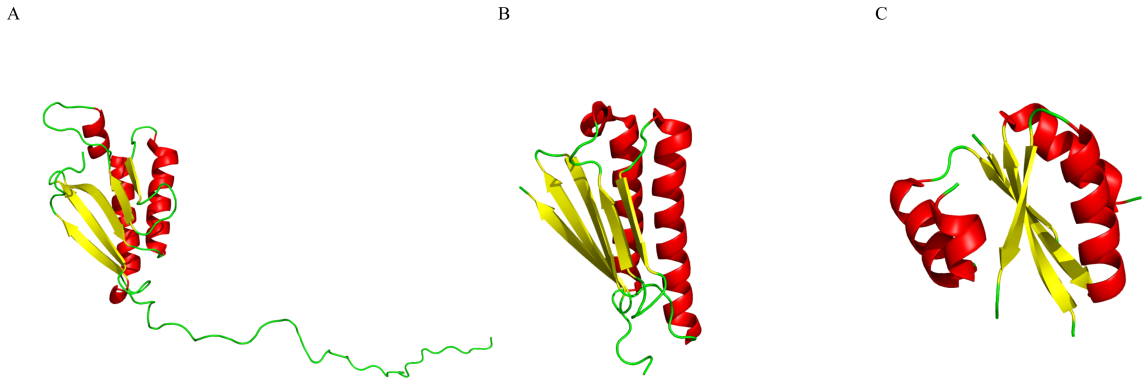

Figure 17: Structures of CD1348 and two example structures from the structural blast.
A) CD1348 model structure calculated via TOP model (D. Mulnaes, unpublished). B) Structure of the SMU.848 protein of *S. mutans* with a cysteine protease sequence domain (PDB code: 2g0j). SMU.848 has similar to the CD1348 protein five ß-sheets and two α-helices, and a similar structure to the head of the CD1348. C) Structure of the Pecwa_4094 protein of *Pectobacterium parmentieri* WPP163 (PDB code: 4olp). It contains four ß-sheets and four α-helices and does not show a high similarity to the CD1348 protein. The α-helices are depicted in red, the ß-sheets in yellow and the loops are coloured in green.

Nevertheless, one interesting result was observed. Four different proteins containing a cysteine proteases Prp sequence domain are identified in the blast. These proteins were identified in *Streptococcus mutans*, *Staphylococcus aureus* and *Streptococcus pneumoniae* which were all human pathogens and one in *Thermotoga Maritima* [227; 228; 229]. This was a promising result because *C. difficile* is also a human pathogen and even when the fitting result is not high based on the RMSD value it provides a further potential function of the CD1348. A closer look to the genome position using the NCBI data base of the four identified proteins shows that these proteins are not encoded in front of an ABC-transporter or two-component system, so this cysteine proteases are not involved in a resistance system. Therefore, a comparison to cysteine proteases Prp was performed and analysed if the CD1348 protein could be part of this protein family. The cysteine protease Prp has a conserved motif of GHxxxxxxGxDxxC (x is any amino acid), and some are known to cleave of ribosomal protein L27 [230]. The amino acid sequence of CD1348 and structure show none of these motifs. CD1348 does not contain the Prp cysteine protease typical residue. In Figure 18 an alignment of the CD1348 protein and the cysteine protease Prp SMU.848 is depicted. The typical cysteine protease Prp residues are coloured red in the SMU.848 (yellow) and are labelled. The corresponding amino acids in CD1348 (blue) at the same structural location are EExxxxxxLxLxxD, depicted in orange. Here it became clear that the residues of a Prp cysteine protease are not located in the CD1348 protein. Also, due to the different length of the α-helices the alignment shows that the structures, even excluding the N-terminal loop region, are not exactly fitting. To determine if CD1348 is another kind of cysteine protease the CD1348 sequence was compared to cysteine protease typical amino acid residues. Cysteine proteases consist of a cysteine, histidine and asparagine triad within the active site [231]. The histidine residue is present in the active site and acts as a proton donor to enhance the nucleophilicity of the cysteine residue. This nucleophilic cysteine residue can then interact with the carbon of the reactive peptide bond [231]. CD1348 also does not contain this triad motif. Both kinds of residues cannot be identified in CD1348. Based on these findings the potential function of CD1348 as Prp cysteine protease and typical cysteine protease can be excluded.

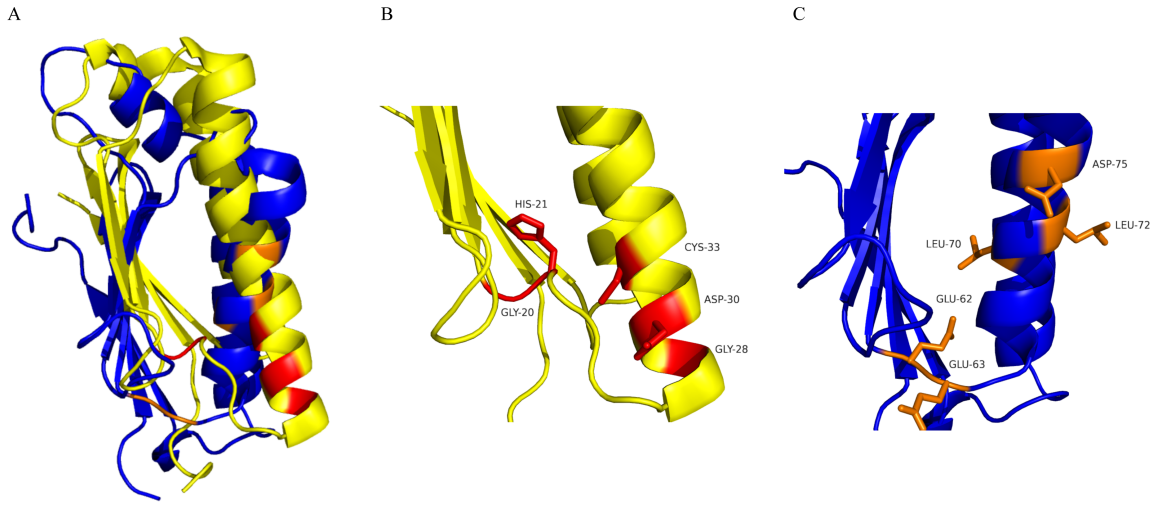

Figure 18: Structure alignment of CD1348 and SMU.848.
A) Depicted are the cartoon representation structures of CD1348 from *C. difficile* (blue) lacking the N-terminal loop domain and the cysteine protease Prp SMU.848 from *S. mutans* (yellow) (PDB code: 2g0j). The typical amino acid sequence in a Prp cysteine protease GHxxxxxxGxDxxC is depicted in red [230]. The structural related amino acids of CD1348 are depicted in orange, the residue of EExxxxxxLxLxxD (x any amino acid) does not share any similarity with the cysteine protease Prp motif. It is shown that the structure alignment shows a similarity. B) Zoom in of the SMU.848 structure and the labelled amino acids of the Prp cysteine protease motif. C) Zoom in of the CD1348 protein and the corresponding amino acids.

To sum up, the purification of the CD1348 protein is established and the protein structure could be solved. The function of the protein is still unknown and even structural and sequence blasts do not result in a possible function. The structure of CD1348 is till date unique and the protein is expressed only in *C. difficile*. The structure shows less similarity to other proteins. The first hypothesis of CD1348 being a lantibiotic resistance protein neither could be excluded or validated in this thesis and the functional analysis has to be carried on. Furthermore, a potential protease function, like *Sa*Nsr, needs to be figured out [169; 171]. Comparing the till date characterized resistance and immunity proteins with the data of analysed CD1348 it became clear that no complete matching could be detected. Interesting is that the *in vitro* analysis of CD1348 results in an interaction with the lantibiotics in a deathly concentration, like in *in vitro* analysis of NisI (Table 2). For NisI the membrane environment is missing so the affinity is reduced [220]. As no resistance *in vivo* could be observed, the interpretation of *in vitro* results for CD1348 is difficult. Maybe a correct substrate will show a resistance *in vivo*.

Table 2: Comparison of immunity protein NisI, resistance protein *Sa*Nsr and the potential resistance protein CD1348.

	NisI	**CD1348**	***Sa*Nsr**
Molecular weight	27.8 kDa	20.6 kDa	36.2 kDa
Localization	Membrane attached/ Lipid-free	Membrane attached	Membrane spanning
Sequence motif	N-terminal signal peptide	N-terminal signal peptide	N-terminal transmembrane helix
Substrate	Nisin	Not determined	Nisin
Function	Nisin binding	Not determined	Nisin cleavage
Mechanism	Cell clustering	Not determined	Activity lowering of nisin
Fold of resistance	8-10	-	20
Binding affinity	Nisin: 1 µM	Nisin: 9.6 µM Gallidermin: 2.4 µM	Not determined
Heat stability	Not determined	Up to 90 °C	Not determined
Structure determined	X-ray crystallography	Modell calculation and NMR	X-ray crystallography
Domains	two	three	three

To identify the substrate, function, mechanism and the fold of resistance of CD1348 interaction studies have to be performed (Table 2). For these experiments different possible substrates have to be used, as it is known that resistance and immunity proteins are highly specific to mostly one lantibiotic.

4.2. Potential substrates of CD1348

Lantibiotic resistance and immunity membrane associated proteins, which have been characterized so far, are highly specific for one substrate. This was analysed in detail for the NisI and SpaI proteins [154; 155]. It is published that the proteins are just performing immunity against the produced lantibiotic of the corresponding strain. NisI recognises nisin but not subtilin although the structures have a high homology [135; 221]. Due to this it is still possible that CD1348 is performing resistance but nisin and gallidermin, which are substrates of the CprABC transporter, are not the correct substrates of CD1348 (Chapter III). The structural analyses performed before show that the CD1348 protein seems to be a unique protein within *C. difficile*. Based on this information an analysis of different bacteriocin producing *Clostridia* seems reasonable to find a possible substrate of the CD1348 protein. *C. difficile* is not known to produce a bacteriocin so other *Clostridia* were analysed with the Bagel 3 and Bagel 4 program [232], which analyses different genomes to identify possible bacteriocins. Also in publications some bacteriocins produced in *Clostridia* were found

[168]. In Table 3 a list of different bacteriocins produced in *Clostridia* are shown. In this research, different classes of bacteriocins could be identified in various *Clostridia*. Class I (lantibiotics), class II (non-lanthionine unmodified peptides) and class III bacteriocins could be identified [79].

Due to the fact that the CprABC transporter is active against class I bacteriocins, like nisin and gallidermin, three possible candidates were still left [157; 158]. The class I bacteriocin produced by *Clostridium maddingley* (*C. maddingley*), *Clostridium perfringens* (*C. perfringens*) and *Clostridium beijerinckii* (*C. berijerinckii*) [168]. Comparing the amino acid sequence with the lantibiotics the ABC-transporter could be active against two bacteriocins, maddinglicin and fringenlicin. The comparison with the ABC-transporter is done as it could be suspected that CD1348 will have a substrate also interacting with the ABC-transporter. The ABC-transporter is unspecific in binding different substrates in a resistance system [135; 152; 170].

Table 3: Different bacteriocins produced by various *Clostridia* species.
In green the Class I bacteriocins, in yellow the class II and in red the class III bacteriocins are depicted [168; 232].

Bacteriocin	Bacteria	Sequence	Name
Class I	*Clostridium maddingley*	ITSKSLCTPGCITGVLMCITQNSCVSCKSCIKC	Maddinglicin
	Clostridium perfringens	ITSVAYCTPGCLTGELCGSSECGLTRSCTNTWLCS	Fringenlicin
	Clostridium beijerinckii	MFLVAGALGVQTAAATTIVNVILNAGTLVTVLGIIASIASGGAG TLMTIGWATFKATVQKLAKQSMARAIAY	Circularin_A
Class II	*Clostridium perfringens*	MENLNLNQLENINGGYWKTIWAVGPGLYQRDTETGKYRWIQT QDNLSYTTNVIANGWAGSAAGGYFSGR	Lactococcin_A
	Clostridium botulinum	MQKPEIISADLGLCAVNEFVALAAIPGGAATFAVCQMPNLDEIV SNAAYV	Boticin_B
	Clostridium perfringens	MDSELFKLMATQGAFAILFSYLLFYVLKENSKREDKYQNIIEEL TELLPKIKEDVEDIKEKLNK	UviB
Class III	*Clostridium perfringens*	MANNIIPNVSSGDLVGSTPTFPPNAVVRGDFLYLRDVDGNQIPG RTVSDGDEITVLFISNEKNIVLVQYPTSSGYRQGYVTNATSIIKY KDDYSWVNGSTPEPVYDFDKTTQIGTLDPRERAVVLYKVDGM TYVAYDTGKGKLTKSGLVHYEGSGSSTGGGSFNGVAPGEVVP GGFTYENNAEVVGDELYLRDANGNLIPGRSVSVGDKITVLDVG YTKQLALVQYPAGDVVRQGYVTNATNLIRYFNQYSWHNG	Bacteriocin_ BCN5
	Clostridium tyrobutyricum	MRKVFLRSIISTLVMCAFVSSSFSVNADESKPNDEKIINNIENVTT TKDIVKSNKNNIVYLDEGVMSIPLSGRKPIAIKDDNNKEDLTVT LPIKNTGDISKISSNGTILYKNNSSNSSNIALQPKNDGFKALININ DKLANKEYEFTFNLPKNSKLISAATYLGKEYDTKEVFVVDKNNI ITSIISPAWAKDANGHNVSTYYKIVSNNKLVQVVEFTENTAFPV VADPNWTKIGKCAGSIAWAIGSGLFGGAKLIKIKKYIAELGGLQ KAAKLLVGATTWEEKLHAGGYALINLAAELTGVAGIQANCF	Closticin_574

Two interesting class I bacteriocins were found [168]. One is maddinglicin from *C. maddingley* and one is an uncharacterized bacteriocin from *C. perfringens* [168; 233]. These possible substrates are interesting as both sharing a high similarity to the ring A and B from nisin. Maddinglicin shares a higher similarity than fringenlicin but both contain the ring B motif proline and glycine. This motif seems to be necessary for the CprABC transporter as recognition structure [157]. The predicted structures of the peptides are calculated with the RIPPMiner to see structural differences to nisin (Figure 19) [234]. The lantibiotic maddinglicin shows a higher similarity to nisin. The first two rings are highly similar to nisin and also the third ring is similar. But after the third ring the structure is not homolog to nisin anymore. The flexible hinge region is missing and maddinglicin contains four rings instead of two at the C-terminus. The mentioned four rings are all intertwined. Maddinglicin contains three lanthionine rings and four methyllanthionine rings. Because of the amino acid sequence and the first three rings, which are highly similar to nisin maddinglicin should be able to bind lipid II [101; 102].

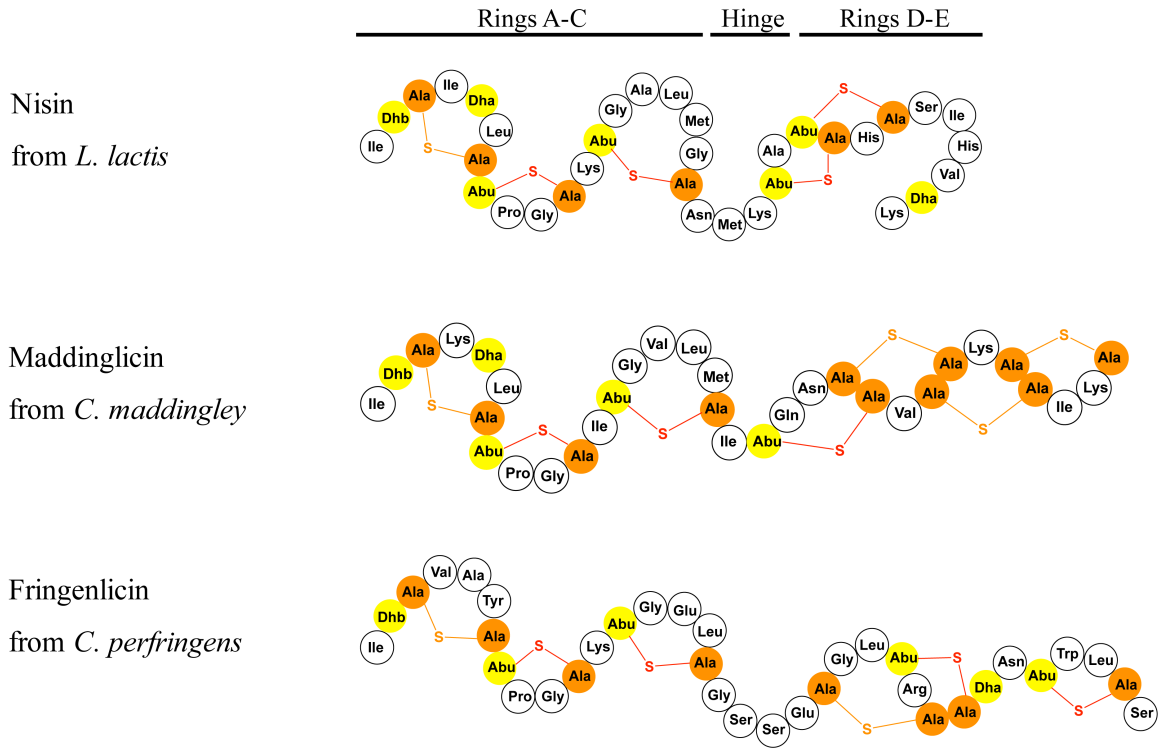

Figure 19: Potential substrates of CD1348 compared to nisin.
Schematic structures of three lanthipeptides. First depicted is nisin, one of the best characterized lantibiotics. The N-terminal part contains the (methyl-) lanthionine rings A-C, ring C is followed by the flexible hinge region and the last two lanthionine rings D-E. The CprABC transporter of *C. difficile* is recognising the second ring. Maddinglicin and fringenlicin are two possible substrates of CD1348. They are sharing a high similarity in the N-terminus of the peptide, and in special the second ring. The C-terminus is different in comparison to nisin. The dehydrated amino acids and the cysteines of the lanthipeptides are highlighted in yellow and orange. The (methyl-)lanthionine rings are visualized in orange and red.

It has still to be determined if maddinglicin forms pores. Because of the missing hinge region and the four intertwined rings, it does not seem flexible enough to flip in the membrane to form pores, like nisin does [99; 103; 235].

The uncharacterized lantibiotic, here named fringenlicin, shows similarity to nisin in the first two rings. The other rings are different to nisin. A flexible hinge region like in nisin is present in fringenlicin. Beside this the C-terminus contains three rings instead of two intertwined compared to nisin.

Because of our measurements in *L. lactis* it is suspected that the CD1348 protein is not recognising the N-terminus with the rings A and B like the CprABC transporter [157]. A theory is that CD1348 recognises the C-terminus of the lantibiotic, like *Sa*Nsr does [169; 171]. So, both lanthipeptides could be promising candidates of the CD1348 protein. *C. maddingley* is a *Clostridia* isolated from coal-seam gas formation water in Victoria, Australia [233]. Because less is known about *C. maddingley* and no information is available if it is a human pathogen, it is unknown if it would be useful for *C. difficile* to be resistant against a lantibiotic produced by this organism [233]. *C. perfringens* is a human pathogen like *C. difficile* so it is possible that both organisms get in contact. *C. perfringens* is found in the gastrointestinal tract of human and animals. The Gram-positive bacteria is the cause of human diseases such as gas gangrene and food poisoning [236]. *C. difficile* is a multi-resistant pathogen causing infections in the gastrointestinal tract resulting in a chronical disease and inflammation of the colon [237; 238]. Due to the fact that *C. difficile* and *C. perfringens* are both present in the gastrointestinal tract. *C. difficile* could be resistant to a lantibiotic produced by *C. perfringens* as they are competitors in the human body.

A blast of the sequence of CD1348 and the genome of *C. perfringens* and *C. maddingley* using NCBI data base does not show any similar protein in these bacteria. CD1348 seems to be a unique protein only present in *C. difficile*.

Further interaction studies with the described lantibiotics and the CD1348 protein have to be done. The lantibiotics can be modified and purified with the established *Lactococcus lactis* system containing the modification enzymes of the nisin system [163; 239]. The CprABC transporter should also be tested in presence and absence of the CD1348 protein to assure that the protein function is correctly determined, like for NisI. If a substrate can be identified also the mechanism description can be detected if it is cooperative with the transporter like NisI and NisFEG [154; 161; 162; 163]. These tests can also identify if the CD1348 may support the transporter in presence of one special lantibiotic like a mechanism known in *S. aureus* with a small transmembrane protein VraH. VraH supports the ABC-

transporter VraDE. Interestingly, VraH is only important for resistance against gallidermin. The nisin and bacitracin resistance of the transporter appears to be independent of VraH [240].

In conclusion, the research of possible substrates still can go on to prove a function as resistance protein against lantibiotics of CD1348. There are still bacteriocins as candidates for research and these candidates can also be interesting without the CD1348 protein as new lantibiotics, which can be interesting for disease treatment in medicine. Not only interaction with CD1348 and CprABC are interesting for further research of this described possible substrates, beside this also the mode of action could be of interest as only less is known about them till date.

4.3. Lipid composition of *L. lactis*

In the second major topic of this thesis the lipid composition of *L. lactis* NZ9000 was determined. Lipids have several major functions in cells. Of course, they are involved in the membrane structural components, but they can also be energy and heat sources, signalling molecules, protein recruiting platforms and substrates for protein-lipid modification [241; 242; 243; 244; 245]. The understanding of lipids is an important step in biology. Membrane lipids like phospholipids are important in many mechanisms. An interesting aim is to check the influence of changing lipid compositions. A change in lipid composition is not only inevitably resulting in changes of membrane properties. Lipids are involved in protein interaction and activity so a change can also have an effect on integral membrane and non-membrane proteins [241].

In this thesis, the lipid composition of *L. lactis* NZ9000 was determined which was not available in detail till date. The Gram-positive bacterium *Lactococcus lactis* has become a good system for overexpression of membrane proteins over the last 20 years [246; 247; 248; 249; 250]. One major reason is the nisin-controlled expression system (NICE). This system contains the two-component system, a regulatory system NisK and NisR which is involved in the production of nisin A [251; 252]. There are also some other reasons why *L. lactis* is suitable for prokaryotic and eukaryotic membrane protein expression beside the different *E. coli*. The benefits of *Lactococcus* are a rapid growth and the high cell density without aeration in comparison to *E. coli* or yeast [249; 250]. It is not able to produce endotoxins and is a food-grade organism. One major advantage is that expressing of eukaryotic membrane proteins in *L. lactis* does not result in inclusion bodies [246; 247; 249]. One

example is the KDEL receptor while expression in *E. coli* results in inclusion bodies, *L. lactis* is targeting exclusively to the cytoplasmic membrane [253; 254]. Other advantages are the low protease activity, no spore forming like other Gram-positive bacteria and containing only one membrane. Due to the fact that there is only one membrane, transport and binding assays can be performed with whole cells [249; 250]. In 2003 Kunji et al. published different examples for overproduction of eukaryotic membrane proteins in *L. lactis*. Here the focus was on mitochondrial transporters and carriers [249]. In this paper, it was shown that mitochondrial proteins are easy and functional overexpressed with the help of the NICE system. The tested carriers have been overproduced in *E. coli* in large amount before, but the protein was found in inclusion bodies, misfolded or non-functional [249; 255]. Mitochondrial carrier can also be overexpressed in yeast mitochondria, but their purification from carriers with overlapping substrate specificities is difficult [256; 257]. *L. lactis* does not show such problems therefore it is a good expression system also for mitochondrial carriers [256; 257]. Some disadvantages are the AT-rich codon usage of the organism and the relatively high resistance against lysis. The disadvantages are negligible in comparison to the advantages. The good results of already expressed membrane proteins in this organism are showing that *L. lactis* NZ9000 is a good candidate for membrane protein expression [246; 247; 248; 249]. Because of its rising use in protein purification the lipid composition is a further step to optimize protein expression.

Due to the fact membrane proteins are able to interact with phospholipids like cardiolipin (CL), phosphatidylglycerol (PG), phosphatidylethanolamine (PE) and phosphatidylcholine (PC) it is important to know the significant lipids for the protein of choice. One example is ABCB10 a human mitochondrial ATP-transporter binding to CL [258; 259]. Membrane proteins are not such easy to purify as soluble proteins and some proteins can be inactive without the right phospholipid. So the lipid composition of the different expression systems like *E. coli*, *L. lactis* or yeast has to be known and maybe compared to the one of the host organism (Table 4) [260]. This knowledge helps the scientists to choose the right expression system for the membrane protein of interest.

Table 4: Phospholipid composition of three different used expression systems.

Organism	Phospholipids	Reference [260]
Escherichia coli	Inner membrane: PE 70 -80%; PG 15-20%; CL 5%	[261]
Lactococcus lactis	CL 48.9%; PC 33.1%; PG 6.9 %; LPC 5.4%; PE 3.2%; SM 1.4%; LPE 1%	Chapter IV
Saccharomyces cerevisiae	Plasma membrane: PC 17%; PE 20%; PI 18%; PS 34%; PA 4%; Cl 0.2% Mitochondrial membrane: PC 40%; PE 26%; PI 15%; PS 3%; PA 2%; CL 13%	[262]

The lipid composition of these bacteria and other used expression systems can be compared and the best expression system could be used for the membrane proteins expression. Some membrane proteins are known to need CL or PG for correct folding or activity [242; 263; 264]. So, an expression system containing these phospholipids should be used. If a wrong expression system is used this may result in a wrong folded purified protein and due to this the protein is inactive.

Comparing Gram-positive bacteria lipid compositions can be used to show that these bacteria are varying a lot in the composition (Chapter IV, Table 3). Even different treatment in the growth of bacteria can change the lipid composition of one organism like in *S. cereus*. For this bacteria it could be shown that the lipid composition is changed in different growth temperatures while at 37° C the PE value is 43 % the value increased at a growth temperature at 15 °C up to 70% [265]. Resulting in a high variety of composition.

Not only the membrane charge is depending of the lipid composition also the membrane curvature can be influenced by different phospholipids [241]. The head group and the hydrophobic tails have a high effect on the lipid shape and the curvature of the membrane [266]. The fluidity of the membrane can also have an influence on the system therefore the fatty acids are important. While long and saturated fatty acids make membranes thicker and less fluid, unsaturated fatty acids do the opposite [241; 242; 267]. All this causes different membranes which are important for proteins.

In *L. lactis* the major phospholipids are CL (48.9 %) and PC (33.1 %) so this system can be a candidate for overproduction of membrane proteins and especially mitochondrial proteins. CL is one major component in the inner mitochondrial membrane and it is known that some membrane proteins bind to CL like the ADP/ATP carrier, which is responsible for of ADP

transport into the mitochondria [258; 268]. Also, PC is a common phospholipid in membranes. Some proteins are known binding this phospholipid like the cytochrome bc_1 from yeast [269]. Comparing this to *E. coli* lipid composition of CL (5%) and no PC this could be an indication for inclusion bodies or misfolded mitochondrial membrane proteins expressed in *E. coli* [246; 249; 250; 255; 260; 261]. Based on the lipid composition in *L. lactis* it seems to be a good expression system for eukaryotic membrane proteins. The lipid composition can be one reason for the good expression results of mitochondrial membrane proteins in *L. lactis* [246; 249; 250; 258; 268].

The expression of proteins is not the only field for which the knowledge about major phospholipids could be helpful. It is also known that a change in lipids can results in a resistance against lantibiotics [67; 106]. Bacteria are able to change the lipids to be more resistant against drugs, like lantibiotics. To be able to see the reason for this resistance the difference in lipid composition to the non-resistant strain has to be verified.

In this thesis, a multi resistant *L. lactis* NZ9000 strain was identified and analysed (Chapter IV). This strain is resistant against several antibiotics and lantibiotics. To determine the reason for resistance several analyses were performed. All tested antibiotics and lantibiotics are targeting the cell wall synthesis so the peptidoglycan and the lipid composition was analysed. The reason for these analyses was the knowledge of other strains performing resistance with the help of a modified cell wall or cell membrane modification [67; 106]. The peptidoglycan, cell wall, analyses does not show significant modifications but in the lipid analysis it was able to determine a different lipid composition of the resistant strain compared to the original NZ9000. The changes were surprising as results did not match with a first hypothesis of changes. It was expected that the membrane is less negatively charged like it is published for *L. monocytogenes* Scott A. This strain developed a resistance against nisin because the membrane contains more PG than CL than a not resistant strain [67; 124]. Here the membrane contains more negative charged CL than the original strain. So, it is possible that this strain developed a new way of lipid composition change to perform a different kind of resistance. The effects like membrane fluidity or thickness were not tested in this thesis so this needs to be analysed in further studies to find the reason for the resistance. In sum, the composition of lipids has a big influence on organisms.

Knowing the lipid composition of *L. lactis* is one step forward to understand the influence of phospholipids in more detail. Based on composition an expression system can be chosen to reduce the possibility of inactive proteins only because an essential lipid is missing for the correct folding. Also, one highly resistant *L. lactis* strain was analysed which seems to

be resistant because of a changed lipid composition. Lipids have a huge influence in bacteria and understanding the function of lipid more in detail can change the understanding of membranes, membrane proteins and resistance mechanism of bacteria a lot.

5. Literature

[1] A. Fleming, On the antibacterial action of cultures of a penicillium, with special reference to their use in the isolation of *B. influenzae*. 1929. Bull World Health Organ 79 (2001) 780-90.
[2] A.H. van Hoek, D. Mevius, B. Guerra, P. Mullany, A.P. Roberts, and H.J. Aarts, Acquired antibiotic resistance genes: an overview. Front Microbiol 2 (2011) 203.
[3] A. Coates, Y. Hu, R. Bax, and C. Page, The future challenges facing the development of new antimicrobial drugs. Nat Rev Drug Discov 1 (2002) 895-910.
[4] A.R. Coates, G. Halls, and Y. Hu, Novel classes of antibiotics or more of the same? Br J Pharmacol 163 (2011) 184-94.
[5] G.S. Bbosa, N. Mwebaza, J. Odda, D.B. Kyegombe, and M. Ntale, Antibiotics/antibacterial drug use, their marketing and promotion during the post-antibiotic golden age and their role in emergence of bacterial resistance. Health 06 (2014) 410-425.
[6] A.M. Geddes, K.P. Klugman, and G.N. Rolinson, Introduction: historical perspective and development of amoxicillin/clavulanate. Int J Antimicrob Agents 30 Suppl 2 (2007) S109-12.
[7] M.A. Kohanski, D.J. Dwyer, and J.J. Collins, How antibiotics kill bacteria: from targets to networks. Nat Rev Microbiol 8 (2010) 423-35.
[8] G. Kapoor, S. Saigal, and A. Elongavan, Action and resistance mechanisms of antibiotics: A guide for clinicians. J Anaesthesiol Clin Pharmacol 33 (2017) 300-305.
[9] K. Drlica, and X. Zhao, DNA gyrase, topoisomerase IV, and the 4-quinolones. Microbiol Mol Biol Rev 61 (1997) 377-92.
[10] D.C. Hooper, Quinolone mode of action. Drugs 49 Suppl 2 (1995) 10-5.
[11] D.C. Hooper, Mechanisms of action and resistance of older and newer fluoroquinolones. Clin Infect Dis 31 Suppl 2 (2000) S24-8.
[12] S. Schwarz, C. Kehrenberg, B. Doublet, and A. Cloeckaert, Molecular basis of bacterial resistance to chloramphenicol and florfenicol. FEMS Microbiol Rev 28 (2004) 519-42.
[13] D. Moazed, and H.F. Noller, Chloramphenicol, erythromycin, carbomycin and vernamycin B protect overlapping sites in the peptidyl transferase region of 23S ribosomal RNA. Biochimie 69 (1987) 879-884.
[14] F. Schlunzen, R. Zarivach, J. Harms, A. Bashan, A. Tocilj, R. Albrecht, A. Yonath, and F. Franceschi, Structural basis for the interaction of antibiotics with the peptidyl transferase centre in *eubacteria*. Nature 413 (2001) 814-21.
[15] R.J. Henry, The Mode of Action of Sulfonamides. Bacteriol Rev 7 (1943) 175-262.
[16] A. Muller, A. Klockner, and T. Schneider, Targeting a cell wall biosynthesis hot spot. Nat Prod Rep 34 (2017) 909-932.
[17] K.F. Kong, L. Schneper, and K. Mathee, Beta-lactam antibiotics: from antibiosis to resistance and bacteriology. APMIS 118 (2010) 1-36.
[18] P. Fulco, and R.P. Wenzel, Ramoplanin: a topical lipoglycodepsipeptide antibacterial agent. Expert Rev Anti Infect Ther 4 (2006) 939-45.
[19] T. Pelaez, L. Alcala, R. Alonso, A. Martin-Lopez, V. Garcia-Arias, M. Marin, and E. Bouza, *In vitro* activity of ramoplanin against *Clostridium difficile*, including strains with reduced susceptibility to vancomycin or with resistance to metronidazole. Antimicrob Agents Chemother 49 (2005) 1157-9.
[20] L.P. Kotra, and S. Mobashery, β-Lactam antibiotics, β-lactamases and bacterial resistance. Bulletin de l'Institut Pasteur 96 (1998) 139-150.

[21] A.T. Terico, and J.C. Gallagher, Beta-lactam hypersensitivity and cross-reactivity. J Pharm Pract 27 (2014) 530-44.
[22] E.M. Wise, Jr., and J.T. Park, Penicillin: its basic site of action as an inhibitor of a peptide cross-linking reaction in cell wall mucopeptide synthesis. Proc Natl Acad Sci U S A 54 (1965) 75-81.
[23] D.J. Tipper, and J.L. Strominger, Mechanism of action of penicillins: a proposal based on their structural similarity to acyl-D-alanyl-D-alanine. Proc Natl Acad Sci U S A 54 (1965) 1133-41.
[24] M.S. Butler, K.A. Hansford, M.A. Blaskovich, R. Halai, and M.A. Cooper, Glycopeptide antibiotics: back to the future. J Antibiot (Tokyo) 67 (2014) 631-44.
[25] E. Binda, F. Marinelli, and G.L. Marcone, Old and New Glycopeptide Antibiotics: Action and Resistance. Antibiotics (Basel) 3 (2014) 572-94.
[26] J. Pootoolal, J. Neu, and G.D. Wright, Glycopeptide antibiotic resistance. Annu Rev Pharmacol Toxicol 42 (2002) 381-408.
[27] D.H. Williams, The glycopeptide story--how to kill the deadly 'superbugs'. Nat Prod Rep 13 (1996) 469-77.
[28] T. Schneider, A. Muller, H. Miess, and H. Gross, Cyclic lipopeptides as antibacterial agents - potent antibiotic activity mediated by intriguing mode of actions. Int J Med Microbiol 304 (2014) 37-43.
[29] B. Cavalleri, H. Pagani, G. Volpe, E. Selva, and F. Parenti, A-16686, a new antibiotic from *Actinoplanes* I. Fermentation, isolation and preliminary physico-chemical characteristics. The Journal of Antibiotics 37 (1984) 309-317.
[30] D.K. Farver, D.D. Hedge, and S.C. Lee, Ramoplanin: a lipoglycodepsipeptide antibiotic. Ann Pharmacother 39 (2005) 863-8.
[31] D.G. McCafferty, P. Cudic, B.A. Frankel, S. Barkallah, R.G. Kruger, and W. Li, Chemistry and biology of the ramoplanin family of peptide antibiotics. Biopolymers 66 (2002) 261-84.
[32] J.M. Willey, and W.A. van der Donk, Lantibiotics: peptides of diverse structure and function. Annu Rev Microbiol 61 (2007) 477-501.
[33] C. Chatterjee, M. Paul, L. Xie, and W.A. van der Donk, Biosynthesis and mode of action of lantibiotics. Chem Rev 105 (2005) 633-84.
[34] Y. Hu, J.S. Helm, L. Chen, X.Y. Ye, and S. Walker, Ramoplanin inhibits bacterial transglycosylases by binding as a dimer to lipid II. J Am Chem Soc 125 (2003) 8736-7.
[35] J.B. Hamburger, A.J. Hoertz, A. Lee, R.J. Senturia, D.G. McCafferty, and P.J. Loll, A crystal structure of a dimer of the antibiotic ramoplanin illustrates membrane positioning and a potential Lipid II docking interface. Proc Natl Acad Sci U S A 106 (2009) 13759-64.
[36] G.D. Wright, Molecular mechanisms of antibiotic resistance. Chem Commun (Camb) 47 (2011) 4055-61.
[37] J.M. Blair, M.A. Webber, A.J. Baylay, D.O. Ogbolu, and L.J. Piddock, Molecular mechanisms of antibiotic resistance. Nat Rev Microbiol 13 (2015) 42-51.
[38] N. Weston, P. Sharma, V. Ricci, and L.J.V. Piddock, Regulation of the AcrAB-TolC efflux pump in *Enterobacteriaceae*. Res Microbiol (2017).
[39] R.E. Hancock, and D.P. Speert, Antibiotic resistance in *Pseudomonas aeruginosa*: mechanisms and impact on treatment. Drug Resist Updat 3 (2000) 247-255.
[40] E.P. Abraham, and E. Chain, An Enzyme from Bacteria able to Destroy Penicillin. Nature 146 (1940) 837-837.
[41] R.P. Ambler, The structure of beta-lactamases. Philos Trans R Soc Lond B Biol Sci 289 (1980) 321-31.

[42] K. Bush, G.A. Jacoby, and A.A. Medeiros, A functional classification scheme for beta-lactamases and its correlation with molecular structure. Antimicrob Agents Chemother 39 (1995) 1211-33.
[43] H. Ozturk, E. Ozkirimli, and A. Ozgur, Classification of Beta-lactamases and penicillin binding proteins using ligand-centric network models. PLoS One 10 (2015) e0117874.
[44] G. Conrads, D.M. Citron, and E.J. Goldstein, Genetic determinant of intrinsic quinolone resistance in *Fusobacterium canifelinum*. Antimicrob Agents Chemother 49 (2005) 434-7.
[45] L.J.V. Piddock, Mechanisms of Fluoroquinolone Resistance: An Update 1994–1998. Drugs 58 (1999) 11-18.
[46] L.S. Redgrave, S.B. Sutton, M.A. Webber, and L.J. Piddock, Fluoroquinolone resistance: mechanisms, impact on bacteria, and role in evolutionary success. Trends Microbiol 22 (2014) 438-45.
[47] B. Weisblum, Erythromycin resistance by ribosome modification. Antimicrob Agents Chemother 39 (1995) 577-85.
[48] J.M. Munita, and C.A. Arias, Mechanisms of Antibiotic Resistance. Microbiol Spectr 4 (2016).
[49] C.T. Walsh, S.L. Fisher, I.S. Park, M. Prahalad, and Z. Wu, Bacterial resistance to vancomycin: five genes and one missing hydrogen bond tell the story. Chem Biol 3 (1996) 21-8.
[50] P.E. Reynolds, and P. Courvalin, Vancomycin resistance in *enterococci* due to synthesis of precursors terminating in D-alanyl-D-serine. Antimicrob Agents Chemother 49 (2005) 21-5.
[51] B. Perichon, and P. Courvalin, VanA-type vancomycin-resistant *Staphylococcus aureus*. Antimicrob Agents Chemother 53 (2009) 4580-7.
[52] P.D. Stapleton, and P.W. Taylor, Methicillin resistance in *Staphylococcus aureus*: mechanisms and modulation. Sci Prog 85 (2002) 57-72.
[53] J. Cleveland, T.J. Montville, I.F. Nes, and M.L. Chikindas, Bacteriocins: safe, natural antimicrobials for food preservation. Int J Food Microbiol 71 (2001) 1-20.
[54] P.D. Cotter, R.P. Ross, and C. Hill, Bacteriocins - a viable alternative to antibiotics? Nat Rev Microbiol 11 (2013) 95-105.
[55] R.E. Hancock, and R. Lehrer, Cationic peptides: a new source of antibiotics. Trends Biotechnol 16 (1998) 82-8.
[56] M. Malmsten, Antimicrobial peptides. Ups J Med Sci 119 (2014) 199-204.
[57] A.A. Bahar, and D. Ren, Antimicrobial peptides. Pharmaceuticals (Basel) 6 (2013) 1543-75.
[58] A. Fleming, On a Remarkable Bacteriolytic Element Found in Tissues and Secretions. Proceedings of the Royal Society B: Biological Sciences 93 (1922) 306-317.
[59] L.A. Rogers, The Inhibiting Effect of *Streptococcus Lactis* on *Lactobacillus Bulgaricus*. J Bacteriol 16 (1928) 321-5.
[60] E.O.W. L.A.Rogers, Limiting factors in the lactic fermentation. . Journal of bacteriology 16 (1928) 211-229.
[61] Z. Wang, and G. Wang, APD: the Antimicrobial Peptide Database. Nucleic Acids Res 32 (2004) D590-2.
[62] H. Jenssen, P. Hamill, and R.E. Hancock, Peptide antimicrobial agents. Clin Microbiol Rev 19 (2006) 491-511.
[63] M. Pasupuleti, A. Schmidtchen, and M. Malmsten, Antimicrobial peptides: key components of the innate immune system. Crit Rev Biotechnol 32 (2012) 143-71.
[64] D.G. Lee, D.H. Kim, Y. Park, H.K. Kim, H.N. Kim, Y.K. Shin, C.H. Choi, and K.S. Hahm, Fungicidal effect of antimicrobial peptide, PMAP-23, isolated from *porcine*

myeloid against *Candida albicans*. Biochem Biophys Res Commun 282 (2001) 570-4.
[65] J. Alberola, A. Rodriguez, O. Francino, X. Roura, L. Rivas, and D. Andreu, Safety and Efficacy of Antimicrobial Peptides against Naturally Acquired *Leishmaniasis*. Antimicrobial Agents and Chemotherapy 48 (2004) 641-643.
[66] M. Wachinger, A. Kleinschmidt, D. Winder, N. von Pechmann, A. Ludvigsen, M. Neumann, R. Holle, B. Salmons, V. Erfle, and R. Brack-Werner, Antimicrobial peptides melittin and cecropin inhibit replication of human immunodeficiency virus 1 by suppressing viral gene expression. J Gen Virol 79 (Pt 4) (1998) 731-40.
[67] K.L. Nawrocki, E.K. Crispell, and S.M. McBride, Antimicrobial Peptide Resistance Mechanisms of Gram-Positive Bacteria. Antibiotics (Basel) 3 (2014) 461-92.
[68] G. Diamond, N. Beckloff, A. Weinberg, and K.O. Kisich, The roles of antimicrobial peptides in innate host defense. Curr Pharm Des 15 (2009) 2377-92.
[69] J.D. Hale, and R.E. Hancock, Alternative mechanisms of action of cationic antimicrobial peptides on bacteria. Expert Rev Anti Infect Ther 5 (2007) 951-9.
[70] G. Wang, Improved methods for classification, prediction, and design of antimicrobial peptides. Methods Mol Biol 1268 (2015) 43-66.
[71] A. Giuliani, G. Pirri, and S. Nicoletto, Antimicrobial peptides: an overview of a promising class of therapeutics. Open Life Sciences 2 (2007) 1-33.
[72] H.G. Boman, Peptide antibiotics and their role in innate immunity. Annu Rev Immunol 13 (1995) 61-92.
[73] T.R. Klaenhammer, Genetics of bacteriocins produced by lactic acid bacteria. FEMS Microbiol Rev 12 (1993) 39-85.
[74] S.C. Yang, C.H. Lin, C.T. Sung, and J.Y. Fang, Antibacterial activities of bacteriocins: application in foods and pharmaceuticals. Front Microbiol 5 (2014) 241.
[75] E. Cascales, S.K. Buchanan, D. Duche, C. Kleanthous, R. Lloubes, K. Postle, M. Riley, S. Slatin, and D. Cavard, Colicin biology. Microbiol Mol Biol Rev 71 (2007) 158-229.
[76] C. Kleanthous, Swimming against the tide: progress and challenges in our understanding of colicin translocation. Nat Rev Microbiol 8 (2010) 843-8.
[77] S. Rebuffat, Microcins in action: amazing defence strategies of *Enterobacteria*. Biochem Soc Trans 40 (2012) 1456-62.
[78] K. Severinov, E. Semenova, A. Kazakov, T. Kazakov, and M.S. Gelfand, Low-molecular-weight post-translationally modified microcins. Mol Microbiol 65 (2007) 1380-94.
[79] P.D. Cotter, C. Hill, and R.P. Ross, Bacteriocins: developing innate immunity for food. Nat Rev Microbiol 3 (2005) 777-88.
[80] B. Jarvis, J. Jeffcoat, and G.C. Cheeseman, Molecular weight distribution of nisin. Biochimica et Biophysica Acta (BBA) - Protein Structure 168 (1968) 153-155.
[81] G. Bierbaum, C. Szekat, M. Josten, C. Heidrich, C. Kempter, G. Jung, and H.G. Sahl, Engineering of a novel thioether bridge and role of modified residues in the lantibiotic Pep5. Appl Environ Microbiol 62 (1996) 385-92.
[82] H.G. Sahl, and G. Bierbaum, Lantibiotics: biosynthesis and biological activities of uniquely modified peptides from gram-positive bacteria. Annu Rev Microbiol 52 (1998) 41-79.
[83] P.J. Knerr, and W.A. van der Donk, Discovery, biosynthesis, and engineering of lantipeptides. Annu Rev Biochem 81 (2012) 479-505.
[84] P.G. Arnison, M.J. Bibb, G. Bierbaum, A.A. Bowers, T.S. Bugni, G. Bulaj, J.A. Camarero, D.J. Campopiano, G.L. Challis, J. Clardy, P.D. Cotter, D.J. Craik, M. Dawson, E. Dittmann, S. Donadio, P.C. Dorrestein, K.D. Entian, M.A. Fischbach, J.S. Garavelli, U. Goransson, C.W. Gruber, D.H. Haft, T.K. Hemscheidt, C.

Hertweck, C. Hill, A.R. Horswill, M. Jaspars, W.L. Kelly, J.P. Klinman, O.P. Kuipers, A.J. Link, W. Liu, M.A. Marahiel, D.A. Mitchell, G.N. Moll, B.S. Moore, R. Muller, S.K. Nair, I.F. Nes, G.E. Norris, B.M. Olivera, H. Onaka, M.L. Patchett, J. Piel, M.J. Reaney, S. Rebuffat, R.P. Ross, H.G. Sahl, E.W. Schmidt, M.E. Selsted, K. Severinov, B. Shen, K. Sivonen, L. Smith, T. Stein, R.D. Sussmuth, J.R. Tagg, G.L. Tang, A.W. Truman, J.C. Vederas, C.T. Walsh, J.D. Walton, S.C. Wenzel, J.M. Willey, and W.A. van der Donk, Ribosomally synthesized and post-translationally modified peptide natural products: overview and recommendations for a universal nomenclature. Nat Prod Rep 30 (2013) 108-60.

[85] L. Xie, and W.A. van der Donk, Post-translational modifications during lantibiotic biosynthesis. Curr Opin Chem Biol 8 (2004) 498-507.

[86] O. Koponen, M. Tolonen, M. Qiao, G. Wahlstrom, J. Helin, and P.E. Saris, NisB is required for the dehydration and NisC for the lanthionine formation in the post-translational modification of nisin. Microbiology 148 (2002) 3561-8.

[87] Q. Zhang, Y. Yu, J.E. Velasquez, and W.A. van der Donk, Evolution of lanthipeptide synthetases. Proc Natl Acad Sci U S A 109 (2012) 18361-6.

[88] B. Li, J.P. Yu, J.S. Brunzelle, G.N. Moll, W.A. van der Donk, and S.K. Nair, Structure and mechanism of the lantibiotic cyclase involved in nisin biosynthesis. Science 311 (2006) 1464-7.

[89] N.M. Okeley, M. Paul, J.P. Stasser, N. Blackburn, and W.A. van der Donk, SpaC and NisC, the cyclases involved in subtilin and nisin biosynthesis, are zinc proteins. Biochemistry 42 (2003) 13613-24.

[90] S. Kodani, M.E. Hudson, M.C. Durrant, M.J. Buttner, J.R. Nodwell, and J.M. Willey, The SapB morphogen is a lantibiotic-like peptide derived from the product of the developmental gene *ramS* in *Streptomyces coelicolor*. Proc Natl Acad Sci U S A 101 (2004) 11448-53.

[91] A. Plat, A. Kuipers, R. Rink, and G. N. Moll, Mechanistic Aspects of Lanthipeptide Leaders. Current Protein & Peptide Science 14 (2013) 85-96.

[92] Y. Goto, B. Li, J. Claesen, Y. Shi, M.J. Bibb, and W.A. van der Donk, Discovery of unique lanthionine synthetases reveals new mechanistic and evolutionary insights. PLoS Biol 8 (2010) e1000339.

[93] G. Jung, Sahl, H.-G., Nisin and Novel Lantibiotics. Springer Netherlands (1991).

[94] M. Zasloff, Antimicrobial peptides of multicellular organisms. Nature 415 (2002) 389-95.

[95] L. Karam, C. Jama, N. Nuns, A.S. Mamede, P. Dhulster, and N.E. Chihib, Nisin adsorption on hydrophilic and hydrophobic surfaces: evidence of its interactions and antibacterial activity. J Pept Sci 19 (2013) 377-85.

[96] F.J. Van de Ven, H.W. Van den Hooven, R.N. Konings, and C.W. Hilbers, NMR studies of lantibiotics. The structure of nisin in aqueous solution. Eur J Biochem 202 (1991) 1181-8.

[97] E. Gross, and J.L. Morell, Nisin. The assignment of sulfide bridges of beta-methyllanthionine to a novel bicyclic structure of identical ring size. J Am Chem Soc 92 (1970) 2919-20.

[98] E. Gross, and J.L. Morell, The structure of nisin. J Am Chem Soc 93 (1971) 4634-5.

[99] I. Wiedemann, E. Breukink, C. van Kraaij, O.P. Kuipers, G. Bierbaum, B. de Kruijff, and H.G. Sahl, Specific binding of nisin to the peptidoglycan precursor lipid II combines pore formation and inhibition of cell wall biosynthesis for potent antibiotic activity. J Biol Chem 276 (2001) 1772-9.

[100] E. Breukink, and B. de Kruijff, Lipid II as a target for antibiotics. Nat Rev Drug Discov 5 (2006) 321-32.

[101] S.T. Hsu, E. Breukink, E. Tischenko, M.A. Lutters, B. de Kruijff, R. Kaptein, A.M. Bonvin, and N.A. van Nuland, The nisin-lipid II complex reveals a pyrophosphate cage that provides a blueprint for novel antibiotics. Nat Struct Mol Biol 11 (2004) 963-7.
[102] H.E. Hasper, B. de Kruijff, and E. Breukink, Assembly and stability of nisin-lipid II pores. Biochemistry 43 (2004) 11567-75.
[103] E. Breukink, C. van Kraaij, R.A. Demel, R.J. Siezen, O.P. Kuipers, and B. de Kruijff, The C-terminal region of nisin is responsible for the initial interaction of nisin with the target membrane. Biochemistry 36 (1997) 6968-76.
[104] E. Breukink, Use of the Cell Wall Precursor Lipid II by a Pore-Forming Peptide Antibiotic. Science 286 (1999) 2361-2364.
[105] A. Abts, A. Mavaro, J. Stindt, P.J. Bakkes, S. Metzger, A.J. Driessen, S.H. Smits, and L. Schmitt, Easy and rapid purification of highly active nisin. Int J Pept 2011 (2011) 175145.
[106] L.A. Draper, P.D. Cotter, C. Hill, and R.P. Ross, Lantibiotic resistance. Microbiol Mol Biol Rev 79 (2015) 171-91.
[107] V. Nizet, Antimicrobial peptide resistance mechanisms of human bacterial pathogens. Curr Issues Mol Biol 8 (2006) 11-26.
[108] R.E. Hancock, and A. Rozek, Role of membranes in the activities of antimicrobial cationic peptides. FEMS Microbiol Lett 206 (2002) 143-9.
[109] C. Bastos Mdo, M.L. Coelho, and O.C. Santos, Resistance to bacteriocins produced by Gram-positive bacteria. Microbiology 161 (2015) 683-700.
[110] J.B. Ward, Teichoic and teichuronic acids: biosynthesis, assembly, and location. Microbiol Rev 45 (1981) 211-43.
[111] C. Weidenmaier, S. Kristian, and A. Peschel, Bacterial Resistance to Antimicrobial Host Defenses - An Emerging Target for Novel Antiinfective Strategies? Current Drug Targets 4 (2003) 643-649.
[112] C. Weidenmaier, and A. Peschel, Teichoic acids and related cell-wall glycopolymers in Gram-positive physiology and host interactions. Nat Rev Microbiol 6 (2008) 276-87.
[113] A. Peschel, M. Otto, R.W. Jack, H. Kalbacher, G. Jung, and F. Gotz, Inactivation of the dlt operon in *Staphylococcus aureus* confers sensitivity to defensins, protegrins, and other antimicrobial peptides. J Biol Chem 274 (1999) 8405-10.
[114] S.M. McBride, and A.L. Sonenshein, The dlt operon confers resistance to cationic antimicrobial peptides in *Clostridium difficile*. Microbiology 157 (2011) 1457-65.
[115] E. Abachin, C. Poyart, E. Pellegrini, E. Milohanic, F. Fiedler, P. Berche, and P. Trieu-Cuot, Formation of D-alanyl-lipoteichoic acid is required for adhesion and virulence of *Listeria monocytogenes*. Mol Microbiol 43 (2002) 1-14.
[116] M. Perego, P. Glaser, A. Minutello, M.A. Strauch, K. Leopold, and W. Fischer, Incorporation of D-alanine into lipoteichoic acid and wall teichoic acid in *Bacillus subtilis*. Identification of genes and regulation. J Biol Chem 270 (1995) 15598-606.
[117] M. Kovacs, A. Halfmann, I. Fedtke, M. Heintz, A. Peschel, W. Vollmer, R. Hakenbeck, and R. Bruckner, A functional *dlt* operon, encoding proteins required for incorporation of d-alanine in teichoic acids in gram-positive bacteria, confers resistance to cationic antimicrobial peptides in *Streptococcus pneumoniae*. J Bacteriol 188 (2006) 5797-805.
[118] Z. Abi Khattar, A. Rejasse, D. Destoumieux-Garzon, J.M. Escoubas, V. Sanchis, D. Lereclus, A. Givaudan, M. Kallassy, C. Nielsen-Leroux, and S. Gaudriault, The *dlt* operon of *Bacillus cereus* is required for resistance to cationic antimicrobial peptides and for virulence in insects. J Bacteriol 191 (2009) 7063-73.

[119] F.C. Neuhaus, and J. Baddiley, A Continuum of Anionic Charge: Structures and Functions of D-Alanyl-Teichoic Acids in Gram-Positive Bacteria. Microbiology and Molecular Biology Reviews 67 (2003) 686-723.

[120] B. Schwartz, J.A. Markwalder, and Y. Wang, Lipid II: total synthesis of the bacterial cell wall precursor and utilization as a substrate for glycosyltransfer and transpeptidation by penicillin binding protein (PBP) 1b of *Escherichia coli*. J Am Chem Soc 123 (2001) 11638-43.

[121] N.E. Kramer, S.A. van Hijum, J. Knol, J. Kok, and O.P. Kuipers, Transcriptome analysis reveals mechanisms by which *Lactococcus lactis* acquires nisin resistance. Antimicrob Agents Chemother 50 (2006) 1753-61.

[122] A. Gravesen, K. Sorensen, F.M. Aarestrup, and S. Knochel, Spontaneous nisin-resistant *Listeria monocytogenes* mutants with increased expression of a putative penicillin-binding protein and their sensitivity to various antibiotics. Microb Drug Resist 7 (2001) 127-35.

[123] R.P. Huijbregts, A.I. de Kroon, and B. de Kruijff, Topology and transport of membrane lipids in bacteria. Biochim Biophys Acta 1469 (2000) 43-61.

[124] A. Verheul, N.J. Russell, T.H.R. Van, F.M. Rombouts, and T. Abee, Modifications of membrane phospholipid composition in nisin-resistant *Listeria monocytogenes* Scott A. Appl Environ Microbiol 63 (1997) 3451-7.

[125] X. Ming, and M.A. Daeschel, Nisin Resistance of Foodborne Bacteria and the Specific Resistance Responses of *Listeria monocytogenes* Scott A. Journal of Food Protection 56 (1993) 944-948.

[126] A.S. Mazzotta, and T.J. Montville, Nisin induces changes in membrane fatty acid composition of *Listeria monocytogenes* nisin-resistant strains at 10 °C and 30 °C. J Appl Microbiol 82 (1997) 32-8.

[127] B. Martinez, and A. Rodriguez, Antimicrobial susceptibility of nisin resistant *Listeria monocytogenes* of dairy origin. FEMS Microbiol Lett 252 (2005) 67-72.

[128] A. Peschel, R.W. Jack, M. Otto, L.V. Collins, P. Staubitz, G. Nicholson, H. Kalbacher, W.F. Nieuwenhuizen, G. Jung, A. Tarkowski, K.P. van Kessel, and J.A. van Strijp, *Staphylococcus aureus* resistance to human defensins and evasion of neutrophil killing via the novel virulence factor MprF is based on modification of membrane lipids with l-lysine. J Exp Med 193 (2001) 1067-76.

[129] C.M. Ernst, P. Staubitz, N.N. Mishra, S.J. Yang, G. Hornig, H. Kalbacher, A.S. Bayer, D. Kraus, and A. Peschel, The bacterial defensin resistance protein MprF consists of separable domains for lipid lysinylation and antimicrobial peptide repulsion. PLoS Pathog 5 (2009) e1000660.

[130] C.M. Ernst, and A. Peschel, Broad-spectrum antimicrobial peptide resistance by MprF-mediated aminoacylation and flipping of phospholipids. Mol Microbiol 80 (2011) 290-9.

[131] S.A. Kristian, M. Durr, J.A.G. Van Strijp, B. Neumeister, and A. Peschel, MprF-Mediated Lysinylation of Phospholipids in *Staphylococcus aureus* Leads to Protection against Oxygen-Independent Neutrophil Killing. Infection and Immunity 71 (2003) 546-549.

[132] P. Staubitz, and A. Peschel, MprF-mediated lysinylation of phospholipids in *Bacillus subtilis* – protection against bacteriocins in terrestrial habitats? Microbiology 148 (2002) 3331-3332.

[133] E. Maloney, D. Stankowska, J. Zhang, M. Fol, Q.J. Cheng, S. Lun, W.R. Bishai, M. Rajagopalan, D. Chatterjee, and M.V. Madiraju, The two-domain LysX protein of *Mycobacterium tuberculosis* is required for production of lysinylated phosphatidylglycerol and resistance to cationic antimicrobial peptides. PLoS Pathog 5 (2009) e1000534.

[134] R.J. Heath, and C.O. Rock, Enoyl-acyl carrier protein reductase (fabI) plays a determinant role in completing cycles of fatty acid elongation in *Escherichia coli*. J Biol Chem 270 (1995) 26538-42.
[135] S. Gebhard, ABC transporters of antimicrobial peptides in *Firmicutes* bacteria - phylogeny, function and regulation. Mol Microbiol 86 (2012) 1295-317.
[136] A.M. Stock, V.L. Robinson, and P.N. Goudreau, Two-component signal transduction. Annu Rev Biochem 69 (2000) 183-215.
[137] T. Mascher, Intramembrane-sensing histidine kinases: a new family of cell envelope stress sensors in *Firmicutes* bacteria. FEMS Microbiol Lett 264 (2006) 133-44.
[138] R. Ohki, Giyanto, K. Tateno, W. Masuyama, S. Moriya, K. Kobayashi, and N. Ogasawara, The BceRS two-component regulatory system induces expression of the bacitracin transporter, BceAB, in *Bacillus subtilis*. Molecular Microbiology 49 (2003) 1135-1144.
[139] T. Mascher, N.G. Margulis, T. Wang, R.W. Ye, and J.D. Helmann, Cell wall stress responses in *Bacillus subtilis*: the regulatory network of the bacitracin stimulon. Molecular Microbiology 50 (2003) 1591-1604.
[140] S. Dintner, A. Staron, E. Berchtold, T. Petri, T. Mascher, and S. Gebhard, Coevolution of ABC transporters and two-component regulatory systems as resistance modules against antimicrobial peptides in *Firmicutes* Bacteria. J Bacteriol 193 (2011) 3851-62.
[141] L.C. Wang, L.K. Morgan, P. Godakumbura, L.J. Kenney, and G.S. Anand, The inner membrane histidine kinase EnvZ senses osmolality via helix-coil transitions in the cytoplasm. EMBO J 31 (2012) 2648-59.
[142] S. Jordan, A. Junker, J.D. Helmann, and T. Mascher, Regulation of LiaRS-dependent gene expression in *bacillus subtilis*: identification of inhibitor proteins, regulator binding sites, and target genes of a conserved cell envelope stress-sensing two-component system. J Bacteriol 188 (2006) 5153-66.
[143] M. Kawada-Matsuo, Y. Yoshida, T. Zendo, J. Nagao, Y. Oogai, Y. Nakamura, K. Sonomoto, N. Nakamura, and H. Komatsuzawa, Three distinct two-component systems are involved in resistance to the class I bacteriocins, Nukacin ISK-1 and nisin A, in *Staphylococcus aureus*. PLoS One 8 (2013) e69455.
[144] T.M. Bergholz, S. Tang, M. Wiedmann, and K.J. Boor, Nisin resistance of *Listeria monocytogenes* is increased by exposure to salt stress and is mediated via LiaR. Appl Environ Microbiol 79 (2013) 5682-8.
[145] M. O'Connell-Motherway, D. van Sinderen, F. Morel-Deville, G.F. Fitzgerald, S.D. Ehrlich, and P. Morel, Six putative two-component regulatory systems isolated from *Lactococcus lactis subsp. cremoris* MG1363. Microbiology 146 (Pt 4) (2000) 935-47.
[146] T. Mascher, S.L. Zimmer, T.A. Smith, and J.D. Helmann, Antibiotic-inducible promoter regulated by the cell envelope stress-sensing two-component system LiaRS of *Bacillus subtilis*. Antimicrob Agents Chemother 48 (2004) 2888-96.
[147] L. Schmitt, and R. Tampe, Structure and mechanism of ABC transporters. Curr Opin Struct Biol 12 (2002) 754-60.
[148] E. Rietkotter, D. Hoyer, and T. Mascher, Bacitracin sensing in *Bacillus subtilis*. Mol Microbiol 68 (2008) 768-85.
[149] Y. Yoshida, M. Matsuo, Y. Oogai, F. Kato, N. Nakamura, M. Sugai, and H. Komatsuzawa, Bacitracin sensing and resistance in *Staphylococcus aureus*. FEMS Microbiol Lett 320 (2011) 33-9.
[150] A. Staron, D.E. Finkeisen, and T. Mascher, Peptide antibiotic sensing and detoxification modules of *Bacillus subtilis*. Antimicrob Agents Chemother 55 (2011) 515-25.

[151] H. Tsuda, Y. Yamashita, Y. Shibata, Y. Nakano, and T. Koga, Genes Involved in Bacitracin Resistance in *Streptococcus mutans*. Antimicrobial Agents and Chemotherapy 46 (2002) 3756-3764.
[152] R. Clemens, J. Zaschke-Kriesche, S. Khosa, and S.H.J. Smits, Insight into Two ABC Transporter Families Involved in Lantibiotic Resistance. Front Mol Biosci 4 (2017) 91.
[153] M. Otto, A. Peschel, and F. Gotz, Producer self-protection against the lantibiotic epidermin by the ABC transporter EpiFEG of *Staphylococcus epidermidis* Tu3298. FEMS Microbiol Lett 166 (1998) 203-11.
[154] T. Stein, S. Heinzmann, I. Solovieva, and K.D. Entian, Function of *Lactococcus lactis* nisin immunity genes *nisI* and *nisFEG* after coordinated expression in the surrogate host *Bacillus subtilis*. J Biol Chem 278 (2003) 89-94.
[155] T. Stein, S. Heinzmann, S. Dusterhus, S. Borchert, and K.D. Entian, Expression and functional analysis of the subtilin immunity genes *spaIFEG* in the subtilin-sensitive host *Bacillus subtilis* MO1099. J Bacteriol 187 (2005) 822-8.
[156] K. Okuda, Y. Aso, J. Nakayama, and K. Sonomoto, Cooperative transport between NukFEG and NukH in immunity against the lantibiotic nukacin ISK-1 produced by *Staphylococcus warneri* ISK-1. J Bacteriol 190 (2008) 356-62.
[157] J.M. Suarez, A.N. Edwards, and S.M. McBride, The *Clostridium difficile cpr* locus is regulated by a noncontiguous two-component system in response to type A and B lantibiotics. J Bacteriol 195 (2013) 2621-31.
[158] S.M. McBride, and A.L. Sonenshein, Identification of a genetic locus responsible for antimicrobial peptide resistance in *Clostridium difficile*. Infect Immun 79 (2011) 167-76.
[159] M. Kawada-Matsuo, Y. Oogai, T. Zendo, J. Nagao, Y. Shibata, Y. Yamashita, Y. Ogura, T. Hayashi, K. Sonomoto, and H. Komatsuzawa, Involvement of the novel two-component NsrRS and LcrRS systems in distinct resistance pathways against nisin A and nukacin ISK-1 in *Streptococcus mutans*. Appl Environ Microbiol 79 (2013) 4751-5.
[160] Z. Alkhatib, A. Abts, A. Mavaro, L. Schmitt, and S.H. Smits, Lantibiotics: how do producers become self-protected? J Biotechnol 159 (2012) 145-54.
[161] R. Ra, M.M. Beerthuyzen, W.M. de Vos, P.E. Saris, and O.P. Kuipers, Effects of gene disruptions in the nisin gene cluster of *Lactococcus lactis* on nisin production and producer immunity. Microbiology 145 (Pt 5) (1999) 1227-33.
[162] Z. AlKhatib, M. Lagedroste, I. Fey, D. Kleinschrodt, A. Abts, and S.H. Smits, Lantibiotic immunity: inhibition of nisin mediated pore formation by NisI. PLoS One 9 (2014) e102246.
[163] Z. AlKhatib, M. Lagedroste, J. Zaschke, M. Wagner, A. Abts, I. Fey, D. Kleinschrodt, and S.H. Smits, The C-terminus of nisin is important for the ABC transporter NisFEG to confer immunity in *Lactococcus lactis*. Microbiologyopen 3 (2014) 752-63.
[164] C. Klein, and K.D. Entian, Genes involved in self-protection against the lantibiotic subtilin produced by *Bacillus subtilis* ATCC 6633. Appl Environ Microbiol 60 (1994) 2793-801.
[165] A. Peschel, and F. Gotz, Analysis of the *Staphylococcus epidermidis* genes *epiF*, *-E*, and *-G* involved in epidermin immunity. J Bacteriol 178 (1996) 531-6.
[166] A. Peschel, N. Schnell, M. Hille, K.D. Entian, and F. Gotz, Secretion of the lantibiotics epidermin and gallidermin: sequence analysis of the genes *gdmT* and *gdmH*, their influence on epidermin production and their regulation by EpiQ v. 254 (1997).

[167] S.R. Ra, M. Qiao, T. Immonen, I. Pujana, and E.J. Saris, Genes responsible for nisin synthesis, regulation and immunity form a regulon of two operons and are induced by nisin in *Lactoccocus lactis* N8. Microbiology 142 (Pt 5) (1996) 1281-8.
[168] A.J. van Heel, T.G. Kloosterman, M. Montalban-Lopez, J. Deng, A. Plat, B. Baudu, D. Hendriks, G.N. Moll, and O.P. Kuipers, Discovery, Production and Modification of Five Novel Lantibiotics Using the Promiscuous Nisin Modification Machinery. ACS Synth Biol 5 (2016) 1146-1154.
[169] S. Khosa, Z. AlKhatib, and S.H. Smits, NSR from *Streptococcus agalactiae* confers resistance against nisin and is encoded by a conserved *nsr* operon. Biol Chem 394 (2013) 1543-9.
[170] J. Reiners, M. Lagedroste, K. Ehlen, S. Leusch, J. Zaschke-Kriesche, and S.H.J. Smits, The N-terminal Region of Nisin Is Important for the BceAB-Type ABC Transporter NsrFP from *Streptococcus agalactiae* COH1. Front Microbiol 8 (2017) 1643.
[171] S. Khosa, B. Frieg, D. Mulnaes, D. Kleinschrodt, A. Hoeppner, H. Gohlke, and S.H. Smits, Structural basis of lantibiotic recognition by the nisin resistance protein from *Streptococcus agalactiae*. Sci Rep 6 (2016) 18679.
[172] Z. Sun, J. Zhong, X. Liang, J. Liu, X. Chen, and L. Huan, Novel mechanism for nisin resistance via proteolytic degradation of nisin by the nisin resistance protein NSR. Antimicrob Agents Chemother 53 (2009) 1964-73.
[173] L.M. Repka, J.R. Chekan, S.K. Nair, and W.A. van der Donk, Mechanistic Understanding of Lanthipeptide Biosynthetic Enzymes. Chem Rev 117 (2017) 5457-5520.
[174] R. Pozzi, M. Coles, D. Linke, A. Kulik, M. Nega, W. Wohlleben, and E. Stegmann, Distinct mechanisms contribute to immunity in the lantibiotic NAI-107 producer strain *Microbispora* ATCC PTA-5024. Environ Microbiol 18 (2016) 118-32.
[175] S. Khosa, M. Lagedroste, and S.H. Smits, Protein Defense Systems against the Lantibiotic Nisin: Function of the Immunity Protein NisI and the Resistance Protein NSR. Front Microbiol 7 (2016) 504.
[176] P.M. Sharp, and B.H. Hahn, Origins of HIV and the AIDS pandemic. Cold Spring Harb Perspect Med 1 (2011) a006841.
[177] E.O. Freed, HIV-1 assembly, release and maturation. Nat Rev Microbiol 13 (2015) 484-96.
[178] S. Modrow, Molekulare Virologie. (2010).
[179] G. Yang, and X. Xiong, Viral infectivity factor: a novel therapeutic strategy to block HIV-1 replication. Mini Rev Med Chem 13 (2013) 1047-55.
[180] G. Maartens, C. Celum, and S.R. Lewin, HIV infection: epidemiology, pathogenesis, treatment, and prevention. The Lancet 384 (2014) 258-271.
[181] A.D. Frankel, and J.A. Young, HIV-1: fifteen proteins and an RNA. Annu Rev Biochem 67 (1998) 1-25.
[182] N.M. Bell, and A.M. Lever, HIV Gag polyprotein: processing and early viral particle assembly. Trends Microbiol 21 (2013) 136-44.
[183] E.O. Freed, HIV-1 gag proteins: diverse functions in the virus life cycle. Virology 251 (1998) 1-15.
[184] J. Nkeze, L. Li, Z. Benko, G. Li, and R.Y. Zhao, Molecular characterization of HIV-1 genome in fission yeast *Schizosaccharomyces pombe*. Cell Biosci 5 (2015) 47.
[185] R.H. Miller, and N. Sarver, HIV accessory proteins as therapeutic targets. Nature Medicine 3 (1997) 389-394.
[186] D. Trono, HIV accessory proteins: leading roles for the supporting cast. Cell 82 (1995) 189-92.
[187] M. Emerman, HIV-1 Regulatory/Accessory Genes: Keys to Unraveling Viral and Host Cell Biology. Science 280 (1998) 1880-1884.

[188] M. Emerman, HIV-1, Vpr and the cell cycle. Current Biology 6 (1996) 1096-1103.
[189] M. Kogan, and J. Rappaport, HIV-1 accessory protein Vpr: relevance in the pathogenesis of HIV and potential for therapeutic intervention. Retrovirology 8 (2011) 25.
[190] R.A. Lamb, and L.H. Pinto, Do Vpu and Vpr of human immunodeficiency virus type 1 and NB of influenza B virus have ion channel activities in the viral life cycles? Virology 229 (1997) 1-11.
[191] A. Bagashev, and B.E. Sawaya, Roles and functions of HIV-1 Tat protein in the CNS: an overview. Virol J 10 (2013) 358.
[192] M. Zhou, M.A. Halanski, M.F. Radonovich, F. Kashanchi, J. Peng, D.H. Price, and J.N. Brady, Tat modifies the activity of CDK9 to phosphorylate serine 5 of the RNA polymerase II carboxyl-terminal domain during human immunodeficiency virus type 1 transcription. Mol Cell Biol 20 (2000) 5077-86.
[193] L.S. Turner, HIV Tat, xPharm: The Comprehensive Pharmacology Reference, Elsevier, New York, 2008, pp. 1-2.
[194] J. Fernandes, B. Jayaraman, and A. Frankel, The HIV-1 Rev response element: an RNA scaffold that directs the cooperative assembly of a homo-oligomeric ribonucleoprotein complex. RNA Biol 9 (2012) 6-11.
[195] M. Bentham, S. Mazaleyrat, and M. Harris, Role of myristoylation and N-terminal basic residues in membrane association of the human immunodeficiency virus type 1 Nef protein. J Gen Virol 87 (2006) 563-71.
[196] M. Williams, J.F. Roeth, M.R. Kasper, R.I. Fleis, C.G. Przybycin, and K.L. Collins, Direct Binding of Human Immunodeficiency Virus Type 1 Nef to the Major Histocompatibility Complex Class I (MHC-I) Cytoplasmic Tail Disrupts MHC-I Trafficking. Journal of Virology 76 (2002) 12173-12184.
[197] A. Rosa, A. Chande, S. Ziglio, V. De Sanctis, R. Bertorelli, S.L. Goh, S.M. McCauley, A. Nowosielska, S.E. Antonarakis, J. Luban, F.A. Santoni, and M. Pizzato, HIV-1 Nef promotes infection by excluding SERINC5 from virion incorporation. Nature 526 (2015) 212-7.
[198] P. Henklein, R. Kinder, U. Schubert, and B. Bechinger, Membrane interactions and alignment of structures within the HIV-1 Vpu cytoplasmic domain: effect of phosphorylation of serines 52 and 56. FEBS Letters 482 (2000) 220-224.
[199] M. Widera, F. Hillebrand, S. Erkelenz, A.A. Vasudevan, C. Munk, and H. Schaal, A functional conserved intronic G run in HIV-1 intron 3 is critical to counteract APOBEC3G-mediated host restriction. Retrovirology 11 (2014) 72.
[200] J.F. Arias, T. Koyama, M. Kinomoto, and K. Tokunaga, Retroelements versus APOBEC3 family members: No great escape from the magnificent seven. Front Microbiol 3 (2012) 275.
[201] J.D. Salter, R.P. Bennett, and H.C. Smith, The APOBEC Protein Family: United by Structure, Divergent in Function. Trends Biochem Sci 41 (2016) 578-594.
[202] R.S. LaRue, S.R. Jonsson, K.A. Silverstein, M. Lajoie, D. Bertrand, N. El-Mabrouk, I. Hotzel, V. Andresdottir, T.P. Smith, and R.S. Harris, The artiodactyl APOBEC3 innate immune repertoire shows evidence for a multi-functional domain organization that existed in the ancestor of placental mammals. BMC Mol Biol 9 (2008) 104.
[203] C. Munk, A. Willemsen, and I.G. Bravo, An ancient history of gene duplications, fusions and losses in the evolution of APOBEC3 mutators in mammals. BMC Evol Biol 12 (2012) 71.
[204] H.C. Smith, R.P. Bennett, A. Kizilyer, W.M. McDougall, and K.M. Prohaska, Functions and regulation of the APOBEC family of proteins. Semin Cell Dev Biol 23 (2012) 258-68.

[205] B. Romani, S. Engelbrecht, and R.H. Glashoff, Antiviral roles of APOBEC proteins against HIV-1 and suppression by Vif. Arch Virol 154 (2009) 1579-88.
[206] J.M. Binning, A.M. Smith, J.F. Hultquist, C.S. Craik, N. Caretta Cartozo, M.G. Campbell, L. Burton, F. La Greca, M.J. McGregor, H.M. Ta, K. Bartholomeeusen, B.M. Peterlin, N.J. Krogan, N. Sevillano, Y. Cheng, and J.D. Gross, Fab-based inhibitors reveal ubiquitin independent functions for HIV Vif neutralization of APOBEC3 restriction factors. PLoS Pathog 14 (2018) e1006830.
[207] X. Yu, Y. Yu, B. Liu, K. Luo, W. Kong, P. Mao, and X.F. Yu, Induction of APOBEC3G ubiquitination and degradation by an HIV-1 Vif-Cul5-SCF complex. Science 302 (2003) 1056-60.
[208] A. Mehle, J. Goncalves, M. Santa-Marta, M. McPike, and D. Gabuzda, Phosphorylation of a novel SOCS-box regulates assembly of the HIV-1 Vif-Cul5 complex that promotes APOBEC3G degradation. Genes Dev 18 (2004) 2861-6.
[209] A. Mehle, B. Strack, P. Ancuta, C. Zhang, M. McPike, and D. Gabuzda, Vif overcomes the innate antiviral activity of APOBEC3G by promoting its degradation in the ubiquitin-proteasome pathway. J Biol Chem 279 (2004) 7792-8.
[210] P. Barraud, J.C. Paillart, R. Marquet, and C. Tisne, Advances in the structural understanding of Vif proteins. Curr HIV Res 6 (2008) 91-9.
[211] R.A. Russell, and V.K. Pathak, Identification of two distinct human immunodeficiency virus type 1 Vif determinants critical for interactions with human APOBEC3G and APOBEC3F. J Virol 81 (2007) 8201-10.
[212] A. Mehle, H. Wilson, C. Zhang, A.J. Brazier, M. McPike, E. Pery, and D. Gabuzda, Identification of an APOBEC3G binding site in human immunodeficiency virus type 1 Vif and inhibitors of Vif-APOBEC3G binding. J Virol 81 (2007) 13235-41.
[213] Z. He, W. Zhang, G. Chen, R. Xu, and X.F. Yu, Characterization of conserved motifs in HIV-1 Vif required for APOBEC3G and APOBEC3F interaction. J Mol Biol 381 (2008) 1000-11.
[214] H. Wang, B. Liu, X. Liu, Z. Li, X.F. Yu, and W. Zhang, Identification of HIV-1 Vif regions required for CBF-beta interaction and APOBEC3 suppression. PLoS One 9 (2014) e95738.
[215] Z. Xiao, E. Ehrlich, Y. Yu, K. Luo, T. Wang, C. Tian, and X.F. Yu, Assembly of HIV-1 Vif-Cul5 E3 ubiquitin ligase through a novel zinc-binding domain-stabilized hydrophobic interface in Vif. Virology 349 (2006) 290-9.
[216] A. Mehle, E.R. Thomas, K.S. Rajendran, and D. Gabuzda, A zinc-binding region in Vif binds Cul5 and determines cullin selection. J Biol Chem 281 (2006) 17259-65.
[217] Y. Yu, Z. Xiao, E.S. Ehrlich, X. Yu, and X.F. Yu, Selective assembly of HIV-1 Vif-Cul5-ElonginB-ElonginC E3 ubiquitin ligase complex through a novel SOCS box and upstream cysteines. Genes Dev 18 (2004) 2867-72.
[218] N.A. Christ, S. Bochmann, D. Gottstein, E. Duchardt-Ferner, U.A. Hellmich, S. Dusterhus, P. Kotter, P. Guntert, K.D. Entian, and J. Wohnert, The First structure of a lantibiotic immunity protein, SpaI from *Bacillus subtilis*, reveals a novel fold. J Biol Chem 287 (2012) 35286-98.
[219] J.H. Jeong, and S.C. Ha, Crystal Structure of NisI in a Lipid-Free Form, the Nisin Immunity Protein, from *Lactococcus lactis*. Antimicrob Agents Chemother 62 (2018).
[220] C. Hacker, N.A. Christ, E. Duchardt-Ferner, S. Korn, C. Gobl, L. Berninger, S. Dusterhus, U.A. Hellmich, T. Madl, P. Kotter, K.D. Entian, and J. Wohnert, The Solution Structure of the Lantibiotic Immunity Protein NisI and Its Interactions with Nisin. J Biol Chem 290 (2015) 28869-86.
[221] T.M. Takala, and P.E. Saris, C-terminus of NisI provides specificity to nisin. Microbiology 152 (2006) 3543-9.

[222] M.C. Thompson, N.M. Wheatley, J. Jorda, M.R. Sawaya, S.D. Gidaniyan, H. Ahmed, Z. Yang, K.N. McCarty, J.P. Whitelegge, and T.O. Yeates, Identification of a unique Fe-S cluster binding site in a glycyl-radical type microcompartment shell protein. J Mol Biol 426 (2014) 3287-3304.
[223] S. Nath, R. Banerjee, and U. Sen, A novel 8-nm protein cage formed by *Vibrio cholerae* acylphosphatase. J Mol Biol 426 (2014) 36-8.
[224] D.H. Shin, Y. Lou, J. Jancarik, H. Yokota, R. Kim, and S.H. Kim, Crystal structure of TM1457 from *Thermotoga maritima*. J Struct Biol 152 (2005) 113-7.
[225] B.E. Jones, P. Rajagopal, and R.E. Klevit, Phosphorylation on histidine is accompanied by localized structural changes in the phosphocarrier protein, HPr from *Bacillus subtilis*. Protein Sci 6 (1997) 2107-19.
[226] I. Kufareva, and R. Abagyan, Methods of protein structure comparison. Methods Mol Biol 857 (2012) 231-57.
[227] D. Ajdic, W.M. McShan, R.E. McLaughlin, G. Savic, J. Chang, M.B. Carson, C. Primeaux, R. Tian, S. Kenton, H. Jia, S. Lin, Y. Qian, S. Li, H. Zhu, F. Najar, H. Lai, J. White, B.A. Roe, and J.J. Ferretti, Genome sequence of *Streptococcus mutans* UA159, a cariogenic dental pathogen. Proc Natl Acad Sci U S A 99 (2002) 14434-9.
[228] G.L. Archer, *Staphylococcus aureus*: A Well–Armed Pathogen. Clinical Infectious Diseases 26 (1998) 1179-1181.
[229] M. Prudhomme, L. Attaiech, G. Sanchez, B. Martin, and J.P. Claverys, Antibiotic stress induces genetic transformability in the human pathogen *Streptococcus pneumoniae*. Science 313 (2006) 89-92.
[230] E.A. Wall, J.H. Caufield, C.E. Lyons, K.A. Manning, T. Dokland, and G.E. Christie, Specific N-terminal cleavage of ribosomal protein L27 in *Staphylococcus aureus* and related bacteria. Mol Microbiol 95 (2015) 258-69.
[231] S. Verma, R. Dixit, and K.C. Pandey, Cysteine Proteases: Modes of Activation and Future Prospects as Pharmacological Targets. Front Pharmacol 7 (2016) 107.
[232] A.J. van Heel, A. de Jong, M. Montalban-Lopez, J. Kok, and O.P. Kuipers, BAGEL3: Automated identification of genes encoding bacteriocins and (non-)bactericidal posttranslationally modified peptides. Nucleic Acids Res 41 (2013) W448-53.
[233] C.P. Rosewarne, P. Greenfield, D. Li, N. Tran-Dinh, M.I. Bradbury, D.J. Midgley, and P. Hendry, Draft Genome Sequence of *Clostridium sp. Maddingley*, Isolated from Coal-Seam Gas Formation Water. Genome Announc 1 (2013).
[234] P. Agrawal, S. Khater, M. Gupta, N. Sain, and D. Mohanty, RiPPMiner: a bioinformatics resource for deciphering chemical structures of RiPPs based on prediction of cleavage and cross-links. Nucleic Acids Res 45 (2017) W80-W88.
[235] E. Breukink, I. Wiedemann, C. van Kraaij, O.P. Kuipers, H.G. Sahl, and B. de Kruijff, Use of the cell wall precursor lipid II by a pore-forming peptide antibiotic. Science 286 (1999) 2361-4.
[236] J.I. Rood, and S.T. Cole, Molecular genetics and pathogenesis of *Clostridium perfringens*. Microbiol Rev 55 (1991) 621-48.
[237] A. Ofosu, *Clostridium difficile* infection: a review of current and emerging therapies. Ann Gastroenterol 29 (2016) 147-54.
[238] D.A. Leffler, and J.T. Lamont, *Clostridium difficile* infection. N Engl J Med 372 (2015) 1539-48.
[239] A. Mavaro, A. Abts, P.J. Bakkes, G.N. Moll, A.J. Driessen, S.H. Smits, and L. Schmitt, Substrate recognition and specificity of the NisB protein, the lantibiotic dehydratase involved in nisin biosynthesis. J Biol Chem 286 (2011) 30552-60.
[240] P. Popella, S. Krauss, P. Ebner, M. Nega, J. Deibert, and F. Gotz, VraH Is the Third Component of the *Staphylococcus aureus* VraDEH System Involved in Gallidermin

and Daptomycin Resistance and Pathogenicity. Antimicrob Agents Chemother 60 (2016) 2391-401.
[241] T. Harayama, and H. Riezman, Understanding the diversity of membrane lipid composition. Nat Rev Mol Cell Biol 19 (2018) 281-296.
[242] G. van Meer, D.R. Voelker, and G.W. Feigenson, Membrane lipids: where they are and how they behave. Nat Rev Mol Cell Biol 9 (2008) 112-24.
[243] M.T. Nakamura, B.E. Yudell, and J.J. Loor, Regulation of energy metabolism by long-chain fatty acids. Prog Lipid Res 53 (2014) 124-44.
[244] T. Shimizu, Lipid mediators in health and disease: enzymes and receptors as therapeutic targets for the regulation of immunity and inflammation. Annu Rev Pharmacol Toxicol 49 (2009) 123-50.
[245] A.E. Saliba, I. Vonkova, and A.C. Gavin, The systematic analysis of protein-lipid interactions comes of age. Nat Rev Mol Cell Biol 16 (2015) 753-61.
[246] M.S. King, C. Boes, and E.R. Kunji, Membrane protein expression in *Lactococcus lactis*. Methods Enzymol 556 (2015) 77-97.
[247] S. Schlegel, M. Klepsch, D. Gialama, D. Wickstrom, D.J. Slotboom, and J.W. de Gier, Revolutionizing membrane protein overexpression in bacteria. Microb Biotechnol 3 (2010) 403-11.
[248] S. Schlegel, A. Hjelm, T. Baumgarten, D. Vikstrom, and J.W. de Gier, Bacterial-based membrane protein production. Biochim Biophys Acta 1843 (2014) 1739-49.
[249] E.R.S. Kunji, D.-J. Slotboom, and B. Poolman, *Lactococcus lactis* as host for overproduction of functional membrane proteins. Biochimica et Biophysica Acta (BBA) - Biomembranes 1610 (2003) 97-108.
[250] M. Monne, K.W. Chan, D.J. Slotboom, and E.R. Kunji, Functional expression of eukaryotic membrane proteins in *Lactococcus lactis*. Protein Sci 14 (2005) 3048-56.
[251] O.P. Kuipers, P.G. de Ruyter, M. Kleerebezem, and W.M. de Vos, Controlled overproduction of proteins by lactic acid bacteria. Trends Biotechnol 15 (1997) 135-40.
[252] O.P. Kuipers, P.G.G.A. de Ruyter, M. Kleerebezem, and W.M. de Vos, Quorum sensing-controlled gene expression in lactic acid bacteria. Journal of Biotechnology 64 (1998) 15-21.
[253] M.M. Klepsch, J.O. Persson, and J.W. de Gier, Consequences of the overexpression of a eukaryotic membrane protein, the human KDEL receptor, in *Escherichia coli*. J Mol Biol 407 (2011) 532-42.
[254] D. Drew, D.J. Slotboom, G. Friso, T. Reda, P. Genevaux, M. Rapp, N.M. Meindl-Beinker, W. Lambert, M. Lerch, D.O. Daley, K.J. Van Wijk, J. Hirst, E. Kunji, and J.W. De Gier, A scalable, GFP-based pipeline for membrane protein overexpression screening and purification. Protein Sci 14 (2005) 2011-7.
[255] G. Fiermonte, J.E. Walker, and F. Palmieri, Abundant bacterial expression and reconstitution of an intrinsic membrane-transport protein from bovine mitochondria. Biochem J 294 (Pt 1) (1993) 293-9.
[256] E.R.S. Kunji, The role and structure of mitochondrial carriers. FEBS Letters 564 (2004) 239-244.
[257] F. Palmieri, The mitochondrial transporter family (SLC25): physiological and pathological implications. Pflugers Arch 447 (2004) 689-709.
[258] P.L. Yeagle, Non-covalent binding of membrane lipids to membrane proteins. Biochim Biophys Acta 1838 (2014) 1548-59.
[259] C.A. Shintre, A.C. Pike, Q. Li, J.I. Kim, A.J. Barr, S. Goubin, L. Shrestha, J. Yang, G. Berridge, J. Ross, P.J. Stansfeld, M.S. Sansom, A.M. Edwards, C. Bountra, B.D. Marsden, F. von Delft, A.N. Bullock, O. Gileadi, N.A. Burgess-Brown, and E.P.

Carpenter, Structures of ABCB10, a human ATP-binding cassette transporter in apo- and nucleotide-bound states. Proc Natl Acad Sci U S A 110 (2013) 9710-5.
[260] M. Opekarová, and W. Tanner, Specific lipid requirements of membrane proteins—a putative bottleneck in heterologous expression. Biochimica et Biophysica Acta (BBA) - Biomembranes 1610 (2003) 11-22.
[261] W. Dowhan, Molecular Basis for Membrane Phospholipid Diversity: Why Are There So Many Lipids? Annual Review of Biochemistry 66 (1997) 199-232.
[262] E. Zinser, and G. Daum, Isolation and biochemical characterization of organelles from the yeast, *Saccharomyces cerevisiae*. Yeast 11 (1995) 493-536.
[263] D. Marsh, Lateral pressure profile, spontaneous curvature frustration, and the incorporation and conformation of proteins in membranes. Biophys J 93 (2007) 3884-99.
[264] W. Dowhan, E. Mileykovskaya, and M. Bogdanov, Diversity and versatility of lipid-protein interactions revealed by molecular genetic approaches. Biochim Biophys Acta 1666 (2004) 19-39.
[265] M.A. Haque, and N.J. Russell, Strains of *Bacillus cereus* vary in the phenotypic adaptation of their membrane lipid composition in response to low water activity, reduced temperature and growth in rice starch. Microbiology 150 (2004) 1397-404.
[266] R. Ernst, C.S. Ejsing, and B. Antonny, Homeoviscous Adaptation and the Regulation of Membrane Lipids. J Mol Biol 428 (2016) 4776-4791.
[267] E. Sezgin, I. Levental, S. Mayor, and C. Eggeling, The mystery of membrane organization: composition, regulation and roles of lipid rafts. Nat Rev Mol Cell Biol 18 (2017) 361-374.
[268] H. Nury, C. Dahout-Gonzalez, V. Trezeguet, G. Lauquin, G. Brandolin, and E. Pebay-Peyroula, Structural basis for lipid-mediated interactions between mitochondrial ADP/ATP carrier monomers. FEBS Lett 579 (2005) 6031-6.
[269] C. Lange, J.H. Nett, B.L. Trumpower, and C. Hunte, Specific roles of protein-phospholipid interactions in the yeast cytochrome bc1 complex structure. EMBO J 20 (2001) 6591-600.

6. Curriculum vitae

Personal Data

Date of Birth	30.08.1989, born in Neuss
Nationality	German

Work Experience

Since 1/2015	Ph.D. student at the Institute of Biochemistry, Heinrich Heine University, Duesseldorf with Prof. Dr. Lutz Schmitt and Dr. Sander H. J. Smits.

Academic Education

03/2013-12/2014	Master of Science (M.Sc.) Graduation Master of Business Chemistry at the Heinrich Heine University, Duesseldorf
10/2009-02/2013	Bachelor of Science (B.Sc.) Graduation Bachelor of Business Chemistry at the Heinrich Heine University, Duesseldorf

School Education

08/2000-06/2009	Abitur, Erasmus Gymnasium Grevenbroich

Professional Memberships

2015-present	Member, of Interdisciplinary Graduate and Research Academy Duesseldorf

Workshops and Conferences

07/2017	FEMS 2017, 7th Congress of European Microbiologists, Valencia Spain
07/2015	22. Arbeitstagung Mikromethoden in der Proteinchemie, Zeche Zollern Dortmund

7. List of Publications

Bialek, S., **Clemens, R.**, & Reiss, G.J. (2014). (Di-methyl-phosphor-yl)methanaminium hydrogen oxalate-oxalic acid (2/1). Acta Crystallographica *Section E Structure Reports Online*, 70 (Pt3), o312.

Reiners, J., Abts, A., **Clemens, R.**, Smits, S.H.J. & Schmitt, L. (2017). Stoichiometry and structure of a lantibiotic maturation complex. *Scientific Reports*. 7 42163.

Clemens, R., Zaschke-Kriesche, J., Khosa, S. & Smits, S.H.J. (2017). Insight into Two ABC transporter families involved in lantibiotic resistance. *Frontiers Molecular Biosciences*. 4 91

8. Acknowledgment

Am Ende meiner Arbeit möchte ich mich noch bei den wichtigsten Menschen auf meinem Weg bedanken.
Als Erstes möchte ich Dr. Sander Smits dafür danken mich darauf gebracht zu haben, überhaupt den Gedanken an eine Doktorarbeit zu haben. Ohne seine Unterstützung wäre ich nicht hier. Vielen Dank für die Projekte und alle Diskussionen und neue Ideen. Ich fand die Zeit immer sehr lehrreich und nehme viel für die Zukunft mit. Ohne ihn wäre es nur halb so gut geworden. Er hat mich immer unterstützt und wusste, wann ich den Kopf freibekommen musste, um weiter kommen zu können. Seine Ruhe in wichtigen Situationen war immer sehr hilfreich und ich danke ihm für seine Geduld bei der Korrektur dieser Arbeit. Vielen Dank für die tolle Zeit hier, ich werde sie nie vergessen.

Ein weiterer großer Dank geht an Prof. Dr. Lutz Schmitt. Ich danke ihm für die Möglichkeit in seinem Institut arbeiten zu können. Ohne seine großartige Unterstützung wäre diese Arbeit nicht möglich gewesen. Vielen Dank für die Übernahme dieser Arbeit und für die zahlreichen Hilfestellungen. Außerdem möchte ich mich bei ihm für die zahlreichen Denkanstöße durch Diskussionen in den Montagsmeetings bedanken.

Ein großes Dankeschön geht an PD Dr. Ulrich Schulte, durch ihn habe ich erst das Interesse an der Biochemie entdeckt. Ohne seine Vorlesung wäre ich wahrscheinlich nie für meine Bachelorarbeit ins Institut für Biochemie gekommen, was meinen weiteren Weg doch sehr geprägt hat. Vielen Dank.

Ich bedanke mich bei Prof. Dr. Holger Gohlke für die Übernahme des Koreferats.

Diana Kleinschrodt und Iris Fey möchte ich für die Unterstützung bei der Klonierung danken und für die vielen Diskussionen und Fragen, die sie mir beantwortet haben.

Astrid und Stefanie möchte ich für ihre Unterstützung bei der Kristallographie danken, ebenso wie Cordula für immer wieder tolle Unterhaltungen. Außerdem möchte ich mich sehr bei Frau Blum bedanken, ohne sie wären alle Verwaltungsangelegenheiten wesentlich komplizierter gewesen. Vielen Dank für alles.

Meinen wundervollen Bürokollegen möchte ich auch danken, ich hätte mir keine besseren wünschen können.
Danke Katja für die tolle Zeit. Mit dir konnte man immer über alles reden und sehr viel Spaß haben. War es mal wieder Zeit einen Wagen zu bauen oder einfach mal wieder die Stimmung nach Kaffee, auf meinen Kaffeekumpel konnte ich immer zählen. Ohne sie wäre die Zeit nur halb so lustig gewesen und ich hoffe, wir werden uns auch nach der Zeit noch viel zu erzählen haben.
Auch Martina möchte ich für alles danken. Sie hat immer alle meine Fragen beantwortet und wenn ich Hilfe brauchte, war sie immer da. Auch wenn ich zu ihr gekommen bin, wenn mal was kaputtgegangen ist (und nein ich habe nicht alles kaputt gemacht), hat sie immer ruhig reagiert. Ich danke ihr für die tolle Zeit im Labor und für unsere Gespräche, mit ihr war es nie langweilig.
Natürlich darf ich hier nicht Julia, unsere Kölner Frohnatur, und Isabelle (Isa-Bernd) vergessen, die unser Büro erst vollständig gemacht haben. Ihr beide seit so schnell in unserem Büro heimisch geworden als wäret ihr schon immer da gewesen. Wir haben so viel zusammen gelacht und Späßchen gemacht, da konnte gar keine schlechte Laune aufkommen. Ein spezieller Dank geht an Julia, ohne ihre Unterstützung wäre ich am Ende der Arbeit aufgeschmissen gewesen. Vielen Dank für alles.
Mein ganz spezieller Dank geht auch an Jens, er hat nie aufgehört mein Masterarbeitsbetreuer zu sein. Ich danke ihm für seine ganze Hilfe bei den Äktas und allen anderen Dingen, die er mir beigebracht hat. Er war immer da, um bei Problemen zu helfen, dafür möchte ich ihm danken. Er hat immer neue Ideen und Vorschläge in meine Projekte eingeworfen. Und ich weiß bis heute nicht, wie er es in unserem Büro mit all den verrückten Hühnern ausgehalten hat.

Dem Nachbarbüro möchte ich auch für alles Danken, ihr habt mich immer aufgenommen und wir konnten immer über unsere Projekte und Probleme reden. Besonders möchte ich mich hier bei Kalpana und Katharina bedanken. Ihr beide wart, seitdem ich angefangen habe, da und habt mich immer unterstützt. Katharinas Aufkleber, damit auch ja keiner ihre Laborgeräte wegnehmen möchte, werde ich nie vergessen und auch nicht, was wir immer für einen Spaß im Labor hatten. Und Kalpana wir haben uns immer so viel zu sagen gehabt und hatten immer viel Spaß.

Olivia unsere Nagellack- und Einhorn-Liebhaberin möchte ich für all die flotten Sprüche danken, die alle immer zum Lachen bringen. Ohne dich und Tobi war der Mensabesuch immer nur halb so lustig.
Auch bei Silke und bei Kerstin möchte ich mich bedanken unsere Unterhaltungen waren immer lustig.

So kommen wir zum Büro unten. Marcel, danke ich das er bei allen Fragen, die ich bezüglich Lactis hatte, immer ein offenes Ohr hatte und ich immer seine Tricin-Gel-Lösungen nutzen durfte, er ist einfach unser Lactis King. Ich fand es immer gut mit ihm über unsere Themen zu sprechen, da er immer eine eigene Sicht hatte und mir oft Tipps gegeben hat, die ich ausprobieren konnte.
Martin möchte ich für die tollen Diskussionen und unsere Unterhaltungen danken, es war immer spaßig.
Tobias, was hätten wir nur alle ohne dein „unnützes Wissen“ gemacht. Ganz ehrlich wie kann er all diese Sachen wissen. Es war immer ein Spaß ihm zuzuhören, ob es ums Kochen, neuste Serien, Geschichte oder Politik ging, er weiß einfach immer alles. Ich fand es immer schön mit ihm zu diskutieren und über unsere Projekte zu reden.
Manuel und Tim meine Flüssigstickstoff-Crew. Mein Gott was haben wir diese Aufgabe immer gehasst, aber dennoch war es immer ein Spaß mit euch alle drei Wochen den Flüssigstickstoff zu holen. Manuel war immer an den Themen der anderen interessiert und hat immer ein paar Ideen auf Lager. Tim mit dir konnte man immer super lachen, da dein Lachen einfach ansteckend ist. Unsere Monatlichen -80° Schrank Reinigungen werde ich zwar nicht vermissen, aber das hat einfach mit der Aufgabe zu tun und nicht mit dir. Du hast die Aufgabe immer mit Humor versetzt.

So kommen wir zu denen die leider nicht mehr im Institut sind, die ich aber trotzdem nicht vergessen will.
Sakshi what else can I say than THANK YOU. I do not know the institute without her, in my bachelor she was there in my master and even in the main time of my Ph.D. she was always there and I mean always, we discussed so many times our toppings and she helped me so much. She told me her tricks and how everything is working. She was always so kind and had always a helpful hand. Or she was just listening. Without her it would not be such a nice time. I thank her for the help of correcting my thesis and I hope we will see us soon again.

Auch möchte ich mich bei Michael und Sven bedanken. Unsere Busfahrten nach Hause waren immer ein Spaß. Es war sehr seltsam als beide weg waren und ich freue mich immer wieder sie zusehen.
Ananda, Carsten Münk, Philipp Neudecker, und Irina möchte ich für die Unterstützung und Kooperation danken. Auch Sandra, Hilke, Andreas, Jose und Jan-Peter möchte ich für alles Danken.

Ich fand es wirklich immer toll mit euch. Unsere gemeinsame Zeit wird mir immer in Erinnerung bleiben, von den Weihnachtsmarktbesuchen, den Filmabenden, den Grillabenden, Lasertag spielen, den TNT-Abenden (die Leute die es betrifft werden es verstehen) oder auch einfach unsere Kuchenzeiten oder auch die vielen (und ich meine viele) gemeinsamen Kaffees. Ohne euch alle wäre meine Zeit nicht so schön gewesen, wie sie war. Danke!

Allen meinen Freunden außerhalb der Arbeit möchte ich eben so danken. Danke, dass ihr es verstanden habt, wenn ich Verabredungen abgesagt oder zu spät gekommen bin. Egal was war, ihr habt mich immer unterstützt. Speziell möchte ich mich bei Marina, Sandra, Carina und Lisa bedanken.

Außerdem möchte ich hier meiner Familie danken. Meinen Eltern, sie haben mich bei allem unterstützt und waren immer da. Sie haben mir alle Möglichkeiten gegeben und mich beim Studium und vor allem bei der Doktorarbeit unterstützt. Sie haben sich immer für alles interessiert und haben immer mit Rat und Tat zur Seite gestanden. Auch wenn es nicht gut lief, waren sie da und haben zugehört. Danke.
Auch meinen Großeltern möchte ich danken, sie haben sich immer für alles interessiert und standen immer hinter mir in allen Phasen meines Lebens. Ich freue mich immer ihnen alles zu erzählen.
Meiner Schwester möchte ich besonders danken, sie ist einfach immer da. Sie hat mich immer aufgemuntert und hat bei allem zugehört und mich unglaublich unterstützt Außerdem danke ich ihr, dass sie meine Arbeit mit korrigiert hat.

Zu guter Letzt, möchte ich mich bei meinem Freund bedanken. Er war immer da und hat mich immer aufgebaut. Er hat mich immer unterstützt und war mein Rückhalt.

9. Declaration

Ich, Frau Rebecca Clemens, versichere an Eides statt, dass die vorliegende Dissertation von mir selbstständig und ohne unzulässige fremde Hilfe unter Beachtung der „Grundsätze zur Sicherung guter wissenschaftlicher Praxis an der Heinrich-Heine-Universität Düsseldorf“ erstellt worden ist.
Diese Dissertation wurde in der vorgelegten oder in ähnlicher Form noch bei keiner anderen Institution eingereicht. Ich habe bisher keine erfolglosen Promotionsversuche unternommen.

Düsseldorf, der

(Rebecca Clemens)